BINDING STUDIES OF

CYCLODEXTRIN-SURFACTANT COMPLEXES

A Thesis Submitted to the College of

Graduate Studies and Research

in Partial Fulfillment of the Requirements

for the Degree of Doctor of Philosophy

in the Department of Chemistry

University of Saskatchewan

Saskatoon

By

Lee Douglas Wilson

Fall 1998

UNIVERSITY OF SASKATCHEWAN

College of Graduate Studies and Research

SUMMARY OF DISSERTATION

Submitted in partial fulfillment

of the requirements for the

DEGREE OF DOCTOR OF PHILOSOPHY

by

Lee Wilson

Department of Chemistry

University of Saskatchewan

Fall 1998

Examining Committee:

Dr. R. Khandelwal	Dean's Designate, Chair College of Graduate Studies and Research
Dr. D. B. Russell	Chair of Advisory Committee, Department of Chemistry
Dr. R. E. Verrall	Supervisor, Department of Chemistry
Dr. R. P. Steer	Department of Chemistry
Dr. D. E. Ward	Department of Chemistry
Dr. G. A. Hill	Department of Chemical Engineering

External Examiner:

Dr. V. C. Reinsborough
Department of Chemistry
Mount Allison University
Sackville, New Brunswick
E4L 1G8

BINDING STUDIES OF CYCLODEXTRIN-SURFACTANT COMPLEXES

This dissertation deals primarily with a comprehensive study of the complexes formed between cyclodextrin (host) and surfactant (guest) systems in aqueous solution (cf. Scheme 1).

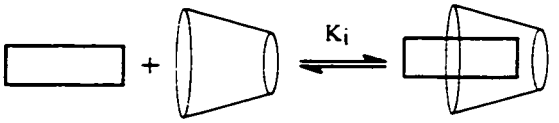

Guest Host Inclusion Complex

Scheme 1: The formation of an host-guest inclusion complex where K_i (i=1:1) is the equilibrium binding constant and i denotes the host-guest stoichiometry.

The cyclodextrin compounds studied are: α-CD, β-CD, 6-O-(2-hydroxypropyl) β-CD (HP-β-CD), 2,6-di-O-methyl β-CD (DM-β-CD), 2,3,6-tri-O-methyl β-CD (TM-β-CD), and randomly methylated β-CD (RAMEB). The hydrocarbon (hc) and fluorocarbon (fc) guest systems consisted of a homologous series of sodium alkyl carboxylate salts [$C_xH_{2x+1}CO_2Na$, x=5,7,9,11,13] and a series of sodium perfluoroalkyl carboxylate salts [$C_xF_{2x+1}CO_2Na$, x=1,3,6-9]. The use of thermodynamic and spectroscopic techniques has provided information about the magnitude of the binding constant, the type of host-guest stoichiometry, and the host-guest inclusion mode for the complexes studied here. In all cases, quantitative analysis of the data involved the use of different models to represent complexed and uncomplexed species according to the host-guest stoichiometry such as 1:1, 1:1 plus 2:1, and 1:1 plus 1:2 complexes.

This study has contributed to a further understanding of the factors that govern the stability of CD-surfactant complexes and the calculation of binding constants from different physical techniques. The main source of complex stability is the hydrophobic effect as shown by the dependence of K_i on alkyl chain length of the surfactant, the greater binding affinity of fc surfactants relative to hc surfactants with a common host, and the linear relation observed between -log $K_{1:1}$ and log CMC of the surfactants. The various types of host-guest stoichiometry and inclusion modes illustrate that complex formation can maximize hydrophobic and hydrophilic interactions within the CD interior and at the

host-guest interface while minimizing unfavourable hydrophobic hydration of the surfactant alkyl chain. The results indicate that desolvation and solvation processes play a significant role in the formation of CD-S complexes, as expected for processes involving hydrophobic hydration and hydrophobic interactions.

The significance of the results in this study can be extended to numerous fields that involve the exploitation of noncovalent host-guest interactions, e.g.; 1) quantification for biochemical model systems, 2) development of drug delivery systems, 3) selective phases for affinity chromatography, 4) new analytical and diagnostic procedures, 5) development of molecular sensors and switches, and 6) catalysis and synthesis in water as a solvent.

BIOGRAPHICAL

May, 1969	Born in St. Boniface, Manitoba
August, 1992	B. Sc., Chemistry, University of Winnipeg

HONOURS

Taube Medal, Department of Chemistry, University of Saskatchewan, 1998

Graduate Teaching Fellowship, University of Saskatchewan, 1993-1997

Johansson Memorial Scholarship, University of Saskatchewan, 1995

Department of Chemistry Achievement Award, University of Saskatchewan, 1993

Dr. A. B. Baird Bursary, University of Winnipeg, 1991.

PERMISSION TO USE

In presenting this thesis in partial fulfillment of the requirements for a Postgraduate degree from the University of Saskatchewan, I agree that the Libraries of this University may make it freely available for inspection. I further agree that permission for copying of this thesis in any manner, in whole or in part, for scholarly purposes may be granted by Professor Dr. R. E. Verrall who supervised my thesis work or, in his absence, by the Head of the Department or the Dean of the College in which my thesis work was done. It is understood that any copying or publication or use of this thesis or parts thereof for financial gain shall not be allowed without my written permission. It is also understood that due recognition shall be given to me and to the University of Saskatchewan in any scholarly use which may be made of any material in my thesis.

Requests for permission to copy or to make other use of material in this thesis in whole or part should be addressed to:

Head of the Department of Chemistry
University of Saskatchewan
110 Science Place
Saskatoon, Saskatchewan
S7N 5C9

ABSTRACT

A systematic thermodynamic and spectroscopic binding study of the complexes formed between cyclodextrin (CD) hosts and surfactant (S) guest systems has been carried out at 25.000±0.001°C and 25±1°C, respectively. The cyclodextrins (CDs) studied are α-CD, β–CD, 2,6-di-O-methyl-β-CD (DM-β-CD), 2,3,6-tri-O-methyl-β-CD (TM-β-CD), 2,3,6-randomly methylated β-CD (RAMEB), and 6-(2-hydroxypropyl)-β-CD (HP-β-CD). The surfactant (S) systems studied are a series of sodium alkyl carboxylate (hc) [$C_xH_{2x+1}CO_2Na$, x=2,5,7-9,11,13] salts and a series of sodium perfluoroalkyl carboxylate (fc) [$C_xF_{2x+1}CO_2Na$, x=1,3,4,6-9] salts. NMR spectroscopy, high precision densimetry, and optical spectrophotometry were used to obtain the binding constants (K_i, where i=1:1, 2:1, or 1:2), the stoichiometry, and the inclusion mode of the CD-S complexes that are formed.

The spectral displacement technique was used to obtain estimates of $K_{1:1}$ for the CD-S systems investigated. The method involves the measurement of absorbance changes of phenolphthalein in the presence of a competing guest and is relatively sensitive and suitable for strongly bound inclusates. NMR chemical shifts of the host and guest nuclei were measured because they are relatively sensitive to medium effects and they provide useful structural and quantitative information about the host-guest complex. The apparent molar volume (AMV) of the host and guest species were obtained because this property is sensitive to processes that involve hydrophobic transfer. Consequently, the NMR chemical shifts and AMV properties obtained are useful for assessing the role of solute-solute, solute-solvent, and solvent-solvent interactions in aqueous solutions. The

NMR complex induced shift (CIS) values and AMV properties of host and guest systems were found to depend on several factors: *i)* the magnitude of the binding constant (K_i), *ii)* the alkyl chain length (C_x) of the surfactant, *iii)* the mole ratio of the host to guest species, *iv)* the host-guest stoichiometry, *v)* the host-guest inclusion mode, *vi)* the conformation of the guest, and *vii)* the lipophilic character of the host and guest. In cases where complexes are formed, the magnitude of these physical measurements are proportional to the amount of bound or unbound host and guest. It is because of this correlation that binding constants (K_i) have been obtained from the analysis of these properties using equilibrium models in which 1:1, 1:1 plus 1:2, and 1:1 plus 2:1 complexes, and uncomplexed species are present.

In general, K_i increases as C_x increases and it is observed that fc surfactants possess systematically greater binding constants than the hc surfactants with a common host. In the case of 1:1 complexes, $K_{1:1}$ for CD-fc surfactant complexes are in the range 10^2-10^5 M^{-1} while the binding constants for CD-hc surfactant complexes are systematically lower and in the range 10^1-10^4 M^{-1}. The differences in binding affinity, stoichiometry, and inclusion mode between the CD hosts with a common guest are interpreted in terms of the lengthening of the annulus and steric exclusion effects created by the introduction of alkyl groups in the annulus region of the cyclodextrin. In the case of fc surfactants, differences in binding affinity between CD hosts were attributed to the occurrence of ion-dipole interactions between the carboxylate head group and the hydroxyl groups in the CD annulus. Ion-dipole interactions are not as pronounced for the hc surfactants because the carboxylate head group is more highly hydrated than in the case of the fc surfactants.

Inclusion complexes were formed by all CD-S systems except in the case of α-CD-fc surfactant and 2:1 β-CD-sodium perfluorooctanoate (SPFO) systems where noninclusion binding occurs between the second CD annulus and the apolar region of the fc chain. HP-β-CD forms 1:1 CD-S complexes with all hc and fc surfactants, α-CD forms 1:1 (C_x<9) and 2:1 (C_x≥9) complexes with hc surfactants whereas noninclusion complexes with all of the fc surfactants. β-CD forms 1:1 (C_x<11) and 2:1 (C_x≥9) complexes with hc surfactants and 1:1 (C_x<7) and 2:1 (C_x≥7) complexes with fc surfactants. The methylated CDs (RAMEB, DM-β-CD, and TM-β-CD) form 1:1 complexes with the hc surfactants and a 1:2 complex is formed between DM-β-CD and sodium tetradecanoate. The methylated CDs form 1:1(C_x≤6) and 1:2 (C_x≥7) complexes with fc surfactants. The various types of host-guest stoichiometry and inclusion modes demonstrate that complex formation maximizes hydrophobic and hydrophilic interactions within the CD interior and at the host-guest interface, respectively, while minimizing unfavourable hydrophobic hydration of the surfactant alkyl chain.

Considerable evidence is obtained that suggests the hydrophobic effect is the main source of stability in the formation of CD-S complexes. For example; K_i increases as C_x increases, -log $K_{1:1}$ increases as log CMC of the surfactant increases, there is correlation of inclusion modes and stoichiometry of the complexes with C_x, the binding affinity of fc surfactants is greater than hc surfactants with a common host, and the Gibbs energy of transfer per CH_2 and CF_2 groups from the bulk solvent to form a β-CD-S complex is similar to the Gibbs energy of transfer of those residues from the bulk solvent to a hc or fc micelle.

Solute-solvent and solvent reorganization processes are expected to play a major role in processes that involve hydrophobic hydration and hydrophobic interactions, as in the case of complexes formed between cyclodextrins and surfactants. The relative importance of solute-solvent and solvent-solvent interactions to the stability of the complex can be related to physical properties of the guest such as the CMC, and the molecular surface area or volume of the alkyl chain of the guest. The strong correlation between the apolar surface area of the guest and the Gibbs energy of complex formation underlines the importance of solvent-solvent interactions. Thus, it is the rearrangement of the H-bonded network of water that accompanies complex formation which provides a significant part of the driving force in the formation of inclusion complexes.

The use of NMR spectroscopy, high precision densimetry, and spectrophotometry has provided complementary and self-consistent information regarding the values of K_i, host-guest stoichiometry, and inclusion modes for complexes formed between cyclodextrins and surfactants in aqueous solution.

ACKNOWLEDGEMENTS

I would like to express my sincere appreciation to my supervisor, Dr. R. E. Verrall, who provided me with considerable guidance, support, and understanding throughout the course of my Ph. D. studies. The work presented herein would not have been possible without his supervision. The combination of his scientific skills and humanitarian qualities are truly impressive. I will always be thankful for the opportunity to have worked in his laboratory to further my scientific career.

I would like to acknowledge the Department of Chemistry for the use of the facilities and the support staff for their assistance in maintaining the equipment. I wish to thank all of the professors that gave the inspiring lectures during my graduate course work. I wish to thank the members of my Ph. D. advisory committee for their expert guidance; Dr. D. B. Russell, Dr. R. P. Steer, Dr. D. E. Ward, Dr. G. A. Hill, Dr. J. B. Senior, Dr. R. Woods, and Dr. V. C. Reinsborough.

I would like to thank Mrs. Stephanie Siddall for her assistance with the spectral displacement studies, Dr. Gong Zhang for his assistance with computer programming, and Dr. D. Jobe for helpful discussions. Many thanks to the research group for their assistance and helpful discussions; D. Hart, Dr. H. Huang, K. Jenkins, X. Wen, and S. Wettig. A special thanks to Dr. D. B. Russell for all of his guidance and encouragement. As well, I wish to thank Ron and Grace for their hospitality and kindness that they provided throughout the course of my Ph. D. studies.

I wish to thank Mom, Marcel, "little brother" Jason, Dad, Joan, and Marlys for their support during the course of my Ph. D. studies.

Financial assistance from the Natural Sciences and Engineering Research Council of Canada and the University of Saskatchewan is gratefully appreciated.

DEDICATION

This work is dedicated

to the memory of a special

friend

Guenther Gensler

and

to my wonderful

son

Quinn (*Boo-Boo*)

PUBLICATIONS

1. Wilson, L. D.; Verrall, R. E. "A Spectral Study of the Binding Constants of Cyclodextrin/Hydrocarbon and Fluorocarbon Surfactant Inclusion Complexes" *Can. J. Chem.* **1997**, 75, 927.

2. Wilson, L. D.; Verrall, R. E. "A Volumetric Study of β-Cyclodextrin/Hydrocarbon and /Fluorocarbon Surfactant Inclusion Complexes in Aqueous Solutions" *J. Phys. Chem. B* **1997**, 101, 9270.

3. Wilson, L. D.; Verrall, R. E. "A Volumetric Study of Modified β-Cyclodextrin/Hydrocarbon and /Fluorocarbon Surfactant Inclusion Complexes in Aqueous Solutions" *J. Phys. Chem. B* **1998**, 102, 480.

4. Wilson, L. D.; Verrall, R. E. "A ^{1}H NMR Study of Cyclodextrin/Hydrocarbon Surfactant Inclusion Complexes in Aqueous Solutions" *Can. J. Chem.* **1998**, 76, 25.

5. Wilson, L. D.; Verrall, R. E. "^{19}F and ^{1}H NMR Investigation of Cyclodextrin/Sodium Perfluoroalkyl Carboxylate Surfactant Inclusion Complexes" In press, Langmuir, October 1998.

TABLE OF CONTENTS

LIST OF TABLES

LIST OF FIGURES

LIST OF SCHEMES

GLOSSARY

Abs	Absorbance
AMV	apparent molar volume
CD	cyclodextrin
α-CD	cyclohexaamylose or cyclomaltohexaose or alpha-cyclodextrin
β-CD	cycloheptaamylose or cyclomaltoheptaose or beta-cyclodextrin
γ-CD	cyclooctaamylose or cyclomaltooctaose or gamma-cyclodextrin
CIS	complexation induced shift
$C_{\beta\text{-CD}}$	concentration of β-CD
$C_{R\text{-}\beta\text{-CD}}$	concentration of R-β-CD
CMC	critical micelle concentration
ΔC_p	change in heat capacity
C_S	concentration of surfactant
C_x	alkyl chain length of the surfactant where x=number of carbon atoms for surfactants of the form $C_xH_{2x+1}CO_2Na$ and $C_xF_{2x+1}CO_2Na$
$\Delta\delta$	chemical shift change or CIS value
δ_i	chemical shift of bound species where i=1:1, 2:1 or 1:2
δ_f	chemical shift of unbound species where f =free
δ_{obs}	observed chemical shift
DM-β-CD	2,3-di-O-methyl β-CD
DMF	dimethyl formamide
DMSO	dimethyl sulfoxide
DSS	4,4-dimethyl-4-silapentane sodium sulphonate
emf	electromotive force
fc	perfluorocarbon or perfluoroalkyl
γ_w	surface tension of water
ΔG	Gibbs energy change
ΔG_{comp}	Gibbs energy of complex formation
ΔG_{mic}	Gibbs energy of micelle formation
g/t	gauche/trans
hc	hydrocarbon
HH	hydrophobic hydration
HI	hydrophobic interaction
HLB	hydrophile lipophile balance
HP-β-CD	6-O-(2-hydroxypropyl) β-CD
$K_{CD\text{-}P}$	1:1 equilibrium binding constant for the β-CD-phenolphthalein complex
K_i	equilibrium binding constant, where i is the host-guest stoichiometry
MLPs	molecular lipophilicity profiles
NLLS	nonlinear least squares
NMR	nuclear magnetic resonance
"o"	the superscript "o" denotes infinite dilution conditions in the context of apparent molar volume quantities

P_c	cohesive pressure
phth	phenolphthalein
R	host-guest or guest-host mole ratio, ie., $C_{\beta\text{-}CD}/C_S$ or $C_{\beta\text{-}CD}/C_S$
RAMEB	randomly methylated β-CD at positions 2, 3, or 6
R-β-CD	alkyl substituted β-CD, where R=methyl or hydroxypropyl
s-s	solute-solute
s-w	solute-water
S	surfactant
SDec	sodium decanoate
SDodec	sodium dodecanoate
SDS	sodium dodecyl sulfate
SHep	sodium heptanoate
SHex	sodium hexanoate
SN	sodium nonanoate
SO	sodium octanoate
SP	sodium propanoate
SPFA	sodium perfluoroacetate
SPFB	sodium perfluorobutanoate
SPFD	sodium perfluorodecanoate
SPFH	sodium perfluoroheptanoate
SPFN	sodium perfluorononanoate
SPFO	sodium perfluorooctanoate
SPFP	sodium perfluoropentanoate
ST	sodium tetradecanoate
TFA	trifluoroacetic acid
TM-β-CD	2,3,6-tri-O-methyl β-CD
type i)	experimental methods that involve measurement of bulk solution properties
type ii)	experimental methods that involve measurement of solute activity
$V_{\phi,i}$	apparent molar volume of bound species where i=1:1, 2:1 or 1:2
$V_{\phi,f}$	apparent molar volume of unbound species where f =free
$V_{\phi,S}$	apparent molar volume of surfactant
$V_{\phi,CD}$	apparent molar volume of cyclodextrin
ΔV_S	transfer volume of surfactant
ΔV_{CD}	transfer volume of cyclodextrin
X_i	mole fraction of bound host or guest species where i=1:1, 2:1 or 1:2 complex
X_f	mole fraction of unbound host or guest species where f=free
w-w	water-water

1. INTRODUCTION

1.1 Rationale

Cyclodextrins (CDs) are of considerable practical and theoretical interest because of their ability, as host molecules, to form stable noncovalent inclusion complexes with numerous inorganic and organic guest molecules,[1] as shown in Scheme 1-1.

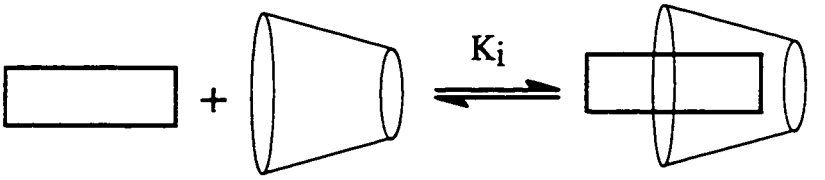

Guest Cyclodextrin Host Inclusion Complex

Scheme 1-1: The formation of an host-guest inclusion complex where K_i (i=1:1) is the equilibrium binding constant and i denotes the host-guest stoichiometry.

The formation of stable inclusion complexes in aqueous solutions may be attributed, in part, to the fact that CDs possess an apolar cavity with a well-defined geometry. CD inclusion complexes can be useful models of biomolecule-ligand complexation processes since there is a similarity in their thermodynamic properties[2] of binding when compared to antigen-antibody, DNA-ligand, enzyme-substrate, and protein-carbohydrate complexes.[3] Examples of applications that exploit the inclusion properties of CDs include biomimetic devices,[4] phase transfer agents,[5] nonlinear optical devices,[6] chromatography of enantiomers,[7] light harvesting complexes,[8] pharmaceutical excipients,[9] lipid extraction,[10] thin films,[11] *de novo* protein synthesis,[12] and organic synthesis.[13] The use of α-, β-, and γ-CD as drug carriers *in vivo* has been limited due to hemolytic effects. However, the development of chemically modified CDs with favorable water solubility and lower hemolytic properties has circumvented this problem.[14,15] The hemolysis of erythrocytes by

CDs has been attributed to two possible effects;[16] *i)* the inducement of an osmotic hypotonic effect and *ii)* the complexation of lipid components such as cholesterol or phospholipids. The work presented, herein, of studies of the interactions between CDs and surfactants could improve our understanding of the hemolytic effect and enhance the use of some CDs as pharmaceutical excipients.

The feverish level of research activity in the field of cyclodextrins continues unabated and there have been many studies concerning the formation and stability of CD-inclusate complexes. Unfortunately, there is considerable variation in the magnitudes of the reported binding constants and a lack of agreement concerning the key factors that govern the formation and stability of CD-inclusate complexes.[17] Binding constants provide a quantitative measure of the stability of a complex and a complete understanding of complex formation is impeded by uncertainty in the value of a binding constant. Thus, there is a need to carry out binding studies of suitable host-guest systems in which the molecular structure of the host and/or guest are varied, systematically, to allow for correlation of chemical structure parameters with stability of the complex. This study has two primary objectives: *i)* to obtain and compare binding constant(s) for such systems using NMR spectroscopy, spectrophotometry, and high precision densimetry and *ii)* to elucidate the relative importance of solute-solute and solute-solvent interactions in the formation and stabilization of CD-inclusate complexes.

The host systems studied in this work include α-CD, β-CD, and alkyl-substituted β-CD (R-β-CD) derivatives: 6-O-2-hydroxypropyl (HP-β-CD), 2,6-di-O-methyl (DM-β-CD), randomly methylated β-CD (RAMEB), and 2,3,6-tri-O-methyl (TM-β-CD). The

guest systems studied are a homologous series of hydrocarbon (hc) [$C_xH_{2x+1}CO_2Na$, x=2-13] and fluorocarbon (fc) [$C_xF_{2x+1}CO_2Na$, x=1-9] surfactants (S) at concentrations below the critical micelle concentration (CMC). Premicellar concentration conditions were chosen to eliminate any complications due to the formation of micelles.

A systematic study of the type described above is preferred to studies where the hosts and/or guests possess multivariate structural characteristics, since a correlation between chemical structure and factors that affect complex stability may be more feasible.[17] For example, a systematic study of a homologous series of surfactants of increasing alkyl chain length (C_x) provides an opportunity to assess contributions to the binding process that arise from; *i)* variation in the lipophilic character of the surfactant, *ii)* dehydration of the CD cavity, and *iii)* coiling of the alkyl chain of surfactant within the host.[18-20] On the other hand, a systematic study of β-CD and R-β-CD hosts provides an opportunity to study the effect of alkyl substitution in the annulus region of the CD on complex formation in terms of; *i)* van der Waals, dipolar, and H-bonding interactions between the host and guest, *ii)* cavity extension, and *iii)* steric exclusion.[21-23]

The use of techniques such as NMR, thermodynamic methods, and optical spectrophotometry provide an opportunity to measure different physical properties associated with complex formation and a better means to achieve the objectives described above. For example, information about the inclusion mode, stoichiometry, and binding constant(s) of the host-guest complex can be derived from NMR.[24] Also, the relative contributions of solute-solute and solute-solvent interactions can be estimated from NMR chemical shift changes and dipolar couplings[25] of the host and guest nuclei. The spectral

displacement technique[26] provides an independent method for estimating binding constants and to corroborate the values obtained from other techniques.

The importance of solute-solvent interactions in solvation and desolvation phenomena can be assessed from the volumetric properties of the host-guest complexes.[1] Kinetic studies[27] (ultrasonic absorption) can provide information regarding the volumetric changes upon complex formation, however, the accuracy of the data is inferior to apparent molar volume data obtained from direct density measurements. The role of solvent in biochemical and physicochemical processes, such as protein folding,[28] DNA-ligand binding,[29] and micelle formation and solubilization,[30] has been interpreted by means of volumetric studies. The significance of the hydrophobic effect is evident in processes involving the transfer properties of apolar solutes from water to a nonaqueous environment, e.g., the formation of CD-guest complexes. The scarcity of published volumetric data[31] for CD-guest complexes suggested that a study, as described herein, should have the potential to reveal important new facts. In conjunction with computer modeling of the data, estimates of the binding constants and host-guest stoichiometry were derived from the experimental data obtained in this study.

1.2 Hydration phenomena

1.2.1 Characteristics of water

Although there are a number of comprehensive reviews[32-35] about the physicochemical properties of water, it is useful to provide a brief review of the salient features in order to pinpoint the key aspects of hydration phenomena as they relate to the

studies in this thesis. The hydration of solutes is directly related to the physicochemical properties of water and the types of intermolecular interactions it can undergo.[36] Water is unique among low molecular weight hydrides as it possesses a low molecular polarizability, small molar volume, high melting and boiling points, low isothermal compressibility, large latent heat of vaporization, and a high internal cohesive energy. The cohesive pressure (P_c) measures the total molecular cohesion per unit volume of solvent and is related to the energy required to create cavities for the solute in the liquid phase

$$P_c = \Delta U_{vap}/V_m = (\Delta H_{vap}\text{-}RT)/V_m \qquad (1.2.1\text{-}1)$$

where V_m is the molar volume of the solvent, and ΔU_{vap} and ΔH_{vap} are the internal energy and enthalpy of vaporization, respectively. A related term encountered in dissolution processes is the Hildebrand-Scott solubility parameter (δ) which is related to P_c as follows

$$\delta = P_c^{1/2} \qquad (1.2.1\text{-}2)$$

By comparison with typical polar organic solvents, the cohesive interactions between water molecules are greater, as shown by a higher interfacial surface tension (γ_w), larger solubility parameter (δ), and substantially greater dipolar and H-bonding interactions.

The presence of two donor and two acceptor sites in an approximate tetrahedral arrangement allows for H-bonding in three-dimensions. The occurence of a maxima in density near 4°C and in other physical properties, such as heat capacity, at other temperatures further supports the qualitative picture of an "open-like" tetrahedral coordination in water. Evidence for local ordering effects in water derive from physical properties such as heat capacity or compressibility, since these properties are observed to be different when water is located next to an apolar surface compared to bulk water.[35]

The intermolecular H-bonding interactions in water are unexpectedly high compared with other polar solvents, and may be due to their partial "covalent character" as evidenced by a shorter intermolecular (O · · ·H) distance (0.176 nm) relative to the sum of the van der Waals radii of O and H atoms. H-bond strength in water ranges from 10 to 40 kJ mol^{-1}. Enhanced H-bonding interactions in water occurs because of cooperative effects by reason of increasing ease of H-bond formation within successive H-bonds.[33] Cooperative phenomena reflect the complexity of hydration processes and create computational difficulties in theoretical modeling.[34] The organization of water around apolar solutes is an attempt to minimize the loss of H-bonding sites and is related to the hydrophobic effect.

1.2.2 Hydrophobic effect

The structure and function of biological macromolecules can be related to the nature of their hydrated states. The low solubility of apolar compounds and their tendency to self-associate or aggregate in aqueous solutions is attributed to the hydrophobic effect. As well, it is implicated in diverse physicochemical processes such as protein folding, biomembrane stability, micelle formation, and biomolecule-substrate binding.[28,34]

The molecular nature of the hydrophobic effect can be deduced from modeling the thermodynamic transfer properties of an apolar solute from its pure liquid state or a solution in an apolar solvent to water. The hydrophobic effect involves the collective contributions of hydrophobic hydration (HH) and hydrophobic interaction (HI). HH refers to solute-water (s-w) interactions and is defined as the reorganization of water adjacent to an apolar solute, whereas, HI refers to the tendency of apolar molecules to

self-associate in aqueous solution. The Gibbs energy change for a pair-wise hydrophobic interaction (ΔG^{HI}) is defined[34] as

$$\Delta G^{HI} = \Delta G^{\circ}_{E} - 2\Delta G^{\circ}_{M} \qquad (1.2.2\text{-}1)$$

where ΔG°_{E} and ΔG°_{M} are the standard chemical potential for the solvation of gaseous ethane (E) and methane (M), respectively.

The hydrophobic effect involves intermolecular interactions such as solute-water (s-w), water-water (w-w), and solute-solute (s-s) which may promote or screen s-s interactions depending on the chemical nature of the solute. In aqueous solution, the second virial coefficients that characterize pair-wise interactions are small for polyhydroxylic compounds such as carbohydrates, whereas, the values for apolar compounds such as alkanes, are greater.[34] The magnitude of the hydrophobic effect depends upon whether the hydrophobic interactions are pair-wise or include a number of self-aggregating species.[35] The hydrophobic effect is illustrated by a comparison of the binding energy of methane molecules in the gas phase (-2.5×10^{-21} J) compared with that in water (-14×10^{-21} J).[32] Although the main attractive force between s-s and s-w pairs (s=apolar solute and w=water) are London dispersion forces,[34] the greater magnitude of w-w interactions relative to the s-s and s-w interactions provides a driving force for hydrophobic interactions between apolar solutes. This is manifested by the limited solubility of apolar solutes in water and their aggregation behavior. Micelle formation is an example of a spontaneous process that depends upon multiple hydrophobic interactions and cooperative effects.

There are two main models that describe the origins of the hydrophobic effect: *i)* structure-based and *ii)* cavity-based models. Structure-based models infer an increased structuring of water molecules adjacent to the surface of an apolar solute relative to pure water, denoted as hydrophobic hydration. Thus, the transfer of an apolar solute from its pure liquid state or a nonaqueous solution to water is accompanied by a decrease in entropy and a positive increase in heat capacity (ΔC_p^o).[28] In contrast, hydrophobic interactions involve the destruction of the hydrophobic hydration shells resulting in a negative value for ΔC_p^o and an increase in entropy.[34] The thermodynamics of a process involving hydrophobic interactions are illustrated by micelle formation in water at 25° C.

$$\Delta G_{mic} = \Delta H_{mic} - T\Delta S_{mic} \qquad (1.2.2\text{-}2)$$

where ΔG_{mic}, ΔH_{mic}, and ΔS_{mic} are the Gibbs energy, enthalpy, and entropy of micelle formation, respectively. The sign of ΔS_{mic} is positive and $T\Delta S_{mic}$ is greater than ΔH_{mic}, which is usually small, negative or positive. Thus, micelle formation is entropy driven and ΔG_{mic} is strongly favored under these conditions. Concepts such as "structure-making" and "structure-breaking" are simple qualitative models for interpreting the thermodynamics of the hydrophobic effect, however, improper use of the terminology has led to some confusion in the literature.

Cavity-based models, such as the scaled-particle theory[37] (SPT) and Sinanoglu's cavity model,[38] consider the energetics of cavity formation in the solvent to accommodate a solute and the ensuing solute-solvent interactions. The fact that the cohesive pressure of water (cf. eq 1.2.1-1) is large, and the apolar solutes are unable to participate in s-w H-bonding and dipolar interactions, leads to the tendency of these materials to minimize

their overall surface free energy. Hence, hydrophobic interactions between apolar solutes result from the "squeezing effect" of water. A reduction in the interfacial surface area and Gibbs energy (ΔG) is accomplished through apolar association according to

$$\Delta G \approx \gamma_w \Delta A \qquad (1.2.2\text{-}3)$$

where ΔA is the change in apolar surface area of the solute and γ_w is the interfacial tension of water.[39] A criticism of this approach is that the macroscopic parameters ΔA and γ_w may not be applicable at the molecular level.[34] Although the open lattice within the H-bonded water network contributes to the solubility of apolar compounds, these void lattice sites are limited in size. Apolar solutes that exceed this size limit of the void lattice sites begin to perturb the H-bond network and display a correlation of apolar surface area or molecular volume with hydrophobicity.[40] The fact that the onset of surface activity occurs when a surfactant possesses a minimum alkyl chain length[41] is consistent with the cavity-based models and can be related to the physical properties of water.

Muller[42] has questioned the use of specific structural hypotheses to rationalize the hydrophobic effect and suggested the use of simpler models that incorporate the two-state H-bonding equilibria of water. Concepts such as the "structure-making" and "structure-breaking" character of certain apolar solutes were criticized because neutron diffraction studies show that similarities exist between the pair distribution functions of water in the presence and absence of such additives.[36] Evidence that water molecules tend to optimize their H-bonding arrangements in the presence of apolar solutes was also obtained from Raman studies where the existence of pentamer aggregates and bifurcated H-bonds in

water was postulated.[34] These metastable structural motifs allow water to undergo extensive rearrangement in intermolecular H-bonding without a substantial loss in the number of H-bonds and illustrate the general difficulty associated with detecting structural changes in water. Although structure- and cavity-based models are useful as interpretive tools due to their simplicity, the former should not be over utilized in the absence of supporting experimental evidence. Improved knowledge of the structural and physical properties of water in the presence of apolar solutes and data on the Gibbs energy of hydration of apolar solutes are required to better understand the molecular nature of the hydrophobic effect.

1.2.3 Hydrophilic effect

Although there is no formal definition for this phenomenon,[35] the hydrophilic effect refers to the tendency of the solute to be hydrated rather than participate in direct s-s interactions in aqueous solution.[32] A related term, hydrophilic hydration, refers to the ordering of water molecules in the vicinity of a charged or polar group. Hydrophilic hydration exerts a disruptive effect on the w-w dipolar and H-bonding interactions due to the long-range ion-dipole and/or dipole-dipole w-s interactions. Disruptive effects are observed with chaotropic solutes such as guanidinium hydrochloride and urea.[28,34] Pronounced hydrophilic effects between macroscopic surfaces, such as membranes, occur since the interfacial forces extend over several hydration layers. In a recent review,[43] Lemieux argues that interactions between polyamphiphilic surfaces, such as carbohydrates, play an important role in molecular recognition events. The "polar-gate

mechanism"[44] describes how carbohydrates adjust their hydration sheaths through conformational changes to mediate intermolecular interactions with polar molecules. In the foregoing examples, water may function as a molecular chaperone by forming solute-water-solute H-bonds, denoted as "molecular bridging effects".[35] Clearly, the hydrophobic and hydrophilic character of solutes are important characteristics that affect hydration, however, the different water solubility of amylose and cellulose illustrates that size, conformation, and stereochemistry also influence the hydration properties of solutes.

1.3 Formation of cyclodextrin-inclusate complexes

1.3.1 Characteristics of Cyclodextrins

Cyclodextrins are cyclic oligosaccharides formed from the condensation of α-D-(+)-glucopyranose units joined together through α-(1→4) glycosidic bonds. Alpha- (α-), beta- (β–), and gamma- (γ-) CD are the three main types and are comprised of n=6, 7, and 8 glucopyranose rings, respectively, where n is the number of glucopyranose rings Scheme 1-2a denotes the molecular structure and numbering strategy for β–CD and its modified alkyl β–CD derivatives (R-β–CD) whereas Scheme 1-2b illustrates the general toroidal shape of CD compounds.

CDs have the shape of a hollow, truncated cone where the periphery of each end of the torus is comprised of a concentric ring of hydroxyl groups. The wider end consists of 2n secondary hydroxyl groups, located on carbons C(2) and C(3), whereas the narrower end consists of n primary hydroxyl groups on carbon atom C(6) (cf. Scheme 1-2b).

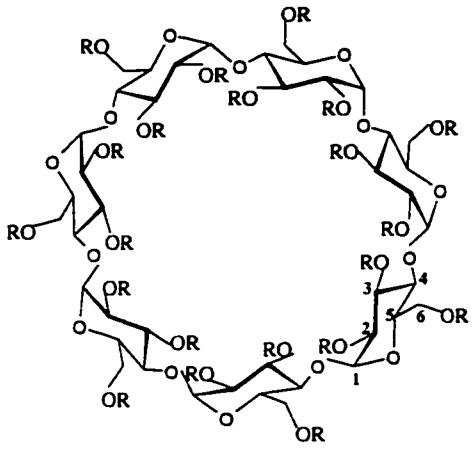

a)

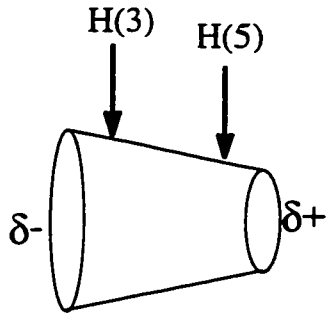

b)

Scheme 1-2: a) Molecular structure and numbering scheme for the ^{1}H nuclei of β-cyclodextrin(β-CD; where R=H) and alkyl-substituted β-CD host systems, and b) The torus shape of the cyclodextrin macrocycle noting the relative position of the H(3) and H(5) protons and the direction of the dipole moment, as denoted by δ^+ and δ^-.

Intramolecular H-bonding between these hydroxyl groups increases the rigidity of the macrocycle and limits rotation about the interglycosidic bonds, as shown from NMR,[45] x-ray crystallography,[23] and Raman[46] studies. The more extensive H-bonding between the secondary hydroxyl groups is supported by their lower pK_a values.[22] Modeling studies indicate that the primary hydroxyl groups possess greater conformational motility and their orientation is strongly affected by solvation effects.[18,47] The hydroxyl groups at the periphery of the annulus impart hydrophilic character that render these compounds soluble in water and polar organic solvents.[48,49] Recent MM2 calculations have demonstrated that a permanent dipole runs along the axis of the CD interior (cf. Table 1-1).[50,51] Lichtenthaler and Immel[52] argue that the wide, secondary end of the CD torus is hydrophilic and the narrow, primary end is hydrophobic. The direction of the dipole moment is denoted by the δ^+ and δ^- signs in Scheme 1-2b. The relative hydrophilic character of the exterior of α-,

β–, and γ–CD has been attributed to variable interglucosidic H-bonding since it affects the hydration character of the macrocycle. The greater solubility and reduced H-bonding of chemically modified CDs at the 2, 3, or 6 hydroxyl positions is consistent with the latter hypothesis.[22]

Table 1-1: Selected Physical Properties of the Cyclodextrins.[(a)]

Property	α-CD	β-CD	γ-CD
number of glucose residues (n)	6	7	8
solubility (g L^{-1})	14.5	1.85	23.2
molecular weight (g mol^{-1})	972	1135	1297
cavity width[(b)] (pm)	470-520	600-640	750-830
dipole moment (D)	7.06	2.03	2.96

[(a)]Obtained from refs. 1 and 17.
[(b)]Determined from Corey-Pauling-Koltun molecular models, where the smaller value is for the diameter at the location of the H(3) protons and the larger value is the diameter at the location of the H(5) protons (cf. Scheme 1-2b).
Each CD has a depth ranging from 790-800 pm.

The apolar character of the CD interior is attributed to the presence of two concentric rings of hydrogen atoms (H(3) and H(5); cf. Scheme 1-2b) and a ring of ether oxygen atoms lining the CD interior (cf. Scheme 1-2a). Chromophores that form inclusion complexes with CD and exhibit polarity dependent photophysical properties such as fluorescence quantum yields, emission lifetimes, and spectral shifts provide estimates of the relative polarity of the CD interior.[6,17,53] While there is general agreement that the CD interior is apolar in nature, there is less agreement about the specifics of assigning the

degree of apolarity. This may be due to the dependence of the photophysical properties of the probe molecule on factors other than polarity, e.g., the inclusion geometry, hydration state, degree of H-bonding with the CD annulus, and motional freedom within the CD interior. The calculated molecular lipophilicity patterns (MLPs) of α-, β–, and γ–CD further support that the interior of the CD cavity is apolar.[52,54]

Chemically modified cyclodextrins are obtained by introducing appropriate alkyl groups (R) at any or all of the C(2), C(3), and C(6) annular hydroxyl group positions[22] (cf. Scheme 1-2a; where R=CH_3 and $CH_2CH(OH)CH_3$). R-β-CDs exhibit greater conformational motility and solubility in water and organic solvents than β-CD due to the differences in the dipolar and H-bonding characteristics. Supporting evidence for this is obtained from NMR,[22] x-ray crystallography,[23] and ultrasonic relaxation studies.[27] As well, R-β-CDs possess a reduced cavity diameter and an increased torus length relative to β-CD.[54] The increased amphiphilic character of certain R-β-CDs is shown by their enhanced surface activity,[55] e.g., the aggregation of R-β-CDs at the air-water interface and the formation of monolayers and mixed films with polymers.[56]

1.3.2 Characteristics of complex formation in aqueous solutions

1.3.2.1 Binding equilibria

Surfactants and colloidal systems can undergo self-assembly and solubilize additives in aqueous solutions.[30] CDs share similar properties; however, the presence of a preorganized lipophilic cavity and a hydrophilic exterior leads to the formation of stable noncovalent complexes with various inorganic and organic guest molecules in aqueous

solution.[1] A number of host-guest stoichiometries can occur for CD-inclusate complexes. The 1:1 complex is the most commonly encountered; however, 2:1 and 1:2 CD-surfactant complexes also have been suggested by Funasaki.[57]

$$CD + S \overset{K_{1:1}}{\rightleftharpoons} CD\text{-}S$$

$$2CD + S \overset{K_{2:1}}{\rightleftharpoons} CD_2\text{-}S$$

$$CD + 2S \overset{K_{1:2}}{\rightleftharpoons} CD\text{-}S_2$$

Scheme 1-3: Various types of host-guest stoichiometry adopted by CD-inclusate complexes; where CD = cyclodextrin and S = surfactant.

Techniques that vary the composition of the components are utilized to estimate the stoichiometry of host-guest complexes. Two techniques are most frequently used: the mole ratio method and the method of continuous variations (Job's method)[58] The latter maintains the sum of the host and guest concentrations constant whereas the mole ratio method maintains a fixed concentration of host or guest while varying that of the other component. In either case, the occurrence of a maximum, discontinuity, or a change in slope of a plot of the measured physical property versus concentration of one of the components provides information about the host-guest stoichiometry.

These complexes are characterized by an equilibrium binding constant, K_i (i=1:1, 1:2, and 2:1), where the subscript i denotes the host-guest stoichiometry.[59] A general expression for the overall binding constant is defined as

$$K_i = \frac{[CD_n - S_m]}{[CD]^n[S]^m} \qquad (1.3.2.1\text{-}1)$$

where CD, S, and CD-S refer to the cyclodextrin, surfactant, and the host-guest complex, respectively (cf. Scheme 1-3). The brackets refer to the equilibrium concentrations and the quantities n and m refer to the stoichiometric coefficients.

In ternary solutions, the formation of host-guest-additive complexes with a 1:1:1, 1:1:2, or 2:1:1 stoichiometries has been reported.[53] The additive may be a different guest or a solvent molecule which functions as a cosolvent, space regulator, or an auxiliary binding partner to enhance the binding stability of the host and guest. However, the precise nature of the interactions is unclear. Increased complex stability is observed for the γ-CD-pyrene-toluene complex (K=869 M^{-1}) compared to the γ-CD-pyrene (K=270 M^{-1}) complex.[60] The formation of 1:1:1:1 quaternary complexes has been reported by Qi *et al.*,[60] and the formation of supramolecular noncovalent polymers between oxidazole derivatives and γ-CD was reported by Agbaria and Gill.[61]

1.3.2.2 Structure of cyclodextrin complexes

X-ray crystallography,[1,23,62] NMR spectroscopy,[1,45] circular dichroism,[63] and molecular modeling[23] are common techniques employed to elucidate the structures of CD-inclusate complexes. However, structural data for the inclusion mode of host-guest complexes derived from the solid-state and solution methods may not be self-consistent.[64] While x-ray crystallographic data provides a single snapshot of a minimum energy structure devoid of significant amounts of solvent, NMR structural data of the host-guest complex in the solution phase are obtained under conditions of dynamic exchange. These differences must be taken into account when comparing the two methods. In cases where solvent

effects are important, theoretical calculations and molecular modeling studies that rely on x-ray data should anticipate this reality. Scheme 1-4 is a typical inclusion mode derived from x-ray crystallographic studies[1,23,62] for a CD-aromatic guest complex where the aromatic guest possesses a charged and/or hydrophilic group.[17]

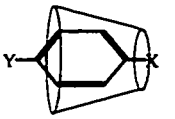

Scheme 1-4: Typical inclusion mode of a 1:1 CD-aromatic guest complex; where X=polar or nonpolar functional group and Y=positive or negative ionic group.

In general, the apolar phenyl ring is included in the CD cavity whereas the charged group (Y) is located at the wider end of the CD torus, near the secondary hydroxyl groups or in the bulk solvent. This type of inclusion mode is observed for the complex formed between α-CD and p-nitrophenolate,[1] as shown in Chapter 5.

In cases where bulky guests are sterically excluded from the apolar CD interior or when favorable interactions occur with the annular hydroxyl groups of the CD, a noninclusion complex is formed, as shown in Scheme 1-5.

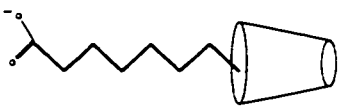

Scheme 1-5: Schematic representation of a noninclusion complex for the 1:1 α-CD-SPFO system; where SPFO=sodium perfluorooctanoate.

In Scheme 1-5, the noninclusion binding in the α-CD-SPFO complex occurs between the primary or secondary annular hydroxyl groups and the apolar region of the surfactant.[65] Noninclusion complexes have also been reported in DMF and water. In water, an axial

orientation was observed whereas an equatorial arrangement was found in DMF.[66] The dependence of the inclusion geometry on the water content in mixed solvents has been reported recently.[67]

In cases where apolar guest molecules are large and the formation of a 1:1 complex does not result in complete encapsulation of the entire apolar surface, there is the possibility that additional CD hosts may be complexed in order to lower the Gibbs energy of solvation. For example, the fluorescent probes, 2-(4-toluidino)naphthalene-6-sulphonate (TNS)[68] and N-methyl-2-anilinonaphthalene-6-sulphonate (MANS)[69] form 2:1 complexes with β-CD. Unfavorable hydration of the naphthyl and phenyl rings of TNS results in the formation of a 2:1 β-CD-TNS complex, as shown in Scheme 1-6.

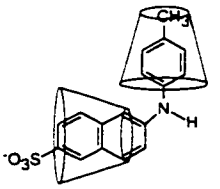

Scheme 1-6: Schematic representation of the inclusion mode for the 2:1 β-CD-TNS complex; where TNS=2-(4-toluidino)naphthalene-6-sulphonate.

Schemes 1-4 to 1-6 illustrate that the optimal stability of CD-guest complexes is achieved through various inclusion modes and host-guest stoichiometries and underlines the importance of steric and electronic complementarity between the host, guest, and solvent.[70]

1.3.2.3 Hypotheses regarding complex stability

The magnitude of CD-inclusate binding constants can vary over a wide range because the stability of a complex depends on many factors.[17,39] Binding constants as

great as 10^{25} M^{-1} have been reported.[71] Although steric and electronic complementarity between the host and guest are important, a complete understanding of the factors governing the stability of these noncovalent complexes is still an important topic of research. The theoretical prediction of a binding constant from first principles for a cyclodextrin-inclusate complex is not yet possible. In part, this may be due to the numerous hypotheses proposed to account for the formation and stability of CD-inclusate complexes. These include: *i)* host-guest geometric compatibility, *ii)* conformational effects, *iii)* dipolar and hydrogen-bonding interactions, *iv)* induction and dispersion forces, *v)* the hydrophobic effect, and *vi)* the displacement of hydrate water from the CD cavity.[1,17]

i) Geometric compatibility

The host and guest must be geometrically compatible in order for an inclusion complex to form. The "goodness-of-fit" between the host and guest is an important requirement since some authors argue that snug fits result in strong binding.[21] On the other hand, others suggest that a certain degree of "looseness" favors strong binding.[72] Yet a third hypothesis specifies that the spatial fit requirements between host and guest should be neither too tight nor too loose.[17,73]

ii) Conformational effects

The release of conformational strain within the α-CD macrocycle is argued to be an exergonic process in complex formation because of the conversion from a "tensed" to a "relaxed" conformation upon guest inclusion.[74] Crystallographic data for α-CD and TM-β-CD indicate that the macrocycle is partially collapsed in the unbound state whereas guest inclusion results in a more open, symmetric arrangement.[62,75] In contrast, NMR

studies of these hosts in solution indicate a symmetrical conformation in the unbound state. Presently, there is little support for the hypothesis of conformational strain.

Increased conformational motility of the modified CDs (R-β-CDs) (cf. § 1.3.1) may allow these host systems to adopt an "induced-fit" mechanism[1,76,77] upon inclusion of a guest. The ability of aliphatic guests to adopt an "induced-fit" is possible because of gauche/trans (g/t) conformational isomerism of the alkyl chain.[18] Castronuovo *et al.*[78] argue that an account of the g/t conformer populations is necessary in order to model their calorimetric data. The coiling of hydrocarbon alkyl chains within the interior of β-CD is supported in experimental[79] and theoretical[18] studies. Conformational changes of the host and/or guest allows for the geometric matching of the binding sites. This lowers the Gibbs energy of complex formation by promoting more favorable steric and electronic interactions.

iii) Dipolar and Hydrogen-bonding interactions

The contributions of H-bonding and dipole-dipole forces in CD-inclusate binding has been confirmed in several studies.[80-86] Some examples include ester hydrolysis[13] and host-guest-alcohol ternary complexes.[53] Guest molecules of the type $CH_3(CH_2)_n$-X, where X=CO_2H, OH, etc., as compared to when X=CH_3, possess greater binding affinity when bound to CDs and affirms the importance of these interactions.[17,86] As well, the greater binding of β-CD with hydrophilic nucleotides relative to lipophilic nucleotides lends additional support.[87]

Dipolar and H-bonding forces are expected to contribute significantly to the stability of host-guest complexes because of their long-range and directional nature.[88]

Comparatively few direct measurements of H-bonding between host and guest in aqueous solution have been made. This is because of the greater ability of water molecules to compete for available donor and acceptor H-bond sites.[3] Compounds, such as nucleotides, undergo intermolecular H-bonding more readily in aqueous solution since their donor and acceptor sites are located near a hydrophobic cleft which excludes water, as seen in the case of base-pairing in DNA.[88] The interaction of two hydrophilic solutes in aqueous solution is conceivable if one considers the formation of H-bonds between a single water molecule and each of the two solutes, denoted as "molecular bridging effects" (cf. § 1.2.3). The latter occcur in antigen-antigen[89] and protein-ligand[90] complexes and are expected to play a role in some CD-inclusate complexes.

iv) Induction and dispersion forces

London dispersion forces, referred to as van der Waals forces, are comprised of dipole-induced dipole and induced dipole-induced dipole contributions. These types of interactions are evidenced by the formation of more stable CD-inclusate complexes with molecules of increasing polarizability, such as halogenated arenes and large inorganic ions.[1] The difference in polarizability of the CD interior and water provides a partial driving force for the inclusion of apolar guests in the CD interior.[70] Tabushi argues that van der Waals interactions are more important than dipolar interactions based on the calculated energetics of complex formation for CD-inclusate complexes.[91] The short-range nature of these forces relative to dipolar interactions indicates that they make a secondary contribution to complex stability. Their significance increases as the number of these interactions increase, e.g., multiple hydrophobic interactions (cf. § 1.2.2).

v) Hydrophobic effects

The involvement of the hydrophobic effect in the formation (cf. § 1.2.2) of CD-inclusate complexes is argued on the basis that the CD possesses a preorganized lipophilic cavity and that binding is enhanced with increasingly apolar solutes in aqueous solution.[92] The fact that the formation of CD-inclusate complexes in aqueous solution is enthalpy dominated does not preclude the hydrophobic effect as a driving force since factors such as dipolar and dispersion forces and the hydration state of the host and guest affect the thermodynamics of binding. In contrast to values obtained in pure water, CD-inclusate binding constants are observed to decrease in organic solvents, water/organic solvents, and aqueous solutions containing chaotropic additives.[93,34] Conversely, "structure making" salts such as LiCl enhance binding due to "salting-in" effects. A detailed treatment of salt effects can be found elsewhere.[94,95] As well, numerous empirical correlations of complex stability with hydrophobic-related markers have been observed: solvent effects, solute structural parameters, thermodynamic properties, water-octanol partition coefficients, various theoretical models, and the compensation effect.[34,39] The foregoing provides support that the hydrophobic effect plays a key role in CD-inclusate complex formation.

vi) Desolvation of the host cavity

According to x-ray crystallography,[62] the hydrate water in the interior of β-CD is relatively disordered with respect to the bulk solvent because of an incomplete network of H-bonds. It is characterized as "high energy" or "enthalpy rich", not unlike water that is next to an apolar surface.[34] Expulsion of the hydrate water from the CD interior upon guest

inclusion is argued to result in a favorable enthalpic contribution due to a net increase in H-bonding with the bulk solvent.

Studies in solution indicate that the dynamics of exchange of labelled water between the CD interior and the bulk solvent is very rapid. [96,97] Calorimetric results indicate a favourable magnitude for the enthalpy of dehydration per water molecule within the β–CD cavity, irrespective of the hydrate content, inferring that dehydration of the CD interior is a concerted or relaxational process.[97] A positive amplitude in the 1-10 MHz region of the ultrasonic aborption spectrum has been attributed to the movement of water molecules in and out of the CD cavity.[27] Furuta *et al.*[98] concluded that a minimum water content in organic solvents was required to promote inclusion binding. The minimum water content coincides with the calculated hydrate content of the CD interior. The thermodynamics of binding for γ- and β-CD with the adamantane carboxylate ion revealed large differences for the enthalpy and entropy of complex formation. These differences between γ- and β-CD are argued on the basis of the different cavity sizes and the relative state of disorder of the hydrate water in the CD interior. [99] Turro *et al.* conclude that dehydration of the CD cavity is rate limiting in the kinetics of complex formation between β-CD and phosphorescing detergents.[100] The foregoing examples illustrate that dehydration of the CD interior may be an important energetic consideration for the inclusion process. However, it is unresolved whether it is the major driving force during complex formation.

There are numerous solute-solvent and solute-solute intermolecular interactions that play a role in the stability and formation of CD-inclusate complexes, as evidenced in the case of large biomolecule-ligand complexes. The relative importance of a single

stabilizing contribution is sometimes difficult to ascertain because of the occurrence of synergistic and cooperative effects. At present, there is some disagreement with regard to the factors which govern the stability of CD-inclusate complexes, particularly the relative role of solute-solvent and solute-solute interactions. An improved knowledge of the factors that govern complex stability should lead to better predictions of binding constants from first principles and a better correlation of structure/stability relationships between the host and guest.

1.4 Overview of the Literature

From a historical point of view, the research activity in the cyclodextrin field can be divided into three eras. The first era dealt with the discovery and characterization of CDs. The second era focused primarily on physicochemical studies of CDs and their inclusion complexes. The third, current, era is devoted to expanding the application of CDs in various fields. There are several reviews which document the three eras of CD research and cover the literature up to the early 1990's.[1,7,55,101-103] A considerable amount of the activity during the second era dealt with the determination of binding constants, stoichiometry and inclusion mode of host-guest complexes in aqueous solutions. Despite the many studies, there still remain some unresolved issues in the cyclodextrin literature and they will be briefly addressed in this section. Two key issues are: *i)* the reliability of CD-inclusate binding constant(s) and *ii)* the importance of solvent effects in host-guest binding. The cyclodextrin literature is vast and the subject of this review will be restricted primarily to β–CD and R-β–CDs since they are the principal host systems

investigated in this work. However, reference will be made to other CD hosts when appropriate. The discussion will focus on studies of CD-inclusate complexes in aqueous solution with emphasis on surfactants as the guest species.

1.4.1. Reliability of the equilibrium binding constant

Traditionally, conductance and optical spectroscopic techniques have been utilized to estimate the binding constants of CD-guest complexes. Other techniques such as NMR spectroscopy, tensiometry, electromotive force (emf), potentiometry, mass spectrometry, calorimetry and sound velocity have also been used. They rely on differences between the properties of the guest or host in the bound or unbound states.[59] The latter methods are useful for aliphatic surfactants that do not possess a suitable chromophore for study by optical methods.[104] Binding constants reflect the stability of the complex and an issue of central importance to host-guest binding is their reliability.[105] Several factors are important in determining their relative reliability. They include: (1) the nature of the physical measurement, (2) the experimental conditions, (3) model assumptions, and (4) the data-fitting procedure.

Physical measurements are divided into two categories; *i)* techniques which involve the measurement of bulk physical properties and *ii)* techniques which involve the direct or indirect measurement of concentration of one or other of the reagents. Type *i)* methods, e.g., NMR, surface tension, heat capacity, and conductance assume that the measured property is proportional to some aspect of the complexation process. Type *ii)* methods involve direct measurement of concentration of bound or unbound species, e.g.,

UV-VIS and fluorescence spectrophotometry,[106] and emf measurements using ion selective electrodes.[107] Indirect methods, such as the spectral displacement technique, yield good estimates of the concentration of unbound species.[26] Type *ii)* methods provide more reliable estimates of the binding constant because the measurement of a specific analyte concentration leads to greater sensitivity in the computer modeling of such data.[105] The sensitivity of type *i)* methods depends on the differences in the measured physical property between bound and unbound species and on the physicochemical characteristics of the solute. The appropriate choice of a technique has been more extensively discussed by Connors.[59]

Experimental conditions such as pH, ionic strength, and relative host and guest concentrations are also important considerations.[59] Factors such as pH and ionic strength can lead to a modification of solvent properties, *vide infra*. The relative concentrations of the host and guest can influence the type of stoichiometry, especially if higher-order 2:1 and 1:2 host-guest complexes are formed. If $K_{2:1} < K_{1:1}$, the formation of a 2:1 complex is favored when $[host]_o >> [guest]_o$, where the subscript "o" infers total concentrations. If $K_{1:2} < K_{1:1}$, the formation of a 1:2 complex is favored when $[guest]_o >> [host]_o$, in accordance with the law of mass-action. An additional consideration when studying the interaction of CDs with surfactant monomers is to keep the concentration of the surfactant below the CMC. At concentrations above the CMC, complications arising from the formation of micelles can occur.

The appropriate choice of model to analyze the data depends on the stoichiometry of the host-guest complex. Complexes of 1:1 stoichiometry are frequently encountered

and are the simplest to deal with; however, higher-order 2:1 and 1:2 complexes have been reported.[57] Clearly, modeling must be adjusted to account for their presence. The type of host-guest stoichiometry can be affirmed using the techniques described in § 1.3.2.1.

Data fitting techniques are divided into two categories; *i)* linear methods and *ii)* nonlinear methods. Linearization procedures that use double-reciprocal plots such as the Benesi-Hildebrand method, have been commonly employed.[108] However, restrictive assumptions[59] and improper weighting of the data have been reported.[105,109] These difficulties can be effectively overcome by using nonlinear fitting techniques.[93,103,110]

An example of the discrepancies that exist among binding constant(s) reported for a host-guest system is shown in Table 1-2 for β-CD-sodium dodecylsulfate (SDS).

Table 1-2: Survey of Binding Constants (K_i) for the β-CD-SDS Complex

K_i	Technique	Reference
4340^1	conductance	111
7230^1	conductance	112
4320 ± 670^1	^{1}H NMR	113
18000^1	visible spectral displacement	114
25600^1, 200^2	fluorescence spectral displacement	115
210000^1, 210^2	emf	116

[1]refers to the 1:1 binding constant ($K_{1:1}$) where the units are M^{-1}
[2]refers to the 2:1 binding constant ($K_{2:1}$) where the units are M^{-2}

The magnitude of K_i varies between 10^2 - 10^5 and the wide range is attributed to the four factors discussed above. For example, consider the values reported for K_i obtained by using the conductance and the spectral displacement methods. The former relies on changes in the macroscopic conductivity property due to variation in the free and

unbound amounts of SDS, whereas, the latter involves the direct measurement of the unbound concentration of chromophore which is linked to bound SDS through coupled equilibria (cf. § 2.1.4). Conductance also monitors changes in the counterion binding of sodium to the surfactant head group and changes in mobilities of these ions are reflected in the macroscopic conductance, as discussed in Chapter 2. The sensitivity of conductance methods has been discussed previously.[117] Type *ii)* methods, such as the spectral displacement method, are expected to be more reliable because the concentration of bound and/or unbound species can be obtained.

The variation in K_i may also be attributed to the models chosen to describe the complexation equilibria. The length of the alkyl chain in SDS allows for the formation of both 1:1 and 2:1 complexes. In such cases, models that assume only the formation of 1:1 complexes[111-113] underestimate the concentration of bound species and the magnitude of $K_{1:1}$.[57] Examples of studies that overlook the presence of 2:1 CD-surfactant complexes can be found in the literature.[78,118-120]

X-ray crystallography,[1,23,62] NMR spectroscopy,[1,45,103] and molecular modeling[23] can provide information on the inclusion mode and quantitative aspects of complex formation (cf. § 1.3.2.2). Structural data that aid in the elucidation of the inclusion mode (cf. Schemes 1-4 to 1-6) of the complex provide support for a chosen binding model and a rational basis upon which to correlate structural parameters of the host and guest. Uncertainty in the inclusion mode can often lead to deficiencies in the intrepretation of data.

Appropriate choice of host and guest systems for study is an important issue if the objective is to correlate complex stability with molecular group additivity parameters. It is

generally not possible to accomplish this by studying host and/or guest systems that possess multivariate structural characteristics. Discrimination between size effects and hydrophobic effects is possible when using a linear homologous series of surfactants, whereas, a comparison of cyclic homologs may be more difficult because of steric exclusion. The α-, β-, and γ-CD hosts are often considered as a homologous series because they differ according to the number of glucopyranose residues that comprise the macrocycle. The different magnitude and sign of the enthalpy and entropy of complex formation with a common guest illustrates that host-guest structural changes are sometimes difficult to intrepret and may not be the only source of complex stability. The different thermodynamics of binding for α-, β-, and γ-CD variation has been attributed to solvent effects, as described below.

1.4.2. Solvent effects

Solute-solute interactions are shown by the formation of CD-inclusate complexes in the solid state whereas solute-solvent interactions are shown from binding studies in solution.[3,121-124] Because of extensive solvation and desolvation processes, Amato *et al.*[125] argue that an account of the role of solvent in complex formation is necessary in order to provide reasonable estimates of the energetics of complex formation. This is consistent with a molecular view of the solvent (water) rather than a continuum model when considering intermolecular forces that occur between s-w and w-w pairs. The importance of solvent effects in CD-guest complex formation is illustrated by considering the overall energetics of the β-CD-benzene sulfonate ion complex,[121] shown in Table 1-3. The values

in Table 1-3 indicate that the inclusion geometry 1a is favored over 1b and that the energetics are dominated by a large solvation contribution. Similarly, Smithrud *et al.* attributed a large part of the enthalpy of complex formation for CD-inclusate complexes to solute-solvent interactions.[124] In aqueous solution, the enthalpy of hydration is appreciable and may contribute substantially to the energetics of complex formation. For example, the heat of solution for 1 mole of H_2O with 1 mole of β-CD is -10.5 kJ mol^{-1}.[122]

Table 1-3: Calculated Interaction Energies for the β-CD-Benzene Sulfonate Ion Complex in Two Different Inclusion Modes.[121]

Inclusion Mode	van der Waals (kJ mol^{-1})	Electrostatic (kJ mol^{-1})	Solvation (kJ mol^{-1})	Total (kJ mol^{-1})
1a	-1.10	-0.007	-4.58	-5.68
1b	-0.70	-0.014	-2.88	-3.59

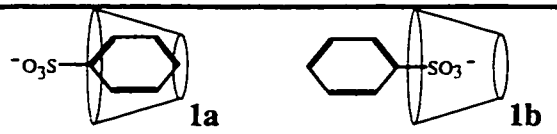

1a **1b**

In a recent calorimetric study[123] of large biomolecule-substrate complexes in H_2O and D_2O, Chervenak and Toone concluded that 25-100% of the enthalpy of ligand binding is due to changes in hydration. In general, the binding affinity of a given CD-inclusate complex is greater in D_2O versus H_2O for apolar inclusates. These results and the different H-bonding characteristics of D_2O and H_2O suggest the importance of the energy required to form cavities (cf. eq 1.2.2-1) in aqueous solution.

The important role of hydration of β–CD is also expected because of the amphiphilic character of the CD macrocycle and this has been reported for studies of β–CD-guest complexes (cf. § 1.3.2.3).[43,126] The dependence of hydration upon the relative stereochemistry of the hydroxyl group of the O(2) and O(4) groups in various monosaccharides was proposed from a recent thermodynamic study. As well, Junquera *et al.*[128] argue that the matching of apolar surfaces is important for the binding of certain guest molecules to carbohydrates whereas Lemieux *et al.*[8] propose that interactions can occur between the hydrophilic surfaces, e.g., proteins and carbohydrates. The latter is referred to as the "polar-gate" mechanism and involves a change in conformation and intramolecular H-bonding of the carbohydrate that results in changes to the hydrophile/lipophile balance (HLB).[44] A similar hypothesis is attributed to the desolvation of β–CD since removal of hydrate water from the CD interior is associated with conformational changes of the macrocycle.[129] The necessary requirement of water in the formation of stable inclusion complexes is supported by recent experimental[130] and theoretical studies.[131] The foregoing examples illustrate the complexity of hydration phenomena of carbohydrates in aqueous solution.

The effect of solute-cosolvent interactions in apolar binding of host-guest systems is shown by the decrease in K_i as the organic cosolvent increases in water/organic cosolvent solutions.[48] A number of hypotheses describing the effect of cosolvents on the stability and formation of CD-inclusate complexes has been outlined.[17] Cosolvents can; *a)* increase solute-solvent dispersion interactions, *b)* participate in other stoichiometric equilibria, e.g.,

act as competitive substrates and to form ternary complexes, and *c)* decrease the hydrophobic effect.

a) In cases where apolar binding occurs in aqueous solution, the presence of an organic cosolvent, such as methanol, lowers the host-guest binding affinity. It is argued that organic cosolvents increase the polarizability of the mixed solvent, resulting in more favorable dispersion interactions with the guest, relative to pure water.[3]

b) The stoichiometric involvement of water in the formation of a host-guest complex is illustrated below

$$\beta\text{-CD}.xH_2O + \text{guest}.yH_2O \overset{K_{app}}{\rightleftharpoons} \beta\text{-CD-guest}.x+y-zH_2O + zH_2O$$

where x, y, and z are the numbers of solvent molecules involved in the overall solvent reorganization process. The apparent binding constant (K_{app}) is given by

$$K_{app} = K_{actual} \times a_w^{\,z} \qquad (1.4.2\text{-}1)$$

where K_{actual} is the thermodynamic equilibrium binding constant and a_W is the activity of water.[132] Equation 1.4.2-1 describes the effect of water activity on K_{app} and provides a rationalization of the effect of additives, such as urea, electrolytes, and low molecular weight alcohols on CD-guest binding. The importance of water activity has also been argued in the case of protein hydration.[133]

Competitive binding between organic cosolvents and inclusates is described below

$$\beta\text{-CD-guest} + \text{cosolvent} \overset{K_{cosolv}}{\rightleftharpoons} \beta\text{-CD-cosolvent} + \text{guest}$$

where K_{cosolv} is the binding constant for the β-CD-cosolvent complex. The occurrence of a competitive equilibrium results in an apparent lowering of the binding constant. The

lowering of the effective host concentration is similar to that described in the spectral displacement method[26] (cf. chapter 2) and can be tested by using known values of K_{cosolv}.[134]

The formation of a β-CD-guest-cosolvent ternary complex[53] may also occur

$$\beta\text{-CD-guest} + \text{cosolvent} \overset{K_{1:1:1}}{\rightleftharpoons} \beta\text{-CD-guest-cosolvent}$$

where $K_{1:1:1}$ is the binding constant for the 1:1:1 ternary complex. Examples of ternary complexes where the guest is naphthalene[53] or bromonaphthalene[135] and the cosolvent is tert-butyl alcohol have been reported. The presence of tert-butyl alcohol increases the binding affinity of these β-CD-guest complexes because of H-bonding to the hydroxyl groups of the CD annulus (cf. § 1.3.2.1).

c) The hydrophobic effect[34,35] is inferred on the basis of a decrease in the hydrophobic driving force because of the presence of organic cosolvents and/or certain solutes in apolar host-guest binding.[136-140] It is well known that such additives decrease the cohesive and structural properties of water, as shown by the reduction in surface tension, heat capacity, and viscosity of their aqueous solutions.[136-140] The β-CD-adamantane carboxylate complex is referred to as a protypical model system for the hydrophobic effect. The binding constant for this complex was observed to decrease as the methanol composition of the aqueous mixture increased and paralleled the decrease in the surface tension of the aqueous solution.[138] The use of an octyl-sepharose stationary phase in affinity chromatography with an aqueous mobile phase containing chaotropic additives resulted in a good separation of α-, β-, and γ-CD, whereas, the use of water as a mobile.

phase resulted in poor separation.[139] These studies demonstrate the importance of solvent cohesion in hydrophobic interactions between apolar solutes in aqueous solution.

Cooperative binding phenomena are known to occur due to allosteric effects in biomolecule-substrate systems.[141] Allosterism is the amplification of binding due to the synergistic effect of multiple binding sites, e.g., the binding of oxygen to hemoglobin. The binding of O_2 to the first heme polypeptide induces a conformational change in one or more of the heme proteins causing a remote site binding effect.

Petter *et al.*[142] observed Hill coefficients[141] greater than unity for the binding of 4-nitrophenol and 4-hydroxybenzoic acid with CDs possessing covalently linked alkyl chains. The cooperative binding was attributed to the micellization of the hosts because the inclusion of a guest resulted in the displacement of the self-included alkyl chain from the CD interior. Self-inclusion of alkyl chains appended to the CD annulus was also reported by Bellanger and Perly.[143] Tabushi[144] argued that cooperative binding occurred in modified CD-guest-transition metal ion ternary complexes because of allosterism due to various electrostatic, van der Waals, and dipolar interactions.

The importance of allosteric effects in apolar CD-guest complexes is unlikely because of the limited conformational motility of CDs, as compared to biomolecules. However, solvent reorganization processes that accompany complex formation can provide the driving force for cooperative binding in CD-guest complexes.[33,145] The involvement of multiple binding sites in cooperative binding processes is consistent with the numerous water molecules that form H-bonds during complex formation [141] and the cooperative H-bonding of water (cf. §1.2.1).

The close connection between solute-solute, solute-water, and water-water interactions in aqueous solution is evident according to the individual contributions to the Gibbs energy of complex formation (ΔG_{comp}) for a host-guest complex

$$\Delta G_{comp} = \Delta G_{w\text{-}w} + \Delta G_{h\text{-}g} + \Delta G_h + \Delta G_g \qquad (1.4.2\text{-}2)$$

where the subscripts w, g, h represent water, guest, and host, respectively. Each Gibbs energy term in eq 1.4.2-2 is affected by hydration due to the extensive solvent reorganization processes that accompany complex formation. Hence, an increase in binding and cooperative behavior in host-guest complexes are explicable in terms of the strong coupling between solute-solute interactions and hydration effects. Theoretical support for the coupling between states due to hydration effects has been argued by Smith and van Gunsteren.[145]

The importance of solvent-solvent interactions as a driving force in host-guest binding processes is based on a linear relationship between enthalpy and entropy, denoted as the "compensation effect" or "isoequilibrium effect". The compensation effect occurs in numerous CD-guest complexes of widely varying chemical structure and provides strong empirical support for this phenomena[1,17,146] There is also ample theoretical support which indicates that the compensation effect is related to solvent reorganization processes. Grunwald *et al.*[147] conducted a dissection of various thermodynamic properties in an attempt to separate out the solute-solvent interaction term from the intrinsic term due to the solute. The theory is a reformulation of thermodynamic properties into intrinsic and interaction terms. In cases where significant changes in a solvent property are accompanied by large changes in enthalpy and entropy, the

interaction terms are large and compensation behavior is predicted. A similar treatment has been presented by Ben Naim.[148] Lumry *et al.*[149] have proposed a closely related interpretation of the compensation effect where the thermodynamics of any process consist of two contributions; a motive (m) and a compensative (com) factor.

$$\Delta H^\circ = \Delta H_m^\circ + \Delta H_{com}^\circ \qquad (1.4.2\text{-}3)$$

$$\Delta S^\circ = \Delta S_m^\circ + \Delta S_{com}^\circ \qquad (1.4.2\text{-}4)$$

$$\Delta G^\circ = \Delta H_m^\circ - T\,\Delta S_m^\circ \qquad (1.4.2\text{-}5)$$

Because of compensation, only the motive parts contribute to the overall free energy of the process. If the quantities ΔH_{com}° and ΔS_{com}° are large, they can be related to the heat capacity changes of the solvent. The formation of CD-inclusate complexes[150] is accompanied by large changes in heat capacity, therefore, enthalpy and entropy are compensated.

According to the Scaled Particle Theory[151] (SPT), the Gibbs energy of transfer (ΔG_{tr}^o) of an apolar solute from the gas phase to a liquid solvent consist of two parts

$$\Delta G_{tr}^o = G_c + G_a \qquad (1.4.2\text{-}6)$$

where G_c is the work required to form a cavity and G_a is the energy released by attractive forces between the solute and solvent. This theory has been criticized because it does not account for the structural characteristics of water, as in the case of the mixture models. In aqueous solutions, G_c is appreciable and can be related to the physicochemical properties of water (cf. eq 1.2.1-1). Sinanoglu[38] has related the enthalpy of complex formation

(ΔH_{comp}) to the work required to make a cavity in solution. The enthalpy term originates from the coalescence of the two solute cavities

$$\Delta H_{comp} = 0.43\ \gamma_w\ A\ T^{-1} - 1.36\ M\ d_o \qquad (1.4.2\text{-}7)$$

where γ_w is the surface tension of water (cf. eq 1.2.2-3), M is the number of solvent molecules per kg of solvent, A is the apolar surface area of the host and guest, and d_o is the density of the solvent.

Connors[17] has introduced a phenomenological model to account for the overall Gibbs energy of complex formation (ΔG_{comp}) which has been applied with some success to α-CD-guest complexes.

$$\Delta G_{comp} = \Delta G^{c}_{intrasol} + (\Delta G^{C}_{w} - \Delta G^{S}_{w} - \Delta G^{L}_{w}) + g\Delta A\gamma_w \qquad (1.4.2\text{-}8)$$

where the superscripts C, S, and L represent the complex, substrate and ligand, respectively, and the subscript w denotes water as a solvent. $\Delta G^{c}_{intrasol}$ describes the substrate-ligand interaction whereas the term in brackets is the overall change in the Gibbs energy of hydration. The term, $g\Delta A\gamma_w$, describes a general medium effect, where g is an empirical term accounting for the curvature of the surface, γ_w is the surface tension of the solvent, and ΔA is the change in apolar surface areas of the ligand and substrate. Solvent effects contribute substantially to the latter terms when apolar host-guest binding occurs. Ravey and Stébé have recently predicted the relative hydrophobicity of fluorocarbon and hydrocarbon compounds based on molecular volumes.[152] Hence, cavity models provide a relatively simple interpretation of hydration phenomena. The extent to which the concept of solvent structuring can be inferred as a driving force, as in the case

of the "iceberg" model, should depend on direct structural evidence, such as that adduced from spectroscopy and neutron diffraction studies.[36]

Molecular modeling of host-guest interactions *in vacuo* is of limited value because of the fact that the solvent plays an integral role in complex stability, as indicated above. In cases where an account of the solvent is made, the dielectric constant of the medium is adjusted. However, this type of theoretical treatment of the solvent is too simplified to use for aqueous solutions given the unique properties of water (cf. § 1.2.1).

1.4.3 Concluding remarks

Recent advances in mass spectrometry[153] have enabled the measurement of molecular ions consisting of intact host-guest complexes. A detailed analysis of the fragmentation patterns of these ions may enable the dissection of the overall energetics of the inclusion process into solute-solute, solvent-solvent, and solute-solvent contributions. As well, thermodynamic binding studies in aqueous solution and in the gas phase may provide similar information. The development of sophisticated multi-pulse NMR experiments are anticipated to yield accurate structural information about the host-guest topology, e.g., the elucidation of intermolecular distances between binding partners and solvent. Neutron diffraction studies have improved our understanding of solvent structural changes in the presence and absence of various additives. Computer simulations of macromolecule-substrate interactions are powerful tools that can provide information which is generally inaccessible by experiment and may furnish a better understanding of the nature of the intermolecular interactions in these processes.[154] Relatively few modeling studies

have incorporated solvent effects in host-guest interactions. However, recent advances have enabled the simulation of hydration phenomena.[34,155] Computer simulations of the formation of host-guest complexes may provide new insight into the relative importance of solute-solute, solute-solvent, and solvent-solvent interactions particularly where they are employed in conjunction with experimental work.[156] Ultimately, a better description of the molecular level events that occur during the formation of CD-inclusate complexes can be achieved.

The potential licensing of CDs as pharmaceutical excipients represents an important area of research due to the development of chemically modified CDs with suitable physicochemical properties. The synthesis of functionalized CDs with pendant groups such as oligosaccarides, amino acids, alkyl groups, etc., may yield agents that possess favorable controlled-release properties and specific targeting of cellular receptor sites.[103,157] Consequently, the increasing use of CDs and their potential application in other fields requires a better understanding of their complexation behavior in solution and in the solid state. The results of systematic studies, such as those presented herein, should contribute to the design of better CD hosts for a particular application and the ability to establish criteria that relate complex stability with structural features of the guest and host. Ultimately, a better understanding of the factors affecting complex stability will lead to the prediction of binding constants for a given host-guest complex from first principles.

2. THEORETICAL BACKGROUND

2.1 Evaluation of binding constants

In Chapter 1, the reliability of host-guest binding constants was assessed in terms of a number of factors (cf. § 1.4.1). This chapter outlines the model equations utilized to describe the host-guest stoichiometry and the nonlinear fitting procedure used to simulate experimental data, two of these important factors.

2.1.1 Models and equations

A model that suitably describes the formation of a host-guest complex must accurately account for all stoichiometric complexes formed.[59] Scheme 2-1 illustrates the complexes that were considered in this work. The host-guest stoichiometry was determined by the method of continuous variations or the mole ratio technique (cf. § 1.3.2.1).[59]

a) $CD + S \overset{K_{1:1}}{\rightleftharpoons} CD\text{-}S$

b) $CD\text{-}S + S \overset{K_{1:2}}{\rightleftharpoons} CD\text{-}S_2$

c) $CD\text{-}S + CD \overset{K_{2:1}}{\rightleftharpoons} CD_2\text{-}S$

Scheme 2-1: Equilibria for the stepwise formation of various types of cyclodextrin-surfactant complexes; where S=surfactant and CD=cyclodextrin. a) 1:1 CD-S complex, b) 1:2 CD-S complex, and c) 2:1 CD-S complex.

According to Scheme 2-1, the formation of higher order 1:2 and 2:1 host-guest complexes occur in a stepwise fashion commencing with a 1:1 complex. The overall

equilibrium expression for the formation of 1:2 and 2:1 host-guest complexes is presented in Scheme 1-3 (cf. § 1.3.2.1).

The mass-action and equilibrium relations for a 1:1 complex (Scheme 2-1a) is described below

$$K_{1:1} = [CD\text{-}S]/[CD][S] \qquad (2.1.1\text{-}1)$$

$$[CD]_o = [CD] + [CD\text{-}S] \qquad (2.1.1\text{-}2)$$

$$[S]_o = [S] + [CD\text{-}S] \qquad (2.1.1\text{-}3)$$

where the brackets denote molar concentrations and the subscript "o" represents the analytical concentration. Eq. 2.1.1-1 may be rewritten in terms of $[CD]_o$, [CD-S], and $[S]_o$

$$K_{1:1} = \frac{[CD-S]}{([CD]_o - [CD-S])([S]_o - [CD-S])} \qquad (2.1.1\text{-}4)$$

Rearrangement of eq 2.1.1-4 yields a quadratic expression of the general form

$$Ay^2 + By + C = 0 \qquad (2.1.1\text{-}5)$$

where y=[CD-S] and A, B, and C are the coefficients. Upon substitution of $[S]_o$, and $[CD]_o$ and an appropriate estimate for $K_{1:1}$, the real value of y was obtained from the negative root of the quadratic equation.[158]

$$y = \frac{1}{2A}\left(-B - \sqrt{B^2 - 4AC}\right) \qquad (2.1.1\text{-}6)$$

Values for [S] and [CD] were obtained from equations 2.1.1-2 and -3.

The mass-action and equilibrium relations for the formation of 1:1 and 1:2 complexes (Scheme 2-1a and b) are described below

$$K_{1:2} = [CD\text{-}S_2]/[CD\text{-}S][S] \qquad (2.1.1\text{-}7)$$

$$[CD]_o = [CD] + [CD\text{-}S] + [CD\text{-}S_2] \quad (2.1.1\text{-}8)$$

$$[S]_o = [S] + [CD\text{-}S] + 2[CD\text{-}S_2] \quad (2.1.1\text{-}9)$$

Equations 2.1.1-1, -7, -8 and -9 yield the following expression for [CD]

$$[CD] = \frac{([CD]_o - [S]_o + [S])}{(1 - K_{1:1}K_{1:2}[S]^2)} \quad (2.1.1\text{-}10)$$

Rearrangement and algebraic manipulation of eq 2.1.1-8 yields a cubic expression in terms of [S]

$$\begin{aligned} &K_{1:1}K_{1:2}[S]^3 + (2K_{1:1}K_{1:2} + K_{1:1} - K_{1:1}K_{1:2}[S]_o)[S]^2 \\ &+(1 + K_{1:1}[CD]_o - K_{1:1}[S]_o)[S] - [S]_o = 0 \end{aligned} \quad (2.1.1\text{-}11)$$

Upon substitution of $[S]_o$, and $[CD]_o$ and an appropriate estimate of $K_{1:1}$ and $K_{1:2}$, the real cubic root of eq 2.1.1-11 was obtained using the Newton-Raphson method.[158,159] Substitution of [S] into equations 2.1.1-8, -9, and -10 yielded [CD], $[CD\text{-}S_2]$, and [CD-S], respectively.

The mass-action and equilibrium relations for the formation of 1:1 and 2:1 complexes (Scheme 2-1a and c) are described below

$$K_{2:1} = [CD_2\text{-}S]/[CD\text{-}S][CD] \quad (2.1.1\text{-}12)$$

$$[CD]_o = [CD] + [CD\text{-}S] + 2[CD_2\text{-}S] \quad (2.1.1\text{-}13)$$

$$[S]_o = [S] + [CD\text{-}S] + [CD_2\text{-}S] \quad (2.1.1\text{-}14)$$

The following expression for [S] is obtained from equations 2.1.1-1, -12, -13, and -14

$$[S] = \frac{([CD]_o - [S]_o - [CD])}{(K_{1:1}K_{1:2}[CD]^2 - 1)} \quad (2.1.1\text{-}15)$$

Rearrangement and algebraic manipulation of eq 2.1.1-13 yields a cubic expression in terms of [CD]

$$-K_{1:1}K_{2:1}[CD]^3 + (K_{1:1}K_{1:2}[CD]_o - 2K_{1:1}K_{1:2}[S]_o - K_{1:1})[CD]^2 + (K_{1:1}[CD]_o - K_{1:1}[S]_o - 1)[CD] + [CD]_o = 0 \quad (2.1.1\text{-}16)$$

Upon substitution of $[S]_o$, and $[CD]_o$ and appropriate estimates of $K_{1:1}$ and $K_{2:1}$, the real cubic root of eq 2.1.1-16 was obtained using the Newton-Raphson method.[158,159] Substitution of [CD] into equations 2.1.1-13, -14, and -15 yielded estimates of [CD], [CD_2-S], and [CD-S], respectively.

2.1.2 Evaluation of binding constants from NMR chemical shifts

The NMR chemical shift (δ) of a nucleus is strongly dependent on the shielding constant which is very sensitive to medium effects.[160,161] Chemical shifts are also dependent on the conformation of molecules, as shown by variations in nuclear shielding of different conformational isomers. This is understood in terms of the changes in internuclear distances through changes in bond angles and torsional angles.[162] The different chemical shifts of axial and equatorial protons in a glucopyranose ring illustrate the dependence of conformation on chemical shift. Accordingly, the total shielding constant (σ_{Total}) of a nucleus can be expressed as follows

$$\sigma_{Total} = \sigma_{nucleus} + \sigma_{medium} \quad (2.1.2\text{-}1)$$

where $\sigma_{nucleus}$ is the intrinsic shielding constant of an isolated atom in a molecule and σ_{medium} is that due to the surrounding medium. The latter term is divisible into five intra- and internuclear contributions as follows

$$\sigma_{medium} = \sigma_a + \sigma_b + \sigma_w + \sigma_e + \sigma_c \quad (2.1.2\text{-}2)$$

where the terms σ_a and σ_b are related to the magnetic susceptibility of the immediate solvation sphere and bulk solvent, respectively; σ_w, σ_e, and σ_c are due to van der Waals, electric field, and complexation interactions between the nucleus and the surrounding medium, respectively. In principle, one can obtain "estimates" of σ_c by rearrangement of eq 2.1.2-2 as shown below

$$\sigma_c = \sigma_{medium} - (\sigma_a + \sigma_b + \sigma_w + \sigma_e) \quad (2.1.2\text{-}3)$$

Although the isolation of σ_c is theoretically feasible, the unequivocal assignment of experimental chemical shift changes to σ_c is complicated because of the numerous contributions to σ_{medium}. Quantitative interpretation of chemical shifts requires explicit calculations of parameters, such as anisotropy and field effects. The computation of these parameters is often accomplished with rigid guests, such as steroids, and becomes more complicated in the case of nonrigid molecules, such as aliphatic guests.[102] As well, changes in the chemical shift of macromolecules involved in complex formation requires some speculation because of the many types of solute-solute and solute-solvent interactions that occur between the host, guest, and solvent. NMR chemical shifts are a type *i)* technique (cf. § 1.4.1) since δ is a physical property proportional to some aspect of the complexation process. Consequently, the observed chemical shifts of host and guest nuclei that form complexes, as shown in Scheme 2-1, can be weighted according to their mass-balance contributions, as described below

$$\delta_{obs} = X_f \delta_f + X_{1:1}\delta_{1:1} \quad (2.1.2\text{-}4)$$

$$\delta_{obs} = X_f \delta_f + X_{1:1}\delta_{1:1} + X_{2:1}\delta_{2:1} \quad (2.1.2\text{-}5)$$

$$\delta_{obs} = X_f \delta_f + X_{1:1}\delta_{1:1} + X_{1:2}\delta_{1:2} \qquad (2.1.2\text{-}6)$$

where X_f, $X_{1:1}$, $X_{2:1}$, and $X_{1:2}$ are the mole fractions (X_i) of the unbound component (S or CD), 1:1 complex, 2:1 complex, and 1:2 complex, respectively, and δ_f, $\delta_{1:1}$, $\delta_{2:1}$, and $\delta_{1:2}$ are the chemical shift (δ_i) values of the unbound species, 1:1 complex, 2:1 complex, and 1:2 CD-S complex, respectively. The observed chemical shift (δ_{obs}) signal is an average value comprised of bound and unbound species, due to fast exchange on the NMR time-scale. The above models are referred to as the two- (eq 2.1.2-4) or three-site (eq 2.1.2-5 and -6) models according to the sum of the bound and unbound components in the expression. The nuclei of the host or guest are amenable to modeling by using equations that account for the NMR chemical shift contributions of different complexes. The binding constants (K_i) can be related to the mole fractions (X_i) by application of eq 1.3.2.1-1. Brereton *et al.*[163] have modeled ^{19}F NMR chemical shift data of host-guest complexes using expressions similar to the two- and three-site models described above.

2.1.3 Evaluation of binding constants from apparent molar volumes

Apparent molar volumes are a useful property for assessing the role of solute-solute(s-s), solute-water(s-w), and water-water(w-w) interactions in aqueous solutions.[33,164] In addition, volume properties are relatively easy to comprehend and can be obtained with a relatively good degree of accuracy.

The partial molar volume of a solute ($\overline{V}_2$) is the change in volume at the specified composition, temperature and pressure when one mole of component 2 is added to a sufficiently large amount of solution such that the addition does not appreciably alter the

concentration.[33] Mathematically, $\overline{V}_2$ is represented as the partial derivative of the total volume (V) with respect to the number of moles of solute at constant T, P, and moles of solvent (n_1).

$$\overline{V}_2 = \left(\frac{\partial V}{\partial n_2}\right)_{T,P,n_1} \qquad (2.1.3\text{-}1)$$

According to Euler's theorem, it can be shown that

$$V = n_1 \overline{V}_1 + n_2 \overline{V}_2 + \ldots \qquad (2.1.3\text{-}2)$$

Although $\overline{V}_2$ can be obtained from density measurements, the apparent molar volume (AMV) of the solute is a more convenient property to measure

$$V_{\phi,2} = \frac{V - n_1 V_1^\circ}{n_2} \qquad (2.1.3\text{-}3)$$

where $V_{\phi,2}$ is the AMV of the solute in a solution containing n_1 moles of solvent and n_2 moles of solute[33] and V_1° is the molar volume of the pure solvent. The difference between $V_{\phi,2}$ and $\overline{V}_2$ is expressed by the following relation

$$\overline{V}_2 = \left(\frac{\partial V}{\partial n_2}\right)_{T,P,n_1} = V_{\phi,2} + n_2\left(\frac{\partial V_{\phi,2}}{\partial n_2}\right)_{T,P,n_1} \qquad (2.1.3\text{-}4)$$

At infinite dilution, $\overline{V}_2^\circ \equiv V_{\phi,2}^\circ$. In terms of the molal concentration scale (m=mol kg^{-1}), n_2 is the number of moles of solute in 1 kg of solvent (n_2=m). On this basis, the AMV of the solute is defined as

$$V_{\phi,2} = \frac{1000(d_o - d)}{m d d_o} + \frac{M_2}{d} \qquad (2.1.3\text{-}5)$$

where d and d_o are the density of the solution and solvent, respectively, and M_2 is the relative molar mass of the solute.

Errors in the value of $V_{\phi,2}$ can arise from three sources; probable errors in concentration (Δm), solution density (Δd), and solvent density (Δd_o). Differentiation of eq 2.1.3-5 with respect to m, d, or d_o yields the probable error in the AMV (ΔV_ϕ) with respect to that parameter, as shown below

$$\Delta V_\phi = 1000\left(\frac{d_o + d}{dd_o}\right)\frac{2\Delta m}{m^2} \qquad (2.1.3\text{-}6)$$

$$\Delta V_\phi = \left(\frac{1000}{m} + M_2\right)\frac{2\Delta d}{d^2} \qquad (2.1.3\text{-}7)$$

$$\Delta V_\phi = \left(\frac{1000}{m}\right)\frac{2\Delta d_o}{d_o^2} \qquad (2.1.3\text{-}8)$$

In pure solvents, the contribution to ΔV_ϕ from d_o is usually insignificant, whereas the error in ternary solutions is greater since the solvent is a binary mixture and d_o is a measured quantity. The probable error in d, d_o, and m are based on the estimated standard deviation of their measured values.[165]

At infinite dilution, the AMV of a solute consists of four contributions[166]

$$V_\phi^\circ = V_m + V_V + V_I + \beta RT \qquad (2.1.3\text{-}9)$$

where V_m is the intrinsic molar volume of the solute, V_v is the void volume adjacent to the surface of the solute in solution, V_I is the interaction volume between the solute and solvent. βRT is the ideal component of the AMV resulting from the motion of the molecule along the translational degrees of freedom and β is the isothermal compressibility of the solvent. The magnitude of βRT ($\approx$1.1 cm^3mol^{-1}) is usually

negligible. The term V_I is related to changes in the solvation and molecular environment of the solute. In cases where the formation of a complex occurs with changes in the AMV of the bound and unbound species, the host-guest binding constant can be evaluated from this data. Apparent molar volume properties are considered as a type *i)* technique because changes in the AMV relate to the term V_I and are anticipated to be proportional to the formation of complexes.

The participation of chemical species in equilibria, such as ionization and complex formation, requires the use of mass-balance and equilibrium relationships to relate the total AMV of a solute in terms of the respective volumetric contributions.[33] The AMV of CD-surfactant complexes depicted in Scheme 2-1 can be analyzed in terms of the volumetric contributions of bound and unbound species according to Young's rule[167]

$$V_\phi = X_f V_{\phi,f} + X_{1:1} V_{\phi,1:1} \qquad (2.1.3\text{-}10)$$

$$V_\phi = X_f V_{\phi,f} + X_{1:1} V_{\phi,1:1} + X_{2:1} V_{\phi,2:1} \qquad (2.1.3\text{-}11)$$

$$V_\phi = X_f V_{\phi,f} + X_{1:1} V_{\phi,1:1} + X_{1:2} V_{\phi,1:2} \qquad (2.1.3\text{-}12)$$

where X_f, $X_{1:1}$, $X_{2:1}$, and $X_{1:2}$ are the mole fractions of the unbound component (S or CD), 1:1 complex, 2:1 complex, and 1:2 complex, respectively, and $V_{\phi,f}$, $V_{\phi,1:1}$, $V_{\phi,2:1}$, and $V_{\phi,1:2}$ are the AMV of the unbound component (S or CD), 1:1 complex, 2:1 complex, and 1:2 complex, respectively. The mole fractions (X_i) of the bound and unbound species can be related to the equilibrium binding constant(s) (K_i) (cf. § 2.1.1). Young's rule is valid near infinite dilution where the solute-water interactions dominate and higher order solute-solute interactions can be neglected To a first approximation, this condition is met in the present

study. The equations describing the AMV of host-guest complexes are referred to as two- or three-site models according to the sum of bound and unbound species in the expression. Høiland *et al.* have analyzed the volumetric data of crown ether-cation complexes using expressions similar to the two- and three-site models presented above.[168]

In ternary solutions, the transfer volume (ΔV) of a solute (component 3) is an important quantity since it is proportional to the formation of complexes

$$\Delta V_3\,(1 \rightarrow 1+2) = V_{\phi,3}\,(1+2) - V_{\phi,3}\,(1) \qquad (2.1.3\text{-}13)$$

where $V_{\phi,3}$ (1+2) and $V_{\phi,3}$ (1) are the AMV of the solute in the mixed binary solvent system (1+2) and the pure solvent (1), respectively. The transfer volume of the host and/or guest molecules from water to solutions containing host-guest complexes provides useful information about the changes in solvation and molecular environment of the host and guest molecules.

2.1.4 Evaluation of binding constants from spectrophotometry

Type *ii)* techniques are divided into direct and indirect methods (cf. § 1.4.1). The spectral displacement technique[26] is an indirect method and Scheme 2-2 illustrates the competitive binding equilibria.

$$\beta\text{-CD-phth} \underset{\text{phth}}{\overset{K_{CD\text{-}P}}{\rightleftharpoons}} \beta\text{-CD} \underset{\text{inclusate}}{\overset{K_{1:1}}{\rightleftharpoons}} \beta\text{-CD-inclusate}$$

Scheme 2-2: Competitive equilibria involved in the spectral displacement technique which utilizes phenolphthalein (phth) as a probe; β-CD=β-cyclodextrin, S=surfactant, and $K_{1:1}$ and $K_{CD\text{-}P}$ are the 1:1 equilibrium binding constants.

The binding of optically transparent compounds to CD can be followed by measuring absorbance changes of a chromophore like phenolphthalein (phth) in the presence of CD and a competing nonchromophoric surfactant (S). Two essential conditions must be met in order to obtain valid estimates of $K_{1:1}$: *i)* competing ligands must not absorb in the wavelength region of interest or interact with the chromophore and *ii)* inclusates must bind exclusively in a 1:1 stoichiometry.

The 1:1 equilibrium binding constants for the CD-S ($K_{1:1}$) and CD-phth ($K_{CD\text{-}P}$) complexes are defined below

$$K_{1:1} = [CD\text{-}S]/[CD]\,[S] \qquad (2.1.4\text{-}1)$$

$$K_{CD\text{-}P} = [CD\text{-phth}]/[CD]\,[phth] \qquad (2.1.4\text{-}2)$$

The spectral displacement technique provides accurate estimates of $K_{1:1}$ because of the large difference in molar absorptivity of the bound and unbound chromophore.

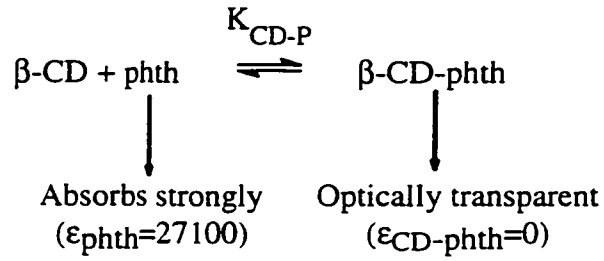

Scheme 2-3: Optical properties of phenolphthalein (phth) in the bound and unbound states at 550 nm where the units of ε are L mol^{-1} cm^{-1}.

In the bound state, the absorbance of the CD-phth complex is zero ($\varepsilon_{CD\text{-}phth}=0$) whereas the absorbance is large for unbound phth. The displacement of phth from the CD cavity by a competitive guest results in an increase in absorbance due to an increasing amount of

unbound phth. The concentration of the unbound phth ([phth]) can be related to its absorbance through the Beer-Lambert law

$$A = \varepsilon_{phth}\, \ell\, c \qquad (2.1.4\text{-}3)$$

where A is the absorbance, ε_{phth} is the molar absorptivity of unbound phth ($Lmol^{-1}cm^{-1}$), ℓ is the path length (cm), and c is the molar concentration of phth (mol L^{-1}). In the case of competitive binding (cf. Scheme 2-2), the absorbance of phth provides an indirect measure of the concentrations of unbound inclusates.

The following equilibrium and mass-balance relations apply to the competitive equilibrium outlined in Scheme 2-2.

$$[S]_o = [S] + [CD\text{-}S] = [S](1+K_{1:1}[CD]) \qquad (2.1.4\text{-}4)$$

$$[phth]_o = [phth] + [CD\text{-}phth] = [phth](1+K_{CD\text{-}P}[CD]) \qquad (2.1.4\text{-}5)$$

$$[CD]_o = [CD] + [CD\text{-}S] + [CD\text{-}phth] \qquad (2.1.4\text{-}6)$$

[CD-S] and [CD-phth] are related to $[S]_o$, $[phth]_o$, $K_{1:1}$, and $K_{CD\text{-}P}$ as follows

$$[CD-S] = [S]_o\left(1+\frac{1}{K_{1:1}[CD]}\right)^{-1} \qquad (2.1.4\text{-}7)$$

$$[CD-phth] = [phth]_o\left(1+\frac{1}{K_{CD-P}[CD]}\right)^{-1} \qquad (2.1.4\text{-}8)$$

Upon substitution into and algebraic manipulation of eq 2.1.4-6, the following cubic expression in terms of [CD] is obtained

$$[CD]^3 + [CD]^2\left(\frac{K_{1:1}+K_{CD-P}}{K_{1:1}K_{CD-P}} + [phth]_o + [S]_o - [CD]_o\right) + [CD]\left(\frac{1}{K_{1:1}K_{CD-P}} + \frac{[S]_o}{K_{CD-P}} + \frac{[phth]_o}{K_{1:1}} - \frac{[CD]_o}{K_{CD-P}} - \frac{[CD]_o}{K_{1:1}}\right) - \left(\frac{[CD]_o}{K_{1:1}K_{CD-P}}\right) = 0 \qquad (2.1.4\text{-}9)$$

The real solution to the cubic root of eq 2.1.4-9 was obtained by application of the Newton-Raphson method[158,159] using appropriate values of $[S]_o$, $[phth]_o$, $K_{1:1}$, and K_{CD-P}. Values for [CD-S], [CD-phth] and [phth] were obtained using eqs 2.1.4-3 to 2.1.4-6.

2.1.5 Evaluation of stoichiometry from conductometry

The specific conductance property is considered as a type *i)* technique and the method of data treatment is analogous to that for chemical shifts (§ 2.1.2) and apparent molar volumes (§ 2.1.3). As mentioned in chapter 1, the use of conductance for the determination of binding constants of CD-inclusate complexes has been criticized on the basis of its relative insensitivity.[117] This problem is exemplified by the small differences in specific conductivity between the unbound surfactant and that which is complexed with CD.

The specific conductance of a solution containing both surfactant and CD can be related to the individual ionic molar conductivity, λ_i, and concentration of each component

$$\kappa_1 = \lambda_{Na^+}.[Na^+] + \lambda_{S^-}[S^-] + \lambda_{CD-S^-}[CD\text{-}S^-] \qquad (2.1.5\text{-}1)$$

$$\kappa_2 = \lambda_{Na^+}.[Na^+] + \lambda_{S^-}[S^-] + \lambda_{CD-S^-}[CD\text{-}S^-] + \lambda_{CD_2-S^-}[CD_2\text{-}S^-] \qquad (2.1.5\text{-}2)$$

$$\kappa_3 = \lambda_{Na^+}.[Na^+] + \lambda_{S^-}[S^-] + \lambda_{CD-S^-}[CD\text{-}S^-] + \lambda_{CD-S_2^{-2}}[CD\text{-}S_2^-] \qquad (2.1.5\text{-}3)$$

where κ_1, κ_2, and κ_3 represent the specific conductance of solutions containing various types of complexes, as depicted in Scheme 2-1. In eqs. 2.1.5-1 to -3, it is assumed that the contribution due to complexes with associated sodium counterions is negligible.

Conductometry was not utilized in this work to obtain binding constants because such studies have been reported previously,[112] and also because of the problems associated with insensitivity, as outlined above. Instead, specific conductance measurements have been used to corroborate the host-guest stoichiometry for certain host-guest complexes. It is anticipated that changes in κ_i may occur because of possible differences in the individual ionic molar conductivities of the surfactant in the various complexes(λ_{CD-S^-} , $\lambda_{CD_2-S^-}$, and $\lambda_{CD-S_2^{-2}}$).

2.1.6 Data Analysis and Modeling

Traditionally, linear fitting methods have been employed to obtain estimates of binding constants of CD-inclusate complexes. The Benesi-Hildebrand technique[108] is commonly used. However, the reliability of the binding constants using this method has been questioned because the assumptions employed are not always satisfied under ordinary conditions. Also, the requirement that the host or guest are in excess of one another involves restrictive experimental conditions. These difficulties are effectively overcome by using nonlinear least squares (NLLS) fitting procedures.[105,169]

Consider a single nonlinear equation of the general form

$$P_{calc,i} = F(x_j, b_1, b_2, ..., b_k) \qquad (2.1.6\text{-}1)$$

where x_j is the independent variable, b_1, b_2, ..., b_k are the unknown parameters, and $P_{calc,i}$ is the calculated physical property. The major premise in NLLS fitting methods is that the best estimates of the unknown parameters (b_1, b_2, ..., b_k) are obtained through a

minimization of the sum of squares of residuals (SSR) with respect to these parameters. The SSR is defined as

$$SSR = \sum_i \left(P_{expt,i} - P_{calc,i}\right)^2 \qquad (2.1.6\text{-}2)$$

where P_{expt} and P_{calc} are the experimental and calculated physical properties, respectively. In this work, the minimization of the SSR was accomplished by using the Marquardt-Levenberg algorithm.[170]

Wyman[171] has shown that a macroscopic thermodynamic property can be related to the properties of the individual components of the system that are linked by coupled equilibria (cf. Scheme 2-1). In this treatment, the calculated physical property (P_{calc}) is given as

$$P_{calc} = X_f P_f + \sum_i X_i P_i \qquad (2.1.6\text{-}3)$$

where X_f and X_i are the mole fractions and P_f and P_i are the physical properties of the free (f) and bound species (i) where i=1:1, 1:2, and 2:1 complexes. Equation 2.1.6-3 is a general form of the models used to simulate experimental physical properties (δ or V_ϕ) of the host and guest for type *i)* methods. The mole fractions (X_f and X_i) can be recast in terms of the binding constants (K_i) of the relevant equilibria (cf. § 2.1.1). Hence, the quantities K_i and P_i are the unknown parameters analogous to b_1, b_2, ..., b_k in eq 2.1.6-1. P_f is usually obtained from independent measurements of the solute (guest or host) in the solvent in the absence of the second component (host or guest). The best fit estimates of these parameters were obtained using a NLLS fitting procedure with commercially available software[172] employing a Marquardt-Levenberg algorithm. In cases where higher order complexes are formed, such as 1:2 or 2:1, the three-site models (cf. § 2.1.3

and § 2.1.2) were required and the Newton-Raphson[158,159] method was used to solve for the concentration of unbound host or guest ([CD] or [S]). Estimates of the errors in K_i and P_i are based on the standard error (SE) of the calculated and experimental physical properties.

The simulation of absorbance data in the spectral displacement technique was accomplished using eqs 2.1.4-3 to -6, and -9. The estimation of $K_{CD\text{-}P}$ involved the simulation of changes in absorbance of phth as the concentration of β-CD increases. The estimation of $K_{1:1}$ involved the simulation of absorbance of phth versus $[S]_o$ for fixed values of $[CD]_o$ and $[phth]_o$. NLLS fitting of phth absorbance versus $[CD]_o$ and phth absorbance versus $[S]_o$ at a fixed value of $[CD]_o$ provided values of $K_{CD\text{-}P}$ and $K_{1:1}$, respectively. Errors in $K_{1:1}$ and $K_{CD\text{-}P}$ are based on the standard deviation in the value of $K_{CD\text{-}P}$.

In all cases, as the solutions studied here were considered dilute, the activity coefficients were taken as unity. In NMR studies, solutions were prepared on a weight or volume basis and the reported binding constants are given in molar concentration units because there was no significant difference with respect to molal concentration units. In apparent molar volume studies, molal concentrations were used throughout and these units have been reported for the calculated binding constants.

3. EXPERIMENTAL METHODS

3.1 Materials

The relevant physical and analytical data for the CD compounds are given in Table 3-1. The cyclodextrin compounds were used as received and their water content was determined using a Karl Fischer titration procedure.[165] This water was included in the calculation of aqueous concentrations.

Table 3-1: Analytical Data for the Cyclodextrin (CD) Compounds Used in this Study.

Cyclodextrin CD	Water Content(%)	Relative MW(g/mol)	Site of Alkyl Substitution	Degree of Substitution	Source
β-CD	12.2 ± 0.1	1135.01	N/A	N/A	Aldrich
RAMEB[(a)]	1.3 ± 0.1	1317	2, 3, or 6	12-13	Am. Maize
DM-β-CD[(b)]	0.6 ± 0.1	1331	2,6[(e)]	14-15	Cyclolab
TM-β-CD[(c)]	0.5 ± 0.1	1429.6	2, 3, 6[(f)]	21	Am. Maize
HP-β-CD[(d)]	3.9 ± 0.1	1384	6[(g)]	4.6	Cyclolab
α-CD	10.0± 0.1	972.86	N/A	N/A	Aldrich

(a) RAMEB=randomly methylated at the 2, 3, and 6 positions, (b) DM=2,6-di-O-methyl, (c) TM=2, 3, 6-tri-O-trimethyl-, (d) HP=6-O-(2-hydroxypropyl)-, (e) purity > 70% as 2,6-regioisomer, (f) purity ~ 95%, (g) purity ~ 95%.

Perfluorocarboxylic acids ($C_xF_{2x+1}COOH$, x=1,3,4,6-9) (Fluorochem and PCR Inc., >99%) were converted to the sodium salts by titration with an equimolar quantity of NaOH (BDH, 99%). The fc alkyl carboxylate salts were recrystallized several times from methanol/chloroform mixtures.[173,174] The majority of hydrocarbon surfactants [$C_xH_{2x+1}CO_2Na$, x=2,5,7,9-13] were obtained as sodium salts from Sigma (99%) except for the propanoic (Fisher, 99%), heptanoic (Sigma, 98%) and nonanoic (BDH, 99%)

compounds which were prepared by converting the acids by titration with an equimolar quantity of NaOH (BDH, 99%). The alkyl carboxylate salts were recrystallized from acetone/methanol mixtures and washed in a Soxhlet extractor with acetone. All sodium salts were dried to constant weight in a vacuum at 50°C.

Phenolphthalein (Aldrich, 99%) was recrystallized from an ethanol/water mixture but no difference between the molar extinction coefficient of the purified and unpurified material was observed. External references for chemical shift measurements, 4,4-dimethyl 4-silapentane sodium sulphonate (Aldrich, 99%) or trifluoroacetic acid (Alfa, 99%) were used as received. The solvent systems for ^{19}F and ^{1}H NMR studies were 50%(w/w) D_2O/H_2O and D_2O (Aldrich, 99.9%), respectively. The p(H+D) of solutions for NMR studies was adjusted between 9-10 with (30%w/w) NaOD(Aldrich, 99.9%) and the pH of solutions for spectrophotometric measurements was buffered at pH 10.5 using 0.1 M Na_2CO_3(BDH, 99%). The water used to make solutions was obtained from a Millipore-Super-Q system and the solution pH was adjusted to 10.5 with NaOH to minimize protonation of the carboxylate anion and dissociation of the β-CD hydroxyl protons($pK_a \approx 12$)[9] and to maintain similar pH conditions as the spectral displacement studies.

3.2 Methods

3.2.1 Measurement of chemical shifts

^{1}H and ^{19}F NMR measurements were recorded on a Bruker AM-300 NMR spectrometer at 300 MHz or 282.4 MHz, respectively, relative to a deuterium lock at

ambient (295 ± 0.5 K) temperature. Chemical shifts were externally referenced to either 5×10^{-3} M 4,4-dimethyl-4-silapentane sodium sulphonate (DSS) (^{1}H, 0 ppm) or trifluoroacetic acid (TFA) (^{19}F, -79.46 ppm). Solutions containing the external references were sealed in 1 mm capillary tubes. An average of 128 transients were collected for each ^{19}F NMR and 8-16 transients for each ^{1}H spectrum and then stored in a 32K data base. All stock solutions were freshly prepared by weight and serially diluted in 5 mm KIMAX® NMR tubes.

Spectral assignments of all ^{19}F and ^{1}H nuclei (cf. Scheme 3-1) were made using two-dimensional correlation spectroscopy (COSY) and identical assignments were found with previous reports for β-CD and the sodium perfluoroalkyl carboxylates.[30,65,175,176]

a)

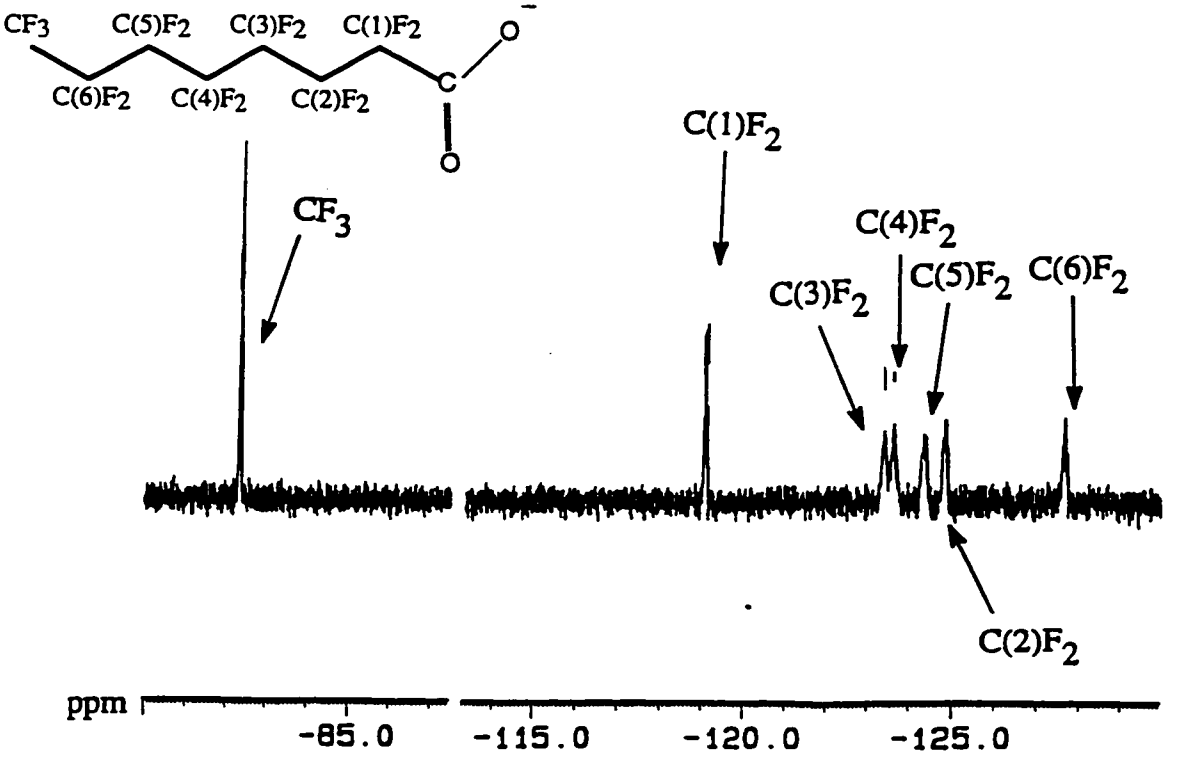

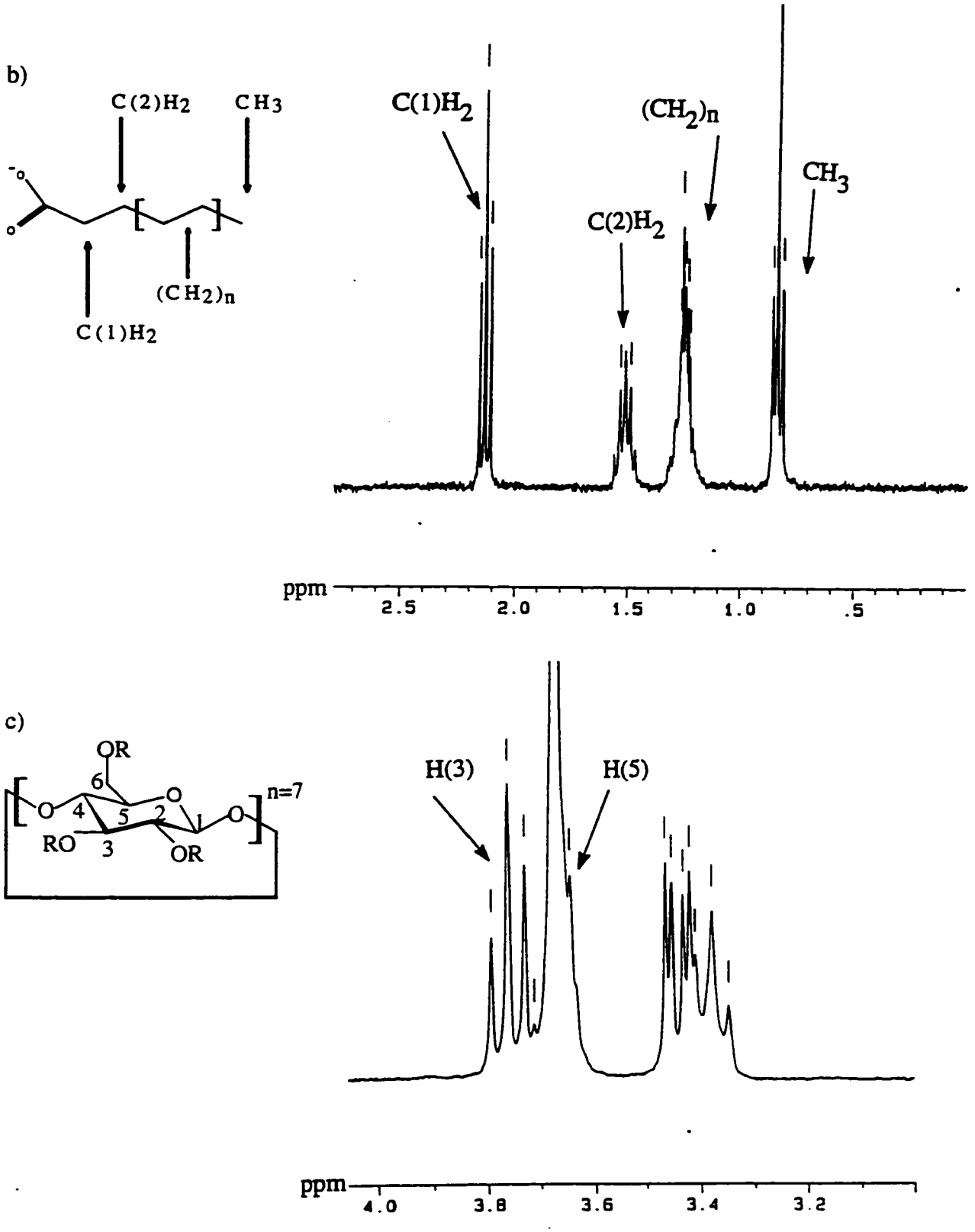

Scheme 3-1: NMR spectra, molecular structure, and numbering assignment for the nuclei investigated in this study: a) ^{19}F nuclei and spectrum of a typical fc alkyl carboxylate, b) ^{1}H nuclei and spectrum of a typical sodium alkyl carboxylate, and c) ^{1}H nuclei and spectrum of β-CD; where R=H.

In order to simplify the spectrum for β-CD, it was twice lyophilized from D_2O to effect an exchange of the hydroxyl protons with deuterium. The overlap of ^1H resonance peaks for the R-β-CDs precluded their use in this study. The complex induced chemical shift (CIS) data for the guest and host, respectively, are presented as a difference ($\Delta\delta$) defined by eqs 3.2.1-1 and -2

$$\Delta\delta = \delta_{obs} - \delta_f \qquad (3.2.1\text{-}1)$$

$$\Delta\delta = \delta_f - \delta_{obs} \qquad (3.2.1\text{-}2)$$

where δ_{obs} is the experimentally observed chemical shift and δ_f is the chemical shift for the unbound host or guest. The chemical shift differences ($\Delta\delta$) for host and guest NMR data were plotted as a function of mole ratio (R), where R = C_S/C_{CD} or C_{CD}/C_S, respectively, and C_S and C_{CD} are the concentrations of the CD and surfactant.

In the case of the ROESY (ROESY=rotating frame nuclear Overhauser effect spectroscopy) experiments,[25] the standard pulse program provided by Bruker was utilized with a 250 ms spinlock time and a 600 μs relaxation delay.

3.2.2 Measurement of density

Density measurements were carried out with a high precision densimeter (Model O2D Sodev Inc.). Period measurements were obtained with a digital frequency meter (Fluke 7261 Universal Counter). Temperature control to 25 ± 0.001°C was maintained by using a closed loop Sodev temperature controller (Model CT-L, Sodev Inc.). The flow rate of solutions through the vibrating tube was controlled either by gravity, through

raising the height of the outlet tube, or with a peristaltic pump set at a constant flow rate of 0.4 ml min^{-1}. The design of the densimeter has been described elsewhere.[177]

The principle behind this method is that the natural vibration frequency of the sample tube changes proportionally to the mass of the fluid circulating through the tube at a uniform rate.[178] The relationship between the density (d) of the fluid in the tube and its period of oscillation (τ) are related by the expression

$$d = A + B\,\tau^2 \qquad (3.2.2\text{-}1)$$

where A and B are instrument constants at a given temperature and are determined by calibration of the instrument with substances of known density. Accurate density values are obtained by measuring differences in period readings of the solution and solvent from the expression

$$d = d_o + B(\tau^2 - \tau_o^2) \qquad (3.2.2\text{-}2)$$

where d and d_o are the density of the solution and the solvent, respectively, and τ and τ_o are the period of vibration of the tube containing the solutions of unknown and known density, respectively. Calibration of the densimeter at 298.15 K was performed using the densities of water (0.997047 g cm^{-3})[179] and nitrogen gas (1.1456×10^{-3} g cm^{-3})[180] as primary standards. Binary (w+S or w+CD) solutions were measured in the sequence water-binary solution-water where water is the solvent of known density in eq 2.1.3-5. Ternary (w+S+CD) solutions were measured in the sequence binary solvent-ternary solution-binary solvent so that the binary (w+S or w+CD) solvent could be used to improve the stability of period readings between successive ternary solutions. The period measurements were averaged over 6-10 readings with a standard deviation not exceeding

± 1 ns. The estimated precision in the density measurements was found to be $\pm 2 \times 10^{-6}$ g cm^{-3} or better, based on a resolution of 100 ns for the period measurements.

3.2.3 Measurement of absorbance

Absorption measurements of phth in the visible region were obtained using a fixed wavelength spectrophotometer(Milton Roy Spectronic 20) at 550 nm and at room temperature (295 ± 0.5 K). A double beam spectrophotometer(Varian CARY 2315) was used to measure absorption versus wavelength, when required. All aqueous solutions were freshly prepared and run within 1.5 h to ensure that absorbance changes due to any instability of phenolphthalein (phth) at pH 10.5 did not contribute to experimental artifacts.[80,99,114,181]

3.2.4 Measurement of specific conductance

The measurement of specific conductance of the surfactants was obtained at 25 ± 0.01°C using a Wayne Kerr Precision Component Analyzer 6425 and an immersion conductivity cell. A series of 10 readings were taken at 5 s intervals and then averaged to give the specific conductance. The solutions were prepared by weight or volume. The measurements were obtained under conditions where the concentration of surfactant was fixed and the concentration of CD was varied using a titrametric dilution method.

3.3 Experimental conditions

The water contents of the CDs (cf. Table 3-1) were accounted for in all calculations. In ^{1}H and ^{19}F NMR experiments, the p(H+D) was adjusted to between 9-10 with (30% w/w) NaOD to minimize protonation of the carboxylate anion[182,183] and dissociation of the β-CD hydroxyl protons ($pK_a \approx 12$)[9]. At the beginning of the study, solutions were prepared individually and spectra were obtained using different NMR tubes. Subsequent measurements involved the use of a single NMR tube where aliquots of the host or guest were titrated with a microsyringe and it was concluded that more accurate chemical shift measurements were obtained in this manner. Stock solutions for NMR analysis were prepared by weight or volume basis and serially diluted. In the study of the ^{1}H nuclei of β-CD, the concentration of the cyclodextrin (C_{CD}) was fixed at 5×10^{-3} mol kg^{-1} and the concentration of surfactant (C_s was varied, with C_s always kept below the critical micelle concentration (CMC). In the case of the ^{1}H and ^{19}F surfactant nuclei, C_s was fixed at 5×10^{-3} mol kg^{-1} such that $C_s \leq$ CMC and C_{CD} was varied. The precision in the chemical shift measurements is estimated to be $\pm2\times10^{-3}$ ppm or better.

In the spectral displacement technique, all solutions were prepared by volume in a 0.1 M Na_2CO_3 buffer adjusted to pH 10.5. The concentration of phenolphthalein (C_{phth}) was 2×10^{-5} M in all experiments. For the determination of the CD-surfactant binding constants, $K_{1:1}$, the concentration of β-CD (C_{CD}) was fixed at 3×10^{-4} M and the concentration of surfactant(C_S) was varied to exceed the 1:1 mole ratio of the CD-surfactant such that C_S<CMC. A stock solution of phth in ethanol was made and aliquots were

utilized to prepare aqueous solutions of phth in buffer. The ethanol content (0.04%; v/v) in aqueous solution was used to increase the solubility of phth.

In volumetric studies, the solvent in the binary solutions is water (w) whereas in ternary solutions it is a mixed solvent, either (w+S) or (w+CD). The details of the calculation of the apparent molar volume (AMV) were given in Chapter 2 (§ 2.1.3). For the determination of $V_{\phi,S}$ in ternary systems, the binary solvent had a fixed value of C_{CD} and C_S was varied but always kept below the CMC. In the case of the determination of $V_{\phi,CD}$ in ternary systems, the binary solvent(w+S) consisted of a fixed C_S and C_{CD} was varied.

The measurement of specific conductance involved fixing the concentration of surfactant (C_S) while the concentration of cyclodextrin (C_{CD}) was varied.

4. RESULTS

4.1 ^{1}H NMR chemical shift studies

4.1.1 ^{1}H nuclei of sodium alkyl carboxylate salts in aqueous cyclodextrin solutions

The ^{1}H NMR chemical shifts (cf. Appendix A1 for experimental data) of the sodium alkyl carboxylate salts (cf. Scheme 3-1b) were measured at conditions where the concentration of surfactant (C_S) was held constant and the concentration of the CD (C_{CD}) was varied so that the mole ratio ($R=C_{CD}/C_S$) exceeded R=1. Data were obtained over a concentration range where the fraction of bound species varied from low to high values over the entire binding isotherm.[184] Figures 4-1a-c illustrate typical plots of chemical shift difference ($\Delta\delta$) (cf. eq 3.1.2-2) versus mole ratio (R). In general, $\Delta\delta$ increases as R increases and then levels off at higher mole ratios. The simulated lines through the data points in Figs. 4-1a-c correspond to the nonlinear least squares (NLLS) fitting predicted by the two- and three-site models presented in § 2.1.2.

Table 4-1 lists the abbreviations used for the sodium alkyl carboxylate salts and the values of the binding constants (K_i) obtained for the CD-surfactant (CD-S) complexes. The simulation of the ^{1}H NMR data utilizes K_i and δ_i as adjustable parameters and δ_f was obtained from measurements of δ of the surfactant in D_2O in the absence of added CD. In all cases, the best fit estimates of K_i were obtained from the NLLS fitting of $\Delta\delta$ versus R for the CH_3 nuclei of the surfactant using equations 2.1.2-4 to -6 because these nuclei displayed the largest CIS values among the guest nuclei that were resolved. In some cases, the C(1)H_2 and C(2)H_2 groups displayed CIS values greater than 0.01 ppm at R=1 and were also utilized to calculate K_i.

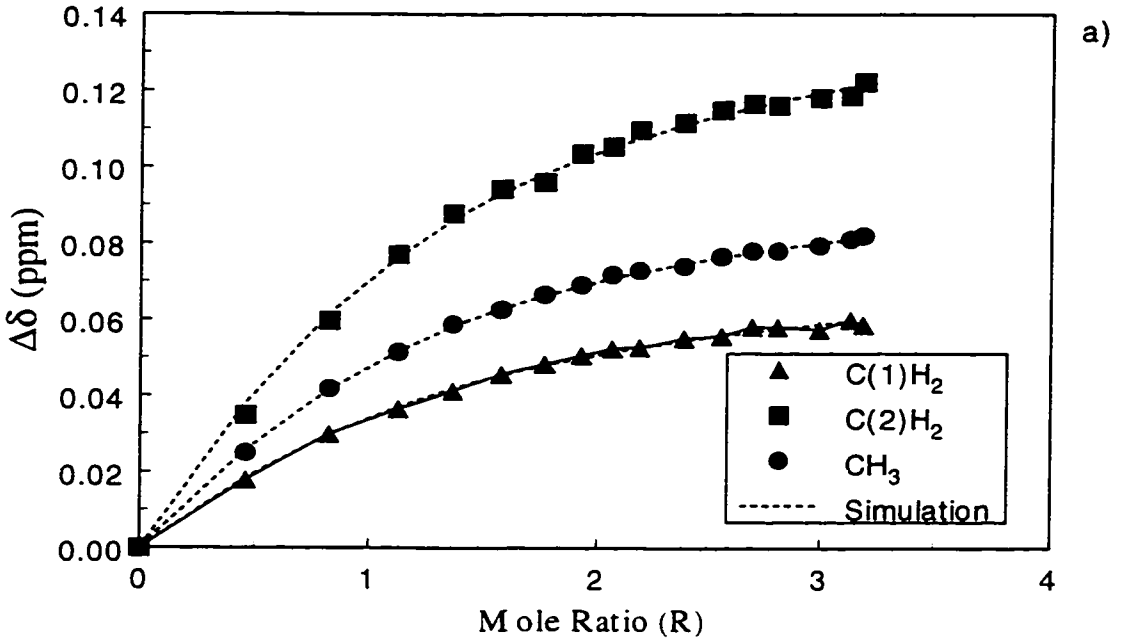
a)
0.14
0.12
0.10
0.08
0.06
0.04
0.02
0.00
Δδ (ppm)
0
1
2
3
4
Mole Ratio (R)
C(1)H2
C(2)H2
CH3
Simulation

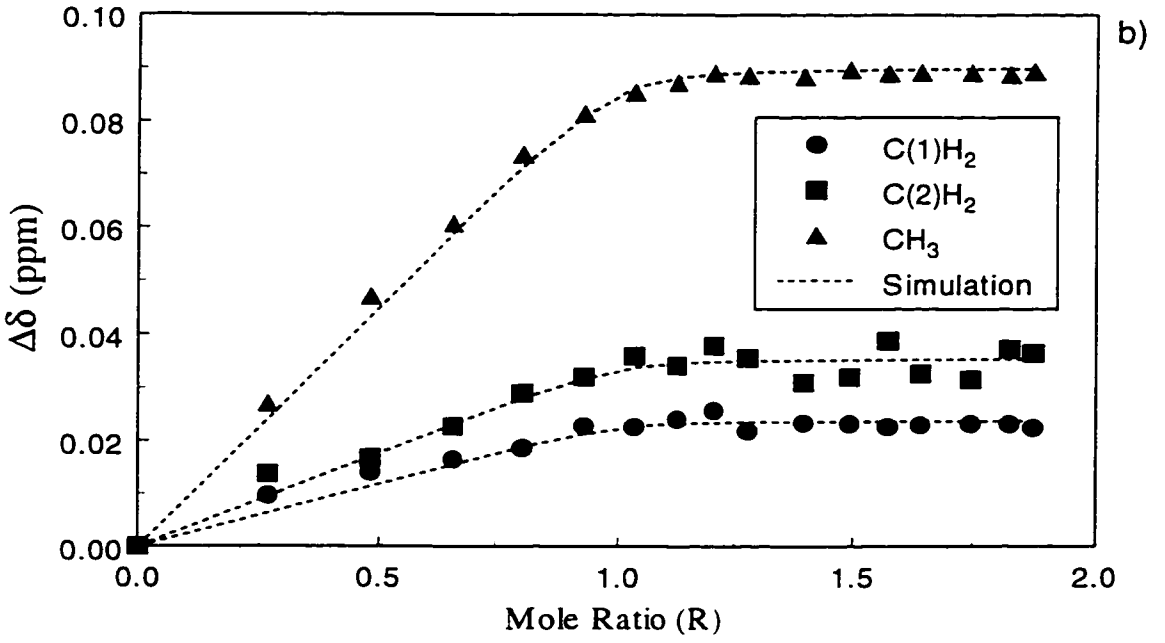
b)
0.10
0.08
0.06
0.04
0.02
0.00
Δδ (ppm)
0.0
0.5
1.0
1.5
2.0
Mole Ratio (R)
C(1)H2
C(2)H2
CH3
Simulation

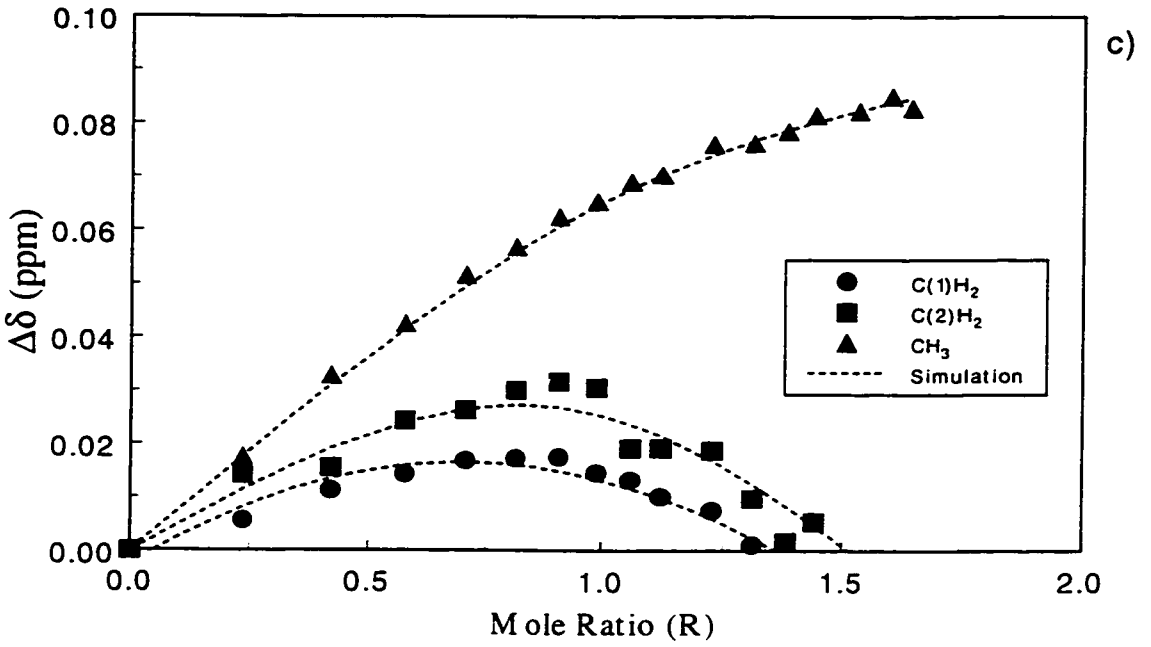

Figure 4-1: ^{1}H chemical shift difference ($\Delta\delta$) versus host-guest mole ratio (R), where R= C_{CD}/C_S, for guest, $C(1)H_2$, $C(2)H_2$, and CH_3 nuclei at T=295 K: a) α-CD-$C_5H_{11}CO_2Na$ system, b) DM-β-CD-$C_{11}H_{23}CO_2Na$ system, and c) α-CD-$C_{11}H_{23}CO_2Na$ system.

In general, K_i (i=1:1 and 2:1) increase as the alkyl chain length (C_x) increases. The magnitude of $K_{1:1}$ ranges from 10^1-10^4 M^{-1} whereas $K_{2:1}$ ranges from 10^2-10^3 M^{-2}. There are some differences amongst the various CDs studied with respect to their relative binding affinity with a common hydrocarbon (hc) surfactant. The binding affinity follows the order: β-CD > α-CD > DM-β-CD > TM-β-CD > HP-β-CD.

Table 4-2 lists the ^{1}H NMR complex induced shift (CIS) values (cf. eq 3.1.2-2) at the 1:1 CD-S mole ratio for the $C(1)H_2$, $C(2)H_2$, and CH_3 groups of the surfactant. These groups were chosen since they were resolved and they can provide information about the

Table 4-1: Binding Constants, (K_i),[a,b] of Various CD-Sodium Alkyl Carboxylate Complexes Obtained From ^{1}H NMR Chemical Shift Measurements of the Guest Protons at 295 K.

Surfactant	α-CD	β-CD	DM-β-CD	TM-β-CD	HP-β-CD
$C_5H_{11}CO_2Na$	[a]$3x10^2(1x10^1)$[c]	[a]$6x10^1(1x10^1)$[c]	[a]$1x10^2(3x10^1)$[c]	[a]$3x10^1(1x10^1)$[c]	[a]$2x10^1(4x10^0)$[c]
SHex	[d]211±12	[d]67.6±1.8, [f]34			
$C_7H_{16}CO_2Na$	[a]$4.7x10^2(7.1x10^1)$	[a]$7.0x10^2(2.9x10^2)$	[a]$3.4x10^2(3.1x10^1)$	[a]$1.0x10^2(1.8x10^2)$	[a]$7.6x10^2(1.6x10^1)$
SO	[d]622±26, [e]2100±12	[d]683±8, [e]420, [f]370			
$C_9H_{19}CO_2Na$	[a]$5.6x10^3(2.8x10^3)$	[a]$8.0x10^3(1.7x10^1)$	[a]$4.8x10^3(3.8x10^2)$	[a]$4.6x10^2(5.7x10^1)$	[a]$2.0x10^3(2.6x10^2)$
SDec	[b]$6.5x10^2(3.3x10^2)$	[d]$7.5±0.9x10^3$, [f]740			
	[d]$1.8x10^3$				
$C_{11}H_{23}CO_2Na$	[a]$2.1x10^4(1.1x10^4)$	[a]$3.3x10^4(1.7x10^4)$	[a]$1.0x10^4(4.5x10^3)$	[a]$4.3x10^3(1.3x10^3)$	[a]$3.8x10^3(1.1x10^3)$
SDodec	[b]$1.2x10^3(6.0x10^2)$	[b]$4.3x10^2(2.2x10^2)$			
		[f]1600			
$C_{13}H_{27}CO_2Na$	[a]$4.0x10^4(2.0x10^4)$	[a]$6.3x10^4(3.2x10^4)$	[a]$5.0x10^4(2.5x10^4)$	[a]$2.3x10^4(3.8x10^3)$	[a]$1.6x10^4(8.2x10^3)$
ST	[b]$6.2x10^3(3.1x10^3)$	[b]$1.6x10^3(8.0x10^2)$			

[a] $K_{1:1}$ (M^{-1}), [b] $K_{2:1}$ (M^{-2}), [c] standard error for K_i obtained in this work is given in parentheses, [d] $K_{1:1}$ from ref. 185, [e] $K_{1:1}$ from ref. 186, [f] $K_{1:1}$ from ref. 187.

host-guest inclusion geometry. In general, the CIS values follow the order: $\Delta\delta(CH_3) > \Delta\delta(C(1)H_2) > \Delta\delta(C(2)H_2)$, and their magnitude increases as C_x increases.

The CIS values for the $(CH_2)_n$ groups are not listed in Table 4-2 because the individual CH_2 groups were not fully resolved and could not be analyzed quantitatively. However, an analysis of the line shapes of the $(CH_2)_n$ resonance line at certain CD-S mole ratios can provide information about the stoichiometry and the maximum number of included alkyl groups in the CD interior. Figure 4-2 illustrates the resonance lines for the $(CH_2)_n$ protons (cf. Scheme 3-1b) for SDec, SDodec, and ST in the presence of α- and β-CD, respectively, at the R=2 mole ratio. The appearance of an asymmetry in this signal, in the presence of CD at R=2, reflects nonequivalent molecular environments due to the presence of complexes of different stoichiometry, and will be discussed in Chapter 5.

4.1.2 ^{1}H nuclei of β-cyclodextrin in aqueous solutions of sodium alkyl carboxylate salts

The measurement of ^{1}H NMR chemical shifts (cf. Appendix A2 for experimental data) of β-CD (cf. Scheme 3-1c) were obtained under conditions where C_{CD} was held constant between 5-10 × 10^{-3} molal and C_S was increased so that the mole ratio ($R = C_S/C_{CD}$) exceeded R=1 but C_S did not exceed the critical micelle concentration (CMC). Figures 4-3a-c illustrate plots of Δδ versus mole ratio (R) for β-CD in the presence of different surfactants. In general, Δδ increases as R increases and then levels off at higher mole ratios. These graphs are typical of the binding behaviour shown by CD-S complexes when the alkyl chain length of the hc surfactant varies from short (Fig. 4-3a)

Table 4-2: ^{1}H NMR Complex Induced Shift[a] (CIS) Values (ppm) of Various Guest Nuclei[b,c,d] at the 1:1 Mole Ratio for Various CD-Sodium Alkyl Carboxylate Complexes at 295 K.

Surfactant	α-CD	β-CD	DM-β-CD	TM-β-CD	HP-β-CD
$C_5H_{11}CO_2Na$	0.033[b], 0.067[c], 0.045[d]	0.002[b], 0.004[c], 0.005[d]	-0.003[b], ≈0[c], 0.001[d]	-0.001[b], -0.001[c], 0.002[d]	-0.020[b], 0.002[c], 0.028[d]
$C_7H_{16}CO_2Na$	0.024[b], 0.049[c], 0.053[d]	0.008[b], 0.019[c], 0.015[d]	-0.007[b], -0.003[c], 0.021[d]	-0.005[b], 0.005[c], 0.022[d]	-0.001[b], 0.009[c], 0.040[d]
$C_9H_{19}CO_2Na$	0.002[b], 0.026[c], 0.054[d]	0.007[b], 0.003[c], 0.058[d]	0.006[b], 0.004[c], 0.055[d]	-0.015[b], -0.002[c], 0.059[d]	-0.003[b], ≈0[c], 0.055[d]
$C_{11}H_{23}CO_2Na$	-0.052[b], -0.035[c], 0.083[d]	0.028[b], 0.023[c], 0.089[d]	0.022[b], 0.032[c], 0.085[d]	≈0[b], 0.013[c], 0.073[d]	0.007[b], 0.011[c], 0.062[d]
$C_{13}H_{27}CO_2Na$	0.016[b], 0.023[c], 0.057[d]	0.036[b], 0.044[c], 0.105[d]	0.025[b], 0.027[c], 0.079[d]	-0.003[b], 0.014[c], 0.064[d]	0.016[b], 0.016[c], 0.060[d]

[a] CIS Value = $\delta_{obs} - \delta_f$; where all δ values are measured relative to the external standard DSS, [b] $C(1)H_2$, [c] $C(2)H_2$, [d] CH_3.

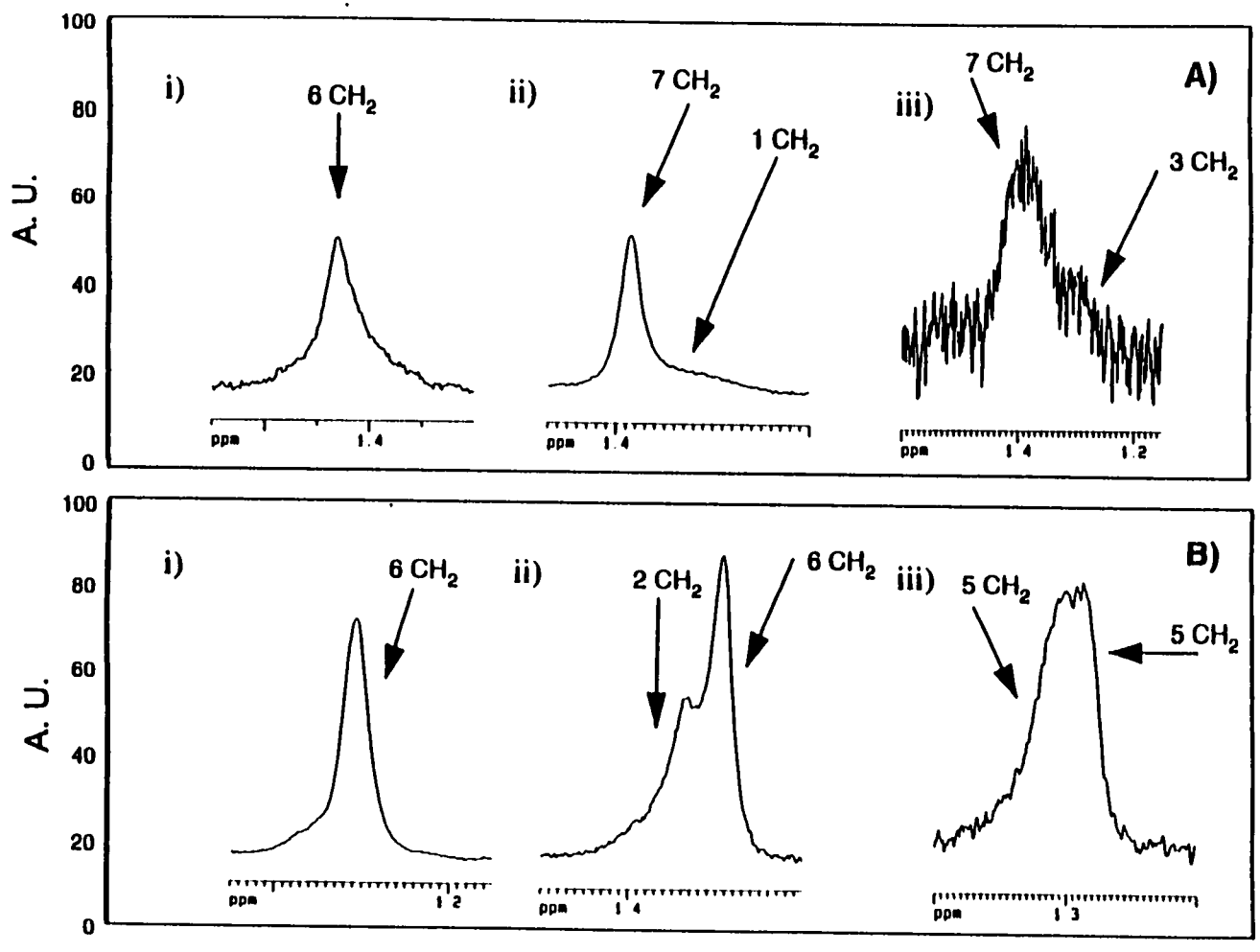

Figure 4-2: Comparison of the ^{1}H NMR signals of the methylene $(CH_2)_n$ protons (cf. Scheme 3) for the surfactants (i) SDec, ii) SDodec, and iii) ST) complexed with A) α-CD and B) β-CD, at R=2 mole ratio and T=295 K.

to long (Fig. 4-3c). The simulated lines through the data points in Figs. 4-3a-c are those predicted according to the two- and three-site models presented in § 2.1.2.

Table 4-3 lists the CIS values for the H(3) and H(5) protons of β-CD at R=1 and the values of K_i obtained for various β-CD-S complexes. The ^1H nuclei of β-CD that are exterior to the cavity did not show any significant change in CIS values upon the addition of surfactant so they were not analyzed. Estimates of K_i were obtained from the NLLS fitting of $\Delta\delta$ versus R for the host nuclei using eqs. 2.1.2-4 to -6. The details of the simulation are similar to those for the ^1H NMR data of the guest (cf. § 4.1.1). In general, the CIS values for H(5) exceed H(3) and their magnitude increases as C_x increases. As well, K_i (i=1:1 and 2:1) increase as C_x increases and there is good agreement with the complementary data, Table 4-1, obtained from the analysis of the nuclei of the guest.

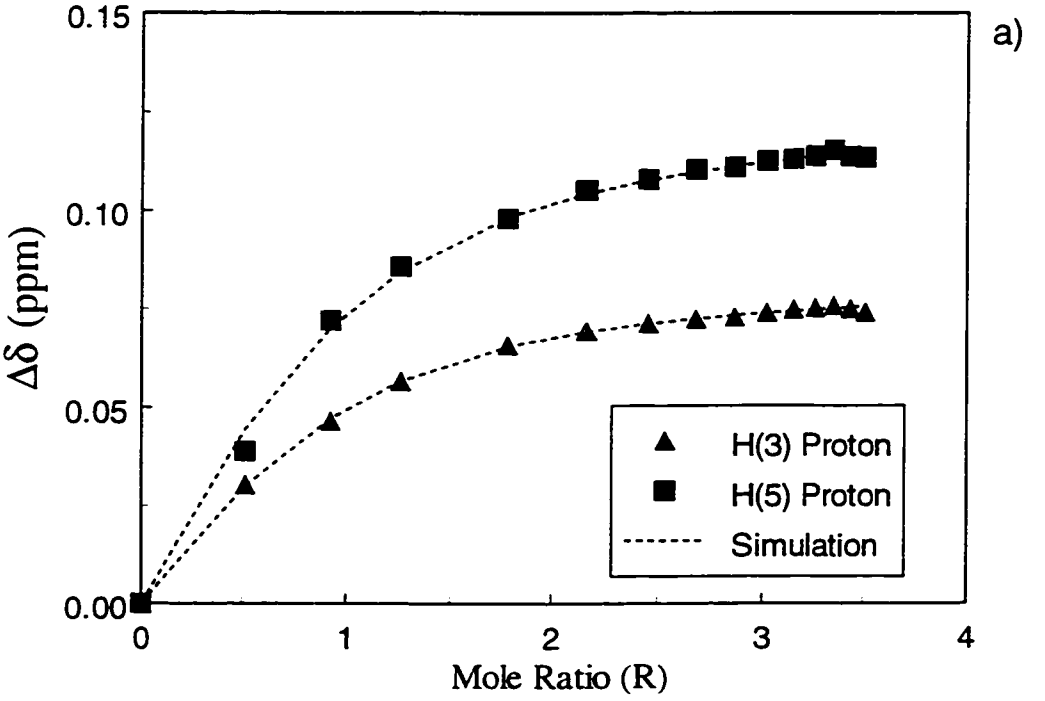

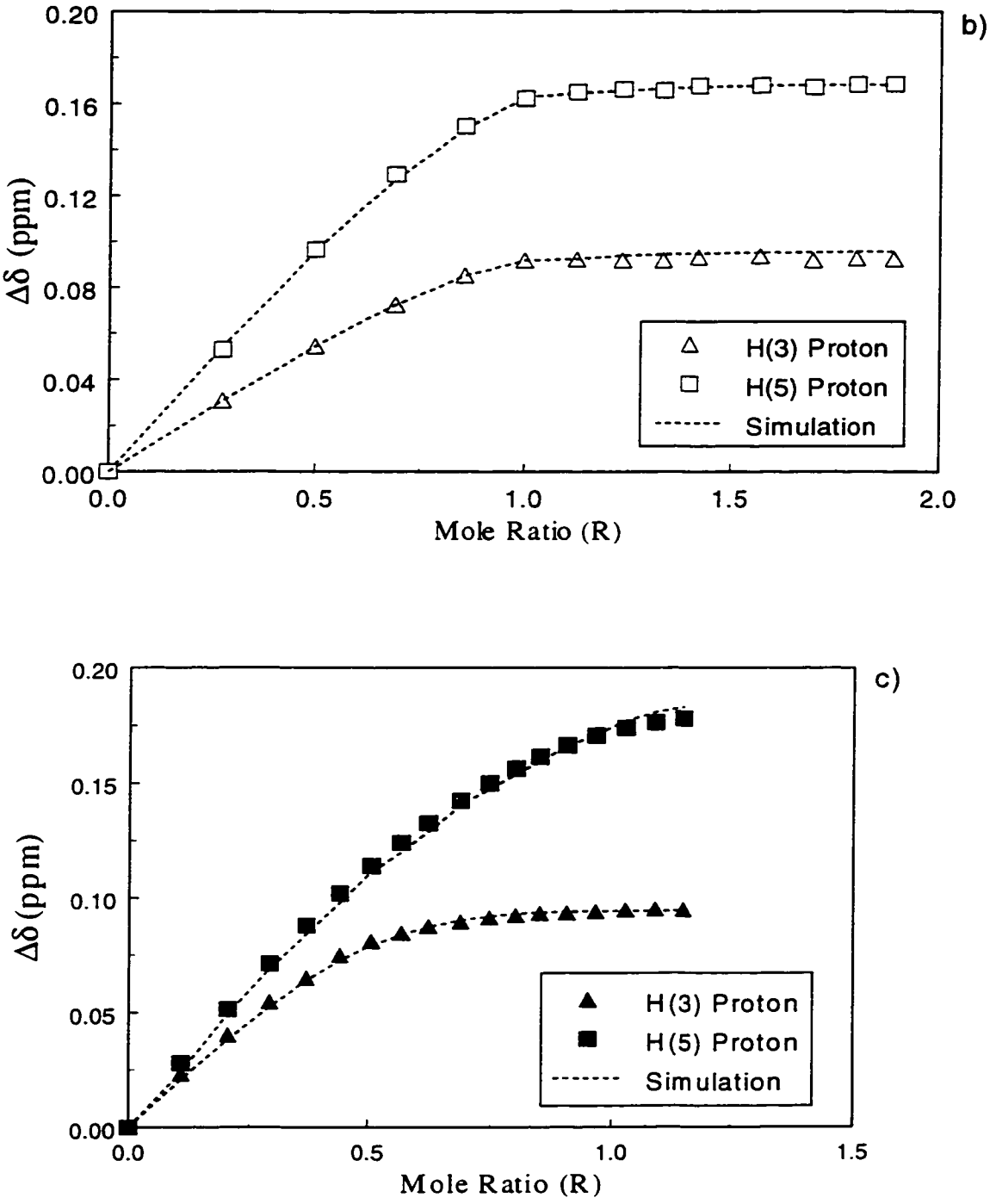

Figure 4-3: ^1H chemical shift difference ($\Delta\delta$) versus mole ratio R, where $R=C_S/C_{\beta\text{-CD}}$, for H(3) and H(5) of β-CD at T=295 K: a) β-CD-$C_5H_{11}CO_2Na$, b) β-CD-$C_{11}H_{23}CO_2Na$, and c) β-CD-Sodium dodecyl sulfate (β-CD-SDS).

Table 4-3: Binding Constants $(K_i)^{a,b}$ of Various β-CD-Sodium Alkyl Carboxylate Complexes and ^1H NMR Complex Induced Shift Values at R=1[c] for the H(3) and H(5) Protons of β-CD at 295 K.

Surfactant	H(3)	H(5)	Δδ(H(3))	Δδ(H(5))
$C_5H_{11}CO_2Na$	[a]1.0×10^2 (1.0×10^1)[d]	[a]1.3×10^2(2.3×10^1)[d]	0.012	0.015
$C_7H_{16}CO_2Na$	[a]7.7×10^2(3.7×10^1)	[a]6.5×10^2(6.6×10^1)	0.049	0.066
$C_9H_{19}CO_2Na$	[a]8.0×10^3(1.5×10^3)	[a]5.2×10^3(7.0×10^2)	0.072	0.122
$C_{11}H_{23}CO_2Na$	[a]5.0×10^4(2.5×10^4)	[a]5.0×10^4(2.5×10^4)	0.089	0.158
	[b]4.0×10^2(2.0×10^2)	[b]4.0×10^2(2.0×10^2)		
$C_{13}H_{27}CO_2Na$*	[a]1.0×10^5(5.0×10^4)	[a]1.1×10^5(5.3×10^4)	0.067	0.125
	[b]1.0×10^3 (0.5×10^3)	[b]2.0×10^3(1.0×10^3)		

[a] $K_{1:1}$ (M^{-1}), [b] $K_{2:1}$ (M^{-2}), [c]Obtained at a surfactant concentration of 5×10^{-3} molal, [d]standard error for K_i is given in parentheses, *Obtained at a surfactant concentration of 1×10^{-3} molal .

Figure 4-4 is a ROESY (ROESY=rotating frame nuclear Overhauser effect Spectroscopy) spectrum of the β-CD-SDodec system. The purpose of the ROESY experiment was to confirm the occurrence of dipolar interactions between the host cavity and the guest, and to provide independent evidence for the formation of inclusion complexes. The main cross-peaks observed are for the $(CH_2)_n$ group (cf. Scheme 3-1b) and the H(3) and H(5) interior cavity protons of β-CD. The intensities of the cross-peaks increase as C_x increases and can be correlated with the binding affinity and the inclusion geometry of the complex. The intermolecular correlation between the $C(1)H_2$, $C(2)H_2$, and CH_3 groups with those of the cavity protons of β-CD appear to be weak or absent.

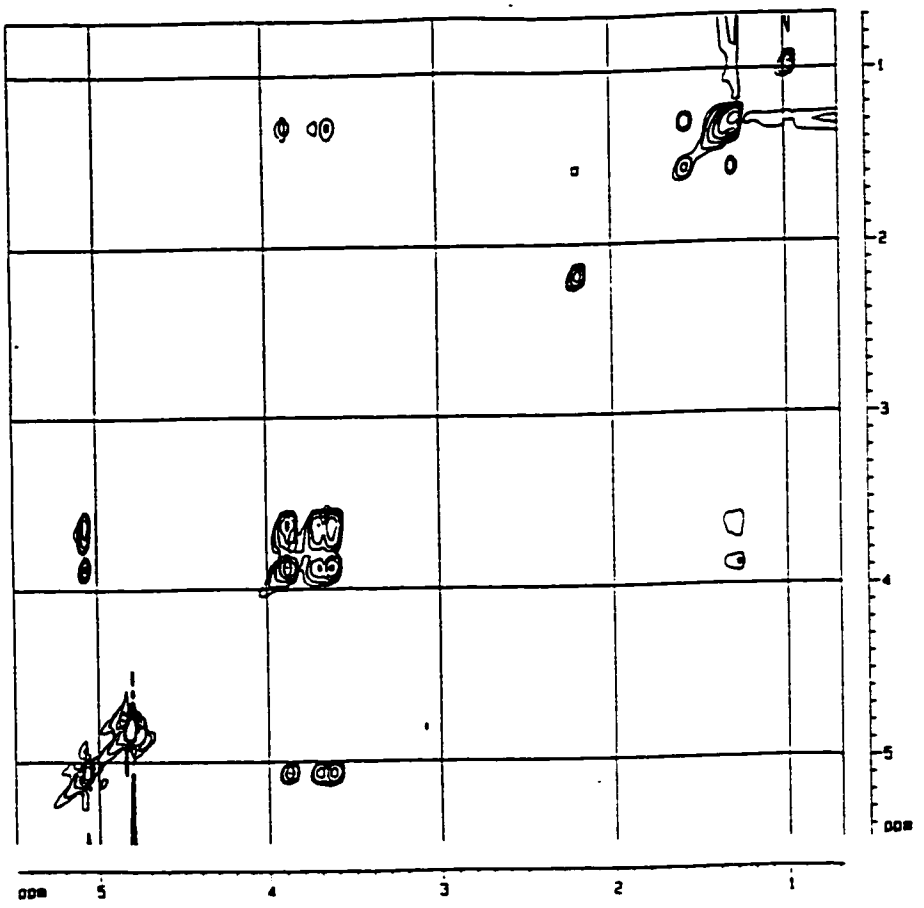

Figure 4-4: ROESY spectrum for β-CD-$C_{11}H_{23}CO_2Na$ system at 295 K with spinlock time of 250 ms and a relaxation delay of 600 μs.

4.2 ^{19}F NMR chemical shift studies

4.2.1 ^{19}F nuclei of sodium perfluoroalkyl carboxylate salts in aqueous cyclodextrin solutions

The ^{19}F NMR chemical shifts (cf. Appendix A3 for experimental data) of the sodium perfluoroalkyl carboxylate salts (cf. Scheme 3-1a) were measured under similar conditions as described in § 4.1.1 for the hc surfactants except that the solvent system was 50%(w/w) D_2O/H_2O and chemical shifts were externally referenced to TFA (cf. § 3.2.1).

Table 4-4 lists the CMC data, the abbreviations used for the sodium perfluoroalkyl carboxylate salts, and the binding constants (K_i) obtained for the CD-fc surfactant systems. The CMC was determined from the inflection in plots of δ versus C_S for the various ^{19}F nuclei of the surfactant. The binding constants (K_i) shown in Table 4-4 are an average value obtained from the analysis of CIS values for several ^{19}F nuclei along the fc surfactant chain that displayed CIS values $\geq$ 0.05 ppm at the R=1 mole ratio. The details of the simulation are similar to that described in § 4.1.1. However, δ_f was allowed to vary as an adjustable parameter within the estimated precision (±0.005 ppm) of the ^{19}F chemical shift. In general, the values of K_i (i=1:1, 1:2, and 2:1) increase as the fc chain length (C_x) increases. The differences in the observed binding affinities among the modified CDs can be correlated with the type of alkyl substitution in the CD annulus region.

Figures 4-5a-f illustrate plots of $\Delta\delta$ versus mole ratio (R) for various CD-S systems. In general, $\Delta\delta$ increases (positive or negative) as R increases and then levels off at higher mole ratios. The simulated curves in Figs. 4-5a-f correspond to the best-fit predicted by the two- and three-site models presented in § 2.1.2.

Figure 4-6 is a plot of specific conductance versus the host-guest mole ratio for various R-β-CD-S systems under conditions similar to which the ^{19}F chemical shifts of the fc surfactants were obtained. In all cases, the specific conductance decreases up to R=1 where a change in slope occurs. As well, a small inflection is observed for the RAMEB-SPFN system at R=0.5 and is consistent with the inflections observed near R=0.5 in Fig. 4-5e.

Table 4-4: Binding Constants[a,b] (K_i)[c-e] of Various Cyclodextrin-Sodium Perfluoroalkyl Carboxylate Complexes and CMC Data for the Sodium Perfluoroalkyl Carboxylates at 295 K.

Surfactant	β-CD	RAMEB	DM-β-CD	TM-β-CD	HP-β-CD	CMC ($\times10^{-3}$ molal)
$C_3F_7CO_2Na$ SPFB	$9.17(1.80)\times10^{2}$[c]	$1.32(0.062)\times10^{2}$[c]	$2.01(0.19)\times10^{2}$[c]	$2.24(0.31)\times10^{1}$[c]	$9.82(0.13)\times10^{1}$[c]	>1000
$C_4F_9CO_2Na$ SPFP	$2.67(0.44)\times10^{3}$[c]	$6.24(0.95)\times10^{2}$[c]	$1.86(0.24)\times10^{3}$[c]	$1.01(0.30)\times10^{2}$[c]	$5.53(0.53)\times10^{2}$[c]	520±15
$C_6F_{13}CO_2Na$ SPFH	$2.35(0.46)\times10^{4}$[c]	$1.05(0.42)\times10^{4}$[c]	$9.59(2.5)\times10^{3}$[c]	$1.48(0.90)\times10^{4}$[c]	$1.40(0.48)\times10^{4}$[c]	81±1 80±2[f]
$C_7F_{15}CO_2Na$ SPFO	$8.85(4.4)\times10^{4}$[c] $7.64(3.8)\times10^{2}$[d] 2.18×10^{4}[c,f]	$3.55(1.4)\times10^{4}$[c]	$2.49(0.81)\times10^{4}$[c]	$2.48(1.7)\times10^{4}$[c]	$3.59(1.1)\times10^{4}$[c]	30±1 32±1[f]
$C_8F_{17}CO_2Na$ SPFN	$1.20(0.60)\times10^{5}$[c] $2.20(1.1)\times10^{3}$[d] 7.2×10^{3}[c,f]	$8.80(4.4)\times10^{4}$[c] $7.00(3.5)\times10^{2}$[e]	$6.20(3.1)\times10^{4}$[c] $4.0(2.0)\times10^{2}$[e]	$6.25(3.12)\times10^{4}$[c] $1.83(0.91)\times10^{3}$[e]	$6.01(1.5)\times10^{4}$[c]	9.8±0.5[g] 9.2±0.2[f]

(a) average value based on several ^{19}F nuclei possessing CIS values > 0.05 ppm at R=1, (b) standard error for K_i is given in parentheses, (c) $K_{1:1}$ (M^{-1}), (d) $K_{2:1}$, (M^{-2}), (e) $K_{1:2}$ (M^{-2}), (f) ref. (65), (g) Obtained at 303 K.

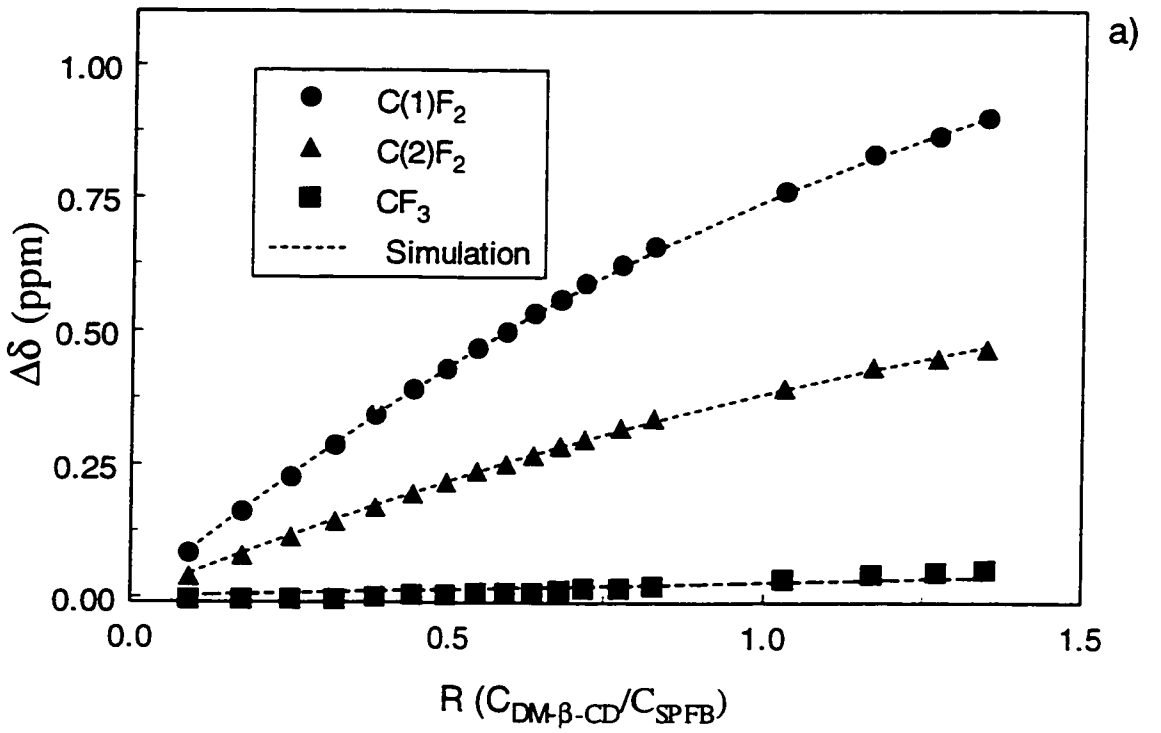
a)
1.00
0.75
0.50
0.25
0.00
Δδ (ppm)
C(1)F2
C(2)F2
CF3
Simulation
0.0
0.5
1.0
1.5
R (CDM-β-CD/CSPFB)

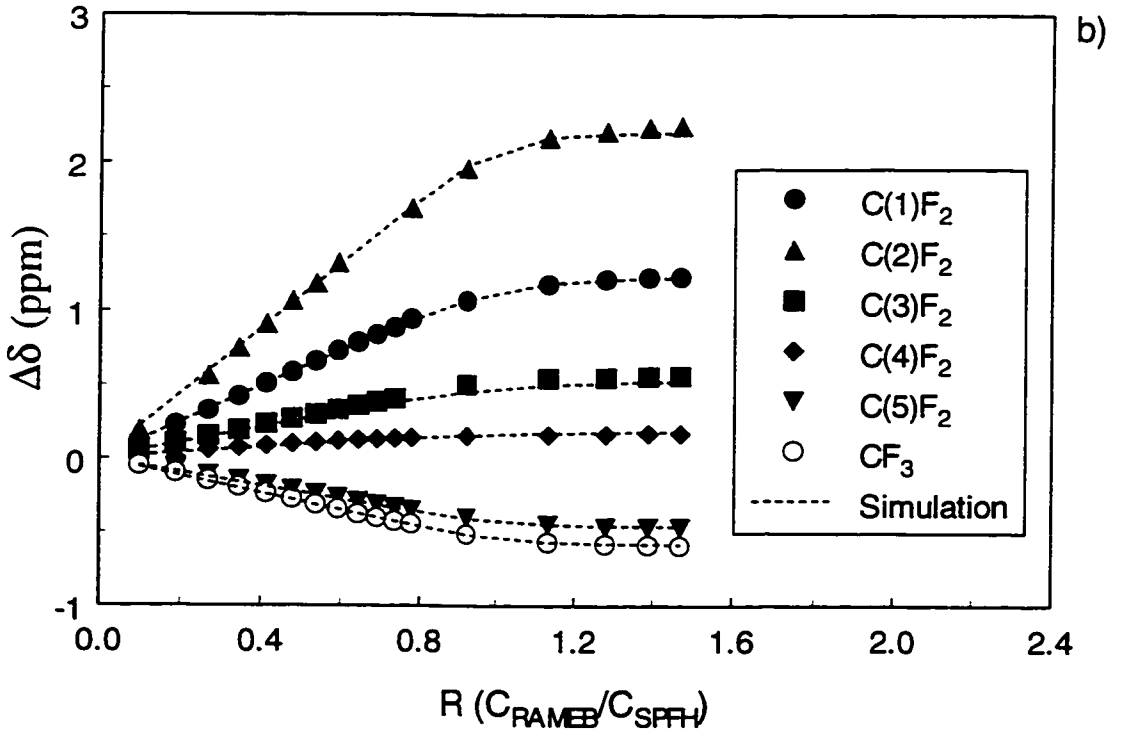
b)
3
2
1
0
-1
Δδ (ppm)
C(1)F2
C(2)F2
C(3)F2
C(4)F2
C(5)F2
CF3
Simulation
0.0
0.4
0.8
1.2
1.6
2.0
2.4
R (CRAMEB/CSPFH)

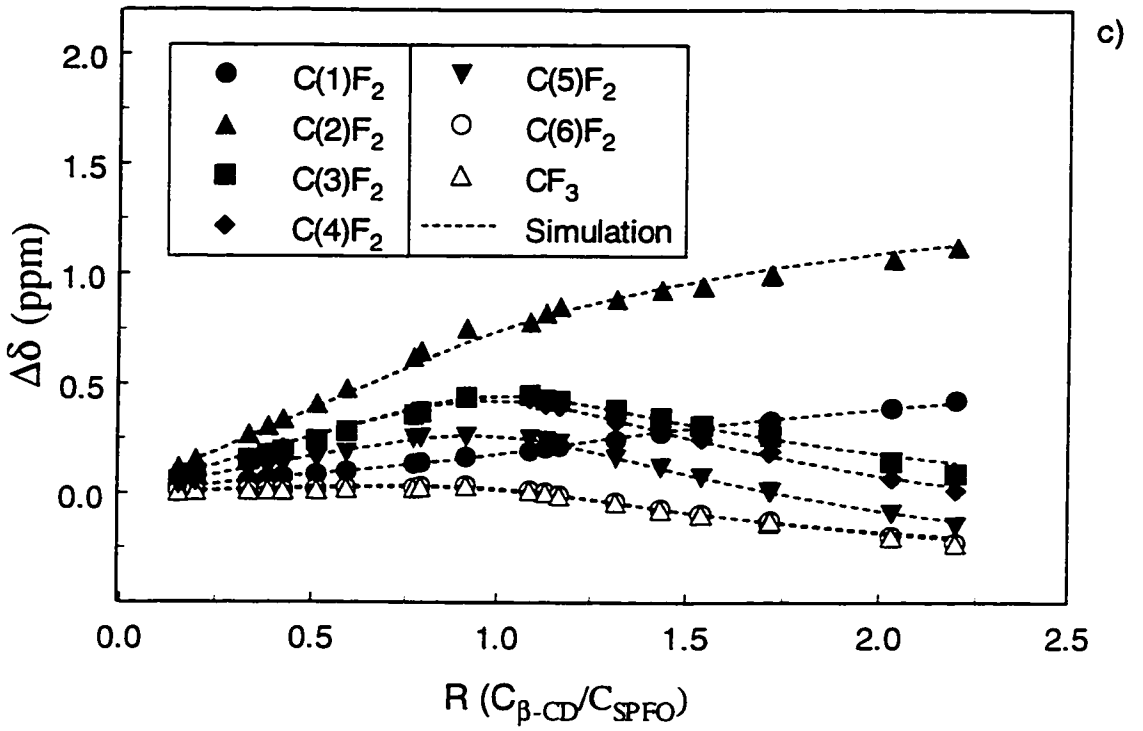
c)
C(1)F2
C(2)F2
C(3)F2
C(4)F2
C(5)F2
C(6)F2
CF3
Simulation
Δδ (ppm)
R (Cβ-CD/CSPFO)

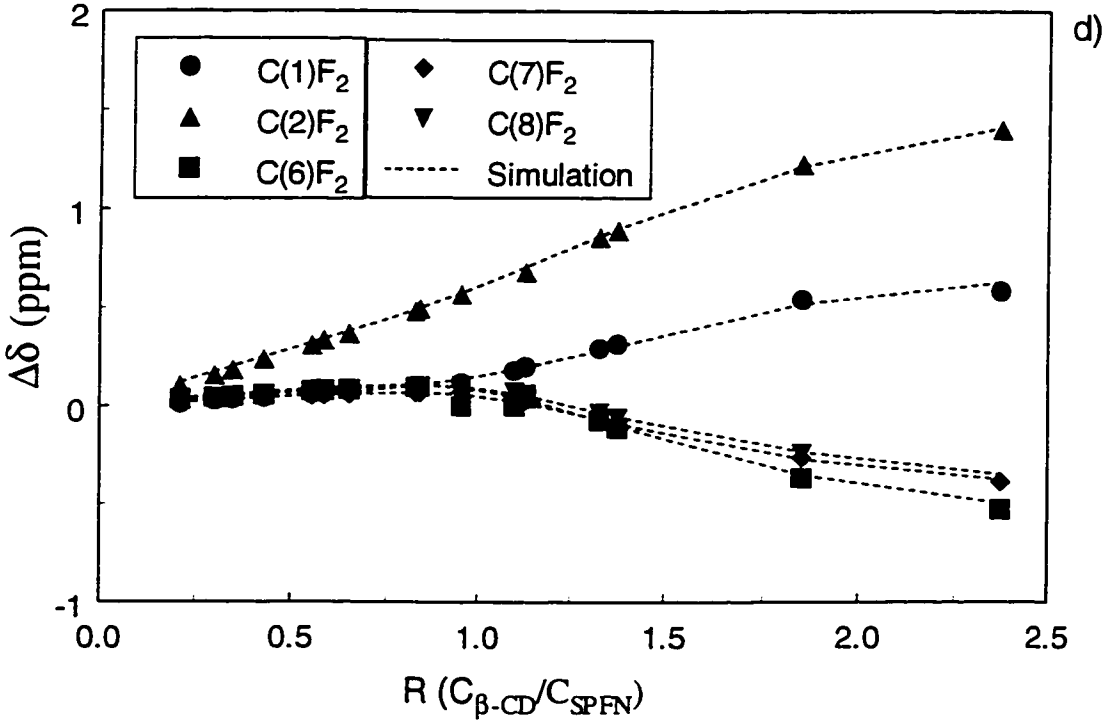
d)
C(1)F2
C(2)F2
C(6)F2
C(7)F2
C(8)F2
Simulation
Δδ (ppm)
R (Cβ-CD/CSPFN)

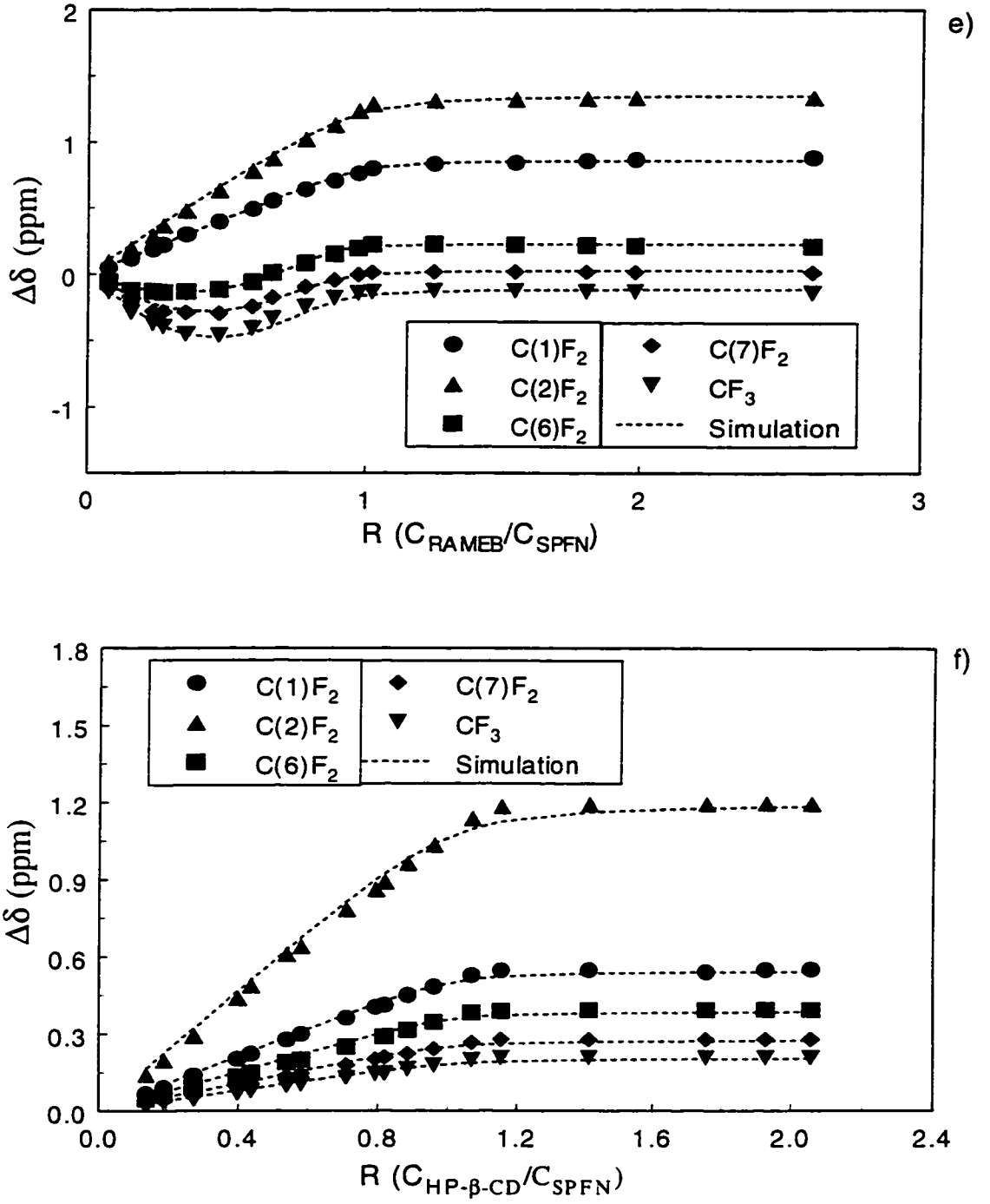

Figure 4-5. ^{19}F chemical shift difference ($\Delta\delta$) for the surfactant plotted against host-guest mole ratio(R=[R-β-CD]/[S]) at a fixed surfactant concentration of 5×10^{-3} molal and T=295 K: a) DM-β-CD-SPFB, b) RAMEB-SPFH, c) β-CD-SPFO, d) β-CD-SPFN, e) HP-β-CD-SPFN, and f) RAMEB-SPFN.

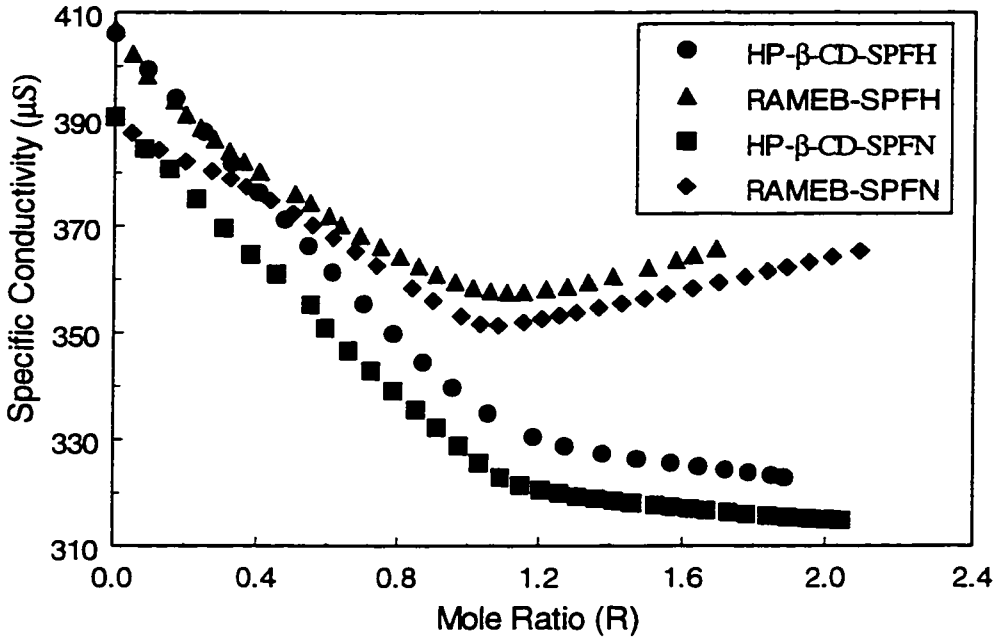

Figure 4-6: Specific conductance versus host-guest mole ratio R, where $R=C_{R\text{-}\beta\text{-}CD}/C_S$ for various R-β-CD-S systems at a fixed surfactant concentration of 5×10^{-3} molal and T=298 K.

Tables 4-5a-e list the CIS values for selected nuclei located near the surfactant head group and the apolar terminus of the fc surfactant chain. These nuclei were chosen because they are expected to provide a basis to elucidate a probable inclusion geometry and an estimate of the optimum alkyl chain length that can be included in the CD cavity. The nuclei adjacent to the carboxylate head group display the largest CIS values whereas the fc nuclei located toward the apolar terminus are much smaller in magnitude. The CIS values at R=1 for some of the fc surfactants follow the general order: SPFB; $C(1)F_2>$ $C(2)F_2>CF_3$, SPFP; $C(2)F_2\geq$ $C(1)F_2>C(3)F_2>$ CF_3, SPFH; $C(2)F_2\geq C(1)F_2>C(3)F_2>>$ $C(4)F_2 > C(5)F_2 > CF_3$.

Table 4-5: ^{19}F CIS Values(ppm) for fc Surfactants in Aqueous Cyclodextrin (CD) Solutions at R=1 and 295 K: a) SPFB, b) SPFP, c) SPFH, d) SPFO, and e) SPFN

a: Sodium Perfluorobutanoate (SPFB)

CD	$C(1)F_2$	$C(2)F_2$	CF_3
α-CD	0.170	0.330	0.361
β-CD	0.660	0.458	0.012
RAMEB	0.751	0.419	0.136
DM-β-CD	0.754	0.392	0.034
TM-β-CD	0.236	0.130	0.110
HP-β-CD	0.633	0.463	0.119

b: Sodium Perfluoropentanoate (SPFP)

CD	$C(1)F_2$	$C(2)F_2$	$C(3)F_2$	CF_3
β-CD	0.695	1.125	0.244	-0.298
RAMEB	1.357	1.278	0.244	-0.157
DM-β-CD	1.212	1.263	0.102	-0.308
TM-β-CD	0.648	0.566	0.069	-0.065
HP-β-CD	0.924	1.185	0.389	-0.015

c: Sodium Perfluoroheptanoate (SPFH)

CD	$C(1)F_2$	$C(2)F_2$	$C(5)F_2$	CF_3
β -CD	0.286	1.170	0.070	-0.063
RAMEB	1.150	1.854	≈0	-0.235
DM-β-CD	0.940	1.640	-0.087	-0.262
TM-β-CD	1.160	2.151	-0.441	-0.533
HP-β-CD	0.715	1.640	0.340	0.132

d: Sodium Perfluorooctanoate (SPFO)

CD	$C(1)F_2$	$C(1)F_2$	$C(6)F_2$	CF_3
α-CD	0.009	0.049	0.114	0.195
β-CD	0.156	0.809	0.020	0.036
RAMEB	0.892	1.458	≈0	-0.155
DM-β-CD	0.664	1.155	-0.094	-0.139
TM-β-CD	0.948	1.525	-0.305	-0.336
HP-β-CD	0.602	1.252	0.311	0.190

e: Sodium Perfluorononanoate (SPFN)

CD	$C(1)F_2$	$C(2)F_2$	$C(7)F_2$	CF_3
β-CD	0.124	0.588	0.054	0.109
RAMEB	0.782	1.261	-0.276†	-0.449†
DM-β-CD	0.649	1.093	-0.043†	-0.121†
TM-β-CD	0.871	1.326	-0.873†	-1.314†
HP-β-CD	0.500	1.073	0.251	0.183

†CIS value obtained at R=0.5

4.2.2 ^1H nuclei of β-cyclodextrin in aqueous solutions of sodium perfluoroalkyl carboxylate salts

The conditions for the measurement of ^1H NMR chemical shifts (cf. Appendix A4 for experimental data) of β-CD were described in § 4.1.2. Figures 4-7a-b illustrate plots of $\Delta\delta$ versus mole ratio (R) for two β-CD-fc surfactant systems. The concentration

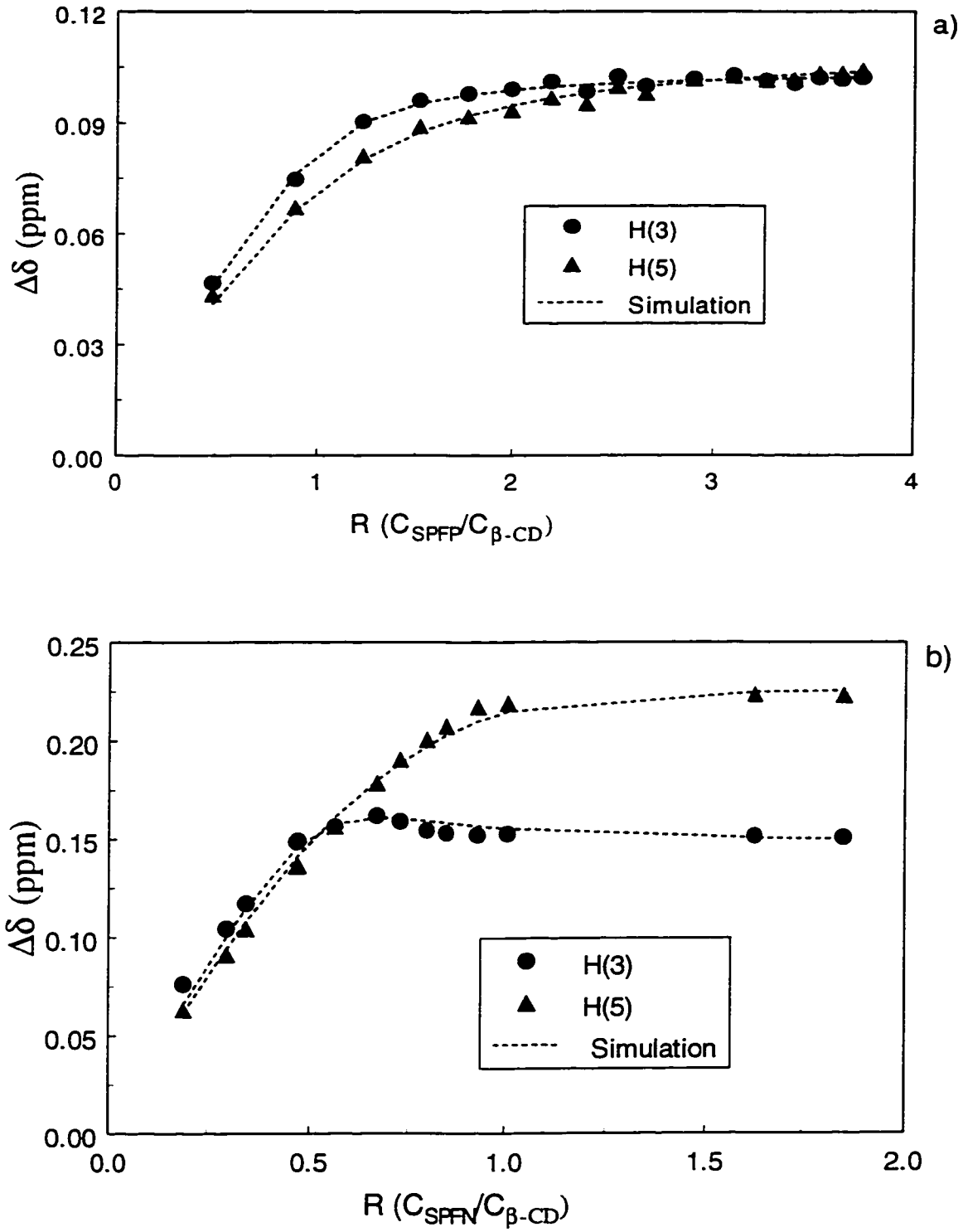

Figure 4-7. ^{1}H chemical shift difference ($\Delta\delta$) for β-CD plotted against mole ratio(R) at a fixed β-CD concentration of 5×10^{-3} molal and T=295 K: a) R=[SPFP]/[β-CD] and b) R=[SPFN]/[β-CD].

dependence of $\Delta\delta$ (cf. eq 3.2.1-1) in Figs. 4-7a-b are representative of fc surfactants that possess short and long alkyl chain length (C_x), respectively. In general, $\Delta\delta$ exhibits a positive increase as R increases and then levels off at higher mole ratios. The simulated curves in Figs. 4-7a-b were obtained using the two- and three-site models presented in § 2.1.2.

Table 4-6 lists the CIS values for the H(3) and H(5) protons of β-CD at R=1 and the values of K_i for various β-CD-S complexes. Values of K_i were obtained from the NLLS fitting of $\Delta\delta$ for H(3) and H(5) versus R using eqs. 2.1.2-4 to -6. The details of the

Table 4-6: Binding Constants[a] $(K_i)^{[b,c]}$ of Various β-CD-Sodium Perfluoroalkyl Carboxylate Complexes and ^{1}H NMR Complex Induced Shift Values at R=1[d] for the H(3) and H(5) Protons of β-CD at 295 K.

Surfactant	H(3) (ppm)	H(5) (ppm)	K_i [b,c]
SPFB	0.052	0.051	$9.8(2.0)\times10^{2}$[b]
SPFP	0.098	0.092	$2.4(0.28)\times10^{3}$[b]
SPFH	0.155	0.178	$2.80(0.90)\times10^{4}$[b]
SPFO	0.158	0.210	$5.00(2.5)\times10^{4}$[b]
			$4.3(2.1)\times10^{2}$[c]
SPFN	0.168[e]	0.226	$1.00(0.50)\times10^{5}$[b]
			$2.20(1.1)\times10^{3}$[c]
SPFD[f,g]	0.196[e]	0.237	$1.53(0.76)\times10^{5}$[b]
			$4.67(2.3)\times10^{3}$[c]

(a) Obtained from CIS values of H(3) and H(5) with standard error given in parentheses. (b) $K_{1:1}$ (M^{-1}), (c) $K_{2:1}$ (M^{-2}), (d) Obtained at a concentration of surfactant 5×10^{-3} molal, (e) Obtained at R=0.5, (f) SPFD=sodium perfluorodecanoate, (g) Obtained at a concentration surfactant of 2×10^{-3} molal.

simulation are analogous to that using the host ^{1}H NMR data in § 4.1.2. In general, the CIS values for H(5) exceed H(3) and their magnitude increases as C_x increases. As well, K_i (i=1:1 and 2:1) increase as C_x increases and the values are in reasonable agreement with the K_i values (Table 4-4) obtained from the guest ^{19}F nuclei.

4.3 Apparent molar volume studies

4.3.1 Apparent molar volume of sodium alkyl carboxylate salts in water and aqueous cyclodextrin solutions

The importance of volumetric changes of the host and/or guest can be related to the extensive involvement of hydration and dehydration processes in host-guest complexation. In this regard, apparent molar volume (AMV) studies are expected to provide new information on the volumetric properties of CD-surfactant complexes.

The details of the measurement of density and AMV (cf. Appendix A5 for experimental data) were given in § 3.2.2 and the equation (cf. eq 2.1.3-5) to determine the AMV was developed in § 2.1.3. The AMV of the surfactant ($V_{\phi,S}$) was obtained in water and in aqueous solutions containing a fixed concentration of CD. $V_{\phi,S}$ was measured as a function of increasing C_S and the mole ratio ($R=C_S/C_{CD}$) exceeded R=1. The AMV of the guest is plotted against the square root of the molality of the surfactant ($C_S^{1/2}$). On the right hand axis, the mole fractions of bound and unbound (X_i) surfactant in 0.013 m β-CD are plotted. The error bars for the AMV data represent the values obtained from the relations described in § 2.1.3. These curves are derived from substitution of

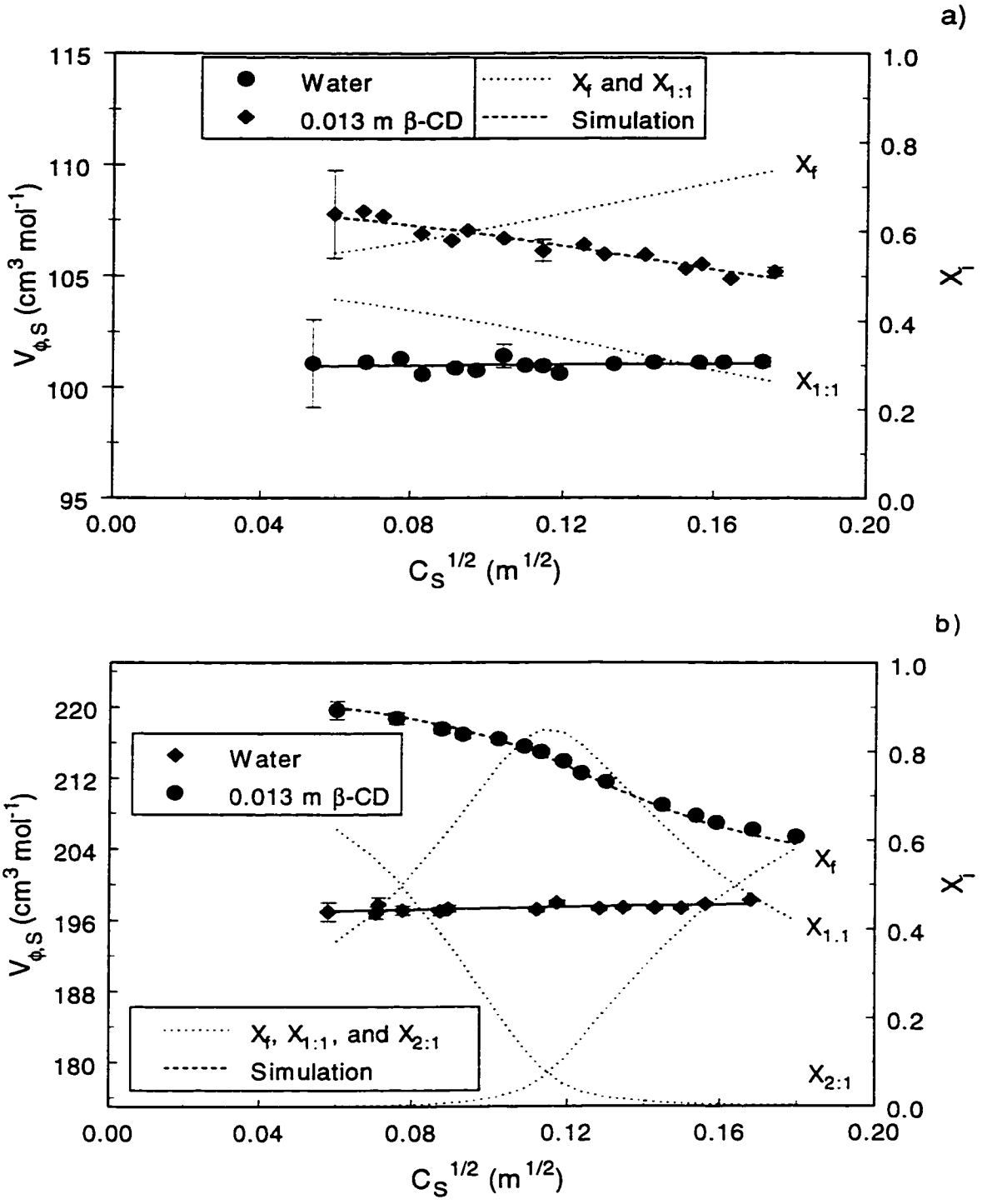

Figure 4-8: $V_{\phi,S}$ versus $C_S^{1/2}$ in water and 0.013 m β-CD at pH 10.5 and T=298 K: a) SHex and b) SDodec. The curves for X_f and $X_{1:1}$ versus $C_S^{1/2}$ are for the surfactant in 0.013 m β-CD.

concentration and K_i values into the appropriate equilibrium expression (eq 1.3.2.1-1). In water, $V_{\phi,S}$ exhibits a slightly positive slope as $C_S^{1/2}$ increases, in agreement with the sign predicted by the Debye Hückel limiting law for a 1:1 electrolyte.[32] The solid line through the $V_{\phi,S}$ data in water represents the least squares linear regression. In aqueous CD solutions, $V_{\phi,S}$ generally displays a linear or nonlinear decrease as $C_S^{1/2}$ increases. At higher surfactant concentrations, the value of $V_{\phi,S}$ in aqueous CD approaches the value of $V_{\phi,S}$ in water. The concentration dependence of $V_{\phi,S}$ in ternary (w+S+CD) systems can be related to the mole fractions of various species weighted by their AMV according to the two- and three-site models presented in § 2.1.3. The simulated lines through the data points in Figs. 4-8a-b correspond to the best-fit curves predicted by the two- and three-site models, respectively, presented in § 2.1.3. The simulation of $V_{\phi,S}$ was performed by allowing the AMV of the bound species ($V_{\phi,i}$; where i=1:1, 2:1, and/or 1:2) and K_i to be adjustable parameters. The value of $V_{\phi,f}$ was taken to be equivalent to the apparent molar volume at infinite dilution, $V^\circ_{\phi,S}$, and was obtained from a linear regression of $V_{\phi,S}$ versus $C_S^{1/2}$ in water.

Tables 4-7 to 4-9 list the AMV of the surfactants at infinite dilution ($V^\circ_{\phi,S}$) in water and in aqueous CD, infinite dilution transfer volume (ΔV°_S), and calculated binding constants (K_i) for the CD-S complexes. In general, the magnitudes of K_i and $V^\circ_{\phi,S}$ increase as the alkyl chain length (C_x) increases. There are some differences in K_i and $V^\circ_{\phi,S}$ for a common guest with different host systems and can be related to the type of alkyl substitution in the CD annulus region.

Table 4-7: Apparent Molar Volume of Sodium Alkyl Carboxylate Salts at Infinite Dilution in Water and Aqueous β-CD Solutions[a] and Calculated Binding Constants[b,c] (K_i)[d,e] for β-CD-Sodium Alkyl Carboxylate Complexes at pH 10.5 and 298 K.

Surfactant	$V^{\circ}_{\phi,S}$ ($cm^3\ mol^{-1}$) Water	$V^{\circ}_{\phi,S}$ ($cm^3\ mol^{-1}$) Aqueous β-CD[a]	ΔV°_S ($cm^3\ mol^{-1}$)[f]	K_i (β-CD-S) from $V_{\phi,S}$ [d,e]
$C_2H_5CO_2Na$ SP	53.8	53.9	≈0	≈0
$C_5H_{11}CO_2Na$ SHex	100.9	110.2	9.3	$7.0\pm1.83 \times 10^{1}$[(d)]
$C_6H_{13}CO_2Na$ SHep	116.6 116.8[g]	130.7	14.1	$1.93\pm0.188 \times 10^{2}$[(d)]
$C_7H_{16}CO_2Na$ SO	133.0 132.4[g]	151.2	18.2	$6.22\pm0.388 \times 10^{2}$[(d)]
$C_8H_{17}CO_2Na$ SN	148.6 148.3[g]	170.3	21.7	$1.59\pm0.892 \times 10^{3}$[(d)]
$C_9H_{19}CO_2Na$ SDec	165.1 164.2[g]	188.6	23.5	$2.14\pm1.94 \times 10^{3}$[(d)]
$C_{11}H_{23}CO_2Na$ SDodec	196.9 195.8[h]	225.0	28.1	$2.80\pm1.40 \times 10^{4}$[(d)] $2.15\pm1.08 \times 10^{2}$[(c)]
$C_{13}H_{27}CO_2Na$ ST	226.7 226.4[g]	270.0	43.3	$3.50\pm1.75 \times 10^{4}$[(d)] $3.00\pm1.50 \times 10^{2}$[(c)]

[a]Concentration of aqueous β-CD approximately 1.3×10^{-2} molal in all cases

[b]Two-site Model: $V_\phi = X_f\, V_{\phi,f} + X_{1:1}\, V_{\phi,1:1}$.

[c]Three-site Model: $V_\phi = X_f\, V_{\phi,f} + X_{1:1}\, V_{\phi,1:1} + X_{2:1}\, V_{\phi,2:1}$.

[d]$K_{1:1}$($kg\ mol^{-1}$) with standard error in parentheses.

[e]$K_{2:1}$($kg^2\ mol^{-2}$) with standard error in parentheses.

[f]$\Delta V^{\circ}_S = V^{\circ}_{\phi,S}$ (β-CD(aq)) - $V^{\circ}_{\phi,S}$ (water), [g]ref 188, and [h]ref 189.

Table 4-8: Apparent Molar Volume of Sodium Alkyl Carboxylate Salts at Infinite Dilution in Water and Aqueous DM-β-CD Solutions[a] and Calculated Binding Constants[b,c] (K_i)[d,e] for DM-β-CD-Sodium Alkyl Carboxylate Complexes at pH 10.5 and 298 K.

Surfactant	$V^{o}_{\phi,S}$ ($cm^3 mol^{-1}$) Water	$V^{o}_{\phi,S}$ ($cm^3 mol^{-1}$) Aqueous DM-β-CD[a]	ΔV^{o}_{S} ($cm^3 mol^{-1}$)[f] Aqueous DM-β-CD	K_1 (DM-β-CD-S) from $V_{\phi,S}$ [d,e]	K_1 (DM-β-CD-S) from $V_{\phi,DM\text{-}\beta\text{-}CD}$ [d,e]
$C_5H_{11}CO_2Na$ SHex	100.9	104.0	3.1	$2.1\times10^2(8.1\times10^1)^d$	$1.0\times10^2(5.0\times10^1)^d$
$C_7H_{16}CO_2Na$ SO	133.0	145.0	12.0	$2.99\times10^2(3.46\times10^1)^d$	$3.15\times10^2(6.37\times10^1)^d$
$C_9H_{19}CO_2Na$ SDec	165.1	184.5	19.4	$3.53\times10^3(9.73\times10^2)^d$	$2.42\times10^3(3.50\times10^2)^d$
$C_{11}H_{23}CO_2Na$ SDodec	196.9	221.3	24.4	$1.68\times10^4(4.42\times10^3)^d$	$1.00\times10^4(2.92\times10^3)^d$
$C_{13}H_{27}CO_2Na$ ST	226.7	255.9	29.2	$8.00\times10^4(4.00\times10^4)^d$ $3.00\times10^3(1.50\times10^3)^e$	$3.56\times10^4(1.28\times10^4)^d$ ND[e]

[a] $C_{DM\text{-}\beta\text{-}CD} \approx 4.0 \times 10^{-3}$ m in all cases

[b] Two-site Model: $V_\phi = X_f V_{\phi,f} + X_{1:1} V_{\phi,1:1}$.

[c] Three-site Model: $V_\phi = X_f V_{\phi,f} + X_{1:1} V_{\phi,1:1} + X_{1:2} V_{\phi,1:2}$.

[d] $K_{1:1}$($kg\ mol^{-1}$) with standard error in parentheses.

[e] $K_{1:2}$($kg^2\ mol^{-2}$) with standard error in parentheses.

[f] $\Delta V^{o}_{S} = V^{o}_{\phi,S}$ (DM-β-CD(aq)) - $V^{o}_{\phi,S}$ (water)

ND=not detected under these experimental conditions

Table 4-9: Apparent Molar Volume of Sodium Alkyl Carboxylate Salts at Infinite Dilution in Water and Aqueous HP-β-CD Solutions[a] and Calculated Binding Constants[b] (K_i)[c] for HP-β-CD-Sodium Alkyl Carboxylate Complexes at 298 K at pH 10.5 and 298 K.

Surfactant	$V^o_{\phi,S}$ ($cm^3 mol^{-1}$) Water	$V^o_{\phi,S}$ ($cm^3 mol^{-1}$) Aqueous HP-β-CD[a]	ΔV^o_S ($cm^3 mol^{-1}$)[d] Aqueous HP-β-CD	K_i (HP-β-CD-S) from $V_{\phi,S}$ [c]	K_i (HP-β-CD-S) from $V_{\phi,HP\text{-}\beta\text{-}CD}$ [c]
$C_5H_{11}CO_2Na$ SHex	100.9	102.1	1.2	$1.0x10^2(6.3x10^1)^c$	$1.2x10^2(4.1x10^1)^c$
$C_7H_{16}CO_2Na$ SO	133.0	145.2	12.2	$3.26x10^2(3.28x10^1)^c$	$1.72x10^2(2.08x10^1)^c$
$C_9H_{19}CO_2Na$ SDec	165.1	182.6	17.5	$5.50x10^3(1.21x10^3)^c$	$1.00x10^3(5.63x10^2)^c$
$C_{11}H_{23}CO_2Na$ SDodec	196.9	219.4	22.5	$4.48x10^3(1.40x10^3)^c$	$2.72x10^3(1.22x10^3)^c$
$C_{13}H_{27}CO_2Na$ ST	226.7	254.0	27.3	$8.00x10^3(2.55x10^3)^c$	$1.00x10^4(4.14x10^3)^c$

[a] $C_{HP\text{-}\beta\text{-}CD} \approx 5.0 \times 10^{-3}$ m in all cases

[b] Two-site Model: $V_\phi = X_f V_{\phi,f} + X_{1:1} V_{\phi,1:1}$.

[c] $K_{1:1}$($kg\ mol^{-1}$) with standard error in parentheses.

[d] $\Delta V^o_S = V^o_{\phi,S}$ (HP-β-CD(aq)) - $V^o_{\phi,S}$ (water)

4.3.2. Apparent molar volume of sodium perfluoroalkyl carboxylate salts in water and aqueous cyclodextrin solutions

The details of the calculation of $V_{\phi,S}$ for the sodium perfluoroalkyl carboxylate salts are analogous to that described in § 4.3.1 for the sodium alkyl carboxylate salts. The primary data for these systems are shown in Appendix A6. Figure 4-9 illustrates the different types of volumetric behaviour for a long chain length fc alkyl carboxylate salt in aqueous solutions containing each of the three different CDs. In water, $V_{\phi,S}$ decreases linearly as $C_S^{1/2}$ increases in contrast to a positive increase for shorter chain length fc surfactants. The amphiphilic nature of the salt should decrease the magnitude of the Debye Hückel slope[32] because of hydrophobic hydration and this is seen to be the case. In ternary solution (w+S+CD), $V_{\phi,S}$ exhibits a complex nonlinear concentration dependence that is consistent with the formation of inclusion complexes.

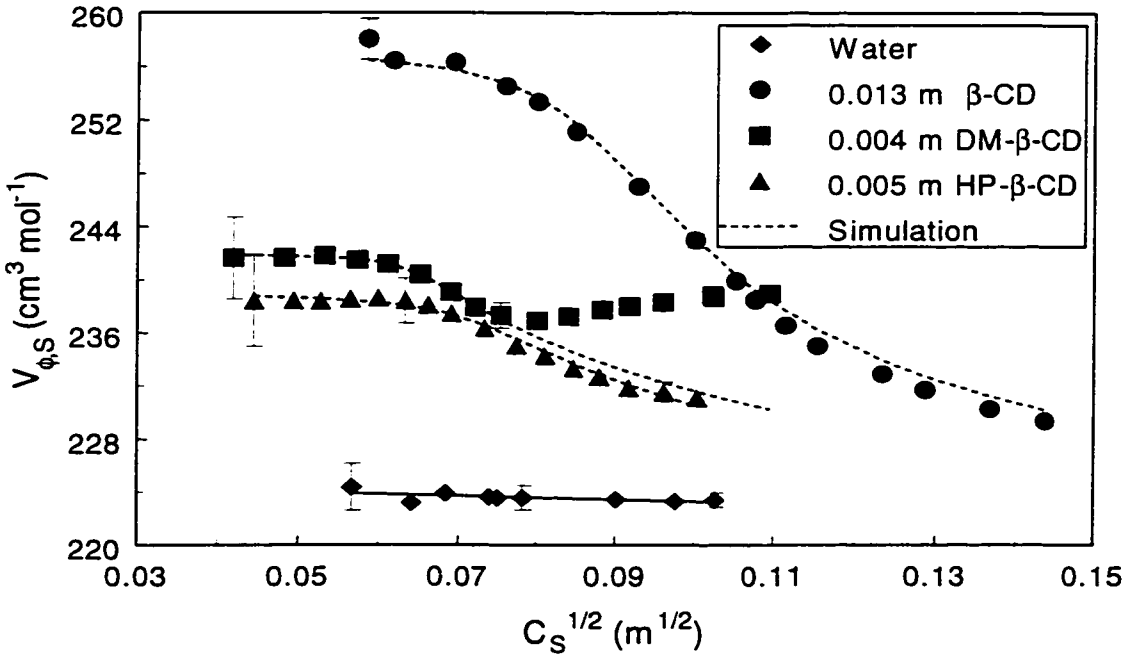

Figure 4-9: $V_{\phi,S}$ versus $C_S^{1/2}$ for SPFN in water and aqueous β-CD, DM-β-CD, and HP-β-CD solutions at pH 10.5 and T=298 K.

The mole fractions (X_i) of the bound species decrease in a similar manner as $V_{\phi,S}$ with increasing concentration. As such, the concentration dependence of $V_{\phi,S}$ in ternary solutions can be explained according to the two- and three-site models presented in § 2.1.3 by substitution of the appropriate mole fractions, X_i and X_f, into these expressions. The lines through the data points in Figures 4-9 correspond to the best-fit curves using eqs 2.1.3-10 to -12.

Tables 4-10 to 4-12 list the AMV of the sodium perfluoroalkyl carboxylates in water and aqueous CD solutions at infinite dilution ($V^{\circ}_{\phi,S}$), the infinite dilution transfer volumes (ΔV°_{S}), and binding constants (K_i) for the CD-S complexes. In general, the magnitude of K_i and $V^{\circ}_{\phi,S}$ increases as C_x increases. There are some differences in K_i and $V^{\circ}_{\phi,S}$ for a common surfactant with different host systems and they can be correlated with the type of alkyl substitution in the CD annulus region.

Table 4-10: Apparent Molar Volume of Sodium Perfluoroalkyl Carboxylate Salts at Infinite Dilution in Water and Aqueous β-CD Solutions[a] and Calculated Binding Constants[b,c] (K_i) [d,e] for β-CD-Sodium Perfluoroalkyl Carboxylate Complexes at pH 10.5 and 298 K.

Surfactant	$V^o_{\phi,S}$ (H_2O) (cm^3mol^{-1})	$V^o_{\phi,S}$ (β-CD)[a] (cm^3mol^{-1})	ΔV^o_S (cm^3mol^{-1})[b]	K_i (β-CD-S) from $V_{\phi,S}$ [d,e]
$C_2F_5O_2Na$ SPFA	56.9 57.2[g],57.28[i]	60.8	3.9	$1.0\pm0.85 \times 10^{2}$ [d]
$C_3F_7CO_2Na$ SPFB	104.7 104.9[g],105.00[i]	117.7	13.0	$1.70\pm0.384 \times 10^{2}$ [d]
$C_4F_9CO_2Na$ SPFP	128.5 128.5[c]	142.9	14.4	$1.64\pm0.260 \times 10^{3}$ [d]
$C_6F_{13}CO_2Na$ SPFH	175.9 175.9[c]	196.7	20.8	$8.75\pm6.60 \times 10^{3}$ [d]
$C_7F_{15}CO_2Na$ SPFO	200.6 199.3[g],199.23[i]	225.1	24.5	$1.00\pm0.500 \times 10^{4}$ [d] $1.20\pm0.600 \times 10^{3}$
$C_8F_{17}CO_2Na$ SPFN	225.1 225±2[h]	260.0	34.9	$6.50\pm3.25 \times 10^{4}$ [d] $2.00\pm1.00 \times 10^{3}$ [e]
$C_9F_{19}CO_2Na$ SPFD	249.0*	290.0	41.0	$7.00\pm3.50 \times 10^{5}$ [d] $3.50\pm1.50 \times 10^{3}$ [e]

[a] $C_{\beta\text{-CD}} \approx 1.3 \times 10^{-2}$ m in all cases

[b] Two-site Model: $V_\phi = X_f V_{\phi,f} + X_{1:1} V_{\phi,1:1}$.

[c] Three-site Model: $V_\phi = X_f V_{\phi,f} + X_{1:1} V_{\phi,1:1} + X_{2:1} V_{\phi,2:1}$.

[d] $K_{1:1}$($kg\ mol^{-1}$) with standard error in parentheses.

[e] $K_{2:1}$($kg^2\ mol^{-2}$) with standard error in parentheses.

[f] $\Delta V^o_S = V^o_{\phi,S}$ (β-CD(aq)) - $V^o_{\phi,S}$ (water)

[g] ref. 190, [h] ref. 191, and [i] ref. 192.

* $V^o_{\phi,S}$ determined from density data at concentrations from $0.5\text{-}2.0 \times 10^{-3}$ m.

Table 4-11: Apparent Molar Volume of Sodium Perfluoroalkyl Carboxylate Salts at Infinite Dilution in Water and Aqueous DM-β-CD Solutions and Binding Constants[b,c] (K_i)[d,e] for DM-β-CD-Sodium Perfluoroalkyl Carboxylate Complexes at 298 K at pH 10.5 and 298 K.

Surfactant	$V^{\circ}_{\phi,S}(H_2O)$ (cm^3mol^{-1})	$V^{\circ}_{\phi,S}$(DM-β-CD)[a] (cm^3mol^{-1})	ΔV°_S(DM-β-CD)[f] (cm^3mol^{-1})	K_i (DM-β-CD-S) from $V_{\phi,S}$ [d,e]	K_i (DM-β-CD-S) from $V_{\phi,DM\text{-}\beta\text{-}CD}$ [d,e]
$C_3F_7CO_2Na$ SPFB	104.7	110.2	5.5	$1.3x10^2(5.6x10^1)^d$	$4.3x10^1(3.9x10^0)^d$
$C_4F_9CO_2Na$ SPFP	175.9	191.2	15.3	$4.00x10^3(1.55x10^4)^d$	$3.00x10^3(1.19x10^4)^d$
$C_6F_{13}CO_2Na$ SPFH	200.6	216.3	15.7	$6.01x10^4(2.65x10^4)^d$	$4.00x10^4(1.87x10^4)^d$
$C_7F_{15}CO_2Na$ SPFO	225.1	240.8	15.7	$7.00x10^4(3.50x10^4)^d$	$6.00x10^4(3.00x10^4)^d$
				$5.00x10^2(2.50x10^2)^e$	$3.00x10^3(1.50x10^3)^e$
$C_8F_{17}CO_2Na$ SPFN	249.0*	264.5	15.5	$1.00x10^5(5.00x10^4)^d$	$1.00x10^5(5.00x10^4)^d$
				$6.00x10^3(2.50x10^3)^e$	$5.00x10^3(2.50x10^3)^e$

[a] $C_{DM\text{-}\beta\text{-}CD} \approx 4.0 \times 10^{-3}$ m in all cases.

[b] Two-site Model: $V_\phi = X_f V_{\phi,f} + X_{1:1} V_{\phi,1:1}$

[c] Three-site Model: $V_\phi = X_f V_{\phi,f} + X_{1:1} V_{\phi,1:1} + X_{1:2} V_{\phi,1:2}$.

[d] $K_{1:1}$($kg\ mol^{-1}$) with standard error in parentheses.

[e] $K_{1:2}$($kg^2\ mol^{-2}$) with standard error in parentheses.

[f] $\Delta V^{\circ}_S = V^{\circ}_{\phi,S}$ (DM-β-CD(aq)) - $V^{\circ}_{\phi,S}$ (water)

* $V^{\circ}_{\phi,S}$ obtained from volume data in the concentration range 0.5-2.0 x 10^{-3} m.

Table 4-12: Apparent Molar Volume of Sodium Perfluoroalkyl Carboxylate Salts at Infinite Dilution in Water and Aqueous HP-β-CD Solutions[a] and Calculated Binding Constants (K_i) for HP-β-CD-Sodium Perfluoroalkyl Carboxylate Complexes at 298 K and at pH 10.5.

Surfactant	$V^{\circ}_{\phi,S}(H_2O)$ (cm^3mol^{-1})	$V^{\circ}_{\phi,S}$(HP-β-CD)[a] (cm^3mol^{-1})	ΔV°_S(HP-β-CD)[d] (cm^3mol^{-1})	K_i (HP-β-CD-S) from $V_{\phi,S}$[c]	K_i (HP-β-CD-S) from $V_{\phi,HP\text{-}\beta\text{-}CD}$[c]
$C_3F_7CO_2Na$ SPFB	104.7	109.5	4.8	$1.3\times10^2(5.6\times10^1)$[c]	$1.8\times10^2(3.5\times10^1)$[c]
$C_4F_9CO_2Na$ SPFP	175.9	189.8	13.9	$1.70\times10^3(7.89\times10^3)$[c]	$1.67\times10^3(7.68\times10^3)$[c]
$C_6F_{13}CO_2Na$ SPFH	200.6	214.7	14.1	$3.14\times10^4(2.10\times10^4)$[c]	$2.61\times10^4(1.05\times10^4)$[c]
$C_7F_{15}CO_2Na$ SPFO	225.1	238.8	13.7	$4.00\times10^4(2.91\times10^4)$[c]	$3.33\times10^4(1.01\times10^4)$[c]
$C_8F_{17}CO_2Na$ SPFN	249.0*	263.0	14.0	$5.00\times10^4(2.02\times10^4)$[c]	$4.10\times10^4(3.02\times10^4)$[c]

[a] $C_{HP\text{-}\beta\text{-}CD} \approx 5.0 \times 10^{-3}$ m in all cases.

[b] Two-site Model: $V_\phi = X_f V_{\phi,f} + X_{1:1} V_{\phi,1:1}$

[c] $K_{1:1}$($kg\ mol^{-1}$) with standard error in parentheses.

[d] $\Delta V^{\circ}_S = V^{\circ}_{\phi,S}$ (HP-β-CD(aq)) - $V^{\circ}_{\phi,S}$ (water)

* $V^{\circ}_{\phi,S}$ Extrapolated from volume data in the concentration range 0.5-2.0 x 10^{-3} m.

4.3.3 Apparent molar volume of cyclodextrins in water

The densities and the calculated AMV of the CDs (cf. Appendix A7 for experimental data) in water were obtained in a manner similar to that described for the surfactants in water, cf. § 2.1.3. The apparent molar volume of β-CD, $V_{\phi,\beta\text{-CD}}$, plotted against the concentration of CD (C_{CD}) is shown in Figure 4-10. Data taken from the literature are shown for comparison.[193,194] The AMV for β-CD shows a slight linear increase with increasing C_{CD} and is in good agreement with the data of Milioto *et al.*[193] Somewhat poorer agreement was found with the data of Paduano *et al.*[194] The latter may be due to inaccuracies in their estimates of the water content of β-CD and/or their density data.

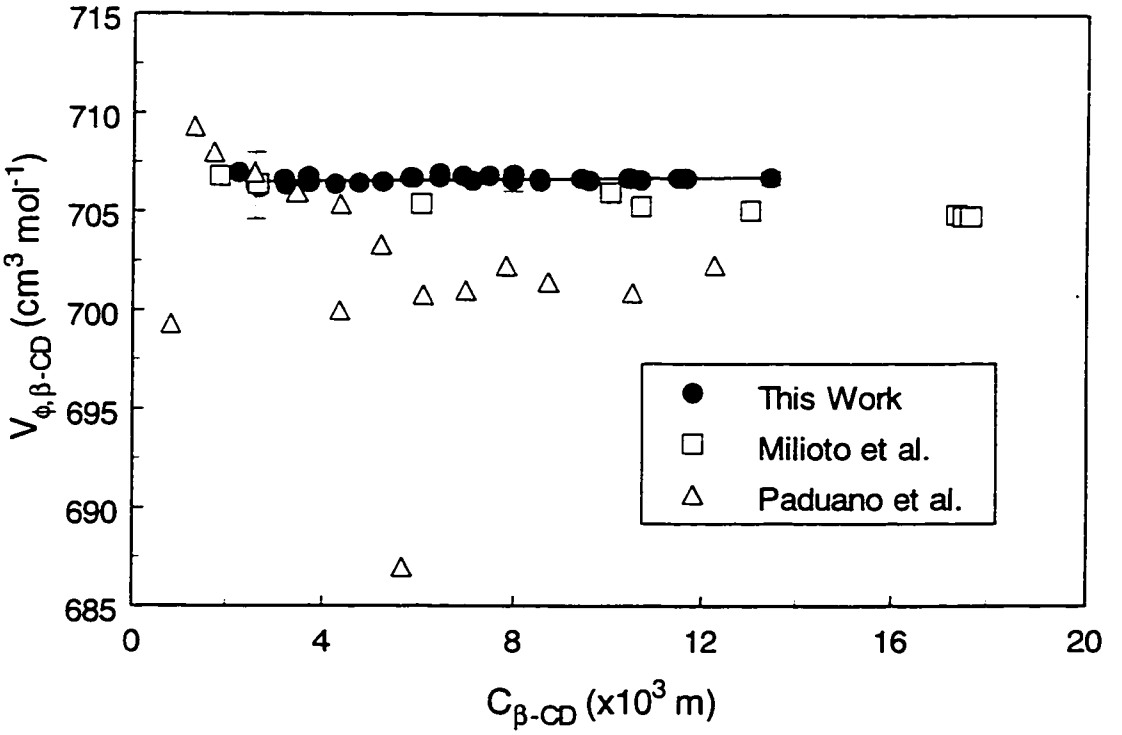

Figure 4-10: $V_{\phi,\beta\text{-CD}}$ versus the concentration of β-CD ($C_{\beta\text{-CD}}$) in water at T=298 K. Experimental data obtained at pH 10.5; pH of literature[193,194] data not stated.

The concentration dependence of $V_{\phi,R\text{-}\beta\text{-}CD}$ (DM-β-CD and HP-β-CD) in water are similar, as shown by analysis of the data according to the relation

$$V_{\phi,CD} = V^{o}_{\phi,CD} + B_v\, m \qquad (4.3.3\text{-}1)$$

where $V^{o}_{\phi,CD}$ is the AMV of the CD at infinite dilution and B_v is the first derivative of $V_{\phi,CD}$ with respect to molality (m). The values obtained for $V^{o}_{\phi,CD}$(cm^3 mol^{-1}) and B_v (cm^3 kg mol^{-2}), respectively, are: β-CD(706.4 and 20.0), DM-β-CD(984.5 and 157), and HP-β-CD(958.2 and 164).

4.3.4 Apparent molar volume of cyclodextrins in aqueous solutions of sodium alkyl carboxylate salts

The AMV of the CDs were determined in water and in aqueous surfactant solutions with C_S held constant and maintained below the CMC while C_{CD} was varied (cf. Appendix A8 for experimental data). The details of the calculation of $V_{\phi,CD}$ are described in § 4.3.4.

Figures 4-11a-b illustrate typical volumetric behaviour of CDs in aqueous solutions of a short and long chain length alkyl carboxylate salts, respectively. Due to differences in $V^{o}_{\phi,CD}$ for each of the CDs investigated, the data are plotted as a volume difference according to the relation

$$\Delta V_{CD} = V_{\phi,CD} - V^{o}_{\phi,CD} \qquad (4.3.4\text{-}1)$$

where ΔV_{CD} is the difference in apparent molar volume at any concentration. This strategy provides a way of comparing volumetric data of different host molecules. The magnitude of ΔV_{CD} decreases as C_{CD} increases and the profiles are linear or nonlinear depending on the chain length of the surfactant. The longest hydrocarbon chain guests display a nonlinear concentration dependence whereas shorter chain hc surfactants display linear behaviour. The concentration dependence of ΔV_{CD} in ternary (w+S+CD) systems were analyzed (simulated results are shown as dashed lines) according to the two- and three-site models presented in § 2.1.3 and the simulated lines through the data points are shown. The simulation of ΔV_{CD} utilizes the AMV of the bound species ($V_{\phi,i}$; where i=1:1, 2:1, and/or 1:2) and K_i as adjustable parameters. The value of $V_{\phi,f} \equiv V^{\circ}_{\phi,CD}$ was obtained from a linear regression of $V_{\phi,S}$ versus $C_S^{1/2}$ in water. Difficulty in the simulation of ΔV_{CD} at higher surfactant concentrations was encountered because of the small change in the AMV over the concentration range studied and it is for this reason that there is an absence of fitted lines in Figures 4-11a-b for these conditions. Also, it is less valid to assume $V_{\phi,f} \equiv V^{\circ}_{\phi,CD}$ at these higher surfactant concentrations, according to Young's rule,[20] and this may contribute to difficulties with the simulation.

Tables 4-13 and -14 list the AMV of the CDs in water and aqueous surfactant solutions at infinite dilution ($V^{\circ}_{\phi,CD}$) and the infinite dilution transfer volume (ΔV°_{CD}). In general, the magnitudes of K_i and $V^{\circ}_{\phi,CD}$ increase as C_x increases. There are some differences between these parameters for a given CD-S complex with a common

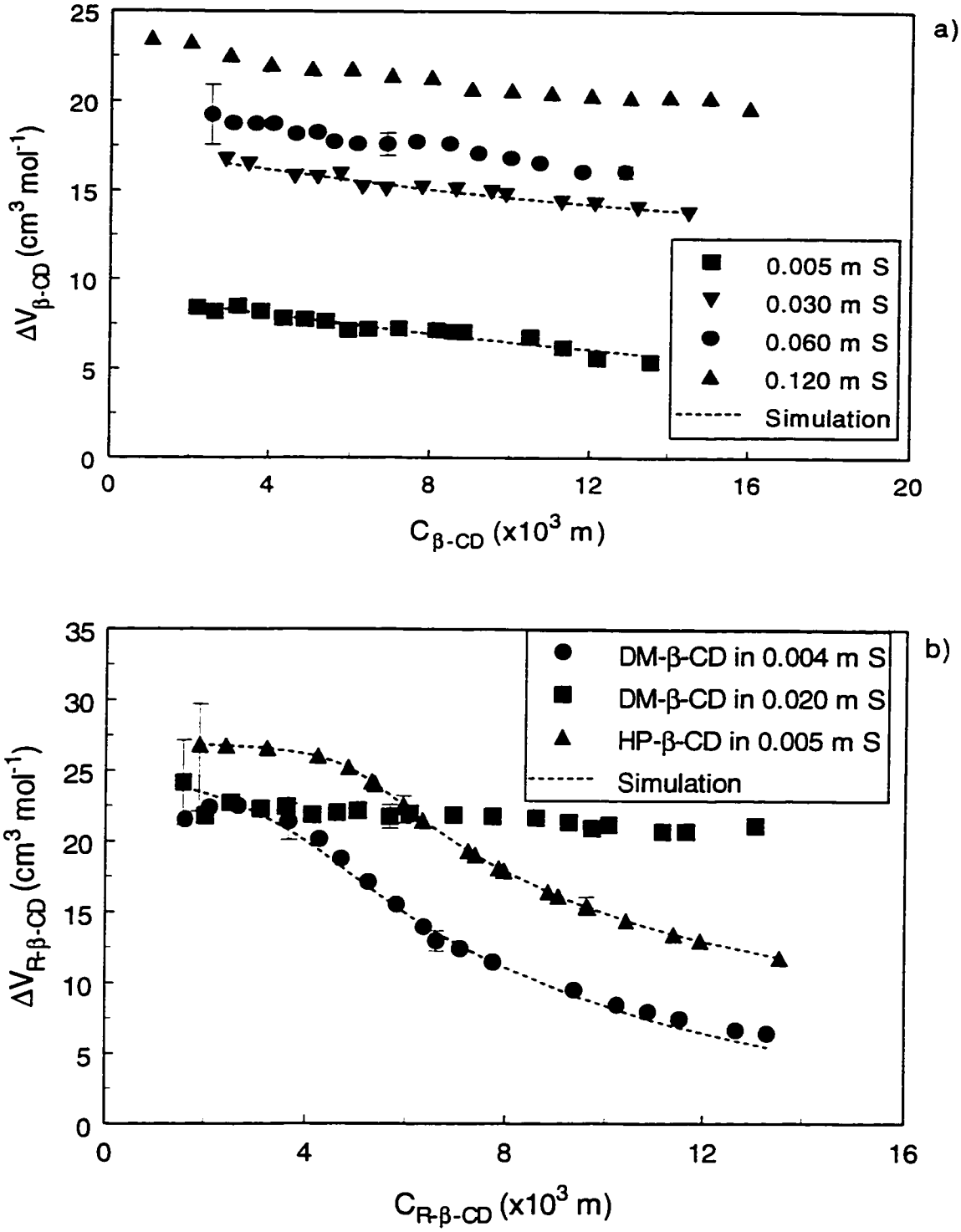

Figure 4-11: ΔV_{CD} versus C_{CD} for β-CD and modified β-CDs in water and aqueous solutions of sodium alkyl carboxylate salts at various concentrations and at pH 10.5 and T=298 K: a) β-CD-S system where S=SHex and b) R-β-CD-S system where S=SDodec.

Table 4-13: Apparent Molar Volume of β-CD at Infinite Dilution in Aqueous Solutions of Sodium Alkyl Carboxylate Salts of Various Concentrations at pH 10.5 and 298 K.

Surfactant	[Surfactant] ($\times 10^3$ molal)	$V^{\circ}_{\phi,\beta\text{-CD}}$ (cm^3mol^{-1})	$\Delta V^{\circ}_{\beta\text{-CD}}$ (cm^3mol^{-1})[a]
$C_5H_{11}CO_2Na$	5, 120, 240	715.5, 726.0, 729.5	9.1, 19.6, 23.1
$C_7H_{15}CO_2Na$	5, 15 120	722.5, 728.0, 733.5	16.1, 21.6, 27.1
$C_9H_{19}CO_2Na$	5, 15, 60	726.0, 728.0, 731.0	21.6, 21.6, 24.6
$C_{11}H_{23}CO_2Na$	5, 10, 20	733.0, 732.5, 732.5	26.6, 26.1, 26.1
$C_{13}H_{25}CO_2Na$	5	732.5	26.1

[a] $\Delta V^{\circ}_{\beta\text{-CD}} = V^{\circ}_{\phi,\beta\text{-CD}}$ (surfactant(aq)) - $V^{\circ}_{\phi,\beta\text{-CD}}$ (water)
$V^{\circ}_{\phi,\beta\text{-CD}} = 706.4\ cm^3\ mol^{-1}$

Table 4-14: Apparent Molar Volumes of DM-β-CD and HP-β-CD at Infinite Dilution in Aqueous Solutions of Sodium Alkyl Carboxylate Salts at pH 10.5 and 298 K.

Surfactant	$V^{\circ}_{\phi,DM-\beta-CD}$ (cm^3mol^{-1})[a]	$\Delta V^{\circ}_{DM-\beta-CD}$ (cm^3mol^{-1})[b]	$V^{\circ}_{\phi,HP-\beta-CD}$ (cm^3mol^{-1})[c]	$\Delta V^{\circ}_{HP-\beta-CD}$ (cm^3mol^{-1})[b]
$C_5H_{11}CO_2Na$	986.7	2.2	961.3	3.1
$C_7H_{15}CO_2Na$	995.3	10.8	970.0	11.8
$C_9H_{19}CO_2Na$	1004.0	19.5	979.0	20.8
$C_{11}H_{23}CO_2Na$	1007.3	22.8	986.0	27.8
$C_{13}H_{25}CO_2Na$	1011.9	27.4	985.7	27.5

[a] $C_s \approx 4.0 \times 10^{-3}$ m in all cases.
[b] $\Delta V^{\circ}_{R-\beta-CD} = V^{\circ}_{\phi,R-\beta-CD}$ (surfactant(aq)) - $V^{\circ}_{\phi,R-\beta-CD}$ (water).
[c] $C_s \approx 5.0 \times 10^{-3}$ m in all cases.
$V^{\circ}_{\phi,DM-\beta-CD} = 984.5\ cm^3\ mol^{-1}$ (water) and $V^{\circ}_{\phi,HP-\beta-CD} = 958.2\ cm^3\ mol^{-1}$ (water)

surfactant which can be correlated with the type of alkyl substitution in the CD annulus region.

4.3.5 Apparent molar volume of cyclodextrins in aqueous solutions of sodium perfluoroalkyl carboxylate salts

The density, AMV, and concentration data for cyclodextrins in aqueous solutions of fc surfactants are listed in Appendix A9. Figures 4-12a-f illustrate the different types of volumetric behaviour of various CDs in aqueous solutions that contain a long chain sodium perfluoroalkyl carboxylate salt. The data are plotted as ΔV_{CD} versus C_{CD} for the reasons described in § 4.3.4. The magnitude of ΔV_{CD} increases or decreases in a linear or nonlinear fashion as C_{CD} increases depending on the chain length of the surfactant. The concentration dependence of ΔV_{CD} in ternary (w+S+CD) can be described by the two- and three-site models presented in § 2.1.3. The best-fit lines through the data points in Figs. 4-12a-f were obtained using the two- and three-site models. The simulation of ΔV_{CD} in ternary solutions was described in § 4.3.4. Similar difficulties were encountered with the simulation of $V_{\phi,CD}$ (cf. § 4.3.4) at higher surfactant concentrations (cf. Figs. 4-12a, e, and f); however, the nonideality was more pronounced than in the case of hydrocarbon guests.

Tables 4-16 and -17 list the AMV of the CDs in water and aqueous surfactant solutions at infinite dilution ($V^{\circ}_{\phi,CD}$) and the infinite dilution transfer volumes (ΔV°_{CD}). In general, the magnitudes of K_i and $V^{\circ}_{\phi,CD}$ increase as C_x increases. There are some differences between these parameters for a given CD-S complex with a common surfactant which can be correlated with the type of alkyl substitution at the CD annulus.

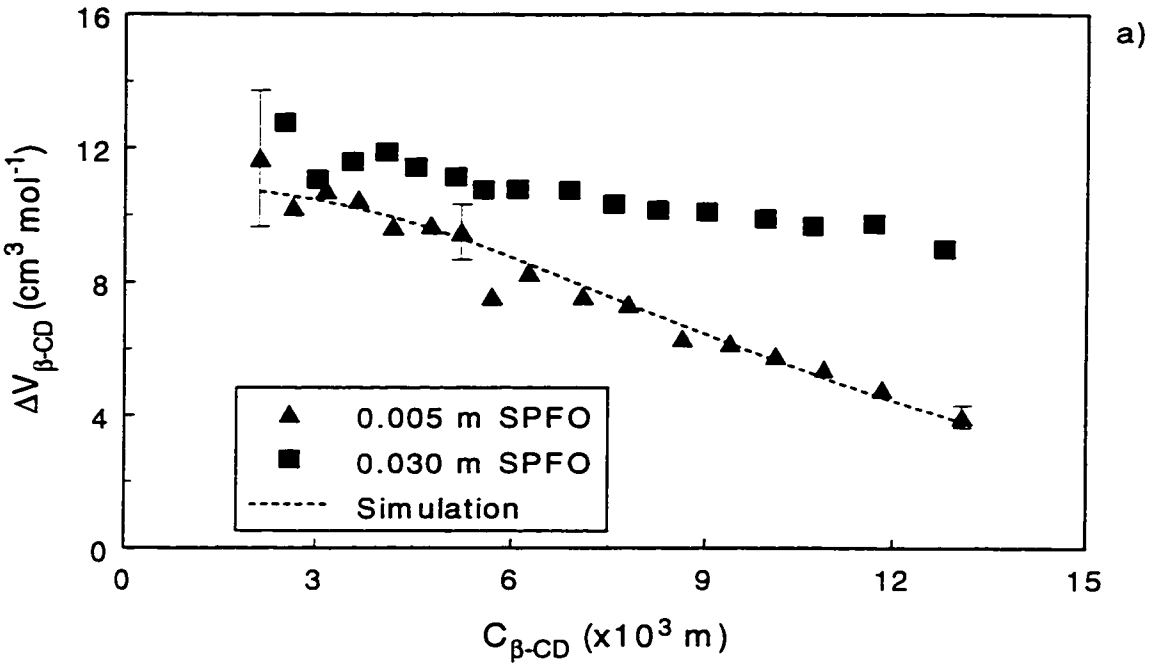
a)
16
12
8
4
0
0
3
6
9
12
15
$\Delta V_{\beta\text{-CD}}$ ($cm^3\ mol^{-1}$)
$C_{\beta\text{-CD}}$ ($x10^3$ m)
0.005 m SPFO
0.030 m SPFO
Simulation

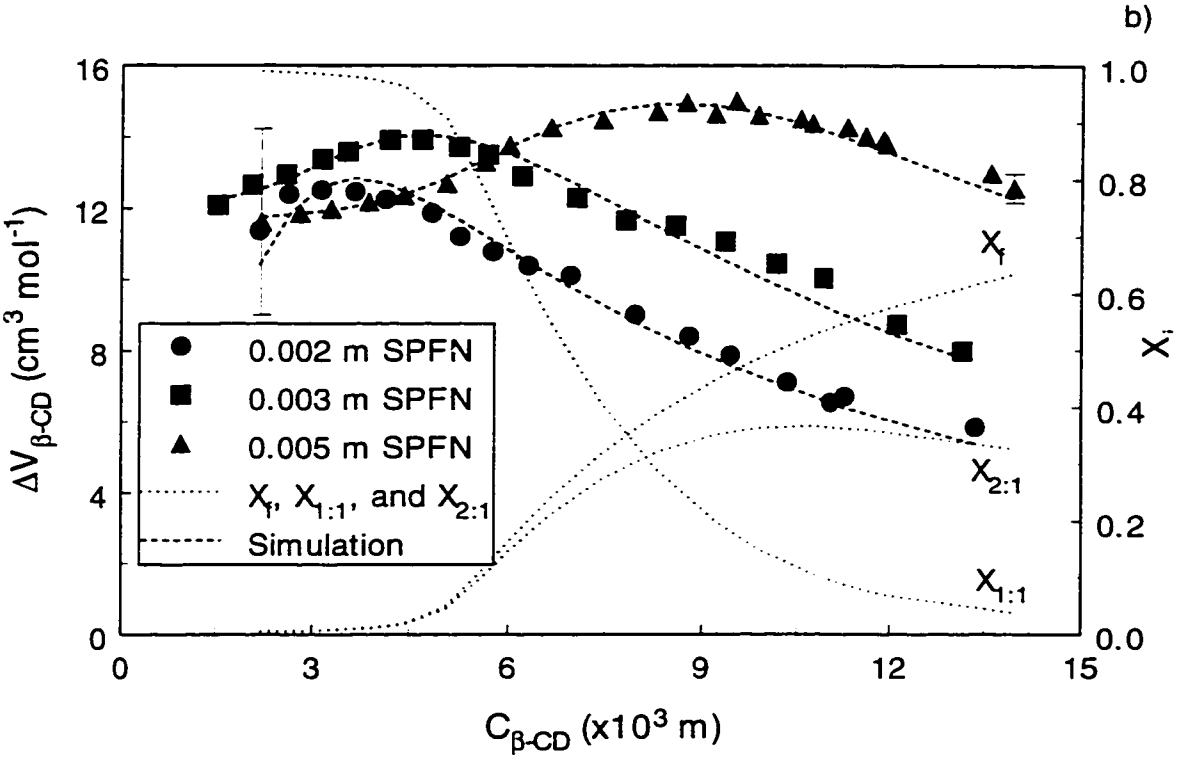
b)
16
12
8
4
0
0
3
6
9
12
15
1.0
0.8
0.6
0.4
0.2
0.0
$\Delta V_{\beta\text{-CD}}$ ($cm^3\ mol^{-1}$)
X_i
$C_{\beta\text{-CD}}$ ($x10^3$ m)
0.002 m SPFN
0.003 m SPFN
0.005 m SPFN
X_f, $X_{1:1}$, and $X_{2:1}$
Simulation
X_f
$X_{2:1}$
$X_{1:1}$

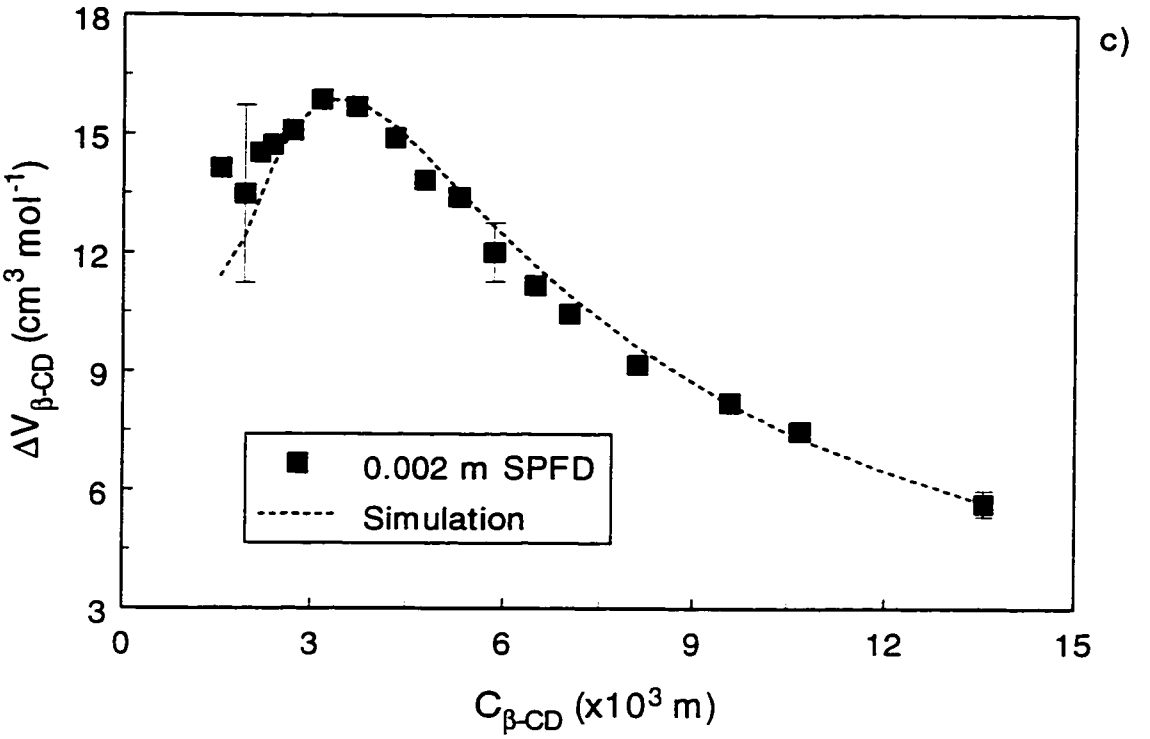
c)
18
15
12
9
6
3
0
3
6
9
12
15
$\Delta V_{\beta\text{-CD}}$ (cm^3 mol^{-1})
$C_{\beta\text{-CD}}$ (x10^3 m)
0.002 m SPFD
Simulation

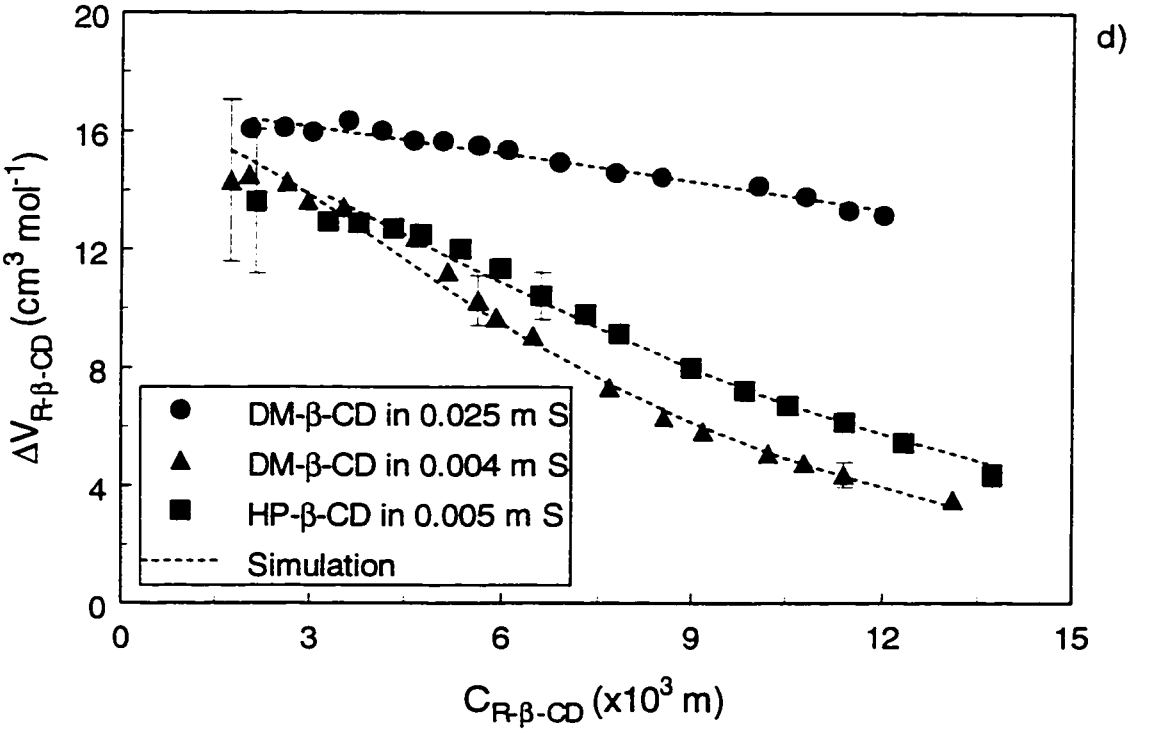
d)
20
16
12
8
4
0
0
3
6
9
12
15
$\Delta V_{R\text{-}\beta\text{-CD}}$ (cm^3 mol^{-1})
$C_{R\text{-}\beta\text{-CD}}$ (x10^3 m)
DM-β-CD in 0.025 m S
DM-β-CD in 0.004 m S
HP-β-CD in 0.005 m S
Simulation

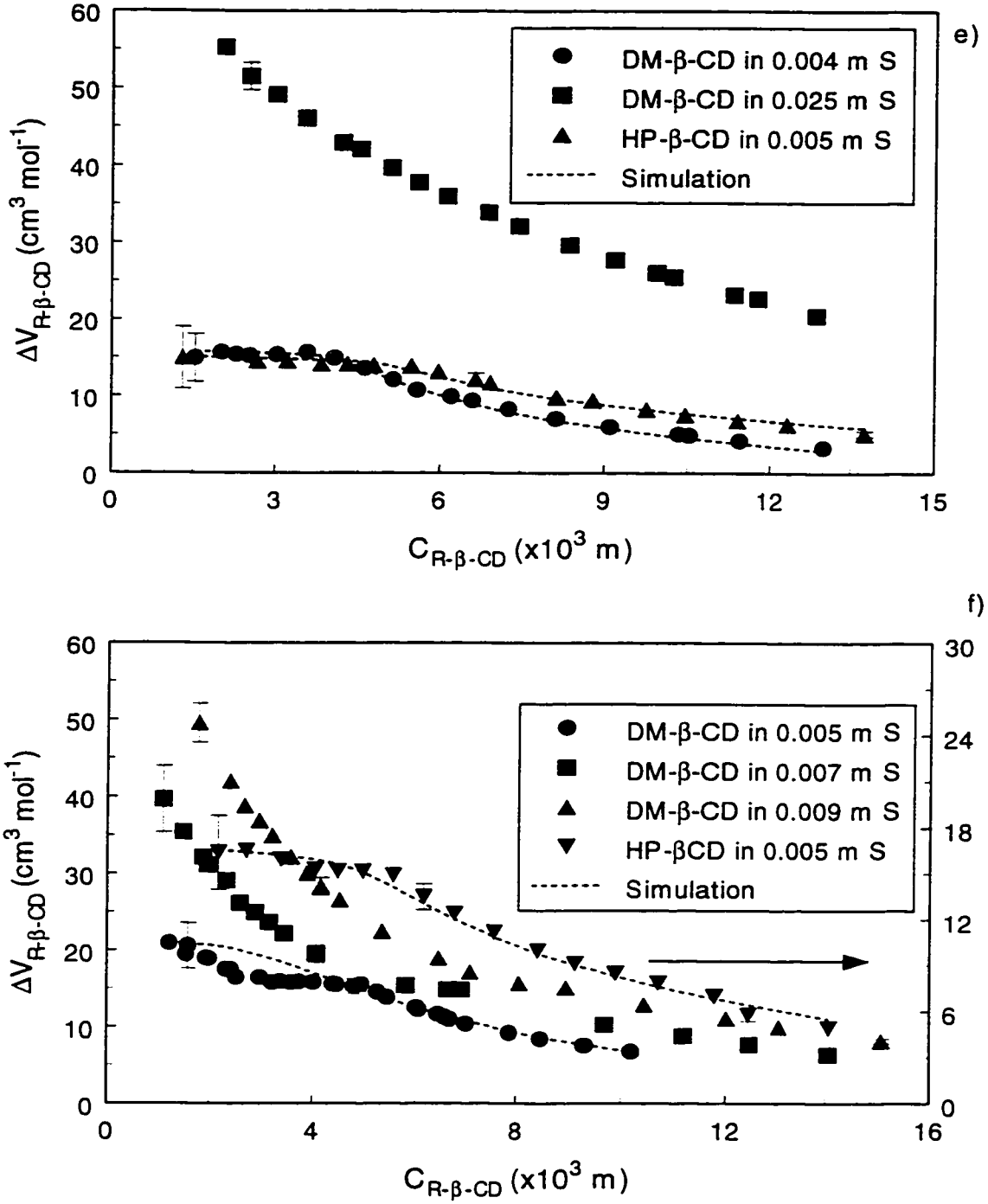

Figure 4-12: ΔV_{CD} versus C_{CD} for CD in aqueous surfactant solutions at pH 10.5 and T=298 K: a) β-CD-SPFO system, b) β-CD-SPFN system; where X_f, $X_{1:1}$ and $X_{2:1}$ are for β-CD in 0.005 m SPFN, c) β-CD-SPFD system, d) DM-β-CD- and HP-β-CD-S systems where S=SPFH, e) DM-β-CD- and HP-β-CD-S systems where S=SPFO, and f) DM-β-CD- and HP-β-CD-S systems where S=SPFN.

Table 4-15: Infinite Dilution Apparent Molar Volume Data of β-CD in Aqueous Sodium Perfluoroalkyl Carboxylate Salt Solutions of Various Concentrations at pH 10.5 and 298 K.

Surfactant	C_S ($\times 10^3$ molal)	$V^o_{\phi,\beta\text{-CD}}$ ($cm^3 mol^{-1}$)	$\Delta V^o_{\beta\text{-CD}}$ ($cm^3 mol^{-1}$)[a]
$C_1F_3CO_2Na$	5	711.9	5.5
$C_3F_7CO_2Na$	5, 60, 120	717.5, 724.1, 731.1	11.1, 17.7, 24.7
$C_6F_{13}CO_2Na$	5, 30, 60	718.0, 721.0, 721.0	11.6, 14.6, 14.6
$C_7F_{15}CO_2Na$	5, 30	718.1, 718.1	11.7, 11.7

[a] $\Delta V^o_{\beta\text{-CD}} = V^o_{\phi,\beta\text{-CD}}$ (surfactant(aq)) - $V^o_{\phi,CD}$ (water)
$V^o_{\phi,\beta\text{-CD}} = 706.4\ cm^3\ mol^{-1}$

Table 4-16: Infinite Dilution Apparent Molar Volumes of β-CD, DM-β-CD, and HP-β-CD in Aqueous Sodium Perfluoroalkyl Carboxylate Salt Solutions at pH 10.5 and 298 K.

Surfactant	$V^o_{\phi,DM\text{-}\beta\text{-CD}}$ ($cm^3 mol^{-1}$)[a]	$\Delta V^o_{DM\text{-}\beta\text{-CD}}$ ($cm^3 mol^{-1}$)[c]	$V^o_{\phi,HP\text{-}\beta\text{-CD}}$ ($cm^3 mol^{-1}$)[b]	$\Delta V^o_{HP\text{-}\beta\text{-CD}}$ ($cm^3 mol^{-1}$)[c]	$V^o_{\phi,\beta\text{-CD}}$ ($cm^3 mol^{-1}$)[b]	$\Delta V^o_{\beta\text{-CD}}$ ($cm^3 mol^{-1}$)[c]
$C_3F_7CO_2Na$	991.3	6.8	964.9	6.7	717.8	11.4
$C_6F_{13}CO_2Na$	1000.4	15.9	972.6	14.4	718.0	11.6
$C_7F_{15}CO_2Na$	1000.3	15.8	973.4	15.2	718.1	11.7
$C_8F_{17}CO_2Na$	1009.0	24.5	975.3	17.1	717.0	10.6
$C_9F_{19}CO_2Na$*	1010.8	26.3	975.6	17.4	716.0	9.6

[a] $C_s \approx 4.0 \times 10^{-3}$ m in all cases, [b] $C_s \approx 5.0 \times 10^{-3}$ m in all cases, *$C_s = 1 \times 10^{-3}$ m.
[c] $\Delta V^o_{R\text{-}\beta\text{-CD}} = V^o_{\phi,R\text{-}\beta\text{-CD}}$ (surfactant(aq)) - $V^o_{\phi,R\text{-}\beta\text{-CD}}$ (water).
$V^o_{\phi,DM\text{-}\beta\text{-CD}} = 984.5\ cm^3\ mol^{-1}$, $V^o_{\phi,HP\text{-}\beta\text{-CD}} = 958.2\ cm^3\ mol^{-1}$, $V^o_{\phi,\beta\text{-CD}} = 706.4\ cm^3\ mol^{-1}$

4.3.6 Transfer volumes from water to ternary aqueous solutions

4.3.6.1 Transfer volume of surfactants from water to aqueous cyclodextrin solutions

Transfer volumes are a useful property (cf. § 2.1.3) since they can be related to the changes in solvation and molecular environment of the host and/or guest molecules. In general, ΔV_S^o increases as C_x increases for fc and hc surfactants in aqueous CD solutions. The relative increase in ΔV_S^o for a homologous series of surfactants with a given CD can be related to the stoichiometry, inclusion geometry, and binding constant(s) of the host-guest complex(es). In aqueous CD solutions, fc surfactants have a greater transfer volume and incremental transfer volume per methylene group than the hc surfactants.

4.3.6.2 Transfer volume of cyclodextrins from water to aqueous surfactant solutions

Transfer volumes for β-CD, DM-β-CD, and HP-β-CD (ΔV_{CD}^o (w→w+S)) are listed in Tables 4-13 to 4-16. In general, ΔV_{CD}^o increases as C_x increases. For a given CD-S system, the magnitude of ΔV_{CD}^o increases as the concentration of the binary solvent system (w+S) increases. Eventually, the magnitude of ΔV_{CD}^o levels off at a certain C_x and concentration of binary solvent (w+S). This result can be correlated with the maximum number of included methylene groups of the surfactant alkyl chain and/or the fraction of bound species in solution through the binding constant (K_i), as will be discussed in chapter 5.

4.4 Spectral displacement studies

4.4.1 β-CD-phenolphthalein binding studies

The measurement of absorbance and the preparation of solutions have been discussed in § 3.2.3 and § 3.3 for the spectral displacement studies (cf. Appendix A10 for experimental data). The molar absorptivity of phenolphthalein (ε_{phth}) at 550 nm and 295 K was determined from plots of absorbance versus C_{phth} using the Beer-Lambert law.

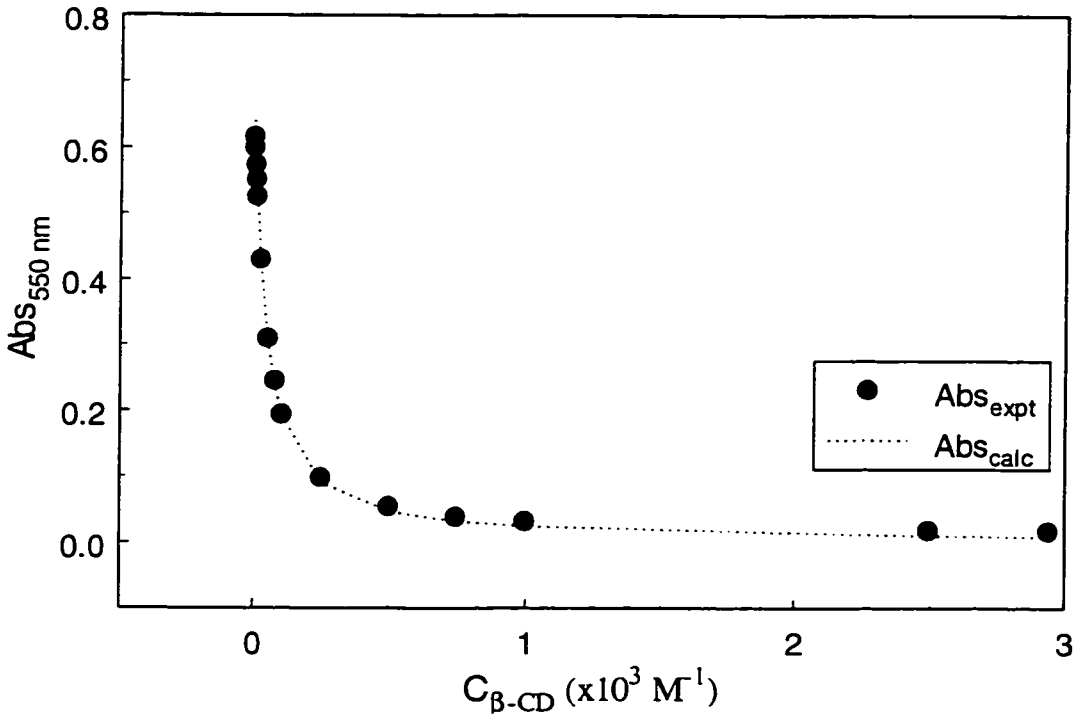

Figure 4-13: Absorbance(abs; λ=550 nm) versus concentration of β-CD ($C_{\beta\text{-CD}}$) in 0.1 M Na_2CO_3 at pH 10.5, [phth]=2×10^{-5} M and T=295 K.

Figure 4-13 is a plot of absorbance of phth at 550 nm versus the concentration of β-CD ($C_{\beta\text{-CD}}$). As $C_{\beta\text{-CD}}$ increases, the absorbance of phth decreases sharply and

approaches zero at higher values of $C_{\beta\text{-}CD}$. The dashed line through the data points corresponds to the NLLS fitting of absorbance versus $C_{\beta\text{-}CD}$ using the 1:1 binding model for the β-CD-phth complex presented in § 2.1.4. The β-CD-phth binding constant ($K_{CD\text{-}P}$=2.5±0.3x10^4 M^{-1}) was determined from several independent measurements and is in good agreement with literature values given in Table 4-17.[134,181,195-201]

Table 4-17: Survey of 1:1 Binding Constants ($K_{CD\text{-}P}$) for the β-CD-Phenolphthalein Complex Taken From the Literature.

$K_{CD\text{-}P}$ (M^{-1})	Conditions	Reference
2.04±0.42 ×10^4	pH=10.2, 0.05 M $NaHCO_3$	196
1.01±0.08 ×10^4	pH=10.0, 0.1 M Na_2CO_3 in 5% ethanol	26(a)
2.1±0.1 ×10^4	pH=10.5, 4×10^{-3} M Na_2CO_3	195
2.3 ×10^4	pH=10.5, 2×10^{-2} M Na_2CO_3	134
3.1±0.3 ×10^4	pH=10.5, 2×10^{-2} M Na_2CO_3	181

4.4.2 β-CD-sodium alkyl carboxylate salt binding studies

The change in absorbance of phth in a solution containing a fixed concentration of phth and β-CD with the addition of a competing sodium alkyl carboxylate surfactant is illustrated in Figures 4-14a-b. The increase in absorbance for a given surfactant can be related to the β-CD-surfactant binding constant ($K_{1:1}$). The model equations presented in § 2.1.4 can be utilized to calculate $K_{1:1}$ provided that the proper conditions are satisfied. The dashed line through the data points in Fig. 4-14a-b corresponds to the best-fit lines predicted using the NLLS binding model presented in § 2.1.4.

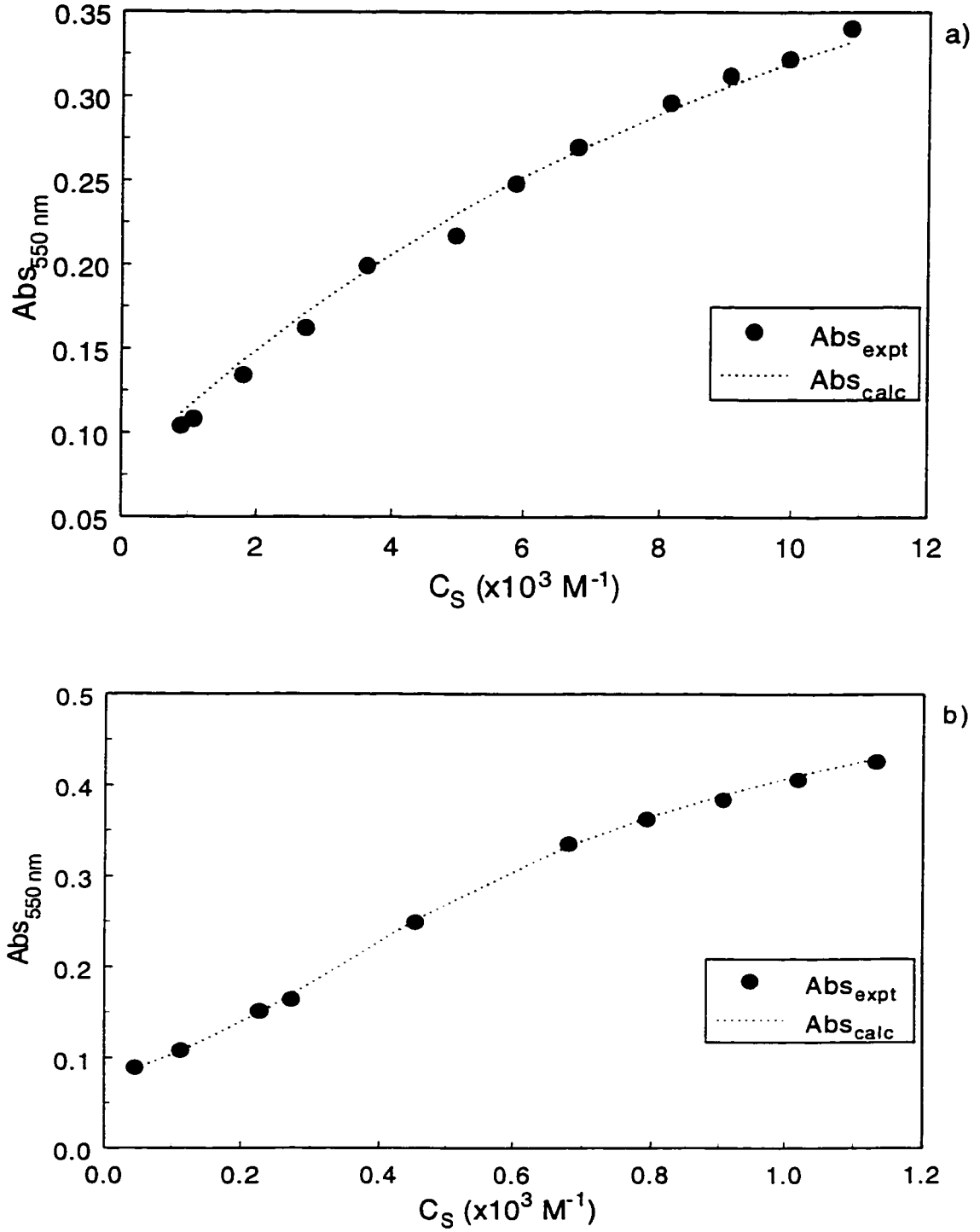

Figure 4-14: Absorbance(abs; λ=550 nm) versus concentration of surfactant (C_S) in 0.1M Na_2CO_3 at pH 10.5, [β-CD]= $3x10^{-4}$ M, [Phth]= $2x10^{-5}$ M and T=295 K: a) sodium hexanoate and b) sodium dodecanoate.

Table 4-18 lists the CMC values for the sodium alkyl carboxylates and the values of $K_{1:1}$ obtained for the β-CD-S complexes. There is good agreement with previously reported values for the β-CD-sodium dodecyl sulfate (SDS) system ($K_{1:1}=1.8x10^4\ M^{-1}$) and the β-CD-sodium octyl sulfate (SOS) system ($K_{1:1}=9.0x10^2\ M^{-1}$).[195,196] The magnitude of $K_{1:1}$ for the β-CD-hc surfactant complexes increases as C_x increases, or as the CMC decreases, of the sodium alkyl carboxylate salts.

Table 4-18: 1:1 Binding Constants*($K_{1:1}$) Obtained from Spectral Displacement Studies of β-CD-Sodium Alkyl Carboxylate Complexes at 295 K and pH 10.5 in 0.1 M Na_2CO_3 Buffer and CMC[(a)] Data in Water.

Surfactant	CMC (M)[(a)]	$K_{1:1}$ (M^{-1})	$\Delta G°$(kJ mol^{-1})[(b)]
$C_8H_{17}SO_3Na$	0.133	$9.0\pm1.1x10^2$	-16.7
$C_{12}H_{25}SO_4Na$	$8.3x10^{-3}$	$1.5\pm0.2x10^4$	-23.6
$C_5H_{11}CO_2Na$	1.57	$5.5\pm0.7x10^1$	-9.8
$C_6H_{13}CO_2Na$	0.95	$2.2\pm0.3x10^2$	-13.2
$C_7H_{15}CO_2Na$	0.35	$6.6\pm0.8x10^2$	-15.9
$C_8H_{17}CO_2Na$	0.23	$2.2\pm0.3x10^3$	-18.9
$C_9H_{19}CO_2Na$	0.096	$5.1\pm0.6x10^3$	-20.9
$C_{11}H_{23}CO_2Na$	0.024	$1.6\pm0.2x10^4$	-23.7
$C_{13}H_{27}CO_2Na$	$6.9x10^{-3}$	$4.8\pm0.6x10^4$	-26.4

*estimated precision is between 5-15% for each $K_{1:1}$ based on the standard deviation of K_{CD-P} for β-CD-phth.
[(a)]CMC values in water at 293-298 K from ref. (41).
[(b)]$\Delta G° = -RT \ln K_{1:1}$

4.4.3 β-CD-sodium perfluoroalkyl carboxylate salt binding studies

Figure 4-15 is a plot of absorbance of phth versus C_S for a long chain fc alkyl carboxylate. The absorbance increases markedly as C_S increases. The line through the data points corresponds to the best-fit value of $K_{1:1}$ using the 1:1 binding model presented in § 2.1.4.

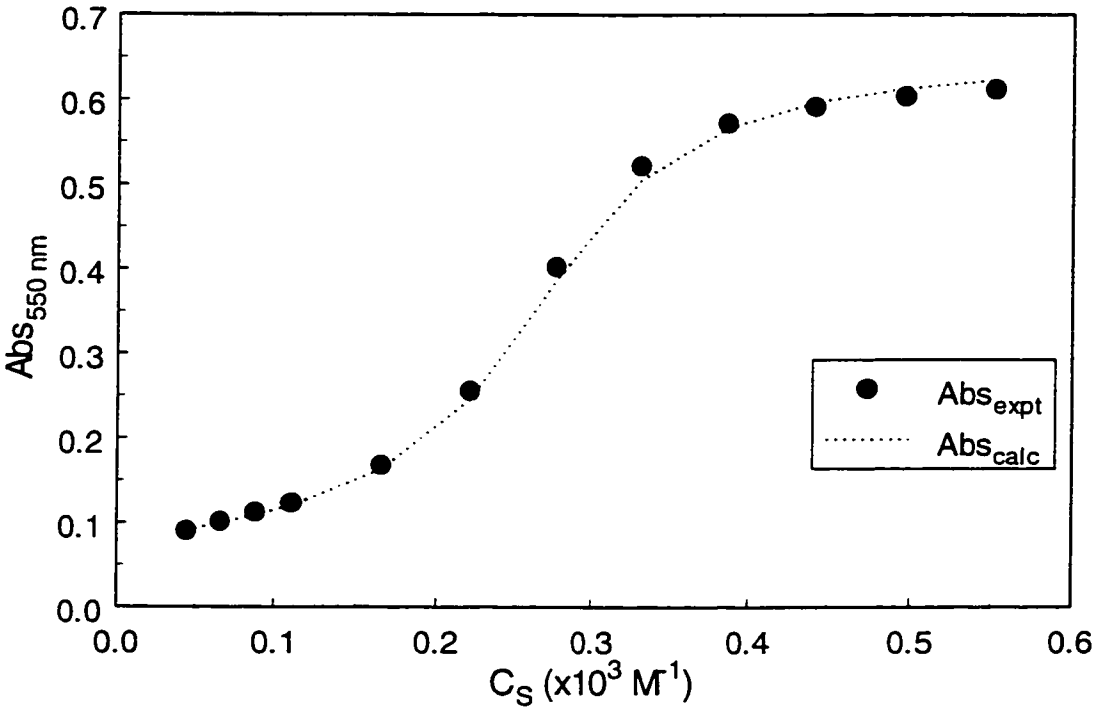

Figure 4-15: Absorbance(Abs; λ=550 nm) versus concentration of surfactant, C_S, where S= SPFN, in 0.1 M Na_2CO_3 at pH 10.5, [β-CD]= $3x10^{-4}$ M, [Phth]= $2x10^{-5}$ M and T=295 K.

Table 4-19 lists the CMC values for the fc alkyl carboxylate salts and $K_{1:1}$ for the β-CD-fc surfactant complexes. The magnitude of $K_{1:1}$ increases as C_x increases and the values are systematically greater than those for the sodium alkyl carboxylates listed in Table 4-18.

Table 4-19: 1:1 Binding Constants ($K_{1:1}$) Obtained from Spectral Displacement Studies of β-CD-Sodium Perfluoroalkyl Carboxylate Complexes at 295 K and pH 10.5 in 0.1 M Na_2CO_3 Buffer and CMC[a] Data in Water at pH 10.5.

Surfactant	CMC (mol L^{-1})[a]	$K_{1:1}$ (M^{-1})	ΔG°(kJ mol^{-1})[b]
$C_3F_7CO_2Na$	>1.000	$2.8\pm0.4\times10^{2}$	-13.8
$C_4F_9CO_2Na$	0.520	$2.6\pm0.3\times10^{3}$	-19.3
$C_6F_{13}CO_2Na$	0.080	$3.7\pm0.9\times10^{4}$	-25.8
$C_7F_{15}CO_2Na$	0.030	$3.3\pm0.4\times10^{5}$	-31.2
$C_8F_{17}CO_2Na$	0.010	$9.4\pm1.2\times10^{5}$	-33.7

[a] CMC values at 295 K and pH 10.5 obtained from ref. (41).
[b] $\Delta G^{\circ} = -RT \ln K_{1:1}$

5. DISCUSSION

5.1 ^{1}H NMR chemical shift studies of cyclodextrin-sodium alkyl carboxylate complexes

5.1.1 ^{1}H NMR chemical shifts of sodium alkyl carboxylate salts

NMR spectroscopy[23,24,102,103] is a useful technique to study host-guest complexes since the ^{1}H NMR chemical shifts (δ) of the interior protons within the β-CD[45] interior and the guest nuclei[197] can be analyzed to provide complementary information about the inclusion mode, stoichiometry, and binding affinity of the inclusion complexes. There are numerous reports of ^{1}H NMR studies[1,25,198] of CD-aromatic guest systems because of the favourable anisotropic properties of the arene ring and the good spectral dispersion of the aromatic protons. However, there have been fewer studies employing aliphatic guest systems.[113,198-200] As mentioned in § 2.1.2, the chemical shift of a nucleus is very sensitive to the surrounding environment and in the case of flexible molecules, to conformational effects. Quantitative analysis of the CIS values (cf. eq 3.2.1-1) is precluded by numerous antagonistic shielding and deshielding effects.[161] For example: *i)* H-bonding between the CD hydroxyl groups and the carboxylate head group is expected to reduce the intramolecular shielding of the C(1)H_2 and C(2)H_2 protons and result in positive CIS values; *ii)* the "goodness of fit" between the alkyl chain of the surfactant and host systems possessing narrower cavities, e.g., α–CD and TM-β-CD, may induce an all-trans conformation of the alkyl chain. This maximizes the distance between adjacent CH_2 groups and decreases the intramolecular shielding within the alkyl chain, resulting in positive CIS values; and *iii)* the apolar environment of the CD interior and/or alkyl

substituents in the annular hydroxyl region result(s) in shielding of the alkyl chain and contributes to negative CIS values. Notwithstanding the differing types, *i)-iii)*, of deshielding and shielding effects on the sign of the CIS values of the guest, consideration of these factors may allow for a semiquantitative interpretation of the CIS values of the guest.

Figures 4-1 a-b illustrate the dependence of $\Delta\delta$ versus mole ratio (R) for a short (SHex) and long (SDodec) alkyl chain hc surfactant in aqueous solutions of α-CD and DM-β-CD, respectively. The positive increase in $\Delta\delta$ for the $C(1)H_2$, $C(2)H_2$, and CH_3 groups indicate that type *i)* and *ii)* effects play a primary role and are consistent with the formation of an inclusion complex. The CIS values of the guest gradually level off at R>3 (Fig. 4-1a) compared to R=1 (Fig. 4-1b) indicating that a greater excess of host is required with SHex compared with SDodec to reach a saturated condition of bound species ($X_{1:1}$),[24] i.e., the value of $X_{1:1}$ for SDodec is greater than for SHex throughout the binding isotherm. The results described above for SHex and SDodec are consistent with behaviour characteristic of weak and strongly bound 1:1 CD-S complexes, as shown by the values of K_i in Table 4-1.

The CIS values of SDodec in Figure 4-1c resemble behaviour that is also typical of a weakly bound 1:1 complex (cf. Fig. 4-1a) because of the nonlinear dependence of $\Delta\delta$ versus R. The CIS values for $C(1)H_2$ and $C(2)H_2$ show a positive increase up to R≈1 with a decrease beyond R>1. This decrease in the CIS values is attributed to type *iii)* shielding effects because the carboxylate head group is removed from the bulk solvent and is located nearby the annular hydroxyl groups. The gradual fall off in $\Delta\delta(CH_3)$ is also

attributed to type *iii)* shielding effects because of 2:1 CD-S complex formation. The latter results from the end-capping of a second CD onto the unbound portion of the alkyl chain of the surfactant that protrudes out of the 1:1 complex. Attempts to simulate the experimental data using only the 1:1 binding model (eq 2.1.2-4) resulted in a poor fit whereas a model accounting for both 1:1 and 2:1 binding (eq 2.1.2-5) provided an excellent fit to the experimental data. The calculated binding constants (Table 4-1) and the results described above indicate that α-CD-SDodec forms a relatively strong 1:1 complex; however, it is the lower binding constant for the 2:1 complex that results in the nonlinear concentration dependence of the CIS values. Previous reports[107,116] indicate that anionic and cationic surfactants of comparable alkyl chain length to SDodec and ST form 2:1 complexes with β-CD and that the value of $K_{1:1}$ exceeds $K_{2:1}$ by one to two orders of magnitude. Other reports indicate that 2:1 CD-S complexes are formed for $C_x \geq 16$.[201] Castronuovo *et al.*[202] have argued that the formation of 2:1 α-CD-S complexes is unlikely for alkyl carboxylate salts having C_x=2-11 due to the hydration requirements of the carboxylate group. However, the results presented here demonstrate that 2:1 α-CD-S complexes are formed for systems with $C_x \geq 9$ (Table 4-1) and that a host-guest stoichiometry of this type optimizes apolar-apolar and minimizes apolar-polar interactions.[34]

In Table 4-1, the value of K_i increases as C_x increases for all of the surfactants investigated. The hosts DM-β-CD, HP-β-CD, and TM-β-CD form 1:1 complexes, exclusively, whereas α-CD and β-CD form 1:1 and 2:1 CD-S complexes. The R-β-CD compounds tend to form only 1:1 complexes because the extended length of the cavity

facilitates the inclusion of guests with longer alkyl chains.[22,23] The onset of 2:1 binding for α-CD, C_x=9 compared to C_x=11 for β-CD, is related to differences in the ability of the surfactant alkyl chain to coil within the CD interior because of the different diameters of each macrocycle. The narrower cavity diameter of α-CD (4.5 Å)[203] causes the hc alkyl chain to adopt an all-trans conformation whereas the greater cavity diameter of β-CD (6.3 Å)[203] allows formation of gauche kinks in the alkyl chain. According to Park and Song,[115] an extended alkyl chain of four carbons is required to span the CD torus. Thus, the tendency of α-CD to form 2:1 complexes more readily than β-CD provides indirect support that coiling of the alkyl chain must occur in β-CD. The relative binding affinity of hc surfactants with the various CDs follows the order β-CD > α-CD > DM-β-CD > TM-β-CD > HP-β-CD. The relative order within the R-β-CD series is consistent with steric effects imposed by the increasing degree of substitution (DS) of methyl groups from DM- to TM-β-CD (cf. Table 3-1). Thus, the relative binding affinity between the host and guest decreases due to greater steric hindrance as the size of the alkyl group and the DS of cyclodextrin increase. While HP-β-CD has a lower DS than DM-β-CD, the hydroxypropyl group is much larger than a methyl group and an additional steric effect that impedes complex formation may arise, due to favourable hydration of the hydroxypropyl group on account of its dipolar character. This effect would be absent in the case of the methyl substituted CDs.

The CIS values of the $C(1)H_2$, $C(2)H_2$, and CH_3 protons shown in Table 4-2 provide information about the inclusion orientation of the guest in the CD-S complex since the $C(1)H_2$ and $C(2)H_2$ groups are adjacent to the hydrophilic carboxylate group

whereas the CH_3 group is in a more lipophilic environment. The relative ordering of the CIS values of the surfactant, $\Delta\delta(CH_3) > \Delta\delta(C(2)H_2) > \Delta\delta(C(1)H_2)$, indicates that protons in the lipophilic region of the alkyl chain are more strongly affected than those near the hydrophilic carboxylate head group. This is consistent with inclusion of the lipophilic alkyl chain in the CD interior while the hydrophilic carboxylate group remains in the bulk solvent or adjacent to the annulus region of the CD, as would be expected for binding processes driven by hydrophobic effects.[34,70] The increase in CIS values of the CH_3 protons with increasing alkyl chain length indicates the importance of type *ii)* deshielding effects. However, this parameter shows a small decrease for x=13 relative to x=11 for α–CD and TM-β-CD. This decrease may be due to a reduction of type *ii)* deshielding effects when the methyl group extends beyond the CD cavity into the facial region.[19]

In cases where 2:1 α-CD-S complexes are formed, the CIS values of the $C(2)H_2$ and $C(1)H_2$ protons of the surfactant decrease for larger values of R because the carboxylate head group is drawn toward the annular hydroxyl groups as the 2:1 CD-S complexes are formed. This is evident from a comparison of the CIS values for $C(1)H_2$ and $C(2)H_2$ protons of SHex, SO, and SDec when they form complexes with α– and β-CD. While the CIS values of the α–CD system decrease as C_x increases, minimal changes in this parameter are observed for β-CD. The decrease observed for α–CD-S systems can be attributed to type *iii)* shielding effects as the carboxylate head group is drawn closer toward the annulus region of α–CD. In contrast to α–CD, the larger cavity diameter of β-CD is not expected to induce substantial changes in the conformation of the alkyl chain of the surfactant, and this is supported by the similar CIS values for the

$C(1)H_2$ and $C(2)H_2$ groups.[19] Hence, smaller CIS values are observed for the $C(1)H_2$ and $C(2)H_2$ protons of the β-CD-S systems as C_x increases because type *ii)* deshielding effects are expected to be less. These results are also consistent with previous conclusions that weak interactions occur between the carboxylate head group of the surfactant and the annular hydroxyl groups of β-CD.[200] In a previous study, the $\Delta\delta$ values at R=1 for the $C(1)H_2$, $C(2)H_2$, and CH_3 protons of a series of n-alkyl amine and n-alkyl carboxylic acid guests were very similar.[200] As well, similar values of ΔC_p° for complexes formed between β-CD and a homologous series of n-alkyl ammonium and n-alkyl carboxylate ions indicates that it is the dehydration of the alkyl chain that contributes to the observed values. Thermodynamic studies have indicated that there is minimal solvent reorganization around hydrophilic groups of a guest species and the hydroxyl groups of the cyclodextrin host upon complex formation.[85] The importance of solvation of the carboxylate head group has also been alluded to in an earlier NMR study.[204] The relatively similar CIS values for the $C(1)H_2$ and $C(2)H_2$ protons of the alkyl carboxylates in complexes with hosts β-CD and R-β-CD further support the contention that the carboxylate head group does not interact strongly with the CD annulus. However, the slightly lower values observed with R-β-CD hosts may be an indication of increased type *iii)* shielding effects because of the alkyl groups in the annulus region. These results indicate that apolar-apolar interactions between the alkyl chain of the surfactant and the CD interior are more important than the interactions between the carboxylate head group of the surfactant and the annular CD hydroxyl groups in complex formation.[204]

The CIS values for the $(CH_2)_n$ groups (cf. Scheme 3-1b) were not quantitatively analyzed because the spectral lines for the individual methylene groups were not fully resolved. However, changes in their CIS values are comparable to that for the CH_3 group. An analysis of the spectral line shape of the $(CH_2)_n$ groups for SDec, SDodec, and ST in complexes formed with α-CD and β-CD can provide information regarding the number of methylene groups that can be included. Since the β-CD-SDec system forms 1:1 complexes, exclusively, it can serve as a useful benchmark for analyzing the effect of the 2:1 complexes on line shape. In Figure 4-2A, the extreme upfield proton signal (closest to DSS) for SDodec and ST is assigned to unbound CH_2 groups residing in the bulk, since the CIS values are similar to a surfactant alkyl chain in D_2O alone, whereas the lower field component of the signal represents 1:1 and 2:1 complexes. Therefore in Figure 4-2B, the low field shoulder appearing in SDodec and ST arises from 2:1 complexes, whereas the high field component is assigned to 1:1 complexes. The integrated area of the low field component of the asymmetric peak (shown above the peak) and its CIS value is consistent with the end-capping of a second CD onto the 1:1 complex. Clearly, as C_x increases the line broadening increases and the intensity of the downfield resonance lines increases, indicating that additional CH_2 groups are bound in a 2:1 complex. On the basis of the relative intensities of the spectral lines and chemical shifts for the $(CH_2)_n$ groups in Fig. 4-2, it is concluded that ca. 5 CH_2 groups can be included within α-CD and ca. 7-8 CH_2 groups within β-CD. These results are in agreement with estimates derived from calorimetry,[85] and whether the alkyl chain of the surfactant is in an all-trans

conformation or whether there are gauche kinks depending on the diameter of the CD annulus.[115]

5.1.2 ^{1}H NMR chemical shifts of β-CD

The chemical shift values of the nuclei of β-CD are also sensitive to similar environmental factors as discussed in § 2.1.2; however, anisotropic effects play a role[45] because of the presence of a dipole moment along the axis of the CD interior (cf. § 1.3.1). Conformational changes of β-CD are limited[23] and the corresponding type *ii)* shielding and deshielding effects are negligible relative to the guest nuclei (cf. § 5.1.1). In general, the formation of inclusion complexes results in positive (increased shielding) CIS values (cf. eq 3.2.1-2) of the host nuclei, H(3) and H(5), because the presence of an apolar guest in the CD interior results in increased shielding of the cavity interior. The presence of hydrate water in the CD interior results in deshielding of the cavity interior and an increase in its relative polarity. Hence, a study of the CIS values of the interior cavity protons of the host can provide confirmation of inclusion binding and may be correlated with the observed ^{1}H CIS values of the guest in § 4.1.1.

Figures 4-3 a-c illustrate the concentration dependence of $\Delta\delta$ versus mole ratio (R) for β-CD with short (SHex) and long (SDodec, SDS) chain hc surfactants, respectively. The positive CIS values for H(3) and H(5) indicate that the surfactants are included in the CD interior. The gradual nonlinear increase and eventual leveling off of the CIS values beyond R=3 for H(3) and H(5) indicate that this system is a weakly bound 1:1 complex. In contrast, Fig. 4-3b represents typical CIS values for a strongly bound β-CD-S complex,

as shown by the approximate linear increase of $\Delta\delta$ up to R=1 and the nearly constant values thereafter. The correlation between the increase in CIS values and the magnitude of K_i for the CD-S complexes (Fig. 4-1a-b) depends upon the fraction of bound species, as described by the two- and three-site models (§ 2.1.2). The dashed lines in Figs. 4-3a-b are the best-fit curves according to eq 2.1.2-4 and the calculated values of K_i are listed in Table 4-3. The CIS values of H(3) and H(5) indicate that SHex and SDodec form weak and strongly bound 1:1 β-CD-S complexes, respectively, in agreement with the results obtained from the guest nuclei in § 4.1.1.

The CIS values of H(3) and H(5) for the β-CD-sodium dodecyl sulfate (SDS) system are shown in Fig. 4-3c. The nonlinear dependence of the CIS values with increasing R resembles that for a weakly bound 1:1 complex (Fig. 4-3a), except that the CIS values for H(3) start to level off at R>0.5. The mole ratio (C_S/C_{CD}), R=0.5, corresponds to the stoichiometry of a 2:1 CD-S complex and the relatively constant CIS values for H(3) beyond R=0.5 indicates that a second CD includes the protruding alkyl chain from the 1:1 complex in its wide, secondary annulus. The eventual saturation of the CIS values for H(5) beyond R=1 indicates that the narrower end of the β-CD interior is less affected because the alkyl chain of SDS does not fully extend into the second CD. Attempts to simulate the data using eq 2.1.2-4 gave poor fits, however, eq 2.1.2-5 was more suitable, as shown by the good agreement between the dashed lines and experimental data points in Fig. 4-3c. The calculated values of $K_{1:1}$ (1.6×10^4 M^{-1}) and $K_{2:1}$ (3.5×10^2 M^{-2}) are in agreement with those from ref. 115 in Table 1-2. Similar differences in the magnitudes of $K_{1:1}$ and $K_{2:1}$ were observed for complexes of β-CD with

long chain anionic and cationic surfactants.[107,111] The occurrence of maxima in $\Delta\delta$ at mole ratios other than 0.5 in Job plots (cf. § 1.3.2.1) of the host and guest ^{1}H NMR data for the β-CD-SDS system corroborates that 2:1 complexes are formed.[205]

Table 4-3 lists the CIS values of H(3) and H(5) protons at R=1 and K_i for various β-CD-hc surfactant complexes. The magnitude of K_i increases as C_x increases and are in good agreement with the values of K_i obtained from the ^{1}H NMR data of the guest (Table 4-1). The CIS values for H(3) and H(5) increase as C_x increases up to x=11 whereas a small decrease is observed for x=13. The lower CIS values for the long alkyl chain length surfactants is consistent with the formation of 2:1 complexes because of the overall lowering of the fraction of bound species (X_i). The CIS values for H(3) and H(5) of β-CD in the presence of SDS at R=1 are 0.095 and 0.175 ppm, respectively. These values exceed those for the β-CD-SDodec system because of possible differences in the extent of inclusion of the alkyl chain. This may be related to the differences in the size of the surfactant head group and its degree of hydration since these factors would affect the ion-dipole interactions with the hydroxyl groups in the annulus region of β-CD, *vide infra*.

The ROESY spectrum in Fig. 4-4 provides evidence that an inclusion complex is formed between β-CD and SDodec because there are indications of intermolecular contacts between the host (H(3) and H(5)) and guest ($(CH_2)_n$) protons due to dipolar correlation between these nuclei. The spectral assignment of the nuclei for a typical hc surfactant and β-CD was shown in Schemes 3-1 b and c. The off-diagonal cross peaks in Fig. 4-4 represent dipolar correlation between the nuclei of β-CD and SDodec. The

cross-peaks of greatest intensity occur between H(3) and H(5) of the host and the $(CH_2)_n$ groups of the surfactant, and their amplitude increases as the alkyl chain length of the guest increases. This may be due to the inclusion of additional methylene groups and/or a greater fraction of bound species. The absence of cross-peaks between $C(1)H_2$ and $C(2)H_2$ protons of the guest and the cavity protons of β-CD may be due to strong hydration of the carboxylate head group, which sterically excludes these methylene groups from favourable contact (≤3Å) with the protons of the CD interior. The absence of dipolar correlation, as described above, is consistent with the small CIS values of the $C(1)H_2$ and $C(2)H_2$ groups (Table 4-2). Correlation between the CH_3 group of the surfactant and host protons is negligible or absent, indicating that the interactions between the host and guest are weak. This may be due to rapidly changing inclusion orientations and/or the presence of competitive intramolecular relaxation pathways. The latter possibility is more likely because it has been argued that relatively large CIS values (Table 4-2) are correlated with the extent of dipolar correlations.[25] For these reasons, it is difficult to ascertain, unequivocally, whether the carboxylate head group in the complex is located at the wide or narrow end of the torus. Previous reports indicate that guest molecules possessing charged groups, such as the p-nitrophenolate anion, locate the charged group at the wide, secondary annulus of β-CD (§ 1.3.2.2).[1] Tee *et al.*[206] have also proposed that the ester functional group locates at this end, based on kinetic studies.

Scheme 5-1 illustrates possible inclusion modes for 1:1 and 2:1 β-CD-S complexes. The two possible inclusion modes for 1:1 complexes are given in Schemes 5-1a) and b). These two possibilities are difficult to distinguish on the basis of the CIS

values of the host and guest nuclei. The tendency for polar and/or charged functional groups to locate near the wide, secondary side of the CD is consistent with the molecular lipophilicity patterns (MLPs) of β-CD.[54] Lichtenthaler and Immel[54,70] argue that the wide, secondary side of the β-CD annulus is more hydrophilic than the narrow, primary side and their molecular modeling studies on the docking of guests within the CD interior support the inclusion mode in Scheme 5-1a, because of the appropriate matching of hydrophilic surfaces.

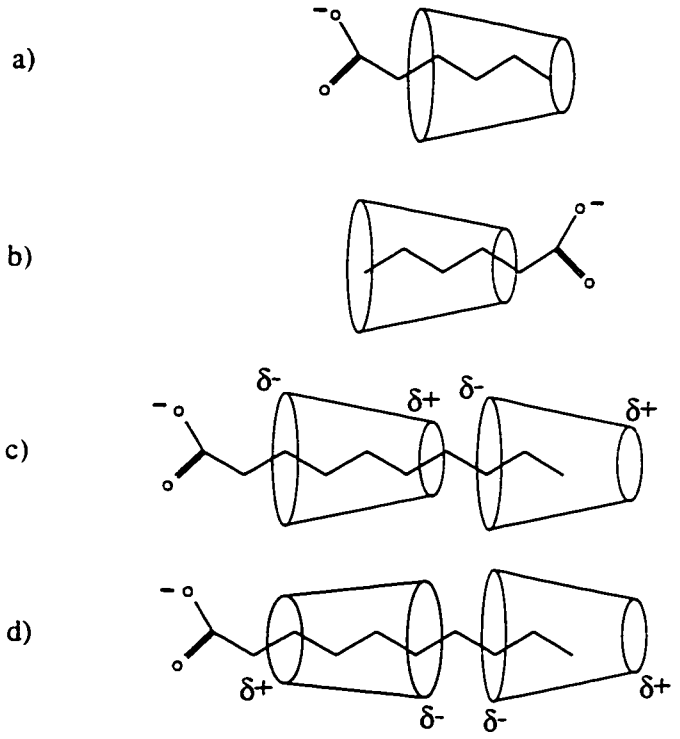

Scheme 5-1: Proposed inclusion modes for 1:1 and 2:1 β-CD-S complexes, as determined from ^{1}H NMR data: a) and b); 1:1 β-CD-S complexes and c) and d); 2:1 β-CD-S complexes.

Indirect support for this inclusion mode of a 1:1 complex is also derived from the ^{1}H CIS values of β-CD for CD-S systems that form 2:1 complexes. The results indicate that the second CD that binds onto the protruding alkyl chain of the 1:1 complex does so from the wide, secondary side of the annulus (Scheme 5-1c-d). The latter result is unexpected on the basis that the narrow annulus region of β-CD is more lipophilic. If one assumes that it is the wide, secondary side of the CD which associates with the apolar end of the hc surfactant (Scheme 5-1a), this inclusion mode is consistent with the appropriate matching of MLPs of the host and guest. The two inclusion modes for 2:1 CD-S complexes (Schemes 5-1 c and d) are reasonable in terms of potential intermoleular H-bonding between macrocycles. It is argued that Scheme 5-1c is favoured relative to Scheme 5-1d in terms of the alignment of the dipoles of each CD. A recent study of polyrotaxane complexes indicated that the "head to tail" arrangement (Scheme 5-1c) was the preferred inclusion mode.[207] Davies and Deary argue that this inclusion mode is also important for 2:1 complexes of α-CD with para alkyl-substituted aryl sulfur compounds.[208] To conclude, Schemes 5-1 a and c are considered to be the most favourable inclusion orientations for 1:1 and 2:1 β-CD-hc surfactant complexes.

5.2 ^{19}F NMR chemical shift studies of cyclodextrin-sodium perfluoroalkyl carboxylate complexes

5.2.1 ^{19}F NMR chemical shifts of sodium alkyl carboxylate salts

Reinsborough *et al.*[209] were the first to examine a cyclodextrin-perfluorocarbon system, β-CD-sodium perfluorooctanoate (SPFO), using ^{19}F NMR. Subsequently, Guo *et*

al.[65] carried out a systematic study of α-, β-, and γ-CD with a homologous series of fc surfactants. In the latter case it was reported that β-CD was bound most strongly with the fc surfactants, and that the magnitude of $K_{1:1}$ increased as the fc alkyl chain length (C_x) increased up to x=7. However, from x=7 to x=8, $K_{1:1}$ showed a large decrease (cf. Table 4-4). The present work has revealed that this result is an artifact of the analysis of the data assuming only the presence of 1:1 complexes, since 2:1 CD-S complexes are shown to occur for x=7 and x=8. This example and the results in Table 1-2 (cf. § 1.4.1) illustrate how an inadequate account of the relevant host-guest stoichiometries results in poor estimates of binding constant(s).[57] Further complications may also arise due to differences in the sensitivity of the measured physical property to complexes other than 1:1, as shown by a comparison of results obtained from conductance (cf. Fig. 4, ref. 120) and sound velocity (cf. Fig. 4, ref. 210) measurements with those reported here (cf. Fig. 4-5c) using ^{19}F NMR for the β-CD-SPFO system.

Various contributions to ^{19}F chemical shifts have been reported: *i)* the decreased shielding of the $C(1)F_2$ and $C(2)F_2$ groups, due to perturbation of the circulating π-electronic currents arising from intermolecular interactions and solvation changes between the CD hydroxyl groups and the carboxylate group of the surfactant;[211] *ii)* the similar diameters of the β-CD cavity and fc chain that induces an all-trans conformation of the fc chain and decreases the shielding between adjacent CF_2 groups;[65] *iii)* the increased shielding of the guest nuclei due to the apolar character and greater polarizability of the CD interior relative to the aqueous phase;[65] and *iv*) the combined shielding and deshielding effects arising from the location of nuclei in the annulus region

that introduces some compensation between effects *ii)* and *iii).*[65] These factors are similar to those outlined in § 5.1.1 for ^{1}H nuclei of the hc surfactants; however, ^{19}F nuclei are more sensitive to medium effects[160] and intra-/intermolecular[212] interactions than ^{1}H nuclei.

Table 4-4 lists the binding constants (K_i) of the CD-S complexes and CMC data for the fc surfactants at 295 K. Most of the CD-SPFB complexes have a value of $K_{1:1} \approx 10^2\ M^{-1}$ (Table 4-4), except for TM-β-CD which has a lower value. The CD-SPFP complexes have a value of $K_{1:1} = 10^2\text{-}10^3\ M^{-1}$ and the binding affinity of TM-β-CD to fc guests is the lowest of the hosts. The magnitude of $K_{1:1}$ for the CD-SPFH systems is ca. $10^4\ M^{-1}$, irrespective of the type of alkyl groups in the annulus of the CD and its degree of substitution (DS). The magnitude of $K_{1:1}$ is similar for the CD-SPFO and -SPFN systems. The binding constant, $K_{2:1}$, increases upon going from β-CD-SPFO to β-CD-SPFN. In cases where complexes are formed between methylated CDs (DM-β-CD, RAMEB, and TM-β-CD) and SPFN, $K_{1:2}$ increases as the DS of methyl groups increases. While small variations in the binding constant may be attributed to steric effects arising from the presence of alkyl groups in the annulus region, it appears that the interior of the CD cavity serves as the principal binding site.

Figures 4-5 a-f illustrate typical plots of $\Delta\delta$ versus mole ratio (R) for the guest nuclei of CD-fc surfactant complexes exhibiting weak or strong binding and with different stoichiometries. The positive nonlinear increase of $\Delta\delta$ as R increases (Fig. 4-5a) for the DM-β-CD-SPFB system gradually levels off when R>1, and is understood in terms of its relatively small binding constant. On the other hand, the near linear increase

in $\Delta\delta$ values up to R=1 that levels off beyond R=1 (Fig. 4-5b) signifies behaviour of a strongly bound CD-S complex.

Figures 4-5c-d illustrate plots of $\Delta\delta$ versus R for the β-CD-SPFO and -SPFN systems, respectively. The CIS values of the ^{19}F nuclei for the $C(1)F_2$ and $C(2)F_2$ groups increase almost linearly up to R=1 and then the slope diminishes beyond R>1 whereas the other ^{19}F nuclei exhibit a negative slope beyond R>1. The concentration dependence of the CIS values beyond R=1 implicates the occurrence of another equilibrium besides the formation of 1:1 complexes. Guo *et al.*[65] postulated the formation of 2:1 β-CD-SPFO complexes, however, no attempt was made to incorporate this fact into the analysis of their NMR data. The "best fit" lines in Figs. 4-5c-d were obtained using eq 2.1.2-5 and includes contributions of 1:1 and 2:1 complexes. The use of eq 2.1.2-4 provides a lower value of $K_{1:1}$ because the fraction of unbound species in solution is overestimated. This accounts for the lower values of $K_{1:1}$ for β-CD-SPFO and β-CD-SPFN reported by Guo *et al.* (cf. Table 4-4). The change in slope at R=1 for the ^{19}F CIS values of the $C(1)F_2$ and $C(2)F_2$ groups can be attributed to increased type *iii)* shielding effects as these groups are drawn closer toward the apolar interior of the CD with the formation of 2:1 complexes. The negative slopes observed for the remaining ^{19}F nuclei are attributed to extensive dehydration and the increased lipophilic environment accompanied by threading two CDs onto the surfactant chain. The fact that 2:1 binding is favoured beyond R=1 is consistent with the fact that $K_{1:1} > K_{2:1}$ (Table 4-4) and that $[CD]_{total}$ exceeds $[S]_{total}$. The observation of negative slopes for groups other than $C(1)F_2$ and $C(2)F_2$ indicates that it is more energetically favourable to hydrate the hydrophilic head group than the hydrophobic

tail for fc surfactants with long alkyl chains (C_x, x>7). The change in the slope of the CIS values for $C(1)F_2$ and $C(2)F_2$ groups (Fig. 4-5c) also occur for fc surfactants at the CMC because of similar dehydration of the fc alkyl chain.[176]

Figures 4-5e-f illustrate plots of $\Delta\delta$ versus R for the guest nuclei of SPFN when it forms complexes with RAMEB and HP-β-CD, respectively. A comparison of these results provides an opportunity to understand the effect of alkyl substitution in the annulus region of the host when complexes with a common guest are formed. In Fig. 4-5 e, the CIS values for all the ^{19}F nuclei increase linearly and level off at R=1, similar to that expected for a strongly bound 1:1 complex. The main difference between Fig. 4-5 e and f is that the nuclei ($C(6)F_2$, $C(7)F_2$, and CF_3) near the lipophilic terminus of the fc chain display different behaviour. The CIS values for these nuclei are negative and reach a minimum near R=0.5 (Fig. 4-5f). Thereafter, they increase up to R=1 and level off, the plateau values being slightly negative for the two ^{19}F nuclei near the terminus of the fc chain. Negative CIS values for these nuclei are consistent with type *iii)* deshielding effects that are expected for a 2:1 complex. Use of equation 2.1.2-5 provided a poor fit in Fig. 4-5f; however, the "best fit" lines (cf. eq 2.1.2-6), which account for contributions arising from 1:1 and 1:2 CD-S complexes, provided an excellent fit. The minimum in CIS values at R≈0.5 represents the transformation from a 1:2 to 1:1 stoichiometry (R=1) and can be qualitatively explained as follows. Although $K_{1:2}<K_{1:1}$ (Table 4-4), the formation of 1:2 complexes is favoured for R≤0.5 because of the mass balance effect, $[S]_{total} >> [CD]_{total}$. Other methylated CDs such as DM-β–CD and TM-β–CD also form, 1:2 CD-S complexes with SPFN. The presence of methyl substituents decreases the

dipolar character of the CD annulus and, therefore, reduces type *i)* deshielding effects, since the presence of alkyl groups may screen favourable ion-dipole interactions between the carboxylate head group and the annular hydroxyl groups of CD. As well, the increased apolar (low CMC value) character of a surfactant such as SPFN, promotes the formation of 1:2 CD-S complexes since this inclusion mode minimizes unfavourable apolar-polar interactions with water. A review of the literature indicates that this is the first direct spectroscopic evidence for a 1:2 CD-fc surfactant complex, and corroborates the thermodynamic results, *vide infra*. The formation of 1:2 CD-dye complexes have been reported[213,214] from fluorescence studies of compounds that exhibit π-stacking interactions, and complex formation with CDs enhances this process. Also, indirect evidence of the formation of 1:2 complexes between β-CD and hexanediols has been suggested from the curve fitting results of surface tension data.[215]

Figure 4-6 is a plot of specific conductance versus R for various R-β-CD-fc surfactant systems. In all cases, the change in the slope (positive or negative) beyond R=1 for the R-β-CD-S systems may be attributed to differences in the degree of counterion binding. It is anticipated that the steric effect created by the hydroxypropyl groups prevents the carboxylate head group from interacting favourably with the hydroxyl groups on the CD annulus. The closer approach of the carboxylate head group to the annular hydroxyl groups of RAMEB offers a microenvironment of lower dielectric constant, which may cause the sodium counterions to associate more strongly and result in a positive slope beyond R=1. The decrease in specific conductivity up to R=1 is mainly due to the decrease in the mobility of the carboxylate ion because of the formation

of an inclusion complex. The inflection at R=1 indicates that 1:1 CD-S complexes are formed. These data corroborate the ^{19}F NMR results discussed above. In the case of HP-β-CD-SPFN, the behaviour is similar to the HP-β-CD-SPFH system; however, a small positive maxima occurs at R=0.5. The latter is attributed to the greater molar conductance of the 1:2 complex relative to the 1:1 complex ($\lambda_{CD-S_2^-} > \lambda_{CD-S^-}$) (cf. § 2.1.5).

Tables 4-5a-e list the ^{19}F CIS values for the sodium perfluoroalkyl carboxylate salts at R=1 for the various CD-S systems investigated. The CIS values of ^{19}F guest nuclei of CD-SPFB complexes are observed to follow the order: $C(1)F_2 > C(2)F_2 > CF_3$. The greater magnitude of the ^{19}F CIS values for $C(1)F_2$ and $C(2)F_2$ groups compared to CF_3 in these complexes suggests that more favourable interactions may be occurring between the carboxylate head group and the β-CD annulus than between the apolar CF_3 group and the β-CD cavity. In order to test the former hypothesis, a NMR study of a monosaccharide, α-D-mannose, in the presence of SPFB and SPFO was carried out. The ^{19}F CIS values for these surfactants were less than 0.02 ppm for $C(1)F_2$ and $C(2)F_2$ groups even though the mole ratio of α-D-mannose-S was increased over a twenty-fold range. These small CIS values for the $C(1)F_2$ and $C(2)F_2$ groups suggest that ion-dipole interactions between the surfactant carboxylate head group and sugar hydroxyl groups are not the reason for the greater CIS values observed in the CD-S complexes. On the other hand, the CIS values for α-CD-SPFB complexes are observed to follow the order: $CF_3 > C(2)F_2 > C(1)F_2$ and their magnitude is consistent with a noninclusion binding between the hydroxyl groups of the α-CD annulus and the CF_3 group of SPFB. This occurs

because the diameter of the α-CD cavity is too small to accommodate the fc chain.[65,54,70] A similar result was obtained for the α-CD-SPFO system (cf. Table 4-5d). A noninclusion complex involving van der Waals interactions between the apolar terminus of the fc chain and the α-CD hydroxyl groups is reasonable because it reduces unfavourable contacts between the fc alkyl chain and water. The CF_3 group is somewhat dipolar in character and this would also favour interactions with the annulus region of α-CD.[216] The similar CIS (Table 4-5a) and $K_{1:1}$ values for TM-β-CD-SPFB and α-CD-SPFB ($K_{1:1}$=38 M^{-1}) support the argument that inclusion complexes between the fc surfactants and TM-β-CD are sterically hindered. However, the apolar region of the fc chain of SPFB is included in the CD interior of β-CD and other R-β-CD compounds because the steric effects are not as pronounced.

In the case of inclusion complexes, the CIS values (Table 4-5) of the nuclei of the guest are greatest near the carboxylate head group and decrease as one moves toward the lipophilic end of the fc alkyl chain. The large CIS values for the $C(1)F_2$ and $C(2)F_2$ groups suggest the importance of type *i)* and *ii)* interactions. The formation of β-CD-fc surfactant complex favours a conformation of the fc chain where it is fully extended due to the comparable van der Waals radii of the CF_2 (5Å) and CF_3 (7 Å) groups[65,217] relative to the diameter of the β-CD (≈7Å) interior. The greater CIS values for the $C(1)F_2$ and $C(2)F_2$ groups of fc surfactants complexed with R-β-CD compounds further support the importance of type *ii)* deshielding effects because of the smaller cavity diameters of these hosts. For longer fc surfactants (C_x, x>7), the hydrophilic head group extends outside the annulus region of β-CD, whereas, the apolar portion of the fc chain is included within the

CD interior to minimize unfavourable apolar-polar interactions with the aqueous phase. In the case of β-CD, the CIS values for $C(1)F_2$ and $C(2)F_2$ groups increase as C_x increases up to C_x=4 and then they decrease with further increase in C_x. The increase is attributed to the occurrence of type *ii)* interactions as the carboxylate head group is drawn closer to the annulus region. The decrease in CIS values is attributed to type *iii)* shielding effects that arises from 2:1 binding.

The CIS values for the CF_3 group are largely affected by type *ii)* and *iii)* interactions. In cases where the CIS values are small and positive, the CF_3 group may reside near the facial region, favouring type *iv)* interactions. Negative CIS values indicate the CF_3 group is highly shielded and located in an apolar environment, such as the CD interior. In the case of β-CD, the CF_3 group may reside near the facial region resulting in the less negative CIS values due to a decrease in type *iii)* shielding effects. This arises as the head group is drawn closer to the annulus region and the alkyl chain extends into the aqueous phase. The CF_3 group is probably located in the CD interior for all CD-SPFP complexes since the CIS values are all negative and become more positive as C_x increases (x>4), except in the methylated host systems. The CIS values of the CF_3 group in longer chain fc surfactants becomes more negative in host systems such as RAMEB, DM-β-CD, and TM-β-CD. Since these macrocycles have an extended cavity depth, they can also form 1:2 CD-S complexes. The degree of inclusion depends on the alkyl chain length of the surfactant and possible steric effects due to substituents in the annulus region of the host.

Schemes 5-1 and 5-2 provide possible types of inclusion modes for the CD-S complexes investigated. Schemes 5-1a, 5-1c, and 5-2 are considered to best describe the current results and other information from the literature. Additional evidence for these structures is presented in the next section from the ^{1}H NMR results of the host. HP-β-CD forms 1:1 CD-S complexes (Scheme 5-1a) with all of the fc surfactants whereas the other CD hosts may form other complexes depending on the alkyl chain length of the surfactant. β-CD forms 2:1 complexes (Scheme 5-1c) with longer fc chain (C_x, x=7-9) surfactants, whereas the methylated CDs form 1:2 complexes (Scheme 5-2) with SPFN.

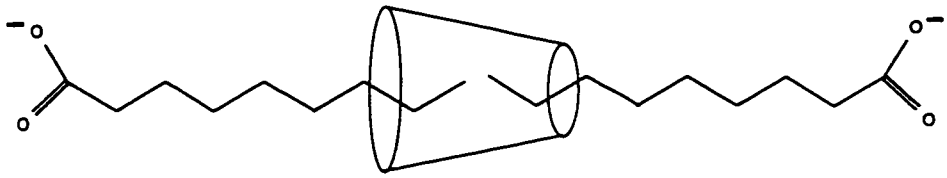

Scheme 5-2: Proposed inclusion mode for the 1:2 CD-SPFN complex, as determined from ^{19}F NMR data; where CD= RAMEB, DM-β-CD, and TM-β-CD.

That the hydrophobic effect is an important factor in these noncovalent interactions is evident from the inclusion modes presented in Schemes 5-1 and 5-2. Complex formation can maximize contact between complementary lipophilic regions[54,70] of the host and guest and minimize unfavourable hydrophobic hydration of the fc alkyl chain.

5.2.2 ^{1}H NMR chemical shifts of β-CD

The ^{19}F nuclei of the fc surfactant show large changes in CIS values in the presence of the various host systems. Although it may seem logical to interpret these data in terms of inclusion phenomena, it is possible that such changes could also be due to

intermolecular interactions between the surfactant and the exterior of the macrocycle. In order to confirm the formation of inclusion complexes, a quantitative study of the CIS values of the host nuclei was also carried out. The environmental factors affecting ^1H chemical shifts of β-CD have been outlined in § 5.1.2.

Figures 4-7a-b show plots of $\Delta\delta$ versus R for the β-CD-SPFP and β-CD-SPFN surfactant systems, respectively. The CIS values in Fig. 4-7a for H(3) and H(5) protons of β-CD display a nonlinear increase up to R=3 and then level off. This pattern of behaviour is consistent with that for a weakly bound 1:1 complex, as seen for the β-CD-SHex system in Fig. 4-3a. The CIS values for H(5) (Fig. 4-7b) exhibit a nonlinear increase up to R=1 and then level off, whereas H(3) levels off beyond R=0.5, similar to that observed for the β-CD-SDS system (Fig. 4-3c). The dashed lines through the data in Figs. 4-7a-b correspond to fitting of the data using eq 2.1.2-4 and eq 2.1.2-6, respectively. The data in Fig. 4-7a-b corroborate the conclusion drawn from ^{19}F NMR results of the guest in § 5.2.1, i.e., β-CD-SPFP forms a 1:1 complex and β-CD-SPFN forms 1:1 and 2:1 complexes.

The greater rate of increase in CIS values for H(3) and the levelling CIS values near R=0.5 for the β-CD-SPFN system (Fig. 4-7b) indicates that it is the wide, secondary side of the annulus that binds onto the unbound portion of the fc alkyl chain of the 1:1 complex. As well, the formation of a 2:1 β-CD-SPFO complex is strongly supported by the ^{19}F results described in § 5.2.1. However, the anticipated break in $\Delta\delta$ of H(3) at R=0.5 is not observed for this system. Provided that the inclusion mode of the 2:1 β-CD-

SPFO complex is similar to that of the 2:1 β-CD-SPFN complex (cf. Scheme 5-1c), the NMR results can be explained for the former system according to Scheme 5-3.

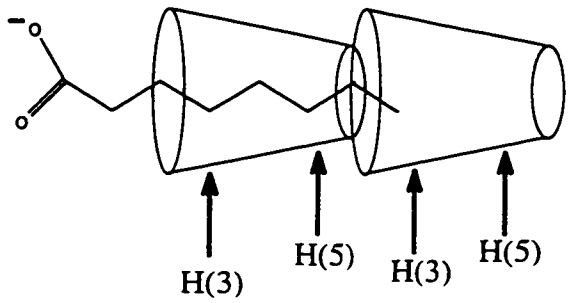

Scheme 5-3: Proposed inclusion mode for the 2:1 β-CD-SPFO complex where the second CD is bound in the wide, secondary annulus region of β-CD, as determined from ^{1}H NMR data.

Therefore, it is concluded that the second CD that binds onto the fc chain of SPFO occurs by means of the secondary annulus region and is bound as a noninclusion complex, as shown in Scheme 5-3. The smaller CIS values of H(3) at R=0.5 for the β-CD-SPFO system relative to the β-CD-SPFN system indicates that the second CD in the 2:1 β-CD-SPFO complex does not fully include the fc chain within the apolar interior. The second CD can be considered as a noninclusion complex since the interactions that occur are primarily between the annular hydroxyl groups of the macrocycle and the apolar end of SPFO. Such binding is also consistent with the small increase in the CIS values of H(3) upon changing the gues from SPFH to SPFO in complexes with β-CD. A similar type of noninclusion binding has been reported[66] for α-CD-fc surfactant complexes (cf. Scheme 1-5). This type of binding is reflected by small CIS values for H(3) and H(5) and is consistent with the results obtained for β-CD-SPFO (Table 4-6). The increase in CIS value of H(3) and H(5) for the β-CD-SPFN and -SPFD systems is related to the extension

of the fc chain into the second CD interior and the concomittant increase in the fraction of bound species due to the increase in K_i (i=1:1 and 2:1).

The CIS values for the host H(3) and H(5) nuclei for various β-CD-S systems and the calculated K_i of the complexes are listed in Table 4-6. In general, the magnitude of K_i increases as the alkyl chain length of the fc surfactant increases. The values are in good agreement with those listed in Table 4-4 and with previous estimates obtained from emf[105,116] studies of long chain hydrocarbon surfactants. Positive $\Delta\delta$ values of H(3) and H(5) indicate that inclusion complexes are formed because of the increase in shielding due to dehydration of the CD interior and subsequent inclusion of a fc alkyl chain. In general, the magnitude of the CIS values for H(3) are less than those for H(5), because of the toroidal shape of the macrocycle, and they both increase as C_x increases.

A comparison of the CIS values of the host interior protons in Tables 4-3 and 4-6 indicates that the CIS values for the CD-fc surfactant complexes are systematically greater than those for CD-hc surfactant systems. This may be due to the closer intermolecular contact between a fc chain and the β-CD interior as compared to a hc chain and the β-CD interior as a result of the greater van der Waals diameter of the former. As well, the fc surfactants possess a systematically higher binding affinity to β-CD than do the hc surfactants.

On the basis of the CIS values of the host and guest nuclei and ROESY data in § 5.1.1 and § 5.1.2, respectively, there is some evidence that the hc surfactant chain is selectively included through the wider, secondary annulus region of β-CD. The relatively similar CIS values for H(3) and H(5) host protons for the β-CD-SPFB and -SPFP systems

are attributed to the extent of inclusion of the fc chain in the CD interior. The partial inclusion of the guest from the wider, secondary side results in a similar shielding effect for both H(3) and H(5) nuclei of β-CD. The offset in CIS values observed for the β-CD-SPFH and -SPFO systems arises because full inclusion of the fc surfactant chain (Scheme 5-4b) occurs. From these arguments, the inclusion geometry expected for a 2:1 CD-fc surfactant complex is shown by Scheme 5-1c.

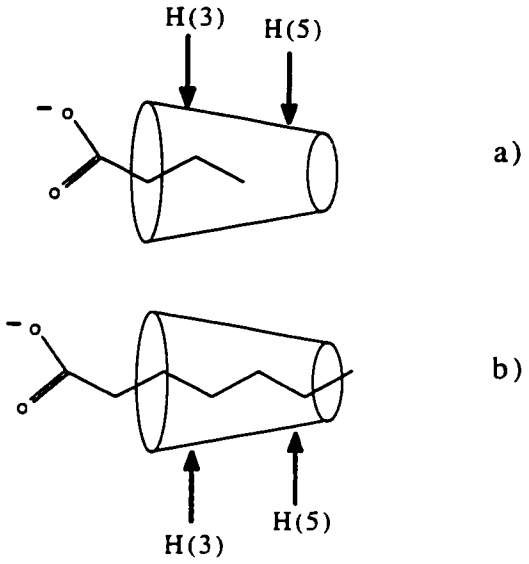

Scheme 5-4: Proposed inclusion modes for the 1:1 β-CD-fc surfactant complexes as determined from ^{1}H NMR data of the host: a) β-CD-SPFB and b) β-CD-SPFH; where the arrows denote the relative position of the H(3) and H(5) nuclei in the β-CD interior.

5.3 Apparent molar volume studies

5.3.1 Apparent molar volume of sodium alkyl carboxylate salts in water and aqueous cyclodextrin solutions

At the start of this study, information on the volumetric properties of CD-inclusate complexes was scarce.[218] Only one study dealing with the thermodynamic properties of

CD-inorganic electrolytes was available.[31] Some indirect information regarding the volume changes associated with complex formation was available for certain complexes from kinetic studies (ultrasonic relaxation).[129,218g] Høiland *et al.*[168] have performed a quantitative analysis of the volumetric data of cation-crown ether complexes using an approach similar to that outlined in § 2.1.3. Unfortunately, the analysis of volumetric data in a recent study of CD-surfactant systems[193] was complicated by the presence of micelle aggregates at the surfactant concentrations investigated. The work in this thesis represents the first major systematic study of the volumes of CD-surfactant systems over a wide range of premicellar concentrations.

The apparent molar volumes (AMV) of the sodium alkyl carboxylate salts were determined in water and in ternary (w+CD+S) aqueous solutions, as shown in Figures 4-8a-b. These plots illustrate the concentration dependence of $V_{\phi,S}$, in the absence and presence of β-CD, and of the mole fractions of complexed (X_i , i=1:1) and unbound surfactant (X_f) for a short chain (SHex) and long chain (SDodec) hc surfactant bound to β-CD, respectively. In water, $V_{\phi,S}$ exhibits a linear dependence (solid line) with a slightly positive slope at low concentration, in agreement with the sign expected from the Debye Hückel limiting law for a 1:1 electrolyte.[33] However, the amphiphilic nature of the salt should decrease the magnitude of the expected theoretical slope because of hydrophobic hydration,[28] and this is seen to be the case for SDodec. In ternary solutions, the magnitude of $V_{\phi,S}$ in the ternary system exceeds that in water, especially near infinite dilution, and decreases with $C_S^{1/2}$ until the values at higher concentrations approach those obtained in water. This is because the magnitude of the AMV of the 1:1 or 2:1 complex exceeds the

value of the dispersed surfactant ($V_{\phi,i} > V_{\phi,f}$) and the amount of unbound surfactant (X_f) increases as $C_S^{1/2}$ increases. In general, the magnitude of the AMV decreases as $C_S^{1/2}$ increases and the profile of the AMV becomes more nonlinear as C_x increases. The magnitude of the AMV depends upon the fraction of bound species, a function of the magnitude of K_i, and the relative concentrations of host and guest. The dashed line through the data points in Fig. 4-8a for SHex in 0.013 m β-CD is the "best fit" according to the two-site model (cf. eq 2.1.3-10). The solid line through the data for SHex in water (Fig. 4-8a) corresponds to the least-squares regression and the curves for $X_{1:1}$ and X_f were derived using $K_{1:1}$ (Table 4-7) and the concentration conditions of the ternary solution.

The ternary solution data in Figs. 4-8 a and b are similar. However, the effect of increased carbon chain length is clearly evident as the magnitude of ΔV_S° is greater for SDodec relative to SHex. (cf. Table 4-4). The concentration dependence of $V_{\phi,S}$ becomes increasingly sigmoidal as C_x increases, consistent with an increase in K_i. The dashed line through the data points for SDodec in 0.013 m β-CD corresponds to the "best fit" according to the three-site model (cf. eq 2.1.3-11) which accounts for the volumes of surfactant in its unbound state, 1:1 and 2:1 complexes. Attempts to simulate the experimental data using eq 2.1.3-10 resulted in poorer fits. These results provide independent support for the existence of 2:1 CD-S complexes, as suggested in § 5.1.1 and § 5.1.2. Generally, the magnitude of $V_{\phi,S}$ for 2:1 complexes exceeds that for 1:1 complexes and the shape of the curves are more sigmoidal. This is consistent with the expectation that the inclusion of additional methylene groups results in more extensive desolvation of the alkyl chain (cf. Scheme 5-5).

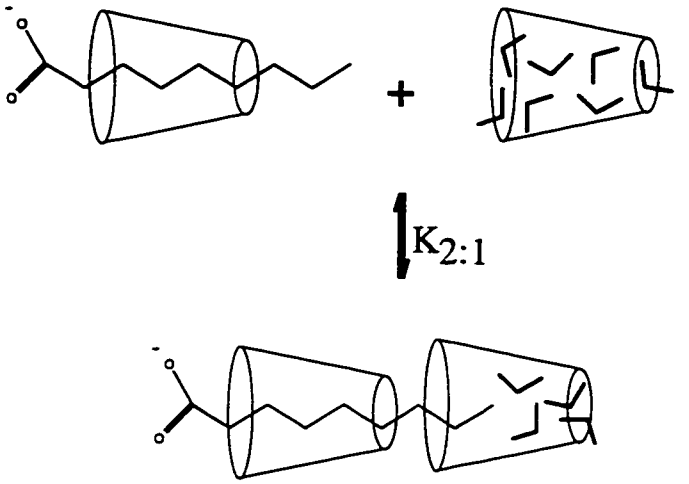

Scheme 5-5: Volumetric changes accompanied by 2:1 CD-S complex formation in aqueous solution; where the "v-shaped" structures represent water molecules.

Tables 4-7 to 4-9 list the AMV at infinite dilution in water and aqueous CD solutions, the transfer volume at infinite dilution (ΔV_S^o), and the binding constants calculated from the AMV data in ternary solutions. The transfer quantities can be interpreted in terms of the change in hydration that accompanies complex formation. The formation of micelles involves positive changes in volume since the carbon chain segments are transferred from an aqueous to an apolar environment.[193] The positive values of ΔV_S^o obtained in this study are consistent with the fact that inclusion complexes are formed since the process involves a similar change in chemical environment of the guest.[28] However, sodium propionate (SP) is an example of an inclusate that does not form an inclusion complex with β-CD under these conditions since $\Delta V_S^o \approx 0$ (Table 4-7). In general the magnitude of ΔV_S^o increases as C_x (or K_i) increases because the fraction of bound species (X_i) increases. The magnitude of the AMV for the unbound species ($V_{\phi,f}$) is less than the AMV for the bound species ($V_{\phi,i}$). As well, $V_{\phi,2:1} > V_{\phi,1:1}$, because the formation of 2:1

complexes involves the transfer of more alkyl groups from the bulk to the complexed state relative to that for 1:1 complexes (cf. Scheme 5-5). The sharp increase in ΔV_S° for $C_x \geq 11$ in Table 4-7 arises because of the formation of 2:1 complexes and corroborates the ^1H NMR results in § 4.1.1. As well, the formation of 2:1 complexes at infinite dilution is favourable because the concentration of host exceeds that of the guest ($C_{CD} >> C_S$), according to mass-balance effects. Because of their extended cavity length, the R-β-CD hosts do not form 2:1 complexes with the alkyl carboxylates studied. This is shown by the smooth monotonic increase in ΔV_S° as C_x increases.

Calculated binding constants (K_i) obtained from an analysis of the volumetric data of the guest using the two- and three-site models are listed in Tables 4-7 to 4-9. K_i increases as C_x increases for all of the CD-S complexes investigated. The binding affinities of the various host systems follow the order: DM-β-CD ≈ HP-β-CD > β-CD. The slightly greater binding affinity of the R-β-CDs relative to β-CD with hc surfactants can be attributed to a possible increase in the hc-hc van der Waals interactions and/or more complete desolvation of the alkyl chain of the surfactant because of the inclusion of additional methylene groups in the R-β-CD hosts. For complexes that form 2:1 complexes, the values of $K_{1:1}$ exceed $K_{2:1}$ by one to two orders of magnitude, in agreement with K_i obtained from emf studies of long alkyl chain cationic and anionic surfactants that form 1:1 and 2:1 complexes with β-CD.[105,116] The small differences between the K_i of the β-CD, DM-β-CD, and HP-β-CD hosts with a common guest suggest that the presence of alkyl substituents in the annulus region of the CD has a marginal effect on the binding affinity with the hc surfactants. The steric exclusion effect of alkyl substituents in the annulus

region in the case of hc surfactants is not pronounced for two main reasons: *i)* the smaller van der Waals diameter of the CH_3 group (4Å)[40] in relation to the diameter of the β-CD annulus and *ii)* the weak contribution of ion-dipole interactions between the surfactant head group and the β-CD annulus due to more favourable hydration of the carboxylate head group (cf. § 5.1.1). The main reason for complex stability is the interaction between the alkyl chain and the CD interior, as shown by the results presented above.

5.3.2. Apparent molar volume of sodium perfluoroalkyl carboxylate salts in water and aqueous cyclodextrin solutions

Figure 4-9 illustrates the concentration dependence of $V_{\phi,S}$ for SPFN in water and aqueous solutions of β-CD, DM-β-CD and HP-β-CD, respectively. In water, SPFN exhibits a slightly negative linear dependence on concentration, though it is a 1:1 electrolyte. This is attributed to hydrophobic hydration effects because of its relatively greater lipophilic character. In 0.005 m HP-β-CD, SPFN shows behaviour typical of a strongly bound 1:1 complex, as shown by the large value of ΔV_S^o, and the sharp decrease in $V_{\phi,S}$ at the 1:1 R-β-CD-S mole ratio. The dashed line shows the "best fit" according to eq 2.1.3-10.

The AMV of SPFN in aqueous DM-β-CD exhibits a complex nonlinear dependence: a gradual decrease at the 1:1 DM-β-CD-S mole ratio, a minimum near the 1:2 mole ratio and an increase beyond the 1:2 mole ratio. The positive increase in the AMV beyond the 1:2 DM-β-CD-S ratio is unexpected and suggests the possible involvement of an additional equilibrium. In general, $V_{\phi,S}$ decreases as $C_s^{1/2}$ increases because of the

increasing mole fraction of unbound surfactant (cf. Fig. 4-8) and its smaller AMV relative to bound surfactant ($V_{\phi,f} < V_{\phi,i}$). The dashed line that passes through the lower concentration range data points represents the "best fit" curve corresponding to eq 2.1.3-12. Evidence for the formation of 1:2 DM-β-CD-SPFN complexes was presented in § 5.2.1. The AMV results presented here indicate that SPFN and ST form 1:2 complexes with DM-β-CD. This type of host-guest stoichiometry provides a favourable means of minimizing surfactant/water interactions and optimizing the CD/surfactant interactions, particularly, when $[S]_{total} >> [CD]_{total}$.

It will be shown in § 5.3.6.2 that the magnitude of the AMV at infinite dilution is strongly dependent on the relative concentrations of the host and guest for weakly bound complexes and relatively independent for strongly bound complexes. The fact that $V^{o}_{\phi,S}$ for SPFN in aqueous DM-β-CD-SPFN exhibits an unusual dependence on the binary solvent concentration, despite the large magnitude of $K_{1:1}$ for this system, indicates that an additional equilibrium may be occurring besides 1:1 and 1:2 complexation. As well, there is disagreement between the "best fit" curve (eq 2.2.3-12) and the experimental data at greater concentrations of SPFN. The poorer fit at host-guest mole ratios greater than 1:2 is due to non-ideal effects.[219] Thus, as the concentration of DM-β-CD increases, deviations between the experimental and calculated AMV data are more pronounced. In 0.004 m DM-β-CD, the positive increase in the AMV of SPFN beyond the 1:2 DM-β-CD-S mole ratio may be due to the formation of a ternary complex, since there is minimal contribution to the volume from unbound surfactant, and the effect is more pronounced as $C_{R\text{-}\beta\text{-}CD}$ or C_S increases. The ternary complex is defined as the binding of surfactant monomers to the

exterior of the macrocycle of a methylated CD-S complex (cf. Scheme 5-6b). Aggregation processes, such as micelle formation, show a sharp increase in AMV at the CMC.[164,188] The increase in AMV beyond the 1:2 CD-S mole ratio may be due to the formation of ternary complexes between the 1:1 and/or 1:2 complexes with unbound SPFN. The following expression provides a semiquantitative intrepretation of the data for the DM-β-CD-SPFN system.

$$V_{\phi,S} = X_f V_{\phi,f} + X_{1:1} V_{\phi,1:1} + X_{1:2} V_{\phi,1:2} + X_{tern} V_{\phi,tern} \qquad (5.3.2\text{-}1)$$

where X_{tern} and $V_{\phi,tern}$ are the mole fraction and AMV of the ternary complex, respectively, and the remaining terms are defined in eq 2.1.3-12. The formation of such complexes between SPFN and DM-β-CD is consistent with the relatively low CMC[65] of SPFN and the decreased dipolar character of the facial region of DM-β-CD relative to β-CD. Further evidence for the latter is also seen from the magnitude of the pair-wise interaction parameter (B_v, cf. § 4.3.3), surface active properties, and the tendency of DM-β-CD to form mixed monolayers.[55,56] Ternary complexes between TM-α-CD and an azo dye compound has been previously reported.[221] Further work will be necessary to characterize these ternary complexes. The presence of an upturn in the AMV for SPFN in aqueous β-CD or HP-β-CD is not expected due to the more hydrophilic character of these cyclodextrins. To illustrate that 2:1 complexes are not the source of the unusual behaviour observed for the DM-β-CD-SPFN system, the AMV data of the β-CD-SPFN system, which forms 2:1 complexes, is shown for comparison.

The β-CD-SPFN system displays a more sigmoidal-shaped curve (Fig. 4-9) relative to that for β-CD-SDodec (Fig. 4-8b) and this may be attributed to the occurrence of positive

binding cooperativity.[33,59] This arises from the rearrangement of H-bonds (§ 1.2.1) within the solvent (H_2O) network because of extensive solvation and desolvation (cf. § 1.4.2) of the host and guest upon formation of the complex. It is expected that the "high energy" water within the β-CD interior (§ 1.3.2.3) and water in the hydration shell about the alkyl chain of the surfactant can assume a more "relaxed" state in the bulk phase when the hc chain is transferred to the β-CD interior. The fact that the β-CD-SPFN system displays more cooperative behaviour than β-CD-SDodec is consistent with its more hydrophobic character, e.g., CMC(SPFN)= 0.01 M and CMC(SDodec)= 0.024 M.

The formation of 2:1 complexes provides a means of increasing apolar/apolar interactions and reducing apolar/polar interactions. It is interesting to note that the onset of 2:1 binding between β-CD-fc and -hc surfactant systems occurs for the guests SPFO and SDodec, respectively. Despite the different physicochemical properties of these surfactants, they possess similar $V^o_{\phi S}$ (cf. Table 4-7 and 4-10) which suggests the energetics of forming a cavity in solution for the guest may be an important factor in the complexation process. Previous experimental[152] and theoretical[220] studies conclude that the relative hydrophobicity may be predicted from molecular sizes and surface areas of apolar alkyl groups.

Tables 4-10 to 4-12 list the AMV at infinite dilution for sodium perfluoroalkyl carboxylate salts in water and aqueous CD solutions, the transfer volume at infinite dilution (ΔV_S^o), and the calculated binding constants. In all cases the values of ΔV_S^o for the fc surfactants are positive and systematically greater than for hc surfactants of a similar chain length. These facts are consistent with the formation of inclusion complexes and the greater volume and hydrophobicity of a fluorocarbon chain compared to a hydrocarbon chain.[216] In

aqueous DM-β-CD and HP-β-CD solutions, ΔV_S^o increases monotonically as C_x increases because of the formation of 1:1 complexes. In aqueous β-CD, ΔV_S^o increases monotonically and shows a sudden increase at C_x=7 because of the formation of 2:1 complexes. The onset of 2:1 binding for the fc surfactants (C_x=7) and hc surfactants (C_x=11) are consistent with the relative lipophilic character of hc and fc surfactants.[40]

The values of K_i increase as C_x increases for all of the CD-S systems and the values are systematically greater for the fc surfactants compared with the hc surfactants of a similar alkyl chain length. The relative binding affinity of a common fc surfactant with different hosts follow the order: β-CD >DM-β-CD>HP-β-CD. The correlation between the fc chain length and the magnitude of K_i suggest that hydrophobic interactions play an important role in complex stability, as mentioned in § 5.2.1 and § 5.2.2. As well, it is likely that ion-dipole interactions between the surfactant head group and the annular hydroxyl groups of the CD contribute in a secondary way to the stability of the complex since the binding affinity decreases with an increase in the number and size of alkyl groups in the CD annulus region. The lower degree of hydration of the carboxylate head group of the fc surfactant is believed to be a reason for ion-dipole interactions being more important than in the case of hc surfactants. The difference in hydration of the hc and fc carboxylate ions is attributed to their relative basicity since pK_a (hydrogenated fatty acids) > pK_a (perfluorinated fatty acids).[37,182] Emf studies[209,222] indicate that sodium counterion binding to the β-CD-$C_7F_{15}COO^-$ complex is greater than for the β-CD-$C_9H_{19}COO^-$ complex and this fact further supports the contention that the carboxylate headgroup of hc surfactants is more strongly hydrated than fc surfactants. Notwithstanding, the interactions between the alkyl chain of

the surfactant and the CD interior, governed by the hydrophobic effect,[28,34] play a primary role in the host-guest binding affinity, as shown by the increase in $K_{2:1}$ as C_x increases. The results of the volumetric work presented above for the CD-fc surfactant complexes corroborate the results obtained from the NMR work described in § 5.2.1 and § 5.2.2.

5.3.3 Apparent molar volume of cyclodextrins in water

As mentioned in § 5.3.1, volumetric data for CD-inclusate systems are relatively scarce, however, there have been AMV studies for α-CD and β-CD in water.[218] Figure 4-10 shows a comparison of $V_{\phi,CD}$ data in water obtained in this work and from the literature.[218,193] The AMV for β-CD is in good agreement with the results of Milioto *et al.* Disagreement with the data of Paduano *et al.* may be due to reasons given in § 2.1.3. The concentration range over which the AMV data can be obtained in water is limited by the solubility of β-CD (1.85 g L^{-1}).[1] It is for this reason that the binding constants (K_i) for the β-CD-S systems were not tabulated because the restricted range of concentration limits the reliability of computer fitting results.[102] The AMV of the CDs in water follow a linear relationship with concentration according to eq 4.3.3-1. The parameter (B_v) is related to the solute-solute pair interaction parameter. The magnitude of B_v for the three CDs varies in the following order: HP-β-CD ≈ DM-β-CD > β-CD. The larger value of B_v for the R-β-CD compounds is related to the presence of alkyl substituents in the annulus region and their greater amphiphilic character. The smaller value for β-CD is attributed to its greater dipolar character and propensity to form intermolecular H-bonds with water.

5.3.4 Apparent molar volume of cyclodextrins in aqueous solutions of sodium alkyl carboxylate salts

Figures 4-11a-b are typical plots of ΔV_{CD} against C_{CD} for certain CD hosts in aqueous solutions of a short (SHex) and long chain (SDodec) hc surfactant, respectively, at different concentrations. Figure 4-11a shows a negative linear dependence of $\Delta V_{\beta\text{-}CD}$ on $C_{\beta\text{-}CD}$ in each of the binary surfactant solutions. As the concentration of the binary solvent (w+S) increases, the magnitude of $\Delta V_{\beta\text{-}CD}$ is shifted to more positive values, as expected for a weakly bound complex (cf. Table 4-10). The negative concentration dependence of $\Delta V_{R\text{-}\beta\text{-}CD}$ with $C_{R\text{-}\beta\text{-}CD}$ is similar to that observed for the complementary AMV of SHex in aqueous β-CD. This is consistent with an increase in the fraction of unbound host (X_f) as $C_{\beta\text{-}CD}$ increases and the fact that $V_{\phi,f} < V_{\phi,i}$, as discussed in § 5.3.3. The "best fit" lines through the ternary solution data in 0.005 m and 0.030 m SHex correspond to the two-site model (cf. eq 2.1.3-10) for 1:1 complexes. The reason for the absence of fitted lines in 0.060 and 0.120 m SHex is because of nonideal solvent effects[105,219] and the sensitivity problems that were outlined in § 4.3.4.

A comparsion of ΔV_{CD} in binary surfactant solutions of SDodec (Fig. 4-11b) with Fig. 4-11a illustrates the effects of increasing the alkyl chain length of the surfactant and of alkyl substituents in the annulus region of the CD. At the lower concentrations of SDodec, ΔV_{CD} for DM-β-CD and HP-β-CD display a sigmoidal concentration dependence and the transfer volume at infinite dilution is greater than that for the β-CD-SHex system at comparable conditions. The results for the R-β-CD-SDodec systems are consistent with that for strongly bound complexes (cf. Table 4-11 and 4-12). The more positive transfer

volume of HP-β-CD relative to DM-β-CD is related to the extended cavity length of the macrocycle because the hydroxypropyl substituents are longer than methyl groups. The inclusion of longer alkyl chain length surfactants and the formation of only 1:1 complexes with each of the surfactants is expected to result in larger transfer volumes because of more desolvation of the host and guest, as discussed for 2:1 complexes in § 5.3.3. In 0.020 m SDodec, ΔV_{CD} for DM-β-CD displays similar behaviour and values to that of β-CD in 0.120 m SHex. This occurs because of the relatively large binding constant for the DM-β-CD-SDodec system and the larger fraction of bound species ($X_{1:1}$) at these concentration conditions.

Table 4-13 lists the values of $V^{\circ}_{\phi,\beta\text{-CD}}$ and $\Delta V^{\circ}_{\beta\text{-CD}}$(w→w+S) for β-CD in aqueous solutions (w+S) containing low, medium, and high concentrations of sodium alkyl carboxylate salts. The corresponding complementary data, $V^{\circ}_{\phi,S}$ and ΔV°_{S}(w→w+CD), for the hc and fc surfactants in aqueous β-CD is not accessible due to the limited solubility of β-CD. Under the experimental conditions for which the data have been obtained, ΔV°_{CD} represents the increase in volume of CD upon transfer from water to the complexed state at infinite dilution when there is an excess of surfactant. The following factors are likely to affect these values: *(i)* the inclusion orientation of the guest in the host, *(ii)* the relative amounts of complexes of different stoichiometry, and *(iii)* the magnitude of the binding constants, K_i. The shorter carbon chain length surfactants exhibit a monotonic increase in $V^{\circ}_{\phi,\beta\text{-CD}}$ and $\Delta V^{\circ}_{\beta\text{-CD}}$ as the binary solvent (w+S) concentration increases, whereas a weaker dependence of the magnitude of $V^{\circ}_{\phi,\beta\text{-CD}}$ and $\Delta V^{\circ}_{\beta\text{-CD}}$ occurs for longer chain surfactants.

These results can be explained in terms of the mole fraction of bound (X_i) host at infinite dilution. Since K_i is smaller for the short chain surfactants, X_i exhibits a strong positive increase as the concentration of the binary (w+S) solvent increases, as shown by the increase in $\Delta V^{o}_{\beta\text{-CD}}$ at such conditions (Fig. 4-11a). Further increases in the binary (w+S) solvent results in relatively constant values of $\Delta V^{o}_{\beta\text{-CD}}$ because $X_{1:1}$ approaches unity for these conditions. The small variation in $V^{o}_{\phi,\beta\text{-CD}}$ and $\Delta V^{o}_{\beta\text{-CD}}$ with increasing concentration of binary (w+S) solvent for longer chain length surfactants is attributed to the large value of K_i and the complete desolvation of the CD cavity, as the surfactant fills the entire CD interior.

The values of $V^{o}_{\phi,R\text{-}\beta\text{-CD}}$ and $\Delta V^{o}_{R\text{-}\beta\text{-CD}}$ (w→w+S) for DM-β-CD and HP-β-CD in aqueous solutions of sodium alkyl carboxylate salts are shown in Table 4-14. $V^{o}_{\phi,R\text{-}\beta\text{-CD}}$ for DM-β-CD and HP-β-CD exhibit an increase of ca. 4.3-4.5 $cm^3\ mol^{-1}$ per CH_2 of the surfactant up to C_x=9 and then a smaller increase of ca. 1.9-1.7 $cm^3\ mol^{-1}$ per CH_2 for C_x>9. These results suggest that the R-β-CDs can include an hc alkyl chain of approximately 10 CH_2 groups. Despite the differences in the nature of the alkyl substituents on HP-β-CD and DM-β-CD, the transfer volumes in Table 4-14 are very similar. These results indicate that the interactions that occur between the CD interior and the alkyl chain are more significant than the interactions that occur in the annulus region. It also corroborates the conclusions presented in § 5.1.1 regarding the diminished interactions between the CD annulus and the surfactant head groups of the hc surfactants. The expectation that alkyl substituents do not substantially increase the hydrophobic character of the CD is consistent with the small,

positive pair-wise interaction term obtained from excess thermodynamic data for methylglucosides compared to the more positive values for organic molecules with polar groups.[223] As well, it has been argued that alkyl groups located within two bond lengths of a heteroatom, such as oxygen, do not exhibit substantial lipophilic character.[164] The main consequence of alkyl substituents in the annulus region is to increase the annulus length and, therefore, to include a greater number of CH_2 groups in the R-β-CD hosts relative to β-CD. This corroborates conclusions drawn from the $V_{\phi,S}$ data in § 5.3.1.

5.3.5 Apparent molar volume of cyclodextrins in aqueous solutions of sodium perfluoroalkyl carboxylate salts

Figures 4-12a-d are typical plots of ΔV_{CD} versus C_{CD} for β-CD and R-β-CD compounds in aqueous solutions of sodium perfluoroalkyl carboxylate salts at various surfactant concentrations. Figure 4-12a illustrates $\Delta V_{\beta\text{-}CD}$ versus $C_{\beta\text{-}CD}$ in 0.005 m and 0.030 m aqueous SPFO. In 0.030 m SPFO, $\Delta V_{\beta\text{-}CD}$ is shifted to more positive values. The similar magnitude of ΔV°_{CD} in these two SPFO solutions can be attributed to the similar fraction of complexed β-CD ($X_{1:1}$) in these systems at infinite dilution because of the large value of K_i (cf. Table 4-10), as discussed in § 5.3.4. In 0.005 m SPFO, the more negative slope of $\Delta V_{\beta\text{-}CD}$ versus $C_{\beta\text{-}CD}$ is due to the increasing amount of unbound species (X_f) as C_{CD} increases. The dashed line through the data in 0.005 m SPFO was obtained by using the three-site model (cf. eq 2.1.3-11). Although β-CD-SPFO forms 2:1 complexes, the relatively small transfer volumes for this system indicates that the second CD which caps onto the 1:1 complex may only encapsulate a small portion of the fc chain, as depicted in Scheme 5-3.

This inclusion mode agrees with the interpretation of the ^{1}H and ^{19}F NMR results in § 5.1.2 and § 5.2.2. In 0.030 m SPFO, the less negative slope is attributed to the greater amount of bound species (X_i) because of the increased concentration of the binary solvent (w+S) system. The absence of a "best fit" line through this data is for reasons similar to that discussed with regard to Figs. 4-11a-b (§ 5.3.4).

Figure 4-12b is a plot of $\Delta V_{\beta\text{-}CD}$ versus $C_{\beta\text{-}CD}$ in aqueous solutions of SPFN at various concentrations. The mole fractions of the bound (X_i) and unbound (X_f) host in 0.005 m aqueous SPFN are plotted on the right hand ordinate and were obtained by using the K_i in Table 4-10. $\Delta V_{\beta\text{-}CD}$ displays a maximum in each binary solvent (w+S) system near the 2:1 CD-S mole ratio. This behaviour is understood in terms of the relative mole fractions of each species and the fact that $V_{\phi,f} < V_{\phi,1:1} < V_{\phi,2:1}$. Complexes of the 1:1 type dominate near infinite dilution up to C_S=C_{CD}. As C_{CD} exceeds C_S, $X_{2:1}$ increases and reaches a maximum at the 2:1 CD-S mole ratio and then decreases thereafter. Consequently, the maxima in the curves for ΔV_{CD} in Fig. 4-12b are related to the formation of 2:1 CD-S complexes. The greater magnitude of the transfer volume of β-CD-SPFN relative to β-CD-SPFO system is related to the deeper inclusion of SPFN into the second CD. The effect is even more pronounced in the β-CD-SPFD system (cf. Fig. 4-12c) as shown by the appearance of a sharper maximum with a larger transfer volume near the 2:1 CD-S mole ratio, and is consistent with the increase in $K_{2:1}$ and $V_{\phi,2:1}$. The dashed lines in Figs. 4-12 b-c were obtained using the three-site model (cf. eq 2.1.3-11). A comparison of Figs. 4-12a-c illustrate the effects of 2:1 CD-S complex formation as the alkyl chain length of the surfactant is increased.

Figures 4-12d-f are plots of $\Delta V_{R\text{-}\beta\text{-}CD}$ vs $C_{R\text{-}\beta\text{-}CD}$ for DM-β-CD and HP-β-CD in aqueous fc surfactant solutions. In all cases, the HP-β-CD-S system forms 1:1 complexes as shown by the dashed line obtained according to eq 2.1.3-10. In Figure 4-12d, the magnitude of $\Delta V^{\circ}_{R\text{-}\beta\text{-}CD}$ in each aqueous solution of SPFH is similar because of the comparable binding constants for these R-β-CD-S complexes. In Fig. 4-12e, $\Delta V^{\circ}_{R\text{-}\beta\text{-}CD}$ for each cyclodextrin is similar in the dilute binary aqueous SPFO solutions; however, the sharper decrease in $\Delta V_{R\text{-}\beta\text{-}CD}$ for DM-β-CD beyond the 1:1 R-β-CD-S mole ratio is because of the greater magnitude of K_i for this system. The greater contribution of unbound DM-β-CD (X_f), when $C_{CD}>C_S$, results in a further lowering of $\Delta V_{R\text{-}\beta\text{-}CD}$. In 0.025 m SPFO, the magnitude of $\Delta V^{\circ}_{R\text{-}\beta\text{-}CD}$ for DM-β-CD in 0.025 m SPFO (>70 cm^3 mol^{-1}) exceeds that in 0.025 m SPFH (≈17 cm^3 mol^{-1}) (Fig. 4-12 d). The large nonlinear increase for $\Delta V_{DM\text{-}\beta\text{-}CD}$ in 0.025 m SPFO near infinite dilution is attributed to hydrophobic interactions between the unbound surfactant and R-β-CD-S complexes because of the increased hydrophobic character of SPFO. This effect is not observed with SPFH in Fig. 4-12d. The "best fit" lines in Fig. 4-12e in the more dilute binary (w+S) solvents for HP-β-CD and DM-β-CD correspond to eq 2.1.3-10 and -12, respectively. Difficulty was encountered in obtaining a suitable fit using the three-site models for the data in 0.025 m SPFO even when $V_{\phi,f}$ was treated as an adjustable parameter. Equation 5.3.2-1 provides a semiquantitative account of how the formation of a supramolecular ternary complex between dispersed surfactant and a CD-S complex could be included in the analysis of the data. However, general application of eq 5.3.2-1 is limited because it involves six adjustable parameters and more extensive experimental data would be required for a reliable quantitative analysis.

Figure 4-12f is a plot of $\Delta V_{R\text{-}\beta\text{-}CD}$ versus $C_{R\text{-}\beta\text{-}CD}$ for DM-β-CD and HP-β-CD in aqueous SPFN. The features of the transfer volume for HP-β-CD are similar to those seen in Fig. 4-12e in 0.005 m SPFO. In the presence of 0.005 m SPFN, the concentration dependence of $\Delta V_{R\text{-}\beta\text{-}CD}$ for HP-β-CD is typical of that for a strongly bound 1:1 complex as shown by the "best fit" line through the data according to eq 2.1.3-10. The nonideal behaviour of DM-β-CD in 0.009 m SPFN is similar to that observed in 0.025 m SPFO (Fig. 4-12e). The magnitude of $\Delta V^{o}_{R\text{-}\beta\text{-}CD}$ and the relative nonlinearity of the curves near infinite dilution increase as the concentration of SPFN increases from 0.005 m to 0.009 m. These results are consistent with the occurrence of ternary complexes between dispersed SPFN and DM-β-CD-SPFN complexes, and corroborates the complementary AMV data of SPFN in 0.004 m DM-β-CD (cf. Fig. 4-9). In 0.005 m SPFN, $\Delta V_{DM\text{-}\beta\text{-}CD}$ was fitted using eq 2.1.3-12; however, the "goodness of fit" decreases near infinite dilution because of these interactions. Complexes of this type are anticipated to increase when $C_S > C_{CD}$. However, when $C_{R\text{-}\beta\text{-}CD}$ increases, the formation of inclusion complexes competes for free monomers more effectively than the process of forming ternary complexes, since the binding constant of the former exceeds the latter.[225] Also, the formation of ternary complexes occurs more readily for the more lipophilic surfactants and methylated hosts, as expected for apolar binding processes. The formation of ternary complexes is not observed for the host HP-β-CD because of the hydrophilic character of its facial region; which is due to the dipolar character of the hydroxypropyl group.

Table 4-15 lists the values of $V^{o}_{\phi,\beta\text{-}CD}$ and $\Delta V^{o}_{\beta\text{-}CD}(w \rightarrow w+S)$ for β-CD in aqueous solutions (w+S) containing low, medium, and high concentrations of sodium perfluoroalkyl

carboxylate salts. The weaker dependence of $V^{\circ}_{\phi,CD}$ and ΔV°_{CD} on alkyl chain length and concentration of fc surfactant is seen from a comparison of data in Tables 4-15 and Table 4-13. It can be related to the differences between the maximum number of included fc and hc groups. The relatively constant values of $V^{\circ}_{\phi,\beta\text{-CD}}$ for $C_x \geq 6$ indicates that the fc surfactant completely fills the CD interior and the value of $X_{1:1}$ is close to unity for these strongly bound complexes. The positive concentration dependence of $V^{\circ}_{\phi,\beta\text{-CD}}$ in SPFB can be attributed to its weak binding affinity with β-CD, as described for the hc surfactants of similar chain length (Table 4-13).

The values of $V^{\circ}_{\phi,CD}$ and ΔV°_{CD} (w→w+S) for β-CD, DM-β-CD and HP-β-CD in aqueous solutions of sodium perfluoroalkyl carboxylate salts are shown in Table 4-16. The positive transfer volumes are consistent with the formation of inclusion complexes, *vide infra*. The transfer volumes of β-CD for the entire homologous series are relatively constant and can be attributed to the fact that only 4 CF_2 groups can be included in the β-CD cavity. There are general features of the data in Table 4-16 that are similar to those observed in aqueous hc surfactant solutions. However, differences occur among the hosts when the guest species have longer fluorocarbon chains. An increase in $V^{\circ}_{\phi,R\text{-}\beta\text{-CD}}$ occurs for both modified CDs up to C_x=6. Then the values remain approximately constant when an additional CF_2 group is added to the surfactant. For $C_x \geq 8$, differences in $V^{\circ}_{\phi,R\text{-}\beta\text{-CD}}$ between DM-β-CD and HP-β-CD arise when the surfactant alkyl chain is lengthened by another CF_2 group. A large increment of ca. 9 cm^3 mol^{-1} is observed for DM-β-CD and a smaller increase of ca. 2 cm^3 mol^{-1} is observed for HP-β-CD. Then $V^{\circ}_{\phi,R\text{-}\beta\text{-CD}}$ remains virtually

constant for HP-β-CD and increases by ca. 2 cm^3 mol^{-1} for DM-β-CD when C_x is increased to x=9. These results are consistent with the formation of 1:1 R-β-CD-S complexes and the ability of these hosts to include ca. 6-7 CF_2 groups of a fc chain. The positive increment in ΔV^o_{CD} for DM-β-CD, when C_x =6-7, and HP-β-CD, when C_x =8, is ca. 5-6 cm^3 mol^{-1}, relative to β-CD. This value is consistent with the presence of alkyl substituents in the annulus region. The data indicate that ca. 7 and 8 fluorocarbon groups can be included in DM-β-CD and HP-β-CD, respectively, compared to 4 in the case of β-CD. The increase in ΔV^o_{CD} for DM-β-CD when $C_x \geq 7$ is consistent with the formation of 1:2 complexes and, possibly, ternary complexes, as described in § 5.3.2.

5.3.6 Transfer volumes from water to ternary aqueous solutions

5.3.6.1 Transfer volume of surfactants from water to aqueous cyclodextrin solutions

The values of V^o_o in Tables 4-7 and 4-10 for hc and fc sodium carboxylate salts in water show an average incremental volume change at infinite dilution per CH_2 and CF_2 group of 15.7 and 23.9 cm^3 mol^{-1}, respectively. Both values are in good agreement with literature values.[218] By comparison, the infinite dilution values per CH_2 and CF_2 groups in 0.013 m β-CD are approximately 18.3 and 27.2 cm^3 mol^{-1}, respectively (cf. Fig. 5-1). Therefore, the infinite dilution transfer volume for CH_2 and CF_2 from water to aqueous 0.013 m β-CD is 2.6 and 3.3 cm^3 mol^{-1}, respectively. Interestingly, the ratio of the CF_2/CH_2 volume data is very similar to the ratio of the volume changes of micellization, ΔV^{mic}(fc) $\approx 1.5\Delta V^{mic}$(hc),[152] and the observation that the CMC(fc) ≈1.5 CMC(hc). These facts are consistent with the relative size and hydrophobicity of these groups.

Figure 5-1 illustrates a plot of ΔV_S^o and $\Delta V_S^{1:1}$ versus C_x , respectively, for the transfer of hc and fc surfactants from water to 0.013 m aqueous β-CD.

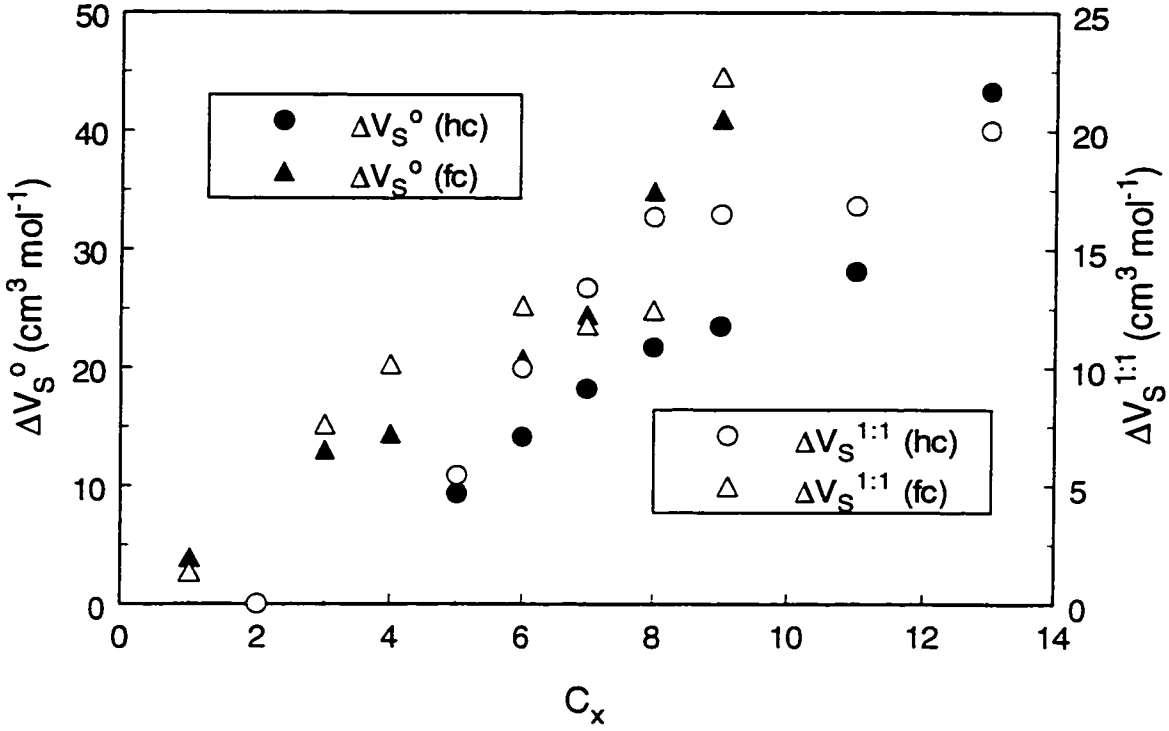

Figure 5-1: , ΔV_S^o and $\Delta V_S^{1:1}$ versus alkyl chain length (C_x) for fluorocarbon (fc) and hydrocarbon (hc) surfactants at infinite dilution and at the 1:1 CD-S mole ratio in 0.013 m β-CD at pH 10.5 and T=298 K.

Generally, ΔV_S^o and $\Delta V_S^{1:1}$ increase as C_x increases and the transfer volumes at infinite dilution are larger than those at the 1:1 CD-S ratio. For the hc surfactants, ΔV_S^o increases monotonically up to C_x=9, then increases less rapidly up to C_x=11, where a further sharp increase in transfer volume occurs for C_x>11. For the fc surfactants, ΔV_S^o increases monotonically with a sharp increase at C_x>6. The initial increase as a function of C_x in each series can be attributed to the increase in $K_{1:1}$ (cf. Table 4-7 and 4-10). If one neglects the

inclusion of the carboxylate group, the maximum number of alkyl groups that can be included within the β-CD core may be inferred from these results, i.e., eight and four for hc and fc surfactants, respectively. The sharp increase in ΔV_S^o for hc (C_x>11) and fc (C_x>6) surfactants corresponds to the onset of 2:1 complex formation due to the end capping of a second CD onto a 1:1 CD-S complex, as shown in Scheme 5-5.

According to Tanford[28], a fully extended alkyl chain consisting of four CH_2 groups can span the β-CD cavity whereas Park and Song[115] indicate that eight CH_2 groups can be accommodated if allowance is made for carbon chain coiling due to the occurrence of gauche kinks. On the other hand, a fc chain is likely to assume an extended conformation, compared to a hc of similar carbon number, because of its higher gauche/trans energy difference (fc chain; 263 J/mol and hc chain; 170 J/mol).[20] Thus the onset of 2:1 complexation that occurs at a lower value of C_x for fc (C_x>6) compared to hc (C_x>11) surfactants can be attributed to differences in the conformation of their alkyl chains. In a 1:1 inclusion complex, it is reasonable to speculate that the carboxylate group is not included and that eight CH_2 groups reside within the CD cavity. For a hc surfactant such as ST (C_x=13), five alkyl groups may remain external to the cavity and project into the bulk solution. This unbound segment of the surfactant carbon chain induces the capping of a second CD onto the 1:1 CD-S complex (cf. Scheme 5-5). Thus, the greater hydrophobicity and preferred all-trans conformation of fc surfactants relative to hc surfactants induces the formation of 2:1 complexes at shorter fc chain length.[216]

Apart from the lower magnitude of $\Delta V_s^{1:1}$ relative to ΔV_s^o, the trends parallel one another. The magnitude of $\Delta V_s^{1:1}$ levels off for hc ($C_x \geq 8$) and fc ($C_x \geq 4$) surfactants and then

increases at higher values of C_x because of the formation of 2:1 CD-S complexes. However, the effect of 2:1 complex formation is more pronounced for the infinite dilution transfer volumes because of the relative excess of host to guest. This is more apparent when C_x is greater.

Table 5-1 lists the molecular group contributions to the van der Waals volume (V_W), molar volume (V_M), and the apparent molar volume at infinite dilution (V_ϕ°) in water for n-alkyl fluorocarbon and hydrocarbon compounds.

Table 5-1: Group Contributions to the van der Waals volume(V_W), Molar Volume(V_M^*) and the Apparent Molal Volume at Infinite Dilution†(V_ϕ°) for n-Alkyl Fluorocarbon and Hydrocarbon Compounds at 298 K.

Group	V_W (cm^3mol^{-1})	V_M^* (cm^3mol^{-1})	V_ϕ° (cm^3mol^{-1})
CH_3	13.7[a]	32.7[c]	26.2[c], 27.1[e]
CH_2	10.2[a]	16.2[b]	15.7[a], 15.7[e]
CF_3	21.3[a]	55.7[b]	39.1[a], 45.7[e]
CF_2	15.3[a]	22.9[b]	23.6[a], 23.9[e], 23.6[f]
COO^-	12.2[a]	21.8[d]	17.8[a]
Na^+	1.25[d]	---	-6.6[a]

[a]ref 224, [b]ref 40, [c]ref 226, [d]ref 227.
[e]Obtained in this work using V_ϕ° for Na^+ and COO^- shown above.
[f]ref 192.
†Obtained from density measurements in water at 298 K.
*Calculated from density data of neat alkane and perfluoroalkane liquids.

The values of V_ϕ° for CH_3 (27.1 cm^3 mol^{-1}) and CF_3 (45.7 cm^3 mol^{-1}) were obtained using the values of V_ϕ° for COO^- and Na^+ in Table 5-1 and the AMV for CH_2 and CF_2 groups, respectively. The values in Table 5-1 can be utilized in an additivity scheme to

interpret the transfer volumes of an hc or fc surfactant from water to an aqueous solution containing CD (w→w+CD).

$$\Delta V_S^\circ (w \rightarrow w+CD) = [x\ V_W(CH_2) + V_W(CH_3) + z\ 18.0] - [x\ V_\phi^\circ(CH_2) + V_\phi^\circ(CH_3)] \quad (5.3.6.1\text{-}1)$$

Equation 5.3.6.1-1, utilizes the values of V_W and V_ϕ° from Table 5-1 and assumes the following: x methylene groups and one methyl group of the surfactant can be included in the CD interior and z water molecules are expelled from the the cyclodextrin cavity during the inclusion process; the carbon chain within the cavity is unsolvated; and neither the COO^- group nor Na^+ ions are included within the β-CD interior. For example: $\Delta V^\circ_{SHex}(W \rightarrow W+CD) = [3(10.2) + 13.7 + 2(18.0)] - [3(15.7) + 27.1] = 6.1\ cm^3\ mol^{-1}$; ΔV°_{SDec} is 20.1 $cm^3\ mol^{-1}$ with x=7 and z=4; ΔV°_{SPFB} is 12.4 $cm^3\ mol^{-1}$ with x=2 and z=3; and ΔV°_{SPFH} is 22.2 $cm^3\ mol^{-1}$ with x=4 and z=4.5. Table 5-2 lists the calculated (eq 5.3.6.1-1) and experimental transfer volumes for various surfactant systems in aqueous cyclodextrin solutions. Good agreement between the calculated and experimental values are obtained using reasonable numbers of methylene groups (x) and displaced water molecules (z), as discussed above.

The predicted number of expelled water molecules (z) may seem low in view of available crystallographic data,[228] For example, Figure 1 in ref. 228 indicates that 4-5 water molecules reside within the hydrophobic interior of β-CD and the remainder are located in the annulus region and interstices of the crystal lattice. However, water molecules are displaced from the hydrophobic interior of CD when it is completely filled by the guest and this contributes mainly to the hydration changes. In the case of DM- and HP-β-CD, the

Table 5-2: Experimental and Calculated[1] Transfer Volumes at Infinite Dilution for Hydrocarbon and Fluorocarbon Sodium Alkyl Carboxylates from water to aqueous cyclodextrin solutions: a) 0.013 m β-CD, b) 0.004 m DM-β-CD, and c) 0.005 m HP-β-CD

Table 5-2 a:

Surfactant	x	z	ΔV_S^o (cm^3 mol^{-1}) Calculated	ΔV_S^o (cm^3 mol^{-1}) Experiment
$C_5H_{11}CO_2Na$	3	4	6.1	9.3
$C_9H_{19}CO_2Na$	7	4	20.1	23.5
$C_3F_7CO_2Na$	2	3	12.4	13.0
$C_6F_{13}CO_2Na$	4	4.4	22.2	20.8

Table 5-2 b:

Surfactant	x	z	ΔV_S^o (cm^3 mol^{-1}) Calculated	ΔV_S^o (cm^3 mol^{-1}) Experiment
$C_5H_{11}CO_2Na$	4	2	3.1	3.1
$C_9H_{19}CO_2Na$	8	4	17.1	19.4
$C_3F_7CO_2Na$	2	2.5	4.0	5.5
$C_7F_{15}CO_2Na$	6	5	15.8	15.7

Table 5-2c:

Surfactant	x	z	ΔV_S^o (cm^3 mol^{-1}) Calculated	ΔV_S^o (cm^3 mol^{-1}) Experiment
$C_5H_{11}CO_2Na$	4	2	3.1	1.2
$C_9H_{19}CO_2Na$	8	4	17.1	17.5
$C_3F_7CO_2Na$	2	2.5	4.0	4.8
$C_7F_{15}CO_2Na$	6	5	15.8	13.7

[1]Calculated according to eq 5.3.6.1-1 where x=number of methylene (CH_2 or CF_2) groups and z=number of water molecules expelled from the CD interior.

value of z is closer to five and this may be due to an increase in the length of the annulus because of the alkyl substituents. The slightly different numbers of cavity hydrate water molecules (z) for the β-CD and R-β-CD hosts suggest that the presence of methyl or hydroxypropyl groups in the annulus region of the CD does not significantly alter the hydration characteristics of the interior of the CD cavity. The minor contribution of hydration changes in the annulus region of the CD upon complex formation is shown by the α-CD-SPFO system. The small diameter of the α-CD prevents inclusion of the guest. However, a noninclusion complex is formed between the annular hydroxyl groups of α-CD and the apolar terminus of the fc alkyl chain, as shown in Scheme 1-5 (cf. § 1.3.2.2). The magnitude of the ΔV_S^o and ΔV_{CD}^o for the α-CD-SPFO system is small (ca. 2 cm^3 mol^{-1}) and indicates that hydration changes in the facial region are not significant. Consequently, it is the volume change due to the removal of the included water molecules from the CD interior that are important in eq 5.3.6.1-1.

There is good agreement between the experimental and calculated transfer volumes, as shown in Table 5-2. The small differences between these values may be due to the simplicity of the model since no provision is made for hydration changes due to the inclusion mode, stoichiometries such as 1:2 and 2:1 CD-S complexes, and coiling of the alkyl chain of the surfactant. All of these factors may affect the relative solute-solute and solute-solvent interactions. Hydrophobic hydration and hydrophobic interactions involve substantial rearrangement of the H-bond network of water and the additivity scheme oultlined above does not explicitly account for these types of volume changes. Kharakoz[166] has estimated the change in volume due to H-bond formation (cf. Table 2, ref. 166).

Volume changes can be significant because the formation of host-guest complexes in aqueous solution may involve extensive desolvation and resolvation processes.[35] Thus, the volumetric contribution of H-bonding due to solvent reorganization may need to be considered in order to obtain a detailed description of the volume changes that occur during complex formation.

Scheme 5-6 summarizes the dependence of stoichiometry on the binary solvent composition for surfactants capable of forming 1:1, 1:2, 2:1, and ternary complexes, according to the experimental conditions used in this work. According to Scheme 5-6, 2:1 and 1:2 CD-S complexes may form depending on the relative mole ratio of the host and guest. The conditions outlined in Scheme 5-6 are satisfied for the AMV of a host or guest near infinite dilution since $[CD]_{total}>[S]_{total}$ or $[S]_{total}>[CD]_{total}$.

a) $$CD + S \underset{\text{excess S}}{\overset{K_{1:1}}{\rightleftharpoons}} CD\text{-}S \underset{\text{excess CD}}{\overset{K_{2:1}}{\rightleftharpoons}} CD_2\text{-}S$$

b) $$CD + S \underset{\text{excess S}}{\overset{K_{1:1}}{\rightleftharpoons}} CD\text{-}S \underset{\text{excess S}}{\overset{K_{1:2}}{\rightleftharpoons}} CD\text{-}S_2 \underset{\text{excess S}}{\overset{K_{tern}}{\rightleftharpoons}} CD_x\text{-}S_y$$

Scheme 5-6: Coupling pathways between the various types of host-guest complexes according to the relative mole ratios of surfactant (S) and cyclodextrin (CD): a) 1:1 and 2:1 CD-S complexes, and b) 1:1, 1:2, and ternary complexes where K_{tern} is the equilibrium constant for the formation of ternary complexes, $x \geq 1$ and $y>2$.

Figure 5-1 illustrates the effect of an excess concentration of host on the transfer volume. The value is considerably different near infinite dilution compared to the 1:1 mole ratio (cf. Figure 5-1). As well, the formation of complexes of different stoichiometries depends on

the alkyl chain length of the surfactant and the magnitude of K_i. Although experimental evidence in favour of 2:1 and 1:2 complexes has been presented, most of the examples given in Table 5-2 are for CD-S systems that form 1:1 complexes. It would be possible to account for the contributions of 2:1 and 1:2 complexes to the transfer volume if their apparent molar volumes were known and weighted by their mole fractions in solution. In conclusion, one may argue that the small differences between the experimental and calculated transfer volumes are fortuitous. Nevertheless, this work has presented a much clearer picture of factors that need to be considered when such complexes are formed.

5.3.6.2 Transfer volume of cyclodextrins from water to aqueous surfactant solutions

Tables 4-13 to 4-16 list the transfer volumes for β-CD and R-β-CD compounds in aqueous hc and fc surfactant solutions, respectively. The transfer volume at infinite dilution of a cyclodextrin from water to an aqueous surfactant solution, ΔV^{o}_{CD}, represents the increase in volume of a CD host upon transfer from water to the complexed form at infinite dilution when there is an excess of surfactant. The factors affecting the transfer volumes were outlined in § 5.3.4. The relatively similar magnitude of $\Delta V^{o}_{R\text{-}\beta\text{-}CD}$ and $\Delta V^{o}_{\beta\text{-}CD}$ (cf. Tables 4-13 and 4-14) in aqueous hc or fc surfactant solutions is related to the similar number of displaced water molecules from each host cavity, as indicated in § 5.3.6.1. As the value of $\Delta V^{o}_{R\text{-}\beta\text{-}CD}$ becomes constant, this indicates that the guest has fully occupied the host cavity and no additional water molecules can be expelled from the CD cavity as the alkyl chain length of the guest is further increased. These results support the argument that the

presence of alkyl substituents in the annulus region of the CD do not contribute substantially to the volumetric behaviour.

The interpretation of ΔV^{o}_{CD} using an expression analogous to eq 5.3.6.1-1 is not straight forward since knowledge of the state of hydration of CD and surfactant in the bound and unbound states is required. It is possible to estimate the number of included alkyl groups in the CD interior using experimental estimates of the incremental transfer volumes (w→w+β-CD) for CH_2 (2.6 cm^3 mol^{-1}) and CF_2 (3.3 cm^3 mol^{-1}) groups (cf. § 5.3.6.1).

It is interesting to note that the value of $\Delta(\Delta V^{o}_{\beta\text{-CD}}) = \Delta V^{o}_{\beta\text{-CD}}(hc) - \Delta V^{o}_{\beta\text{-CD}}(fc)$ is approximately 8 cm^3 mol^{-1} for systems where 1:1 complexes are likely to dominate. As mentioned in § 5.3.6.1, the estimated number of alkyl groups ($C_x \geq 4$; fc surfactants and $C_x \geq 8$; hc surfactants) that fill the β-CD cavity can account for this difference. The difference in volume between transferring 8 CH_2 groups or 4 CF_2 groups from the bulk phase to completely fill the CD cavity, e.g., (8 CH_2 x 2.6 cm^3 mol^{-1}) - (4 CF_2 x 3.3 cm^3 mol^{-1}) = 7.6 cm^3 mol^{-1}, corroborates the results discussed in § 5.3.6.1 and the argument that it is only the hc surfactant homologs that coil within the β-CD cavity. A similar calculation for $\Delta(\Delta V^{o}_{R\text{-}\beta\text{-CD}})$ indicates 9 CH_2 or 5 CF_2 groups are included in DM-β-CD whereas 14 CH_2 or 6 CF_2 groups are included in HP-β-CD. The larger numbers of included alkyl groups for the R-β-CD compounds are consistent with the extended length of the annulus..

5.4 Spectral displacement studies

5.4.1 Evaluation of the β-CD-phenolphthalein binding constant

The NMR chemical shift and apparent molar volume measurements used to study the formation of CD-S complexes are considered as type *i)* methods (cf. § 1.4.1). The spectral displacement technique falls into the category of type *ii)* methods and provides accurate estimates of the 1:1 host-guest binding constants ($K_{1:1}$) when the necessary conditions are fulfilled (§ 2.1.4). [26,134,229] With respect to the first condition, any contribution from micelle/phth interactions was eliminated by carrying out all measurements below the CMC of the surfactants.[114] In a few instances, a very small decrease in the absorbance of phth did occur and it is believed to be due to the formation of small clusters of surfactant around the phth. An appropriate correction was applied to absorbance data in these cases. Condition *ii)* is largely met in this study since it is only some of the surfactants (SDodec, ST, SPFO, and SPFN) with longer alkyl chain lengths that form 2:1 complexes with β-CD. In these cases, the formation of 2:1 complexes are not favoured because of the small excess of host to guest concentrations employed and the value of $K_{CD\text{-}P}$ exceeds $K_{2:1}$ in all cases. The equilibrium between β-CD and phth competes for unbound β-CD thereby suppressing the formation of 2:1 complexes. A further condition is that the competing ligand must fully displace the chromophore and bind as a well-defined CD-guest inclusion complex. For example, the formation of a ternary (CD-phth-guest) complex would not fully displace the chromophore and this could affect the magnitude of $K_{1:1}$.[53] The formation of ternary complexes with neutral and positively charged guests were alluded to by Reinsborough *et al.*;[196] however, this effect is not

anticipated in the case of anionic guests. The monotonic increase in $K_{1:1}$ as a function of increasing alkyl chain length of the surfactant seems to militate against this possibility. Finally, a practical requirement is to have $K_{CD\text{-}P} \geq K_{1:1}$ such that phth is displaced over a suitable range of C_S in order to obtain adequate absorbance changes.[26] This condition is satisfied for most of the surfactants studied in this work.

Figure 4-13 showed a plot of the absorbance of phenolphthalein (phth) versus the concentration of β-CD. Preliminary estimates of $K_{CD\text{-}P}$ were first obtained using classical double reciprocal plots(1/abs against $1/C_{CD}$).[59] Difficulty in obtaining reproducible values of $K_{CD\text{-}P}$ were encountered due to improper weighting of the data and/or the inappropriate assumptions implicated with linearization procedures. Consequently, a NLLS fitting procedure was employed to obtain values of $K_{CD\text{-}P}$ and $K_{1:1}$ (cf. § 2.1.4). A value of $K_{CD\text{-}P}=2.5\pm0.3\times10^4$ M^{-1} was determined from several independent experimental trials and is in agreement with various literature values (cf. Table 4-17). However, the conditions employed, here, utilized lower ethanol compositions than those of Selvidge *et al.*[26a] and the value of $K_{CD\text{-}P}$ obtained is correspondingly larger. This difference may be due to a solvent effect (cf. § 1.4.2).[230] In comparison to the β-CD-4-nitrophenolate complex ($K_{1:1} \approx 10^2$ M^{-1}), the value of $K_{CD\text{-}P}$ is greater. The interpretation for the greater binding affinity is based on the occurrence of multipoint (dispersive and ion-dipole) interactions between phth and β-CD.[181] Although similar dispersion interactions are expected to contribute favourably to both complexes (cf. Scheme 5-7 a and b), the presence of an additional ion-dipole interaction in the β-CD-phth complex results in an increase in binding by at least one order of magnitude.[181] The secondary effect of ion-dipole

interactions on complex stability explains the different binding affinities of fc surfactants with β-CD and R-β-CD compounds discussed in § 5.3.2.

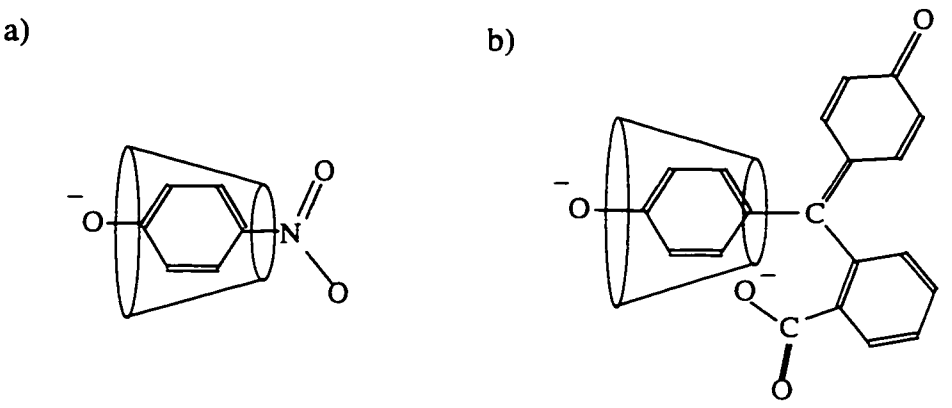

Scheme 5-7: Inclusion modes for β-CD-inclusate complexes with multipoint interactions: a) β-CD-4-nitrophenolate and b) β-CD-phth under alkaline conditions.

The steric exclusion effect in the annulus region due to increasing degree of alkyl substitution has been reported for HP-β-CD.[231] The importance of ion-dipole interactions between the hydroxyl groups of β-CD and the carboxylate group of phth is shown, indirectly, by the decrease in the magnitude of $K_{CD\text{-}P}$ when there is an increase in alkyl substitution in the annulus region.[231]

5.4.2 β-CD-sodium alkyl carboxylate ion binding constants

Figures 4-14a-b illustrate plots of absorbance of phth versus C_S for a short (SHex) and long (SDodec) chain surfactant, respectively. Fig. 4-14a illustrates typical behaviour expected of a weakly bound surfactant, as shown by the gradual parabolic increase in absorbance as C_S increases. Typical behaviour of a strongly bound surfactant is shown by a marked sigmoidal dependence of absorbance on concentration (Fig. 4-14b). The increase in

absorbance with increasing C_S corresponds to the displacement of phth from the CD cavity upon inclusion of the surfactant. The binding constants of the 1:1 complexes are given in Table 4-18 for the β-CD-S systems studied. The error in $K_{1:1}$ is based on the standard deviation in $K_{CD\text{-}P}$. The magnitude of $K_{1:1}$ ranges from 10^1 - 10^4 M^{-1} and increases as C_x increases. As well, values of $K_{1:1}$ for β-CD-sodium dodecyl sulfate (SDS) and β-CD-sodium octane-1-sulphonate (SOS) were obtained to validate the method and the results agree with the literature[195,196] values. The estimates of $K_{1:1}$ are in good agreement with estimates obtained from ^{1}H NMR and AMV studies (cf. Table 4-1 and 4-7). The value of $K_{1:1}$ displays an inverse dependence on the CMC of the surfactant, as shown by the increase in $K_{1:1}$ as the CMC decreases (Table 4-18). Interestingly, the values of $K_{1:1}$ for SDec and SO are similar to those for β-CD-SDS and β-CD-SOS (Table 4-18), respectively. This limited comparison indicates that interactions between the CD interior and the hydrocarbon chain play a greater role in stabilizing the complex than interactions between the surfactant head group and CD.

The spectral displacement technique offers increased sensitivity due to the large magnitude of ε_{phth} and provides a good method for obtaining estimates of $K_{1:1}$ for strongly bound CD-surfactant systems. One drawback associated with this method is the inability to determine binding constants other than $K_{1:1}$. NMR and volumetric studies of β-CD-hc surfactant complexes (cf. § 4.1 and 4.3) indicate that surfactants such as SDec and SDodec form 2:1 CD-S complexes. Thus, the reliability of the calculated values of $K_{1:1}$ for these complexes may be questioned. However, errors arising from the formation of higher order complexes should be minimized because of the following facts: *(i)* $K_{1:1}$ exceeds $K_{2:1}$ by one

to two orders of magnitude, *(ii)* the equilibrium between β-CD and phth minimizes 2:1 binding because $K_{CD\text{-}P}$ ($\approx 10^4$ M^{-1}) exceeds $K_{2:1}$ by one to two orders of magnitude, and *(iii)* the relative concentrations of β-CD and surfactants used.

5.4.3 β-CD-sodium perfluoroalkyl carboxylate ion binding constants

Figure 4-15 is a typical plot of absorbance against C_S for the β-CD-SPFN system. Fig. 4-15 shows features similar to that observed for a strongly bound hc surfactant (Fig. 4-14b), however, the curve is more sigmoidal and the absorbance change is greater over a narrower concentration range. The appearance of sigmoidal curves has been attributed to cooperative binding phenomena (cf. § 5.3.2) Table 4-19 list the values of $K_{1:1}$ obtained for the β-CD-fc surfactant systems investigated. The magnitude of $K_{1:1}$ ranges from 10^2 to 10^5 M^{-1} and increases with increasing C_x for the fc surfactants, the values being systematically greater than the $K_{1:1}$ for the hc surfactant homologues. Schuette *et al.*[230] noted a similar difference in the magnitude of $K_{1:1}$ for the complexation of low molecular weight hc and fc alcohols with β-CD. The magnitudes of $K_{1:1}$ for the various systems are in good agreement with those obtained from ^{19}F NMR and volumetric studies (Tables 4-4 and 4-10).

5.4.4 Molecular additivity schemes for the Gibbs energy of complex formation for β-CD-hydrocarbon and -perfluorocarbon alkyl carboxylate ion complexes

Figure 5-2 shows a plot of ΔG° of 1:1 complex formation versus C_x for both fc and hc surfactants with β-CD. The value of ΔG° exhibits a monotonic decrease (more negative) with increasing value of C_x for both hc and fc surfactants, with the rate of decrease being greater for the latter. This result can be attributed to the differences in the physicochemical properties of the hc and fc surfactants. It is of interest to compare the average change in ΔG° per methylene group determined in this work with values obtained for the Gibbs energy of transfer of a CH_2 or CF_2 group from water to an hexane-water interface, $\Delta\Delta G^{\circ}$ (w→hexane-water), and with the transfer of a methylene group from water to the interior of a micelle. Mukerjee reported values of $\Delta\Delta G^{\circ}$(w→hexane-water) = -5.1 kJ/mol (CF_2) and -3.4 kJ/mol (CH_2).[152] These values are slightly greater than the average Gibbs energy of complexation, -4.4 kJ/mol (CF_2) and -2.7 kJ/mol (CH_2), obtained from the slopes of the curves in Fig. 5-2. The less negative values of $\Delta\Delta G^{\circ}$ per methylene group obtained in this work are closer to the values expected for the transfer of a methylene group from water to the interior of a micelle ($\Delta\Delta G^{\circ}(CH_2)$ = -2.7 to -3.0 kJ/mol).[152] While neither of these processes are perfect models for the formation of a 1:1 complex, the results show that there are some global similarities.

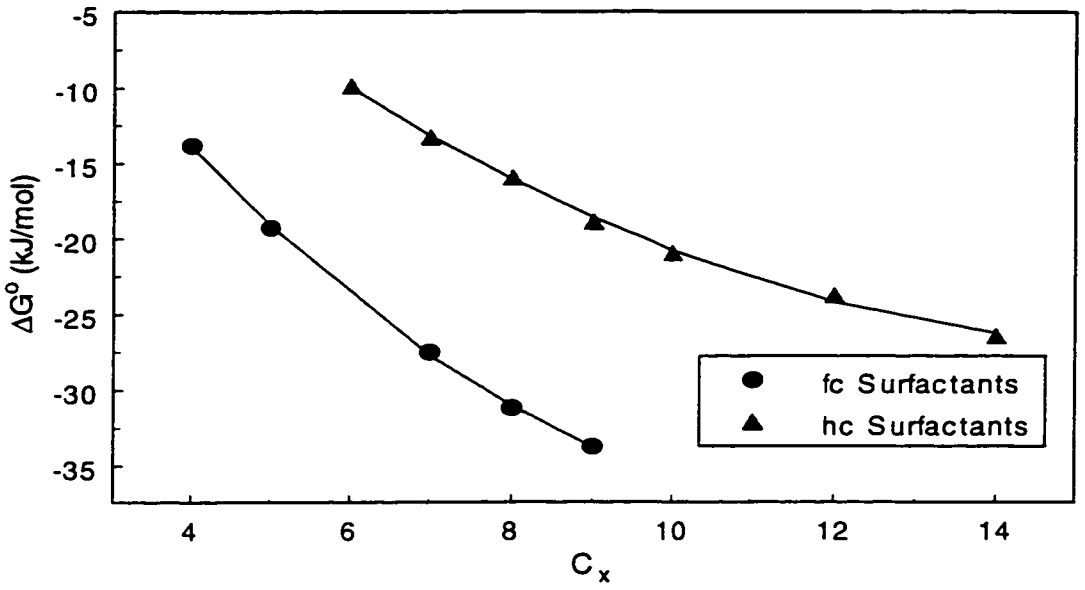

Figure 5-2: ΔG° for the formation of 1:1 complexes of β-CD-sodium alkyl carboxylates and -sodium perfluoroalkyl carboxylates versus alkyl chain length (C_x) of the surfactant.

The nonlinear dependence of ΔG° on the alkyl chain length (C_x) for both surfactant systems can be attributed to the degree of inclusion of the surfactant chain within the CD cavity. As C_x exceeds the depth of the CD cavity, ΔG° decreases less because the additional methylene groups are not included within the CD interior and extend outside of the annulus. In § 5.3.6.1 it was suggested that the β-CD interior can accommodate no more than approximately 8 CH_2 groups if allowance is made for chain coiling. Because of the all-trans conformation of the fc chain (cf. § 5.3.6.1), it is likely that fewer CF_2 than CH_2 groups can be included in the CD interior and the fc series will show greater nonlinearity than the hc series (cf. Figure 5-2). While it can also be argued that the nonlinear dependence of ΔG° on C_x may be due to the contribution of higher order binding phenomena, the experimental range of C_s chosen in this work was done with the view to minimize, as much as possible,

the formation of such complexes. Furthermore, the "goodness of fit" of the experimental data to a 1:1 model does not warrant the consideration of higher order binding phenomena.

The hydrophobic effect has been implicated in various CD-inclusate complexation phenomena.[28,34] Since lipophilic character of a surfactant can be related to the CMC, it is expected that there should be a correlation between the binding constant ($K_{1:1}$) and the CMC. Figure 5-3 is a plot of -log $K_{1:1}$ against log CMC for complexes of β-CD with fc and hc surfactants, respectively. The value of ΔG^{o} exhibits a nonlinear decrease (less negative) as C_x increases for both hc and fc surfactants, with the decrease being more negative for the fc surfactants. This is consistent with the greater hydrophobicity of the fc surfactants.[216] The less negative decrease in -log $K_{1:1}$ as log CMC decreases, is related to the extension of the apolar alkyl chain outside of the β-CD annulus. These results show that the hydrophobic effect[17] is an important factor in the formation of CD-surfactant complexes. Also, they provide an approximate method to obtain estimates of $K_{1:1}$, by extrapolation or interpolating for inclusates within a homologous series of surfactants when only a few values of $K_{1:1}$ are known.

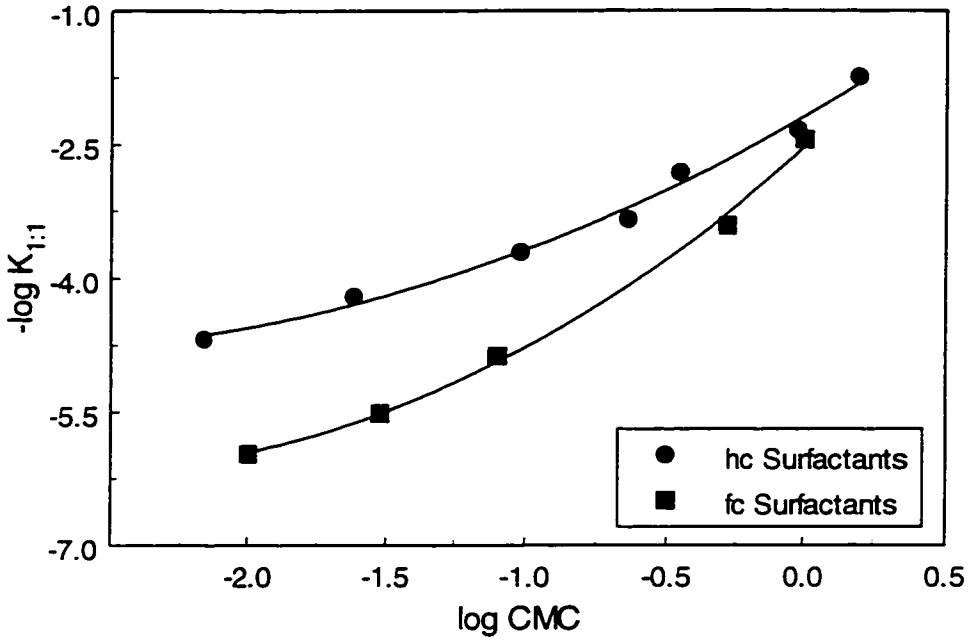

Figure 5-3: -Log $K_{1:1}$ for 1:1 complexes of β-CD-sodium alkyl carboxylates and -sodium perfluoroalkyl carboxylates versus log CMC of the surfactant.

5.5 Correlation of solute-solute interactions with the stability of cyclodextrin-inclusate complexes

Four characteristics of the guest are important in considering the stability of the host-guest complexes studied in this work. They are; geometrical size, conformation, molecular polarizability, and degree of solvation of the carboxylate headgroup. First, the size differences between hc and fc alkyl chains are apparent from a comparison of the van der Waals radii of H(145 pm) and F(160 pm) as well as the van der Waals volumes, $CF_3(21.3) > CF_2(15.3) > CH_3(13.7) > CH_2(10.2)$, where the volumes are in cm^3mol^{-1}.[224] In § 1.3.2.3 it was argued that dispersion interactions can play a role in stabilizing host-guest

complexes. The total intermolecular pair potential in a host-guest complex can be represented by the Lennard-Jones (L-J) potential

$$U_{ij} = 4 \in \left[\left(\frac{r_o}{r_{ij}} \right)^{12} - \left(\frac{r_o}{r_{ij}} \right)^{6} \right] \qquad (5.5\text{-}1)$$

where r_{ij} is the distance of separation between interacting pairs, r_o is the interparticle separation when $U_{ij}=0$, and $\in$ is the depth of the potential well. Dispersion forces are the primary contributor to the attractive interactions that occur between neutral segments of the host interior and guest. Since the dispersive forces operate over very short distances, and are much less orientation dependent than dipolar interactions, the size of the guest is an important factor in determining the strength of these interactions because the "goodness of fit" of the guest within the host cavity will determine r_{ij}.

Conformational changes of the alkyl chain of the surfactant during the course of complexation could enhance the potential energy of interaction by optimizing the distance between the guest and host. This would offset unfavourable size effects (cf. § 1.3.2.3). In the case of the surfactants studied here, there are differences in the size and conformation of hc and fc alkyl chains. The somewhat smaller diameter of a hc chain relative to the host cavity size would make r_{ij} in eq 5.5-1 larger than in the case of fc chains. However, since gauche kinks (cf. § 5.3.6.1) can occur in a hc chain, then r_{ij} can be reduced. This is shown by the fact that β-CD can include a longer hc alkyl chain (C_x=8) than a fc chain segment (C_x=4). As a result, the distance between the carbon chain of the guest and the CD interior may not be significantly different for hc and fc surfactants.

The polarizability of the interacting species is also a critical parameter in determining the contribution of the dispersion energy to U_{ij}, as shown in eq 5.5-2

$$U_{disp} \approx -\alpha_i \alpha_j r_{ij}^{-6} \qquad (5.5\text{-}2)$$

where α_i and α_j are the polarizabilities of the interacting species and r_{ij} is defined in eq 5.5-1. The molecular polarizability of typical hc and fc aliphatic and aromatic compounds are similar, e.g., $\alpha(C_{10}F_8)$ = 17.64 Å^3 and $\alpha(C_{10}H_8)$ = 16.5 Å^3.[232] Thus, differences in the molecular polarizability of hc and fc surfactants are not expected to contribute to significant differences in binding affinity between hosts and guests. However, the interactions between molecules or small particles in a solvent medium can be very different from that of isolated molecules in free space or in a gas. In the former case the excess or effective polarizabilities of the interacting species are important.

It has been shown[35b] that one can calculate the total van der Waals interaction Gibbs energy (w(r)) between two different molecules (1 and 2) in a medium (3)

$$w(r) \approx -\frac{\sqrt{3}h\nu_e a_1^3 a_2^3 N}{2r^6}\left[\frac{\left(n_1^2-n_3^2\right)\left(n_2^2-n_3^2\right)}{\left(n_1^2+2n_3^2\right)^{1/2}\left(n_2^2+2n_3^2\right)^{1/2}\left[\left(n_1^2+2n_3^2\right)^{1/2}+\left(n_2^2+2n_3^2\right)^{1/2}\right]}\right] \qquad (5.5\text{-}3)$$

where a_i is the radius of the solutes (i=1,2), r is the distance of separation, n_i is the refractive index of the solutes (i=1,2) and solvent (i=3), ν_e is the absorption frequency ($\approx 3\times10^{15}$ s^{-1}) and assumed the same for all three media, N is the Avogadro number, and h is the Planck constant (cf. Scheme 5-8).

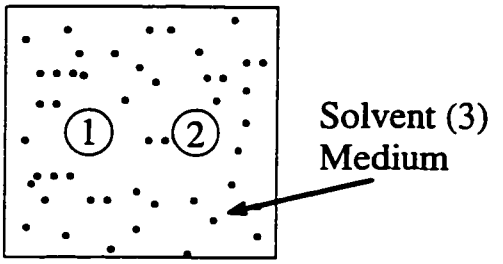

Scheme 5-8: Two different molecules (1 and 2) with radius, a, interacting in a solvent medium (3). Adapted from ref. 35b.

Estimates of w(r) for the interaction of a CH_2 or CF_2 group with the CD interior were calculated from eq 5.5-3 taking the radius of a CH_3 or CF_3 group (a_1=4Å or 7Å),[65,40] respectively, and assuming the CD to be a sphere of radius, a_2, identical to a_1. Since it is the alkyl chain of the hc or fc surfactant that interacts with the CD interior, the values of n for a CH_2 or CF_2 group were approximated using typical values for hc or fc n-alkanes, i.e., n_1(hc alkane)=1.4 or n_1(fc alkane)=1.26, respectively. The refractive index of dioxane (n_2=1.4224) was used to represent the CD interior and the value for water (n_3=1.33) was used for the solvent (3). The calculated values of w(r) per CH_2 or CF_2 group are less than 0.025 kJ mol^{-1} and are two orders of magnitude lower than the average Gibbs energy of complex formation per CH_2 or CF_2 group, -4.4 kJ/mol (CF_2) and -2.7 kJ/mol (CH_2), obtained in this work (cf. § 5.3.4). Equation 5.5-3 illustrates several important points: *i)* repulsive interactions occur between 1 and 2 when n_3 is intermediate between n_1 and n_2, *ii)* weaker attractive interactions occur between 1 and 2 when n_3 is closer to n_1 or n_2, *iii)* stronger attractive interactions occur between 1 and 2 when n_1 and n_2 are similar in value, and *iv)* stronger attractive interactions between apolar solutes occur *in vacuo* (n_3=1) relative to a solvent such as water (n_3=1.33). More importantly, eq 5.5-3 indicates that the stability

of CD-S complexes can not be accounted for by solute-solute dispersion interactions between the host and guest because the calculated values are considerably lower than the experimental Gibbs energy of 1:1 complex formation. The contention that dispersive interactions do not contribute substantially to the overall stability of the complex is further evidenced by a comparison of the relative binding affinity of α- and β-CD with a common guest (cf. Table 4-1). One might expect that the narrower cavity diameter of α-CD relative to β-CD (cf. Table 1-1) would result in stronger dispersion attractive forces between α-CD and a common hc surfactant; however, the differences in the K_i values of these hosts with a common guest are small.

The final factor to be considered with respect to solute-solute interactions is the importance of head group solvation as it relates to ion-dipole interactions between the carboxylate head group and annular hydroxyl groups of the CD (§ 5.3.2). The ^{1}H and ^{19}F NMR results discussed in § 5.1.1 and § 5.2.1 indicate that ion-dipole interactions are more important for fc surfactants because of the weaker hydration of the carboxylate head group, as inferred in Scheme 5-9. The different binding affinity of β-CD and R-β-CD hosts with fc surfactants is related to the screening of ion-dipole interactions by the alkyl groups in the annulus region. The contribution of ion-dipole interactions in a polar solvent such as $CHCl_3$ is ca. 3 kJ mol^{-1}.[102] In aqueous solutions, ion-dipole interactions are expected to decrease because of the greater dielectric constant and dipolar character of water. Therefore, the small magnitude of an ion-dipole interaction can not account for the differences in stability of complexes formed with fc and hc surfactants; however, these interactions may contribute to small differences in complex stability.

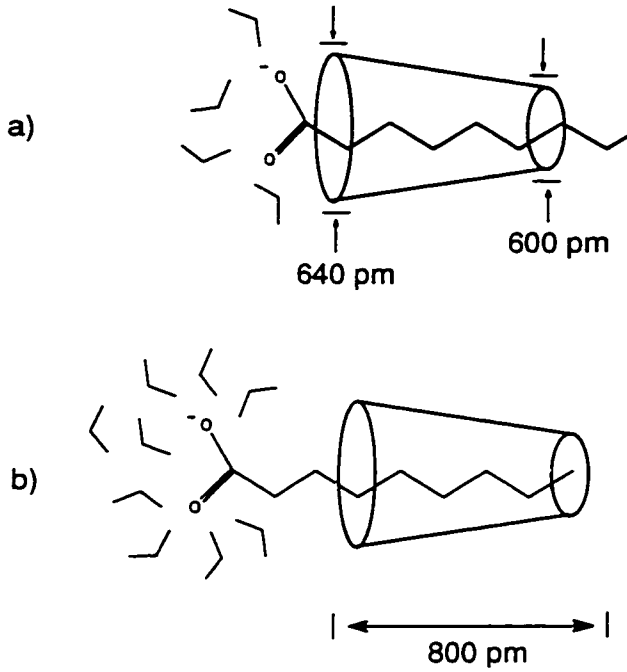

Scheme 5-9: The influence of carboxylate head group solvation on inclusion geometry of β-CD-surfactant complexes: a) β-CD-fc surfactant complex and b) β-CD-hc surfactant complex; where the "v-shaped" structures represent water molecules.

In cases where multiple ion-dipole and dispersive attractive interactions occur as in the case of the β-CD-phth complex (§ 5.3.1), an increase in binding affinity arises because of cooperative binding.[181] Similar examples of cooperative binding have been reported for enzyme-substrate complexes.[233] However, positive cooperativity of this type is not expected for the CD-S systems investigated here.

5.6 Correlation of solute-solvent and solvent-solvent interactions with the stability of cyclodextrin-inclusate complexes

There is considerable evidence that micelle formation and the formation of CD-S inclusion complexes are governed by the hydrophobic effect. Apolar association in aqueous solution is characterized by a relatively large and negative change in heat capacity,

a hallmark signature of the hydrophobic effect.[34] Consequently, apolar binding processes that display a negative change in heat capacity generally involve substantial solvent reorganization because of the release of water from the solvation shells adjacent to apolar surfaces. Consequently, apolar association leads to a reduction in the number of heat absorbing bonds due to a decrease in hydrophobic hydration. Thus, the collective role of hydrophobic interactions and hydrophobic hydration are important factors that govern the stability of CD-inclusate complexes. The relative contribution of solute-solute, solute-solvent, and solvent reorganization processes to the overall energetics of complex formation is a key issue that needs to be addressed. For this reason, the Gibbs energy of complex formation (ΔG_{comp}) is reintroduced (cf. eq 1.4.2-2)

$$\Delta G_{comp} = \Delta G_{w\text{-}w} + \Delta G_{h\text{-}g} + \Delta G_{h} + \Delta G_{g}$$

In § 5.5, it was argued that dispersion interactions do not contribute significantly to the overall stability of the inclusion complex. Therefore, $\Delta G_{h\text{-}g}$ can be neglected in eq 1.4.2-2.

The relatively similar Gibbs energy of transfer ($\Delta\Delta G^{o}$) per CH_2 and CF_2 groups from water to aqueous solutions containing micelles and cyclodextrins (§ 5.3.4) suggests that comparable hydrophobic hydration and solvent reorganization processes occur during micellization and complex formation. These processes generally involve the transfer of the surfactant alkyl chain to a more lipohilic environment and the loss of an apolar solute cavity, with the head group remaining hydrated to a certain extent. The removal of an apolar solute cavity results in a net increase in H-bonding and dipolar interactions between water molecules in the bulk. It is for this reason that the driving force for the formation of complexes is mainly due to favourable enthalpic and entropic contributions from the

substantial solvent rearrangement in bulk water. Hence, it is expected that correlations should exist between the Gibbs energy of complex formation and the hydrophobicity and molecular volumes or solvent accessible surfaces areas of the apolar guest molecule.[17,34]

The greater binding affinity of fc surfactants relative to hc surfactants with CD hosts can be attributed to their greater hydrophobicity, as evidenced by the lower values of CMC and surface tension for the fc surfactants.[152,216,234] The greater volume (cf. Table 5-1) and molecular surface areas of fc relative to hc groups are consistent with this expectation.[152] Thus, the terms relating to the solute-solvent and solvent-solvent interactions ($\Delta G_{w\text{-}w}$, ΔG_h, and ΔG_g) in complex formation are more important.

The occurrence of solvent reorganization processes provides strong support in favour of the cavity based models (cf. § 1.2.2). Equation 1.4.2-8 outlines the factors that contribute to ΔG_{comp}. The term, $\Delta G^c_{intrasol}$, is neglected on the basis of the arguments presented in § 5.5. A number of reports indicate that the change in Gibbs energy of hydration is highly compensated in processes that involve hydrophobic species.[235] Thus, it is anticipated that the terms, (ΔG^C_w - ΔG^S_w -ΔG^L_w), do not contribute significantly to ΔG_{comp}. The omission of these two terms are supported by the results of Lee,[236] where he argues that most subprocesses involving hydrophobic transfer are compensating except for the process of cavity formation. This leads to the following expression

$$\Delta G_{comp} \approx g\Delta A\gamma_w \qquad (5.5\text{-}4)$$

where g is a correction factor accounting for the curvature of the surface, ΔA is the change in nonpolar surface area of the guest, and γ_w is the surface tension of water.

Equation 5.5-4 can be criticized on the basis of the physical significance of the term, g, and the use of γ_w to approximate the interfacial surface tension of a microscopic cavity.[17]

Alternatively the use of the interfacial surface energy (γ_i) in eq 5.5-4 is preferable

$$\Delta G_{comp} \approx \Delta A \gamma_i \qquad (5.5\text{-}5)$$

The use of γ_i of a hydrocarbon/water interface in eq 5.5-5 is a more physically meaningful parameter to describe the microscopic interface between the guest and bulk solvent. The formation of CD-S inclusion complexes necessitates a negative change in the apolar surface area of the guest and contributes favourably to the Gibbs energy of complex formation. Table 5-3 lists some calculated values of ΔG_{comp} using eq 5.5-5. The following assumptions were made: the alkyl chain length is in its extended conformation in the bound and unbound states, the molecular surface area is obtained by treating the shape of the alkyl chain as a cylinder having the diameter of a CH_3 (4Å)[227] or CF_3 (7 Å)[65,40] group, respectively, and the complex is 1:1. The calculation also neglects any contributions that may arise from changes in hydration of the carboxylate head group.

The calculated and experimental values of ΔG_{comp} in Table 5-3 are in reasonable agreement despite the assumptions. If one were to allow for alkyl chain coiling of the surfactant and higher order binding, then the estimated values of ΔG_{comp} would be more negative because of the greater decrease in the apolar surface area of the guest. Further refinements to the model are possible by accounting for the fraction of species undergoing transfer and determining the contributions of the other terms neglected in eqs 5.5-4 and -5 (cf. eq 1.4.2-8). Nevertheless, the calculations in Table 5-3 demonstrate the importance of solvent reorganization processes in complex formation.

Table 5-3: Calculated and Experimental Gibbs Energy of Complex Formation (ΔG_{comp}) of Hydrocarbon and Fluorocarbon Sodium Alkyl Carboxylates of Varying Alkyl Chain Length (C_x) with β-CD.

Surfactant	ΔG_{comp} (kJ mol^{-1}) experiment[a]	ΔG_{comp} (kJ mol^{-1}) calculated[b]
SP (C_x=2)	≈0	-2.9[c]
SO (C_x=7)	-15.9	-6.7[c]
SPFB (C_x=3)	-13.8	-8[d]
SPFO (C_x=7)	-31.2	-13.5[d]

[a] Obtained from the spectral displacement technique, [b] Obtained using eq 5.5-5, [c] Obtained using γ_i(n-hexane/water)=18.2 mJ m^{-2} from ref. 35b, [d] Obtained using γ_i(n-perfluorohexane/water)= 56.4 mJ m^{-2} from ref. 152b.
$l_{hc} = 1.5 + 1.265C_x$ (calculated hc alkyl chain length), ref. 40
$l_{fc} = 2 + 1.34C_x$ (calculated fc alkyl chain length), ref. 40

In conclusion, one may argue that the small differences between the experimental and calculated Gibbs energy of complex formation may be fortuitous because of compensation among terms omitted from eq 1.4.2-8. Notwithstanding, this work has presented a clearer picture of the relative contributions of solute-solute interactions and solvent reorganization to the stability of cyclodextrin-inclusate complexes.

6. CONCLUSIONS AND SUMMARY

A comprehensive study of complexes formed between cyclodextrin (host) and surfactant (guest) systems has been carried out. The cyclodextrin compounds studied are: α-CD, β-CD, 6-O-(2-hydroxypropyl) β-CD (HP-β-CD), 2,6-di-O-methyl β-CD (DM-β-CD), 2,3,6-tri-O-methyl β-CD (TM-β-CD), and randomly methylated β-CD (RAMEB). The hydrocarbon (hc) and fluorocarbon (fc) guest systems consisted of a homologous series of sodium alkyl carboxylate [$C_xH_{2x+1}CO_2Na$, x=5,7,9,11,13] salts and a series of sodium perfluoroalkyl carboxylate [$C_xF_{2x+1}CO_2Na$, x=1,3,6-9] salts. The complexes formed between these host-guest systems were investigated using thermodynamic and spectroscopic techniques to obtain information about the magnitude of the binding constant, the type of host-guest stoichiometry, and the host-guest inclusion mode.

The measured physical properties, e.g., NMR chemical shift, apparent molar volume (AMV), and absorbance, were found to depend on the following factors: *i)* the magnitude of the binding constant (K_i), *ii)* the chain length of surfactant, *iii)* the mole ratio of the host to guest species, *iv)* the host-guest stoichiometry, *v)* the host-guest inclusion mode, and *vi)* the physicochemical properties of the cyclodextrin and surfactant. Because of the correspondence between the measured variable and the fraction of bound species, the binding constants of the cyclodextrin-surfactant (CD-S) complexes have been obtained from an analysis of the changes in a measured physical property using different models to represent the amount of complexed and uncomplexed species. These models

differ in terms of the types of host-guest stoichiometries such as 1:1, 1:1 plus 2:1, and 1:1 plus 1:2 complexes.

In general, the binding constant (K_i, i=1:1, 2:1, and/or 1:2) for complexes formed between cyclodextrins (CDs) and all of the surfactants studied increases as the alkyl chain length (C_x) of the surfactant increases. In the case of complexes that are formed between β-CD-hc surfactants and -fc surfactants, the magnitude of K_i obtained for the latter are systematically greater than the former. The binding affinity of the host systems with the hc surfactants follows the order β-CD> α-CD > DM-β-CD > TM-β-CD > HP-β-CD and that with the fc surfactants follows the order β-CD> RAMEB ≈ DM-β-CD > TM-β-CD > HP-β-CD> α-CD. In the case of 2:1 binding, $K_{2:1}$ increases as C_x increases. For 1:2 binding, $K_{1:2}$ increases as the degree of methyl substitution increases in the CD annulus. The values of K_i for a common hc surfactant that forms complexes with different CD hosts are relatively similar whereas greater differences in K_i are observed for a common fc surfactant with different CD hosts. The differences in the binding affinity of the alkyl substituted β-CD (R-β-CD) compounds arise because of cavity lengthening, steric effects, and differences in ion-dipole interactions created by the presence of alkyl substituents in the annulus region of the macrocycle, particularly for TM-β-CD and HP-β-CD. Tables 6-1 a and b provide a summary of the K_i values for all of the CD-S complexes obtained using the various methods. Figures 6-1 a and b provide a graphic illustration of the values of $K_{1:1}$ for the β-CD-surfactant complexes from each of the three techniques investigated in this study. Notwithstanding the differences in sensitivity of each of the

Table 6-1: Summary of Binding Constants, (K_i),[a,b] of Cyclodextrin-Surfactant Complexes Obtained Using the Various Methods of This Study.

Table 6-1a: Cyclodextrin-Sodium Alkyl Carboxylate Complexes

Surfactant	α-CD	β-CD	DM-β-CD	TM-β-CD	HP-β-CD
$C_5H_{11}CO_2Na$ SHex	[a]$3x10^{2d}$	[a]$6x10^{1d}$ [a]$1.2x10^{2d}$, [a]7.0×10^{1e}, [a]$5.5x10^{1f}$	[a]$1x10^{2d}$, [a]$2.09x10^{2e}$, [a]$1.00x10^{2e}$	[a]$3x10^{1d}$	[a]$2x10^{1d}$, [a]$1.00x10^{2e}$, [a]$1.21x10^{2e}$
$C_7H_{16}CO_2Na$ SO	[a]$4.7x10^{2d}$	[a]$7.0x10^{2d}$, [a]$7.1x10^{2d}$, [a]6.22×10^{2e}, [a]$6.6x10^{2f}$	[a]$3.4x10^{2d}$, [a]$2.99x10^{2e}$, [a]$3.15x10^{2e}$	[a]$1.0x10^{2d}$	[a]$7.64x10^{2d}$, [a]$3.26x10^{2e}$, [a]$1.72x10^{2e}$
$C_9H_{19}CO_2Na$ SDec	[a]$5.6x10^{3d}$ [b]$6.5x10^{2d}$	[a]$8.0x10^{3d}$, [a]$6.6x10^{3d}$, [a]2.14×10^{3c}, [a]$5.1x10^{3f}$	[a]$4.8x10^{3d}$, [a]$3.53x10^{3e}$, [a]$2.42x10^{3e}$	[a]$4.6x10^{2d}$	[a]$2.0x10^{3d}$, [a]$5.50x10^{3e}$, [a]$1.00x10^{3e}$
$C_{11}H_{23}CO_2Na$ SDodec	[a]$2.1x10^{4d}$ [b]$1.2x10^{3d}$	[a]$3.3x10^{4d}$, [a]$5.0x10^{4d}$, [b]$4.3x10^{2d}$, [b]$4.0x10^{2d}$, [a]2.80×10^{4e}, [b]2.15×10^{2e} [a]$1.6x10^{4f}$	[a]$1.0x10^{4d}$, [a]$1.68x10^{4e}$, [a]$1.00x10^{4e}$	[a]$4.3x10^{3d}$	[a]$3.8x10^{3d}$, [a]$4.48x10^{3e}$, [a]$2.72x10^{3e}$
$C_{13}H_{27}CO_2Na$ ST	[a]$4.0x10^{4d}$ [b]$6.2x10^{3d}$	[a]$6.3x10^{4d}$, [a]$1.0x10^{5d}$, [b]$1.6x10^{3d}$, [b]$1.5x10^{3d}$, [a]$3.5\times10^{4(e)}$, [b]$3.00\times10^{2(e)}$ [a]$4.8x10^{4f}$	[a]$5.0x10^{4d}$, [a]$8.00x10^{4e}$, [c]$3.00x10^{3e}$, [a]$3.56x10^{4e}$	[a]$2.3x10^{4d}$	[a]$1.6x10^{4d}$, [a]$8.00x10^{3e}$, [a]$1.00x10^{4e}$

[a] $K_{1:1}$ (M^{-1}), [b] $K_{2:1}$ (M^{-2}), [c] $K_{1:2}$ (M^{-2}), [d] ^1H NMR (guest and/or host), [e]AMV (guest and/or host), [f]Spectrophotometry.
Error estimates of K_i can be found in the Tables given in Chapter 4.

Table 6-1b: Cyclodextrin-Sodium Perfluoroalkyl Carboxylate Complexes

Surfactant	β-CD	RAMEB	DM-β-CD	TM-β-CD	HP-β-CD
$C_3F_7CO_2Na$ SPFB	[a]9.17×10^{2d}, [a]1.7×10^{2c}, [a]2.8×10^{2f}	[a]1.32×10^{2d}	[a]2.01×10^{2d}, [a]1.3×10^{2e}, [a]4.3×10^{1e}	[a]2.24×10^{1d}	[a]9.82×10^{1d}, [a]1.3×10^{2e}, [a]1.8×10^{1e}
$C_4F_9CO_2Na$ SPFP	[a]2.67×10^{3d}, [a]1.6×10^{3e}, [a]2.6×10^{3f}	[a]6.24×10^{2d}	[a]1.86×10^{3d}, [a]4.00×10^{3e}, [a]3.00×10^{3e}	[a]1.01×10^{2d}	[a]5.53×10^{2d}, [a]1.70×10^{3e}, [a]1.67×10^{3e}
$C_6F_{13}CO_2Na$ SPFH	[a]2.35×10^{4d}, [a]8.8×10^{3e}, [a]3.7×10^{4f}	[a]1.05×10^{4d}	[a]9.59×10^{3d}, [a]6.01×10^{4e}, [a]4.00×10^{4e}	[a]1.48×10^{4d}	[a]1.40×10^{4d}, [a]3.14×10^{4e}, [a]2.61×10^{4e}
$C_7F_{15}CO_2Na$ SPFO	[a]8.85×10^{4d}, [a]6.5×10^{4e}, [b]2.0×10^{3e}, [b]7.64×10^{2d}, [a]3.3×10^{5f}	[a]3.55×10^{4d}	[a]2.49×10^{4d}, [a]7.00×10^{4e}, [a]6.00×10^{4e}, [c]5.00×10^{2e}, [c]5.00×10^{3e}	[a]2.48×10^{4d}	[a]3.59×10^{4d}, [a]4.00×10^{4e}, [a]3.33×10^{4e}
$C_8F_{17}CO_2Na$ SPFN	[a]1.20×10^{5d}, [b]2.20×10^{3d}, [a]7.0×10^{5e}, [b]3.5×10^{3e}, [a]9.4×10^{5f}	[a]8.80×10^{4d} [c]7.00×10^{2d}	[a]6.20×10^{4d}, [c]4.0×10^{2d}, [a]1.00×10^{5e}, [a]1.00×10^{5e}, [c]6.00×10^{3e}, [c]5.00×10^{3e}	[a]6.25×10^{4d} [c]1.83×10^{3d}	[a]$6.01\times10^{4(d)}$, [a]5.00×10^{4e}, [a]4.10×10^{4e}

[a] $K_{1:1}$ (M^{-1}), [b] $K_{2:1}$ (M^{-2}), [c] $K_{1:2}$ (M^{-2}), [d] ^{19}F NMR (guest and/or host), [e]AMV (guest and/or host), [f]Spectrophotometry.
Error estimates of K_i can be found in the Tables given in Chapter 4.

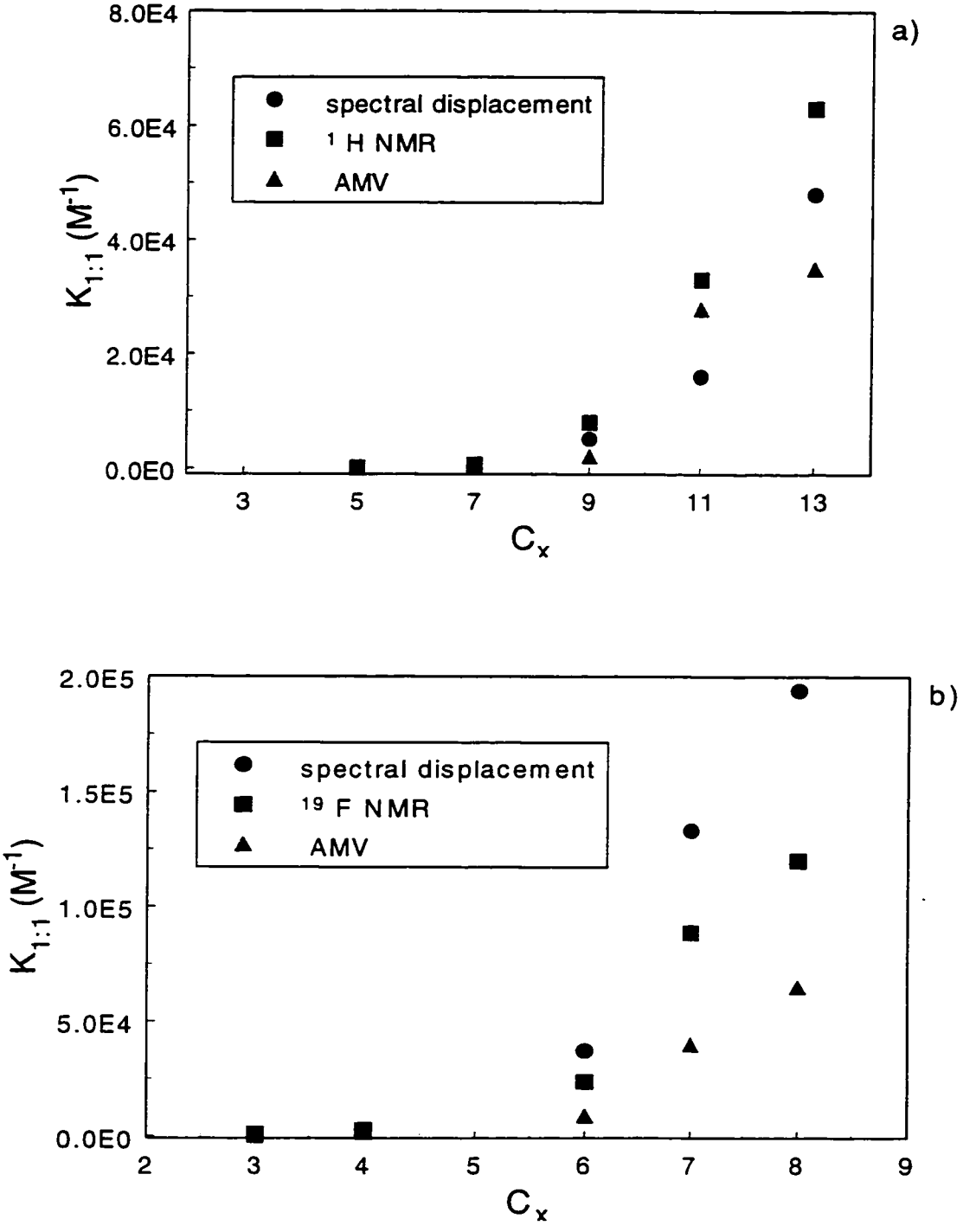

Figure 6-1: Comparison of the 1:1 β-CD-surfactant binding constants ($K_{1:1}$) obtained using the various techniques in this study: a) β-CD-sodium alkyl carboxylates and b) β-CD-sodium perfluoroalkyl carboxylates, where C_x is alkyl chain length.

techniques, the values of K_i obtained from NMR, densimetry, and spectrophotometry are in good agreement with one another on the basis of the estimated errors. The values of K_i obtained using a single technique from the perspective of the host or guest physical property are also in good agreement.

A number of different types of host-guest stoichiometries have been elucidated in this work. The main type of host-guest stoichiometry for the relatively short to medium chain length surfactants is the 1:1 CD-S complex; however, other stoichiometries such as 1:2 and 2:1 are also observed, as summarized in Table 6-2.

Table 6-2: Summary of the Various Types of Stoichiometries Observed in This Work for Complexes Formed Between Cyclodextrin-Surfactant Systems.

a: Surfactant=Sodium Alkyl Carboxylates ($C_xH_{2x+1}COONa$).

Cyclodextrin	1:1	2:1	1:2
α-CD	x=5-7	x=9-13	NF
β-CD	x=2-9	x=11-13	NF
DM-β-CD	x=5-11	NF	x=13
RAMEB	x=5-13	NF	NF
TM-β-CD	x=5-13	NF	NF
HP-β-CD	x=5-13	NF	NF

b: Surfactant=Sodium Perfluoroalkyl Carboxylates ($C_xF_{2x+1}COONa$).

Cyclodextrin	1:1	2:1	1:2
α-CD	NR	NR	NR
β-CD	x=3-6	x=7-9	NF
DM-β-CD	x=3-6	NF	x=7,8
RAMEB	x=3-6	NF	x=7,8
TM-β-CD	x=3-6	NF	x=7,8
HP-β-CD	5-9	NF	NF

NR= not reported
NF= not formed

As well, 2:1 complexes are favored when $[CD]_{total}>>[S]_{total}$, 1:2 complexes are favored when $[S]_{total} >>[CD]_{total}$, and when the surfactant has a relatively long alkyl chain that exceeds the depth of the CD cavity. The fact that R-β-CD hosts do not form 2:1 CD-S complexes is consistent with their extended cavity length created by the presence of alkyl substituents in the annulus region.

This work presents some of the first direct evidence for the formation of a 1:2 CD-S complex, where S=SPFO, SPFN, and ST, and CD= RAMEB, DM-β-CD, and TM-β-CD, as shown from NMR and AMV studies. AMV results show the possible formation of higher order complexes for DM-β-CD with SPFO, SPFN, and ST.

Evidence of inclusion and noninclusion binding is supported from NMR and AMV studies. The inclusion mode for 1:1 (Scheme 5-1a), 2:1 (cf. Scheme 5-1c), and 1:2 (cf. Scheme 5-2) complexes involves the insertion of the apolar alkyl chain into the CD interior while the carboxylate head group of the surfactant remains in the bulk solvent or near the hydroxyl groups in of the CD annulus. In the case of β-CD, inclusion occurs from the wider, secondary side of the CD annulus. Evidence of noninclusion binding was observed for α-CD-fc surfactants and 2:1 β-CD-SPFO complexes, as demonstrated by small transfer volume and CIS values of the nuclei within the host interior.

The number of alkyl groups that can be accommodated within the α- and β-CD interior was deduced from an analysis of the $(CH_2)_n$ NMR spectral line shapes of SDec, SDodec, and ST in the presence of α-CD and β-CD at R=2 ($R=C_S/C_{CD}$). The results indicate that 5 CH_2 groups can be included within α-CD and 7-8 CH_2 groups within β-CD. The greater number of alkyl groups included in β-CD are in agreement with results

from AMV studies and suggests that the alkyl chain of the surfactant can coil by assuming gauche kink conformations. Results from the AMV work indicate that additional methylene groups, at least 10 CH_2 or 6-7 CF_2 groups, are included in the R-β-CD hosts. The additivity scheme used to interpret transfer volumes of hc and fc surfactants from water to ternary solutions provides further evidence of the greater numbers of included alkyl groups in R-β-CD relative to β-CD hosts.

The greater binding affinities of fc surfactants relative to hc surfactants with a common host has been attributed to a number of physicochemical characteristics. In comparison to hc surfactants, fc surfactant systems possess greater hydrophobicity, molecular volumes, and solvent accessible surface areas. The greater binding in fc surfactants can be related to the occurrence of ion-dipole interactions between the carboxylate head group and annular CD hydroxyl groups. The latter is argued to be more important in the case of fc surfactants because of the lower degree of hydration of the carboxylate head group. The ion-dipole interactions are diminished in the R-β-CD hosts because the presence of alkyl groups in the annulus region screen the ion-dipole interactions.

There are differences in binding between R-β-CD and β-CD hosts with a common guest as shown from the NMR and AMV results. The presence of alkyl substituents in the annulus region of β-CD tends to lengthen the macrocycle, resulting in the inclusion of additional alkyl groups, a reduction of the dipolar character of the CD annulus, and steric exclusion effects. These effects depend upon the size of the alkyl substituents and their degree of substitution. According to the additivity scheme used to interpret transfer

volumes, the hydration of the CD interior of the R-β-CD and β-CD hosts is relatively unaffected by the presence of alkyl substituents in the CD annulus.

The main contribution to complex stability is the hydrophobic effect. Although, there are differences in the physicochemical properties of the various host and guest, as mentioned above, it is argued that solute-solute (dispersion, H-bonding, ion-dipole) interactions between the host and guest do not play a significant role in complex stability. These types of interactions can account for only a small fraction of the overall stability of the complex. In aqueous solutions, solute-solvent and solvent reorganization processes are expected to play a major role. The involvement of the hydrophobic effect in these complexation phenomena is demonstrated, indirectly, according to the dependence of K_i on C_x, the greater binding affinity of fc surfactants relative to hc surfactants with a common host, and the agreement between the Gibbs energy of complex formation and that predicted by the cavity model. The various types of host-guest stoichiometry and inclusion modes demonstrate that complex formation can maximize hydrophobic and hydrophilic interactions within the CD interior and at the host-guest interface while minimizing unfavourable hydrophobic hydration of the surfactant alkyl chain. The results indicate that desolvation and solvation processes play a significant role in the formation of CD-S complexes, as expected for processes involving hydrophobic hydration and hydrophobic interactions. The greater binding constants for the CD-fc surfactant systems relative to the CD-hc surfactant systems can be related to the systematic differences in physicochemical properties of the individual surfactants such as CMC, volume, and molecular surface area. Thus, hydrophobicity correlates with molecular volume because it can be related to the

energy required to form a cavity for the solute in water. The results described herein on the binding of CD-surfactant systems indicate that it is the rearrangement of the water network accompanying complex formation which provides a significant driving force for complex formation. Future studies are expected to establish the relative contribution of solvent reorganization to the overall energetics of complex formation.

NMR, thermodynamic, and spectrophotometric studies have provided information regarding the binding constants, stoichiometry, and inclusion mode of cyclodextrin-surfactant complexes. Despite the different sensitivity of each of the techniques to the binding process, the general conclusions derived from each method are complementary and self-consistent. The techniques used in this research are suitable for aliphatic guest molecules that do not possess a chromophore for study by spectroscopic techniques. The study described herein, where the chemical structure of the host and guest species are varied systematically, has provided a better understanding of the factors that govern the formation and stability of cyclodextrin-surfactant complexes, such as the relative contribution of solute-solute, solute-solvent, and solvent reorganization interactions.

7. SIGNIFICANCE OF RESULTS AND SUGGESTIONS FOR FUTURE WORK

7.1 Significance of results

This work represents one of the few comprehensive binding studies of cyclodextrin-surfactant (CD-S) complexes using a variety of spectroscopic and thermodynamic methods in which the chemical structure of the host and guest has been varied systematically. It has produced results that show the importance and benefits to be gained from such systematic studies and information about the factors that contribute to the formation and stability of host-guest complexes.

A significant result arising from this work is the establishment of the validity of the magnitude of the binding constant (K_i) by using different physical methods such as NMR spectroscopy, spectrophotometry, and high precision densimetry. In the case of NMR spectroscopy and densimetry, the physical properties of the host and guest were measured independently and were found to yield consistent values of K_i of a given CD-S complex. The apparent molar volume results obtained from density measurements represent one of the first studies of this type. These results have contributed to a better understanding of the formation, stability, and volumetric properties of CD-S complexes and the utility of AMV measurements as an investigative tool to study CD-S complexes.

There are a number of factors that influence the magnitude of K_i (cf. § 1.4.1). An appropriate choice of models to describe the host-guest stoichiometry and the data fitting procedure are of paramount importance. In the cyclodextrin literature, it is often incorrectly assumed that 1:1 cyclodextrin-inclusate complexes are the predominant equilibrium. However, the results of this study indicate that 2:1 and 1:2 CD-S complexes

are also formed and need to be considered. It is for these reasons that a global analysis of the data was carried out that included a nonlinear least-squares fitting of the data and a thorough accounting of the various types of CD-S complexes formed. This analysis has revealed that many of the discrepancies between reported results of binding constants for host-guest complexes can be traced to analysis of data that neglect contributions arising from all types of CD-S complexes. Hence, the results of this study have contributed substantially to clarifying issues concerning the reliability of binding constants for cyclodextrin-inclusate complexes, as shown by some examples presented in Chapter 5.

In addition to experimental evidence in favor of various stoichiometries of CD-S complexes, a number of different binding modes, e.g., inclusion, noninclusion, and extracavity have been established. This works reports one of the first examples of 1:2 methylated CD-S (where S=ST, SPFO, and SPFN) complexes and a ternary complex consisting of a methylated 1:1 or 1:2 CD-S (where S=SPFO and SPFN) complex bound to monomer surfactants to the exterior of the macrocycle. Previous interpretations of sound velocity[219b,237] and kinetic studies[129] of these systems may need to be reexamined in the light of the results presented in this research.

The information obtained regarding the inclusion mode, stoichiometry, and binding constants has provided important information about the factors that govern complex stability. The various types of binding modes such as inclusion, noninclusion, and extracavity CD-S complexes reaffirm the importance of the hydrophobic effect. The optimal binding geometry in the various types of 1:1, 2:1, and 1:2 CD-S complexes result in

the close matching of apolar-apolar surfaces while minimizing polar-apolar interactions with the solvent.

This study has provided strong evidence for the direction of inclusion of a guest molecule into the host β-CD, as seen in the case of 1:1 and 2:1 CD-S complexes (cf. Schemes 5-1 a and c). Specific directional inclusion of this type is consistent with the calculated MLPs of β-CD. Information about the inclusion mode provides an opportunity to further understand the factors governing complex stability and the prediction of the binding constants of CD-guest complexes. As well, a better design of host systems for applications that involve the exploitation of noncovalent binding with guest molecules may be achieved. The above examples illustrate that hydrophobic interactions play a major role in complex stability and strongly influence the stoichiometry and inclusion mode of CD-S complexes. Solute-solute interactions, such as dispersion, between the alkyl chain of the surfactant and the CD interior or ion-dipole between the carboxylate head group and annular hydroxyl groups of the CD play a secondary role in determining complex stability.

The issue of solvent reorganization processes has not been adequately dealt with in the cyclodextin literature since much of the focus has been on deriving solute-solute correlations between the host and guest that relate to complex stability. The results of this study have established that solvent reorganization needs to be considered, as shown by the good agreement between the Gibbs energy of complex formation and that predicted by a simple cavity model. Solvent reorganization processes play a substantial role in apolar binding interactions in aqueous solution, as demonstrated in the case of the formation of CD-S complexes studied here.

The significance of the results in this study can be extended to numerous applications involving noncovalent host-guest binding interactions, for example; 1) quantification for systems of biological or medicinal interest; enzymes, receptors, immunoglobulins, and antigen-antibody systems, 2) development of drug delivery systems, 3) selective phases for affinity chromatography, 4) new analytical and diagnostic procedures, 5) development of molecular sensors and switches. and 6) catalysis and synthesis in water as a solvent.

7.2 Future work

In order to establish the relative importance of solute-solute, solute-solvent, and solvent-solvent interactions, further theoretical studies that deal with the quantification of these noncovalent interactions in the formation of host-guest complexes is necessary. As such, there is a need to explore the utility of semiempirical molecular mechanics (MM), molecular dynamics (MD), and Monte Carlo (MC) methods to estimate the contribution of van der Waals, ion-dipole, dipole-dipole and H-bonding interactions in complex formation. These techniques can be used to estimate the contribution of Gibbs energy of solvation to the overall energetics of the system. In conjunction with experimental studies, it is anticipated that theoretical calculations should provide a better understanding of the mechanism of the formation of host-guest complexes.[156] In this regard, the results of this systematic study have shown the occurrence of alkyl chain coiling, have estimated the number of alkyl groups included within the CD interior, and have provided new

insights about the inclusion geometry, stoichiometry, and Gibbs energy of binding in aqueous solution and will be of considerable value in supporting computational efforts.

Because the contribution of solvent reorganization to the overall energetics of host-guest complex formation may be considerable, it is necessary to compare calculated energies *in vacuo* and in solution in order to elucidate the relative contribution of solvent reorganization to host-guest binding. Statistical perturbation or free energy perturbation theory makes it possible to calculate changes in Gibbs energy (ΔG) between similar states. Statistical mechanics can be utilized to calculate the energies of the host, guest, and solvent separately which can be utilized as reference states. Complex formation can be treated as a perturbed state. The method is applicable to systems in solution by using appropriate thermodynamic cycles (cf. Scheme 7-1), taking into account the solvent and considering desolvation of the host and guest. In Scheme 7-1, $\Delta G_{CD\text{-}S}$ is the Gibbs energy of formation of the 1:1 CD-S complex and ΔG_x^w(x=CD, S, and CD-S) is the Gibbs energy of hydration of the CD, S, and CD-S species, respectively. The solvent induced part can be computed by comparing $\Delta G_{CD\text{-}S}$ (g, C^o) with $\Delta G_{CD\text{-}S}$ (aq, C^o).

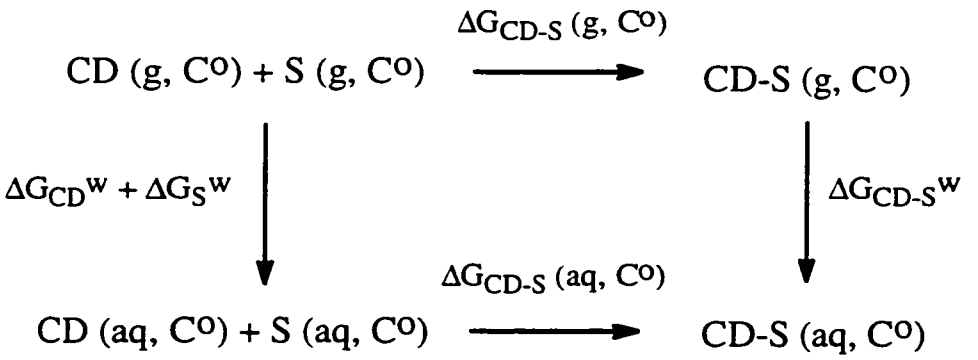

Scheme 7-1: Thermodynamic cycle for the transfer of a cyclodextrin (CD), surfactant (S), and 1:1 CD-S inclusion complex from the gas phase (g) into water (w), where C^o is a standard reference state concentration. Adapted from ref. 34.

A key issue related to the hydrophobic effect is the influence of solute-solute and solute-solvent interactions. Chemical processes in solution consist of "chemical" and "solvation" components and the results of this work indicate that it is the latter which contributes, significantly, to the overall energetics of host-guest complex formation (cf. § 5.5 and § 5.6). Thermodynamic studies in nonaqueous solvents (DMSO, DMF, hydrazine, and propylene carbonate) or in mixed solvent (H_2O/CH_3OH and H_2O/D_2O) systems may provide insight into solvent effects (cf. § 1.4.2) and the interactions that occur in water.[3] The variation in thermodynamic parameters can be correlated to the physicochemical properties of the solvent. The thermodynamics of complex formation for CD-inclusate systems, e.g., enthalpy (ΔH_{comp}) and entropy (ΔS_{comp}) can be subdivided into two components

$$\Delta H_{comp} = \Delta H_i + \Delta H_S \qquad (7.2\text{-}1)$$

$$\Delta S_{comp} = \Delta S_i + \Delta S_S \qquad (7.2\text{-}2)$$

where the subscripts i and s denote the intrinsic and solvent reorganization contributions, respectively. In the case of studies that employ light and heavy water, it may be possible to isolate the contribution due to solvent reorganization.

High precision acoustic and densimetric techniques are known to be able to provide information on the binding induced changes in the hydration of the host and guest. For example, compressibility measurements of aqueous solutions containing host-guest complexes are expected to provide useful information regarding local changes in water structure and hydration.

An investigation of the kinetics of complex formation using ultrasonic relaxation techniques under conditions where the host-guest mixing ratio is varied can provide an increased understanding of the nature of the hydrate water in the CD interior and the kinetics of association and dissociation of the surfactant monomer to and from the host macrocycle. Studies of 1:2 CD-S complexes and ternary complexes using ultrasonic relaxation studies are anticipated to yield important mechanistic details about the dynamics of such processes.

8. REFERENCES

1. *In* Inclusion Compounds, Eds; Atwood, J. L.; Davies, J. E. D., MacNicol, D. D. a) Vol. 2: Structural Aspects of Inclusion Compounds Formed by Organic Host Lattices, b) Vol. 3: Physical Properties and Applications, Academic Press: London, 1984; c) Vol. 4: Key Organic Host Systems; d) Vol. 5: Inorganic and Physical Aspects of Inclusion, Oxford University Press, Oxford, 1991; e) Bender, M. L.; Komiyama, M. Cyclodextrin Chemistry. Springer, Berlin. 1978. f) Clarke, R. J.; Coates, J. H.; Lincoln, S. F. *Adv. Carbohydr. Chem.* **1988**, 46, 205.

2. Izatt, R. M.; Bradshaw, J. S.; Pawlak, K.; Bruening, R. L.; Tarbot, B. J.; *Chem. Rev.* **1992**, 92, 1261.

3. Diederich, D.; Smithrud, B.; Sanford, E. M.; Wyman, T. B.; Fergus, S. B.; Carcanague, D. R.; Chao, I.; Houk, K. N. *Acta. Chem. Scand.* **1992**, 46, 205, and references cited therein.

4. Breslow, R. *Acc. Chem. Res.* **1995**, 28, 146.

5. Farnasier, R.; Marcuzzi, F.; Tonellato, U. *J. Inclusion Phenom. Mol. Recognit. Chem.* **1994**, 18, 81.

6. Ramamurthy, V.; Eaton, D. F. *Acc. Chem. Res.* **1988**, 21, 300.

7. a) Li, S.; Purdy, W. C. *Chem. Rev.* **1992**, 92, 1457. b) Easton, C. J.; Lincoln, S. F. *Chem. Soc. Rev.* **1996**, 163.

8. Jullien, L.; Canceill, J.; Valeur, B.; Bandez, E.; Lefèvre, J.-P.; Lehn, J.-M.; Marchi-Artzner, V.; Pansu, R. *J. Am. Chem. Soc.* **1996**, 118, 5432.

9. Brewster, M. E.; Loftsson, T. *J. Pharm. Sci.* **1996**, 85, 1017, and references cited therein.

10. Rawyler, A.; Siegenthaler, P. A. *Biochim. Biophys. Acta* **1996**, 1278, 89.

11. Parazak, D. P.; Khan, A. R.; D'Souza, V. T.; Stine, K. J. *Langmuir* **1996**, 12, 4046.

12. a) Rozema, D.; Gellman, S. H. *J. Am. Chem. Soc.* **1995**, 117, 2373. b) Mutter, M. Vuilleumier, S. *Angew. Chem. Int. Ed. Engl.* **1989**, 28, 535.

13. Maheswaran, M. M.; Divakar, S. *J. Sci. Ind. Res.* **1994**, 53, 924.

14. Bost, M.; Laine, V.; Pilard, F.; Gadelle, A.; Defaye, J.; Perly, B. *J. Inclusion Phenom. Mol. Recognit. Chem.* **1997**, 29, 57.

15. Leray, E.; Leroy-Lechat, F.; Parrot-Lopez, H.; Duchêne, D. *Supramol. Chem.* **1995**, 5, 149.

16. Irie, T.; Otagiri, M.; Sunada, K.; Uekama, Y.; Ohtani, Y.; Yamada, Y.; Sugiyama, Y. *J. Pharm. Dyn.* **1982**, 5, 741.

17. Connors, K. A. *Chem. Rev.* **1997**, 97, 1325.

18. Botsi, A.; Yannakiopoulou, K.; Hadjoudis, E.; Waite, J. *Carbohydr. Res.* **1996**, 283, 1.

19. Miranda, P. B.; Saijo, V.; Shen, Y. R. *Chem. Phys. Lett.* **1997**, 264, 387.

20. Tiddy, G. J. T. *In* Modern Trends of Colloid Science in Chemistry and Biology, Edited by E. Eicke. Birkhauser Verlag, Basel, 1985, pp. 153.

21. a) Eftink, M. R.; Andy, M. L.; Bystrom, K.; Perlmutter, H. D.; Kristol, D. S. *J. Am. Chem. Soc.* **1989**, 111, 6765. b) Matsui, Y.; Mochida, K. *Bull. Chem. Soc. Jpn.* **1979**, 52, 2808.

22. Wenz, G. *Angew. Chem. Int. Ed. Engl.* **1994**, 33, 803, and references cited therein.

23. Claire Myles, A. M.; Barlow, D. J.; France, G.; Lawrence, M. J. *Biochim. Biophys. Acta.* **1994**, 1199, 27, and references cited therein.

24. Wang, T.; Bradshaw, J. S.; Izatt, R. M. *J. Heterocyclic Chem.* **1994**, 31, 1097.

25. Schneider, H.-J. *Recl. Trav. Chim. Pay-Bas* **1993**, 112, 412.

26. a) Selvidge, L. A.; Eftink, M. R. *Anal. Biochem.* **1986**, 154, 400. b) Inestal, J. J.; González-Velasco, F.; Cebalos, A. *J. Chem. Educ.* **1994**, 71, A297.

27. Jobe, D. J.; Verrall, R. E.; Junquera, E.; Aicart, E. *J. Colloid Interface Sci.* **1997**, 189, 294.

28. Tanford, C. *In* The Hydrophobic Effect: Formation of Micelles and Biological Membranes; 2nd ed.; Wiley: New York, 1980.

29. Chalikian, T. V.; Plum, G. E.; Sarvazyan, A. P.; Breslauer, K. J. *Biochemistry* **1994**, 33, 8629.

30. Huang, H. Ph. D Thesis, University of Saskatchewan, Saskatoon, SK., 1997.

31. Høiland, H.; Harald, L. H.; Kvammen, O. J. *J. Solution Chem.* **1981**, 10, 775.

32. a) Gutman, V.; Resch, G. *In* Lecture Notes on Solution Chemistry, World Scientific: New Jersey, 1995, and references cited therein; b) Reichardt, C. *In* Solvents

and Solvent Effects in Organic Chemistry, 2nd ed.; VCH: Weinheim, 1988. c) *In* Water: A Comprehensive Treatise. The Physics and Physical Chemistry of Water, Ed. Franks, F. Vol. 1., Plenum Press: New York, 1972.

33. *In* Water and Aqueous Solutions: Structure, Thermodynamics, and Transport Processes. Ed.; Horne, R. A., Wiley: New York, 1972, Chapter 13, pp. 519.

34. Blokzijl, W.; Engberts, J. F. B. N. *Angew. Chem. Int. Ed. Engl.* **1993**, 32, 1545.

35. a) Israelachvili, J.; Wennerström. *Nature* **1996**, 379, 219. b) Israelachvili, J. *In* Intermolecular and Surface Forces, 2nd ed., Academic Press: London, 1992. c) F. Kreschek, G. C. *In* Water - A Comprehensive Treatise, Vol. 4. Ed. Franks, F., Plenum: New York, 1975, Chapter 2.

36. Finney, J. L.; Soper, A. K. *Chem. Soc. Rev.* 1994, 1.

37. Lee, B. *Biopolymers* **1991**, 31, 993.

38. Sinanoglu, O. *In* Molecular Association in Biology Ed. Pullman, B., Academic Press: New York, 1968, 427.

39. Connors, K. A. *J. Pharm Sci.* **1996**, 85, 796.

40. Giulieri, F.; Krafft, M. *Colloids and Surfaces A: Physicochem. Eng. Aspects* **1994**, 84, 121.

41. Mukerjee, M.; Mysels, K. J. *In* Critical Micelle Concentration of Aqueous Surfactant Systems, NSRDS-NBS 36, Washington, D.C. 1971.

42. Muller, N. *Acc. Chem. Res.* **1990**, 23, 23.

43. Lemieux, R. U. *Acc. Chem. Res.* **1996**, 29, 373.

44. Lemieux, R. U.; Boullanger, P. H.; Bundle, D. R.; Baker, D. A.; Nagpurkar, A.; Venot, A. *Nouv. J. Chim.* **1978**, 2, 321.

45. Inoue, Y. *Ann. Rep. NMR Spectrosc.* **1993**, 27, 59.

46. Bell, A. F.; Hecht, L.; Barron, L. D. *Chem. Eur.* **1997**, 3, 1292.

47. Margheritis, C.; Sinistri, C. *Z. Naturforsch* **1996**, 51a, 950.

48. Donzé, C.; Chatjigakis, A.; Coleman, A. W. *J. Inclusion Phenom. Mol. Recog. Chem.* **1992**, 13, 155.

49. Coleman, A. W.; Munoz, M.; Chatjigakis, A. K. *J. Phys. Org. Chem.* **1993**, 6, 651.

50. Kitagawa, M.; Hoshi, H.; Sakurai, M.; Inoue, Y.; Chûjô, R. *Carbohydr. Res.* **1987**, 163, C1.

51. Sakurai, M.; Kitagawa, M.; Hoshi, H.; Inoue, Y.; Chûjô, R. *Carbohydr. Res.* **1990**, 198, 181.

52. Lichtenthaler, F. W.; Immel, S. *Tetrahedron: Asymmetry.* **1994**, 2045.

53. Warner, I. M.; Schuette, J. M. *Adv. Mult. Lum.* **1993**, 2, 61.

54. Lichtenthaler, F. W.; Immel, S. *Starch* **1996**, 48, 225.

55. a) Szejtli, L. *In* Cyclodextrin Technology; Kluwer: Dordrecht, The Netherlands, 1988. b) Szejtli, L. *In* Cyclodextrins and Their Inclusion Complexes, Akadèmiai Kiadó: Budapest, Hungary, 1982.

56. Klyamkin, A. A.; Topchieva, I. N.; Zubov, V. P. *Coll. Polym. Sci.* **1995**, 273, 520.

57. Funasaki, N.; Yodo, H.; Hada, S.; Neya, S. *Bull. Chem. Soc. Jpn.* **1992**, 65, 1323.

58. Job, A. *Ann. Chim.* **1928**, 9, 113

59. Connors, K. A. *In* Binding Constants: "The Measurement of Molecular Complex Stability". Wiley: New York, 1987, Chapter 5.

60. Qi, Z. H.; Zhu, L.; Chen, H.; Qi, W. *J. Inclusion Phenom. Mol. Recognit. Chem.* **1997**, 27, 279.

61. Agbaria, R. A.; Gill, D. *J. Photochem. Photobiol. A: Chem.* **1994**, 78, 161.

62. Saenger, W. *Angew. Chem. Int. Ed. Engl.* **1980**, 19, 344.

63. a) Du, Y.-Q.; Nakamura, A.; Toda, F. *J. Inclusion Phenom. Mol. Recognit. Chem.* **1991**, 10, 443. b) Matsushita, A.; Kuwabara, T.; Nakamura, A.; Ikeda, H.; Ueno, A. *J. Chem. Soc. Perkin Trans 2* **1997**, 1705.

64. Alderfer, J. L., Eliseev, A. V. *J. Org. Chem.* **1997**, 62, 8225.

65. Guo, W.; Fung, B. M.; Christian, S. D. *Langmuir* **1992**, 8, 446.

66. Danil de Namor, A. F.; Traboulssi, R.; Lewis, D. F. *J. Chem. Soc. Chem. Commun.* **1990**, 751.

67. Lainé, V.; Coste-sarguet, A.; Gadelle, A.; Defaye, J.; Perly, B. *J. Chem. Soc. Perkins Trans 2* **1995**, 1479.

68. Jobe, D. J.; Verrall, R. E.; Palepu, R.; Reinsborough, V. C. *J. Phys. Chem.* **1988**, 92, 3582.

69. Ito, N.; Yoshida, N.; Ichikawa, K. *J. Chem. Soc., Perkin Trans. 2* **1996**, 965.

70. Lichtenthaler, F. W.; Immel, S. *Starch* **1996**, 48, 145.

71. Impellizzeri, G.; Maccarrone, G.; Rizzarelli, E.; Vecchio, G.; Corradini, R.; Marchelli, R. *Angew. Chem. Int. Ed. Engl.* **1991**, 30, 1348.

72. Schneider, H.-J.; Blatter, T.; Simova, S. *J. Am. Chem. Soc.* **1991**, 113, 1996.

73. Lichtenthaler, F. W. *Angew. Chem. Int. Ed. Engl.* **1994**, 33, 2364.

74. Saenger, W.; Noltmeyer, M.; Manor, P. C.; Hagerty, O., Klar, B. *Bioorg. Chem.* **1976**, 5, 187.

75. Caira, M. R.; Griffith, V. J.; Nassimbeni, L. R. *J. Inclusion Phenom. Mol. Recognit. Chem.* **1995**, 20, 277.

76. Koshland, D. E. Jr. *Angew. Chem. Int. Ed. Engl.* **1994**, 33, 2315.

77. Dodziuk, H.; Nowinski, K. *J. Mol. Structure* **1994**, 304, 61.

78. Castronuovo, G., Elia, V., Fessas, D., Velleca, F., Viscardi, G. *Carbohydrate Res.* **1996**, 287, 127.

79. Turro, N. J. *Langmuir* **1985**, 1, 170.

80. Buvari, Á.; Barcza, L. *Acta. Chim. Hung.* **1989**, 26, 455.

81. Harata, K. *J. Chem. Soc. Perkin Trans 2* **1990**, 799.

82. Jeffrey, G. A.; Saenger, W. *In* Hydrogen Bonding in Biological Structures, Springer Verlag: New York, 1991, Chapter 18.

83. He, Q.; Ke, X.; Wu, Z.; Yoder, C. H.; Chen, S.; Mahalick, J. E. *J. Solution Chem.* **1995**, 24, 601.

84. Biczok, C.; Jicsinszky, L.; Linschitz, H. *J. Inclusion Phenom. Mol. Recognit. Chem.* **1994**, 18, 237.

85. Ross, P. D.; Rekharsky, M. V. *Biophys. J.* **1996**, 71, 2144.

86. Matsui, Y.; Naruse, H.; Mochida, K.; Date, Y. *Bull. Chem. Soc. Jpn.* **1970**, 43, 1909.

87. Eliseev, A. V.; Schneider, H.-J. *J. Am. Chem. Soc.* **1994**, 116, 6081.

88. Schneider, H.-J. *Chem. Rev.* **1994**, 227.

89. Bhat, J. N.; Benley, G. A.; Boulot, G.; Greene, M. I.; Tello, D.; Dáll'Acqua, W.; Souchon, H.; Schwarz, F. P.; Mariuzza, R. A.; Poljak, R. J. *Proc. Natl. Acad. Sci. USA.* **1994**, 91, 1089.

90. Helms, V.; Wade, R. C. *Biophys. J.* **1995**, 69, 810.

91. Tabushi, I.; Mizutani, T. *Tetrahedron* **1987**, 43, 1439.

92. Tabushi, I.; Yamamura, K. *Top. Curr. Chem.* **1983**, 113, 145.

93. Schneider, H.-J.; Simova, S.; Schneider, U. *J. Am. Chem. Soc.* **1988**, 110, 6442.

94. Hakormori, S. *Pure Appl. Chem.* **1991**, 63, 473. b) Reid, D. S. *In* Studies in Molecular Thermodynamics; Ed. Jones, M. N., Elsevier: 1979, Chapter, 5.

95. Drost-Hansen, W.; Clegg, J. *In* Cell-Associated Water, Academic Press: New York, 1979.

96. a) Steiner, T; Moreira da Silva, A. M.; Teixeira-Dias, J. J. C.; Saenger, W. *Angew. Chem. Int. Ed. Engl.* **1995**, 34, 1452. b) Moreira da Silva, A. M.; Steiner, T; Saenger, W.; Empis, J.; Teixeira-Dias, J. J. C. *Chem. Commun.* **1996**, 1871.

97. Marini, A.; Berbenni, V.; Bruni, G.; Massarotti, V.; Mustarelli, P.; Villa, M. *J. Chem. Phys.* **1995**, 103, 7532.

98. Furuta, T.; Yoshi, H.; Miyamoto, A.; Yasunishi, A.; Hirano, H. *Supramol. Chem.* **1993**, 1, 321.

99. Cromwell, W. C.; Bystrom, K.; Eftink, M. R. *J. Phys. Chem.* **1985**, 89, 326.

100. Turro, N. J.; Okubo, T.; Chung, C.-J. *J. Am. Chem. Soc.* **1982**, 104, 1789.

101. a) *In* Comprehensive Supramolecular Chemistry Eds.; Szejtli, J., Osa, T., Pergamon Press: New York, 1996, and references cited therein and b) For a recent review see: *Chem Rev.* **1998**, 98, 1743-2076.

102. *In* Frontiers in Supramolecular Chemistry and Photochemistry, Ed. Schneider, H.-J.; Dürr, H. VCH: Weinheim. 1991, and references cited therein. b) Schneider, H. -J. *Angew. Chem. Int. Ed. Engl.* **1991**, 30, 1417.

103. Perly, B.; Djedaïni, F.; Berthault, P. *In* New Trends in Cyclodextrins and Derivatives, Ed.; Duchêne, D., Editions de Santé: Paris. 1991, Chapter 5.

104. Kaifer, A. E. *Adv. Supramol. Chem.* **1992**, 2, 1.

105. Mwakibete, H.; Cristiantino, R.; Bloor, D. M.; Wyn-Jones, E.; Holzwarth, J. F. *Langmuir* **1995**, 11, 57.

106. Nigam, S.; Durocher, G. *J. Phys. Chem.* **1996**, 100, 7135.

107. Dharmawardana, U. R.; Christian, S. R.; Tucker, E. E.; Taylor, R. W.; Scamehorn, J. F. *Langmuir* **1993**, 9, 2258.

108. Benesi, H.; Hildebrand, H. *J. Am. Chem. Soc.* **1949**, 71, 2703.

109. Loukas, Y. L. *J. Pharm. Pharmacol.* **1997**, 49, 944.

110. Loukas, Y. L. *J. Phys. Chem B* **1997**, 101, 4863.

111. Satake, I.; Ikenoue, T.; Takeshita, T.; Katumitu, H.; Maeda, T. *Bull. Chem. Soc. Jpn.* **1985**, 58, 2746.

112. Palepu, R.; Reinsborough, V. C. *Can. J. Chem.* **1988**, 66, 325, b) Palepu, R.; Richardson, J. M.; Reinsborough, V. C. *Langmuir* **1989**, 5, 218, and c) Palepu, R.; Reinsborough, V. C. *Can. J. Chem.* **1989**, 67, 1550.

113. G. Qing-Xiang, L. Zi-Zhang, R. Tan, Z. Xiao-Qing, and L. You-Cheng. *J. Inclusion Phenom. Mol. Recog. Chem.* **1994**, 17, 149.

114. Sasaki, K. J.; Christian, S. D.; Tucker, E. E. *J. Colloid Interface Sci.* **1990**, 134, 412.

115. Park, J. W.; Song, H. J. *J. Phys. Chem.* **1989**, 93, 6454.

116. Wan Yunus, W. M. Z.; Taylor, J; Bloor, D. M.; Hall, D. G.; Wyn-Jones, E. *J. Phys. Chem.* **1992**, 96, 8979.

117. Okubu, T.; Kitano, H.; Ise, N. *J. Phys. Chem.* **1976**, 80, 2661.

118. Lu, R.; Hao, J.; Wang, H.; Tong, L. *J. Inclusion Phenom. Mol. Recognit. Chem.* **1997**, 28, 213.

119. González-Gaitano, G.; Crespo, A.; Compostizo, A.; Tardajos, G. *J. Phys. Chem. B* **1997**, 101, 4413.

120. Junquera, E.; Peña, L., Aicart, E. *J. Inclusion Phenom. Mol. Recognit. Chem.* **1996**, 24, 233.

121. Harata, K. *Bull. Chem. Soc. Jpn.* **1976**, 49, 2066.

122. Wang, C. X.; Chen, W. Z.; Tran, V.; Doulliard, R. *Chem. Phys. Lett.* **1996**, 251, 268.

123. Chervenak, M. C. Toone, E. J. *J. Am. Chem. Soc.* **1994**, 116, 10533.

124. Smithrud, D. B.; Wyman, T. B.; Diederich, F. *J. Am. Chem. Soc.* **1991**, 113, 5420.

125. Amato, M. E.; Lipkowitz, K. B.; Lombardo, G. M.; Pappolard, G. C. *J. Chem. Soc. Perkins Trans 2* **1995**, 325.

126. Sharon, N.; Lis, H. *Sci. Am.* **1993**, 82.

127. a) Galema, S. A.; Høiland, H. *J. Phys. Chem.* **1991**, 95, 5321. b) Galema, S. A.; Blandamer, M. J.; Engberts, J. F. B. N. *J. Org. Chem.* **1992**, 57, 1995. c) Galema, S. A.; Engberts, J. F. B. N., Høiland, H.; Førland, G. M. *J. Phys. Chem.* **1993**, 97, 6885.

128. a) Jiménez-Barbero, J.; Junquera, E.; Martín-Pastor, M.; Sharma, S.; Vincent, C.; Penadés, S. *J. Am. Chem. Soc.* **1995**, 117, 11198. b) Junquera, E. Laynez, J.; Ménendez, M.; Sharma, S.; Renadés, S. *J. Org. Chem.* **1996**, 61, 6790.

129. Jobe, D. J.; Verrall, R. E.; Reinsborough, V. C. *Can. J. Chem.* **1990**, 68, 2131.

130. Spencer, J. N.; Mihalick, J. E.; Paul, I. M. Petigara, B.; Wu, Z.; Chen, S.; Yader C. H. *J. Solution Chem.* 1996, 25, 747.

131. Klein, C. T.; Köller, G.; Mayer, B.; Mraz, K. Reiter. S.; Vierstein, H.; Wolschann, P. *J. Inclusion Phenom. Mol. Recognit. Chem.* **1995**, 22, 15.

132. Gerasimowicz, W.; Wojcik, J. *Bioorg. Chem.* **1982**, 10, 388.

133. Parsegian, V. A.; Rand, R. P.; Rau, D. C. *Methods Enzymol.* **1995**, 259, 43.

134. Buvari, Á.; Szejtli, J.; Barcza, L. *J. Inclusion Phenom. Mol. Recognit. Chem.* **1983**, 1, 151.

135. Mortelarro, M. A.; Nocera, D. G. *Chemtech* **1996**, 17.

136. Ortstan, A.; Ross, J. B. A. *J. Am. Chem. Soc.* **1987**, 91, 2739.

137. Ramadan, M.; Evans, D. F.; Lumry, R. *J. Phys. Chem.* **1983**, 87, 4583.

138. Harrison, J. C.; Eftink, M. R. *Biopolymers* **1982**, 21, 1153.

139. Janado, M.; Yano, Y.; Umura, M.; Kondo, Y. *J. Solution Chem.* **1995**, 24, 587.

140. Junquera, E.; Aicart., E. *J. Phys. Chem. B* **1997**, 101, 7163.

141. Hill, T. L. *In* Cooperativity Theory in Biochemistry: Steady-State and Equilibrium, Ed. Rich, A., Springer: New York, 1985, Chapter 4.

142. Petter, R. C.; Salek, J. S.; Sikorski, C. T.; Kumaravel, G.; Lin, F. T. *J. Am. Chem. Soc.* **1990**, 112, 3800.

143. Bellanger, N.; Perly, B. *J. Mol. Structure* **1992**, 273, 215.

144. Tabushi, I.; Shimizu, N.; Sugimoto, T.; Shiozuka, M.; Yamamura, K. *J. Am. Chem. Soc.* **1977**, 79, 7100.

145. Smith, P. E.; van Gunsteren, W. F. *J. Phys. Chem.* **1994**, 98, 13735.

146. Irwin, P. L.; King, G.; Hicks, K. B. *Carbohydr. Res.* **1996**, 282, 65.

147. Grunwald, E. *J. Am. Chem. Soc.* **1986**, 108, 5726.

148. Ben-Naim, A. *Biopolymers* **1975**, 24, 813.

149. a) Lumry, R.; Frank, H. S. *Proc. 6th Int. Biophysics Congress* **1978**, VII-30, 554. b) Lumry, R.; Rajender, S. Biopolymers **1970**, 9, 1125. c) Lumry, R. *In* Bioenergetics and Thermodynamics: Model Systems, Ed. Bráibanti, A., Reidel: Dordrecht, 1980, 405.

150. a) Nilsson, S. O.; Wadsö, J. *J. Chem. Thermodyn.* **1986**, 18, 673. b) Hallén, D.; Schön, A.; Schehatta, I.; Wadsö, J. *J. Chem. Soc. Far. Trans* **1992**, 88, 2859.

151. Lee, B. *Biopolymers* **1985**, 24, 813.

152. a) Ravey, J. C.; Stébé, M. *Coll. Surf. A: Physicochem. Eng. Aspects* **1994**, 84, 11, and references cited therein and b) Mukerjee, P. *Coll. Surf. A: Physicochem. Eng. Aspects* **1994**, 84, 1.

153. Przbylski, M.; Glocker, M. O. *Angew. Chem. Int. Ed. Engl.* **1996**, 35, 806.

154. Stoll, S.; Buffle, J. *Chimia* **1995**, 49, 300.

155. Ivanov, P. M.; Jaime, C. *J. Mol. Structure* **1996**, 377, 137.

156. Mayer, B.; Marconi, G.; Klein, C.; Köhler, G.; Wolschann, P. *J. Inclusion Phenom. Mol. Recognit. Chem.* **1997**, 29, 79.

157. a) Imata, H.; Kubota, K., Hattori, K.; Aoyagi, M.; Jindoh, C. *Polymer Journal* **1997**, 29, 563. b) Kubik, S.; Wulff, G. *Macromol. Chem. Phys.* **1994**, 195, 1719.

158. Mortimer, R. G. *In* Mathematics for Physical Chemistry, Macmillan: New York, 1981.

159. Parker, O. J.; Breneman, G. L. *In* Spreadsheet Chemistry, Prentice Hall, New Jersey, 1991, pp. 274-277.

160. Emsley, J. W.; Feeney, J.; Sutcliffe, L. H. *In* Progress in Nuclear Magnetic Resonance Spectroscopy; Pergamon Press: New York, 1971; vol. 7.

161. J. B. Lambert, H. F. Shurvell, D. Lightner, R. G. Cooks *In* Introduction to Organic Spectroscopy. Macmillan Pub. Co., New York, 1987, Chapter 3.

162. de Dios, A. C.; Jameson, C. J. *Ann. Rep. NMR Spectrosc.* **1994**, 29, 1.

163. Brereton, I. M.; Spotswood, T. M.; Lincoln, S. F.; Williams, E. H. *J. Chem. Soc. Far. Trans I* **1984**, 80, 3147.

164. Vikingstad, E. *In* Aggregation Processes in Solution; Eds. Wyn-Jones, E. and Gormally J.; Elsevier: New York, 1983, Vol. 26, Chapter 4.

165. Skoog, D. A.; West, D. M.; Holler, J. F. *In* Fundamentals of Analytical Chemistry; Saunders: New York, 1988; 5th ed., 349.

166. Kharakoz, D. P. *J. Solution Chem.* **1992**, 21, 569.

167. Young, T. F.; Smith, M. B. *J. Phys. Chem.* **1954**, 58, 716.

168. Høiland, H.; Ringseth, J. A.; Vikingstad, E. *J. Solution. Chem.* **1978**, 7, 515.

169. Rusling, J. F.; Kumosinski, T. F. *In* Nonlinear Computer Modeling of Chemical and Biochemical Data, Academic Press: New York, 1996, pp. 7-73.

170. a) Marquardt, D. *J. Soc. Ind. Appl. Math.* **1963**, 2, 431. b) Bates, D. M.; Watts, D. G. *In* Nonlinear Regression Analysis and its Applications, Wiley: New York, 1988, pp. 1-30.

171. Wyman, J. *In* Linked Functions and Reciprocal Effects in Hemoglobin, Advances in Protein Chemistry 1964, 19, pp. 223-286.

172. a) Sigmaplot® V. 2.0 Jandel Corporation, 1986-1994. b) Axum® V. 4.0 Trimetrix Inc., 1994, c) Quattro® V. 3.0 Borland International, 1987.

173. Saint Aman, E.; Servé, D. J. *J. Colloid Interface Sci.* **1990**, 138, 365.

174. Braun, A. M.; Krieg, M.; Turro, N. J.; Aikawa, M.; Gould, I. R.; Graf, G. A.; Lee, P. C. C. *J. Am. Chem. Soc.* **1981**, 103, 7312.

175. Muller, N.; Simsohn, H. *J. Phys. Chem.* **1971**, 75, 942.

176. Clapperton, R. M.; Ottewill, R. H.; Ingram, B. T. *Langmuir* **1994**, 10, 51.

177. Picker, P.; Tremblay, E.; Jolicoeur, C. *J. Solution Chem.* **1974**, 3, 377.

178. Kratky, O.; Leopold, H.; Stabinger, H. *Angew. Phys.* **1969**, 27, 273.

179. Kell, G. S. *J. Chem. Eng. Data* **1967**, 12, 66.

180. CRC Handbook of Chemistry and Physics; Weast, R. C., Ed.; CRC Press: Cleveland Ohio, 54th ed., 1973.

181. Buvári, Á.; Barcza, L.; Kajtár, M. *J. Chem. Soc. Perkin Trans. II* **1988**, 1627.

182. Henne, A. L.; Fox, C. J. *J. Am. Chem. Soc.* 73, 2323 (1951).

183. Schreck, J. O. *In* Organic Chemistry: Concepts and Applications; Mosby: Saint Louis, 1975, pp.237.

184. Deranlau, D. A. *J. Am. Chem. Soc.* **1969**, 91, 4044.

185. R. I. Gelb, L. M. Schwartz *J. Inclusion Phenom. Mol. Recog. Chem.* **1989**, 7, 465.

186. E. Saint Aman, D. Serve *J. Colloid Interface Sci.* **1990**, 138, 365.

187. R. Palepu, J. E. Richardson *Langmuir* **1989**, 5, 218.

188. Vikingstad, E.; Skauge, A.; Høiland, H. *J. Colloid Interface Sci.* **1978**, 66(2), 240.

189. Milioto, S.; Cristantino, R.; De Lisi, R.; Inglese, A. *Langmuir* **1995**, 11, 718.

190. Tamaki, K.; Watanabe, S.; Daikoji, Y. *Bull. Chem. Soc. Jpn.* **1990**, 63, 3681.

191. Johnson, I.; Olofsson, G. *J. Chem. Soc. Far. Trans. I* **1988**, 84(2), 551.

192. Perron, G.; Desnoyers, J. E. *J. Chem. Eng. Data* **1997**, 42, 172.

193. Milioto, S.; Bakshi, M. S.; Cristantino, R.; Delisi, R. *J. Solution Chem.* **1995**, 24, 103.

194. Paduano, L.; Sartorio, R.; Vitagliano, V.; Constantino, L. *J. Solution Chem.* **1990**, 19, 31.

195. Sasaki, K. J.; Christian, S. D.; Tucker, E. E. *Fluid Phase Equilibria* **1989**, 49, 281.

196. Gray. J. E.; MacLean, S. A.; Reinsborough, V. C. *Aust. J. Chem.* **1995**, 48, 551.

197. Tan, Z. J.; Zhu, X. X.; Brown, G. R. *Langmuir* **1994**, 10, 1034.

198. Casu, B.; Grenni, A.; Naggi, A.; Torri, G. T.; Virtuani, M.; Focher, B. *Carbohydr. Res.* **1990**, 200, 101.

199. Watanabe, M.; Nakamura, H.; Matsuo, T. *Bull. Chem. Soc. Jpn.* **1992**, 65, 164.

200. Rekharsky, M. V.; Mayhew, M. P.; Goldberg, R. N.; Ross, P. D.; Yamashoji, Y.; Inoue, Y. *J. Phys. Chem. B* **1997**, 101, 87.

201. Lu, R.; Hao, J.; Wang, H.; Tong, L. *J. Inclusion Phenom. Mol. Recognit. Chem.* **1997**, 28, 213.

202. Castronuovo, G.; Elia, V.; Fessas, D.; Velleca, F.; Viscardi, G. *Carbohydr. Res.* **1996**, 287, 127.

203. F. W. Lichtenthaler, and S. Immel. Liebigs Ann. **1996**, 27.

204. Bergeron, R. J.; Channing, M. A.; McGovern, K. A.; Roberts, W. P. *Bioorg. Chem.* **1979**, 8, 263.

205. Lin, J.; Djedaïni,-Pilard, F.; Guenot, P.; Perly, B. *Supramol. Chem.* **1996**, 7, 175.

206. Tee, O. S.; Gadosy, T. A.; Giorgi, J. B. *J. Chem. Soc. Perkin Trans 2* **1993**, 1705.

207. Harata, A.; Li, J.; Kamachi, M.; Kitagawa, Y.; Katsube, Y. *Carbohydr. Res.* 1998, 305, 127.

208. Davies, D. M.; Deary, M. E. *J. Chem. Soc. Perkin Trans 2* **1995**, 1287.

209. a) Palepu, R.; Richardson, J. M.; Reinsborough, V. C. *Langmuir* **1989**, 5, 218 and b) Palepu, R.; Reinsborough, V. C. *Can. J. Chem.* **1989**, 67, 1550.

210. Junquera, E.; Aicart, E.; Tardajos, G. *Langmuir* **1993,** 9, 1213.

211. Silverstein, R. M.; Basssler, G. C.; Morrill, T. C. *In* Spectrometric Identification of Organic Compounds, 5th ed.; Wiley: New York, 1991, 174.

212. Luck, L. A.; Mason, A. B.; Savage, K. J.; MacGillivray, R. T. A.; Woodworth, R. G. *Magn. Reson. Chem.* **1997**, 35, 477.

213. a) Yang, L.; Takisawa, N.; Kaikawa, T.; Shirahama, K. *Coll. Polym. Sci.* **1997**, 275, 486.

214. Smith, V. K.; Ndou, T. T.; De la Peña, A. M.; Warner, I. M. *J. Inclusion Phenom. Mol. Recognit. Chem.* **1991**, 10, 471.

215. Saito, Y.; Abe, M.; Sato, T.; Scamehorn, J. F.; Christian, S. D. *Coll. Surf. A: Physicochem. Eng. Aspects* **1996**, 119, 149.

216. Riess, J. G. *Coll. Surf. A: Physicochem. Eng. Aspects* **1994**, 84, 33.

217. Chidsey, C. E. D. *Langmuir* **1990**, 6, 682.

218. a) Ortona, O.; Paduano, L.; Constantino, L.; Vitigliano, V. *J. Molecular Liquids* **1995**, 63, 291, b) Bakshi, M. S. *J. Solution Chem.* **1996**, 25,(4), 411, c) Bakshi, M. S. *Indian J. Chem. Sect. A.* **1996**, 35(6), 499, d) Tamaki, K.; Watanabe, S.; Daikoji, Y. *Bull. Chem. Soc. Jpn.* **1990**, 63, 3681, e) Bakshi, M. S. *Indian J. Chem. Sect. A* **1997**, 36, 931, f) Hersey, A.; Robinson, H.; Kelly, H. C. *J. Chem. Soc. Far. Trans I* **1986**, 82, 1271, g) Miyajima, K.; Sawada, M.; Nagaki, M. *Bull. Chem. Soc. Jpn.* **1983**, 56, 3556, h) Nomura, H.; Koda, S.; Miyahara, Y. *In* Studies in Physical and Theoretical Chemistry Eds.; Tanaka, N.; Ohtaki, H.; Tamamushi, R., Elsevier: Amsterdam, 1982, vol. 27, pp.

151, i) Shahidi, F.; Farrell, P. G.; Edward, J. T. *J. Solution Chem.* **1976**, 5, 807, j) Gonz lez-Gaitano, G.; Crespo, A.; Compostizo, A.; Tardajos, G. *J. Phys. Chem. B* **1997**, 101, 4413, and k) Delitalia, C.; Marongiu, B.; Pittau, B.; Porcedda, S. *Fluid Phase Equilibria* **1996**, 126, 257.

219. a) Junquera, E.; Peña, L.; Aicart, E. *Langmuir* **1995**, 11, 4685, and b) Peña, L.; Junquera, E.; Aicart, E. *J. Solution Chem.* **1995**, 24, 1075.

220. Du, Q.; Arteca, G. A. *J. Comp. Mol. Des.* **1996**, 10, 133.

221. Jung, J. H.; Takehisa, C.; Sakata, Y.; Kaneda, T. *Chem. Lett.* **1996**, 147.

222. MacPherson, Y. E. Palepu, R.; Reinsborough, V. C. *J. Inclusion Phenom. Mol. Recognit. Chem.* **1990**, 9, 137.

223. Barone, G. *Thermochim. Acta* **1990**, 162, 17.

224. Gianni, P.; Lepori, L. *J. Solution Chem.* **1996**, 25, 1.

225. Jobe, D. J.; Reinsborough, V. C.; Wetmore, S. D. *Langmuir* **1995**, 11, 2476.

226. Fisher, C. H. *J. Amer. Oil Chem. Soc.* **1995**, 72, 681.

227. Huheey, J. E. *In* Inorganic Chemistry: Principles of Structure and Reactivity; 3rd ed., Harper and Row: New York, 1983, pp. 258.

228. Linder, K.; Saenger, W. *Angew. Chem. Int. Ed. Engl.* **1978**, 17(9), 694.

229. Buvári, Á.; Barcza, L. *Inorg. Chim. Acta* **1979**, 33, L179.

230. Schuette, J. M.; Warner, I. M. *Anal. Lett.* **1994**, 27(6), 1175.

231. Müller, B. W.; Brauns, U. *J. Pharm. Sci.* **1986**, 75, 571. b) Rao, C. T.; Pitha, J.; Lindberg, B.; Lindberg, J. *Carbohydr. Res.* **1992**, 223, 99, and c) Buvári-Baccza, Á, Kajtár, J.; Szente, L.; Barcza, L. *J. Chem. Soc. Perkin Trans. 2* **1996**, 489.

232. CRC Handbook of Chemistry and Physics; Lide, D. R., Ed.; CRC Press: Cleveland Ohio, 76th ed., 1995-96, pp. 10-199 to 10-201.

233. Wiseman, T.; Williston, S.; Brandts, J. F.; Lin, L. *Anal. Biochem.* **1989**, 179, 131.

234. Shinoda, K. *J. Phys. Chem.* **1976**, 80, 2468.

235. a) Ben-Naim, A. *Biopolymers* **1975**, 14, 1337, b) Grunwald, E. *J. Am. Chem. Soc.* **1984**, 106, 5414, and c) Yu, A.-A.; Karplus, M. *J. Chem. Phys.* **1988**, 89, 2366.

236. Lee, B. *Biophys. Chem.* **1994**, 51, 271.

9. Appendices

APPENDIX A1

Table A-1: ^{1}H NMR Chemical Shifts for $C(1)H_2$, $C(2)H_2$, and CH_3 Nuclei of the Sodium Alkyl Carboxylates of Various Cyclodextrin-Surfactant Systems at 295 K.[a]

C_{CD}	$C(1)H_2$	$C(2)H_2$	CH_3	C_{CD}	$C(1)H_2$	$C(2)H_2$	CH_3
			α-CD-SHex System, SHex=4.942×10^{-3} M				
0.000	2.161	1.542	0.865	10.815	2.214	1.651	0.937
2.270	2.179	1.577	0.890	11.827	2.217	1.653	0.939
4.086	2.191	1.601	0.906	12.646	2.217	1.657	0.941
5.571	2.198	1.619	0.916	13.323	2.220	1.658	0.943
6.810	2.203	1.630	0.923	13.891	2.219	1.658	0.943
7.857	2.207	1.636	0.927	14.793	2.219	1.660	0.944
8.755	2.210	1.638	0.931	15.476	2.221	1.660	0.946
9.533	2.212	1.645	0.934	15.759	2.220	1.664	0.947
10.214	2.214	1.647	0.936				
			β-CD-SHex System, SHex=3.751×10^{-3} M				
0.000	2.160	1.539	0.863	1.750	2.165	1.546	0.868
0.417	2.160	1.539	0.865	1.986	2.164	1.544	0.869
0.750	2.160	1.542	0.866	2.172	2.164	1.549	0.868
1.023	2.161	1.542	0.867	2.322	2.166	1.546	0.869
1.250	2.163	1.542	0.867	2.446	2.164	1.549	0.870
1.443	2.162	1.543	0.867	2.501	2.163	1.548	0.869
1.607	2.162	1.546	0.868				
			DM-β-CD-Hex System, SHex=4.942×10^{-3} M				
0.000	2.162	1.542	0.865	10.291	2.158	1.542	0.866
2.160	2.160	1.541	0.865	11.254	2.158	1.542	0.867
3.888	2.160	1.541	0.865	12.034	2.158	1.542	0.867
5.302	2.159	1.541	0.865	12.678	2.157	1.542	0.867
6.480	2.158	1.541	0.865	13.219	2.157	1.542	0.867
7.477	2.158	1.541	0.866	14.077	2.157	1.542	0.867
8.331	2.158	1.541	0.866	14.727	2.157	1.542	0.867
9.072	2.158	1.542	0.866	15.213	2.157	1.542	0.867
9.720	2.158	1.542	0.866				

Table A-1: continued

C_{CD}	$C(1)H_2$	$C(2)H_2$	CH_3	C_{CD}	$C(1)H_2$	$C(2)H_2$	CH_3
			TM-β-CD-Hex System, SHex=4.942×10^{-3} M				
0.000	2.162	1.543	0.865	10.021	2.161	1.542	0.868
2.103	2.162	1.542	0.866	10.959	2.161	1.543	0.869
3.786	2.161	1.541	0.867	11.718	2.161	1.543	0.869
5.162	2.161	1.542	0.867	12.345	2.160	1.542	0.869
6.309	2.162	1.542	0.867	12.871	2.160	1.543	0.869
7.280	2.161	1.541	0.868	13.707	2.160	1.542	0.869
8.112	2.162	1.543	0.868	14.340	2.161	1.543	0.869
8.833	2.161	1.542	0.868	14.836	2.160	1.544	0.870
9.464	2.161	1.542	0.868				
			HP-β-CD-Hex System, SHex=4.942×10^{-3} M				
0.000	2.182	1.542	0.841	9.687	2.159	1.546	0.876
2.033	2.162	1.542	0.866	10.594	2.158	1.548	0.877
3.660	2.161	1.544	0.870	11.328	2.156	1.544	0.875
4.990	2.160	1.542	0.872	11.934	2.156	1.545	0.876
6.099	2.159	1.544	0.871	12.443	2.156	1.544	0.876
7.038	2.157	1.544	0.873	13.250	2.155	1.545	0.877
7.842	2.156	1.543	0.873	13.862	2.155	1.548	0.877
8.539	2.157	1.546	0.873	14.232	2.155	1.545	0.878
9.149	2.157	1.546	0.874				
			α-CD-SO System, SO=5.235×10^{-3} M				
0.000	2.162	1.536	0.853	10.368	2.192	1.604	0.924
2.176	2.174	1.558	0.879	11.339	2.194	1.605	0.927
3.917	2.182	1.578	0.896	12.124	2.193	1.609	0.929
5.341	2.186	1.585	0.906	12.773	2.193	1.614	0.929
6.528	2.188	1.590	0.913	13.318	2.195	1.609	0.930
7.533	2.189	1.597	0.916	13.782	2.193	1.616	0.930
8.394	2.192	1.598	0.919	14.531	2.194	1.617	0.931
9.140	2.193	1.600	0.922	15.108	2.202	1.620	0.940
9.792	2.193	1.609	0.924				
			β-CD-SO System, SO=4.942×10^{-3} M				
0.000	2.161	1.532	0.853	2.040	2.172	1.552	0.872
0.486	2.167	1.535	0.858	2.314	2.171	1.552	0.876
0.874	2.170	1.539	0.862	2.531	2.174	1.552	0.875
1.192	2.172	1.540	0.867	2.706	2.178	1.556	0.875
1.457	2.170	1.549	0.868	2.851	2.177	1.558	0.877
1.681	2.170	1.552	0.871	2.973	2.173	1.555	0.875
1.873	2.173	1.552	0.872	3.026	2.176	1.558	0.878

Table A-1: continued

C_{CD}	$C(1)H_2$	$C(2)H_2$	CH_3	C_{CD}	$C(1)H_2$	$C(2)H_2$	CH_3
			DM-β-CD-SO System, SO=5.234×10^{-3} M				
0.000	2.160	1.532	0.852	10.045	2.151	1.528	0.882
2.108	2.156	1.529	0.862	10.984	2.152	1.525	0.884
3.795	2.153	1.536	0.869	11.745	2.151	1.522	0.885
5.175	2.153	1.528	0.873	12.374	2.150	1.527	0.886
6.324	2.152	1.528	0.877	12.902	2.151	1.527	0.885
7.297	2.151	1.532	0.878	13.352	2.149	1.522	0.886
8.131	2.150	1.523	0.880	14.077	2.150	1.522	0.887
8.854	2.152	1.531	0.881	14.636	2.150	1.522	0.887
9.487	2.151	1.526	0.882				
			TM-β-CD-SO system, SO=5.234×10^{-3} M				
0.000	2.162	1.535	0.854	9.538	2.154	1.540	0.889
2.002	2.161	1.539	0.864	10.431	2.153	1.544	0.891
3.603	2.159	1.539	0.870	11.153	2.153	1.543	0.892
4.914	2.158	1.540	0.875	11.750	2.152	1.542	0.895
6.006	2.157	1.540	0.878	12.251	2.152	1.543	0.895
6.929	2.155	1.542	0.883	12.678	2.153	1.543	0.896
7.721	2.152	1.541	0.881	13.367	2.150	1.547	0.897
8.408	2.153	1.540	0.886	13.899	2.148	1.545	0.896
9.008	2.154	1.539	0.888				
			HP-β-CD-SO System, SO=5.234×10^{-3} M				
0.000	2.158	1.531	0.850	9.761	2.154	1.541	0.907
2.049	2.161	1.539	0.871	10.674	2.153	1.541	0.909
3.687	2.158	1.539	0.882	11.413	2.152	1.538	0.909
5.028	2.157	1.541	0.890	12.024	2.148	1.535	0.910
6.146	2.157	1.540	0.895	12.537	2.153	1.541	0.911
7.091	2.156	1.541	0.899	12.974	2.152	1.540	0.912
7.902	2.156	1.542	0.902	13.679	2.151	1.539	0.912
8.604	2.155	1.538	0.903	14.223	2.154	1.538	0.914
9.218	2.156	1.539	0.905				

Table A-1: continued

C_{CD}	$C(1)H_2$	$C(2)H_2$	CH_3	C_{CD}	$C(1)H_2$	$C(2)H_2$	CH_3
			α-CD-SDec System, SDec=5.819×10^{-3} M				
0.000	2.169	1.543	0.864	6.711	2.169	1.574	0.927
1.409	2.168	1.544	0.869	7.339	2.163	1.582	0.932
2.535	2.173	1.551	0.883	7.848	2.159	1.581	0.936
3.457	2.175	1.552	0.893	8.268	2.155	1.588	0.937
4.226	2.177	1.561	0.903	8.620	2.152	1.585	0.941
4.876	2.176	1.561	0.909	8.921	2.151	1.587	0.943
5.433	2.174	1.566	0.915	9.406	2.154	1.596	0.950
5.916	2.174	1.576	0.920	9.779	2.141	1.598	0.948
6.338	2.168	1.573	0.923				
			β-CD-SDec System, SDec=5.896×10^{-3} M				
0.000	2.163	1.536	0.854	5.948	2.170	1.541	0.915
1.248	2.166	1.538	0.862	6.504	2.170	1.538	0.918
2.247	2.167	1.540	0.872	6.955	2.169	1.538	0.921
3.064	2.169	1.540	0.882	7.327	2.169	1.534	0.921
3.745	2.169	1.541	0.891	7.639	2.169	1.538	0.923
4.321	2.168	1.539	0.896	7.906	2.168	1.535	0.924
4.815	2.170	1.537	0.903	8.335	2.169	1.533	0.924
5.243	2.169	1.537	0.908	8.667	2.170	1.535	0.928
5.617	2.169	1.540	0.913				
			DM-β-CD-SDec system, SDec=5.819×10^{-3} M				
0.000	2.159	1.534	0.851	8.607	2.167	1.543	0.915
1.806	2.161	1.534	0.871	9.412	2.166	1.541	0.916
3.251	2.164	1.536	0.888	10.064	2.168	1.542	0.916
4.434	2.163	1.537	0.897	10.603	2.167	1.539	0.916
5.419	2.165	1.541	0.905	11.055	2.168	1.540	0.917
6.253	2.167	1.538	0.910	11.440	2.169	1.541	0.917
6.967	2.167	1.537	0.912	12.062	2.168	1.541	0.917
7.587	2.165	1.534	0.913	12.541	2.168	1.535	0.917
8.129	2.165	1.539	0.914				

Table A-1: continued

C_{CD}	$C(1)H_2$	$C(2)H_2$	CH_3	C_{CD}	$C(1)H_2$	$C(2)H_2$	CH_3
			TM-β-CD-SDec System, SDec=5.819×10^{-3} M				
0.000	2.163	1.537	0.854	7.389	2.146	1.535	0.922
1.551	2.158	1.537	0.873	8.080	2.145	1.532	0.925
2.791	2.154	1.536	0.887	8.640	2.144	1.531	0.927
3.806	2.152	1.535	0.897	9.102	2.143	1.535	0.929
4.652	2.150	1.536	0.905	9.491	2.144	1.538	0.931
5.368	2.150	1.533	0.909	9.821	2.143	1.531	0.932
5.981	2.144	1.536	0.911	10.355	2.142	1.532	0.932
6.513	2.147	1.539	0.918	10.767	2.143	1.534	0.933
6.978	2.146	1.531	0.920				
			HP-β-CD-SDec System, SDec=5.819×10^{-3} M				
0.000	2.162	1.535	0.853	8.081	2.156	1.540	0.918
1.696	2.161	1.534	0.871	8.837	2.158	1.528	0.919
3.053	2.160	1.535	0.888	9.450	2.157	1.534	0.921
4.163	2.159	1.537	0.896	9.955	2.156	1.534	0.920
5.088	2.159	1.534	0.904	10.380	2.156	1.536	0.922
5.871	2.159	1.536	0.910	10.742	2.156	1.534	0.921
6.542	2.160	1.538	0.913	11.325	2.159	1.534	0.923
7.124	2.156	1.532	0.915	11.776	2.158	1.536	0.921
7.632	2.156	1.531	0.916				
			α-CD-SDodec System, SDodec=5.066×10^{-3} M				
0.000	2.160	1.529	0.848	5.681	2.170	1.548	0.919
1.192	2.166	1.543	0.866	6.212	2.167	1.548	0.924
2.146	2.171	1.544	0.881	6.643	2.161	1.539	0.925
2.927	2.174	1.553	0.891	6.998	2.155	1.531	0.927
3.577	2.177	1.555	0.900	7.297	2.155	1.534	0.930
4.127	2.177	1.559	0.905	7.770	2.150	1.528	0.931
4.599	2.177	1.561	0.911	8.129	2.146	1.529	0.933
5.008	2.174	1.560	0.914	8.346	2.144	1.524	0.931
5.365	2.173	1.548	0.917				

Table A-1: continued

C_{CD}	$C(1)H_2$	$C(2)H_2$	CH_3	C_{CD}	$C(1)H_2$	$C(2)H_2$	CH_3
			β-CD-SDodec System, SDodec=5.011×10^{-3} M				
0.000	2.160	1.534	0.854	5.921	2.190	1.561	0.944
1.243	2.166	1.534	0.869	6.475	2.192	1.552	0.948
2.237	2.173	1.546	0.883	6.923	2.190	1.555	0.949
3.050	2.177	1.551	0.903	7.294	2.190	1.556	0.950
3.728	2.181	1.552	0.912	7.605	2.191	1.558	0.951
4.301	2.186	1.555	0.924	7.870	2.189	1.552	0.950
4.793	2.187	1.554	0.933	8.098	2.188	1.557	0.950
5.219	2.190	1.559	0.940	8.201	2.190	1.559	0.950
			DM-β-CD-SDodec System, SDodec=5.066×10^{-3} M				
0.000	2.159	1.531	0.852	6.467	2.181	1.567	0.940
1.357	2.169	1.545	0.879	7.073	2.182	1.562	0.940
2.443	2.173	1.548	0.899	7.563	2.182	1.563	0.942
3.332	2.176	1.554	0.913	7.967	2.182	1.570	0.941
4.072	2.178	1.560	0.926	8.307	2.182	1.564	0.941
4.699	2.182	1.563	0.933	8.846	2.182	1.563	0.941
5.236	2.182	1.567	0.937	9.255	2.182	1.568	0.941
5.701	2.183	1.565	0.939	9.502	2.181	1.567	0.941
6.108	2.185	1.569	0.941				
			TM-β-CD-SDodec System, SDodec=5.066×10^{-3} M				
0.000	2.161	1.534	0.853	5.492	2.161	1.543	0.928
1.153	2.159	1.536	0.875	6.006	2.162	1.548	0.931
2.075	2.157	1.539	0.889	6.422	2.161	1.543	0.934
2.829	2.157	1.538	0.900	6.766	2.160	1.551	0.933
3.458	2.161	1.548	0.911	7.055	2.161	1.549	0.936
3.990	2.159	1.545	0.917	7.513	2.161	1.546	0.936
4.446	2.161	1.544	0.922	7.859	2.161	1.549	0.936
4.841	2.161	1.551	0.925	8.069	2.162	1.549	0.938
5.187	2.161	1.546	0.926				

Table A-1: continued

C_{CD}	$C(1)H_2$	$C(2)H_2$	CH_3	C_{CD}	$C(1)H_2$	$C(2)H_2$	CH_3
			HP-β-CD-SDodec System, SDodec=5.066×10^{-3} M				
0.000	2.159	1.529	0.851	4.708	2.165	1.537	0.912
0.988	2.160	1.533	0.866	5.148	2.164	1.539	0.913
1.778	2.161	1.535	0.877	5.505	2.167	1.545	0.916
2.425	2.163	1.536	0.886	5.799	2.167	1.542	0.917
2.964	2.163	1.536	0.893	6.047	2.168	1.543	0.919
3.420	2.163	1.535	0.898	6.439	2.169	1.538	0.920
3.811	2.166	1.538	0.903	6.736	2.168	1.547	0.921
4.150	2.165	1.538	0.906	6.916	2.167	1.541	0.921
4.446	2.167	1.539	0.910				
			α-CD-ST System, ST=5.525×10^{-4} M				
0.000	2.159	1.531	0.854	0.432	2.176	1.553	0.913
0.103	2.174	1.551	0.874	0.490	2.175	1.565	0.907
0.185	2.179	1.549	0.885	0.536	2.165	1.546	0.912
0.252	2.189	1.549	0.897	0.573	2.168	1.544	0.908
0.308	2.185	1.541	0.901	0.603	2.167	1.563	0.911
0.356	2.181	1.534	0.905	0.629	2.165	1.553	0.907
			β-CD-ST System, ST=5.011×10^{-3} M				
0.000	2.137	1.509	0.830	3.765	2.174	1.549	0.921
0.389	2.146	1.520	0.843	4.607	2.177	1.555	0.939
1.254	2.152	1.531	0.858	5.264	2.174	1.554	0.943
1.668	2.155	1.533	0.866	5.430	2.175	1.556	0.943
2.240	2.162	1.541	0.883	7.001	2.161	1.547	0.936
3.320	2.171	1.546	0.913	11.967	2.134	1.522	0.917
3.342	2.168	1.545	0.908				
			DM-β-CD-ST System, ST=4.742×10^{-4} M				
0.000	2.160	1.534	0.852	0.635	2.176	1.560	0.930
0.141	2.167	1.545	0.882	0.672	2.188	1.551	0.929
0.254	2.171	1.558	0.910	0.735	2.177	1.580	0.926
0.346	2.179	1.564	0.921	0.786	2.183	1.571	0.927
0.423	2.181	1.561	0.915	0.828	2.177	1.554	0.925
0.489	2.181	1.574	0.927	0.864	2.188	1.595	0.930
0.544	2.178	1.593	0.933	0.920	2.178	1.551	0.926
0.593	2.218	1.555	0.932	0.962	2.179	1.583	0.929

Table A-1: continued

C_{CD}	$C(1)H_2$	$C(2)H_2$	CH_3	C_{CD}	$C(1)H_2$	$C(2)H_2$	CH_3
			TM-β-CD-ST system, ST=5.525×10^{-4} M				
0.000	2.161	1.530	0.850	0.742	2.158	1.545	0.925
0.150	2.160	1.546	0.874	0.808	2.154	1.538	0.927
0.281	2.161	1.539	0.891	0.868	2.162	1.549	0.929
0.396	2.158	1.541	0.904	1.164	2.147	1.561	0.932
0.497	2.162	1.542	0.913	1.349	2.163	1.544	0.931
0.588	2.157	1.555	0.917	1.492	2.166	1.567	0.935
0.669	2.164	1.544	0.923				
			HP-β-CD-ST System, ST=4.742×10^{-4} M				
0.000	2.133	1.534	0.850	0.684	2.177	1.537	0.912
0.152	2.139	1.536	0.875	0.725	2.168	1.544	0.916
0.274	2.165	1.520	0.888	0.792	2.168	1.536	0.911
0.373	2.140	1.536	0.903	0.847	2.179	1.554	0.915
0.456	2.155	1.536	0.920	0.893	2.174	1.555	0.917
0.526	2.158	1.539	0.912	0.931	2.171	1.551	0.918
0.587	2.172	1.541	0.909	0.991	2.169	1.552	0.912
0.639	2.176	1.539	0.918	1.037	2.176	1.537	0.923

[a]Chemical shifts for $C(1)H_2$, $C(2)H_2$, and CH_3 are in ppm relative to DSS and C_{CD} is in mol $L^{-1}(\times10^3)$.

APPENDIX A2

Table A2: ^{1}H NMR Chemical Shifts of the H(3) and H(5) Nuclei of β-CD of Cyclodextrin-Surfactant Systems at 295 K.[a]

C_S	H(3)	H(5)	C_S	H(3)	H(5)	C_S	H(3)	H(5)
			β-CD-SHex System, β-CD=4.752×10^{-3} M					
0.000	3.961	3.844	8.713	3.941	3.821	12.697	3.936	3.815
2.075	3.954	3.834	9.885	3.939	3.819	13.139	3.936	3.814
3.734	3.950	3.830	10.810	3.938	3.817	13.521	3.936	3.813
5.092	3.948	3.827	11.559	3.937	3.817	13.853	3.936	3.813
7.181	3.944	3.824	12.177	3.937	3.815	14.145	3.935	3.813
			β-CD-SO System, β-CD=4.752×10^{-3} M					
0.000	3.960	3.842	10.269	3.891	3.737	14.963	3.885	3.729
2.445	3.930	3.803	11.649	3.889	3.734	15.485	3.885	3.728
4.401	3.914	3.770	12.739	3.888	3.731	15.934	3.884	3.726
6.001	3.904	3.756	13.622	3.887	3.731	16.326	3.885	3.728
8.463	3.894	3.744	14.351	3.886	3.729	16.670	3.886	3.728
			β-CD-SDec System, β-CD=4.752×10^{-3} M					
0.000	3.960	3.843	5.659	3.879	3.707	8.174	3.875	3.698
1.467	3.935	3.800	6.162	3.878	3.703	8.612	3.874	3.696
2.641	3.916	3.767	6.602	3.876	3.700	8.979	3.874	3.696
3.601	3.900	3.740	6.991	3.876	3.700	9.562	3.875	3.697
4.401	3.888	3.725	7.645	3.875	3.697	10.003	3.873	3.694
5.079	3.884	3.713						
			β-CD-SDodec System, β-CD=4.752×10^{-3} M					
0.000	3.959	3.843	4.745	3.867	3.680	7.456	3.866	3.675
1.294	3.928	3.790	5.338	3.867	3.677	8.045	3.867	3.675
2.372	3.905	3.746	5.861	3.867	3.676	8.541	3.867	3.674
3.285	3.887	3.713	6.326	3.868	3.677	8.962	3.867	3.674
4.067	3.874	3.692	6.743	3.866	3.675			
			β-CD-ST System, β-CD=1.213×10^{-3} M					
0.000	3.964	3.851	1.219	3.896	3.725	1.854	3.877	3.693
0.316	3.941	3.811	1.327	3.892	3.718	1.934	3.878	3.691
0.569	3.926	3.785	1.505	3.886	3.709	2.001	3.878	3.688
0.775	3.915	3.762	1.646	3.884	3.700	2.059	3.878	3.690
0.948	3.908	3.746	1.760	3.880	3.697	2.110	3.877	3.689
1.094	3.902	3.733						

Table A2: continued

C_S	H(3)	H(5)	C_S	H(3)	H(5)	C_S	H(3)	H(5)
			β-CD-SDS system, β-CD=1.051×10^{-2} M					
0.000	3.932	3.815	5.063	3.851	3.704	8.501	3.839	3.655
1.083	3.908	3.791	5.657	3.847	3.695	9.060	3.838	3.649
2.049	3.891	3.766	6.204	3.844	3.686	9.658	3.838	3.644
2.918	3.877	3.746	6.866	3.842	3.674	10.272	3.837	3.638
3.702	3.867	3.731	7.464	3.840	3.667	10.883	3.837	3.634
4.414	3.857	3.717	8.007	3.839	3.661	11.477	3.837	3.632

[a]Chemical shifts for H(3) and H(5) are in ppm relative to DSS and C_S is in mol $L^{-1}(\times10^3)$

APPENDIX A3

Table A3: ^{19}F NMR Chemical Shifts for the Nuclei of the Sodium Perfluoroalkyl Carboxylates of Cyclodextrin-Sodium Perfluoroalkyl Carboxylate Systems at 295 K.

C_{CD}	$C(1)F_2$	$C(2)F_2$	CF_3	C_{CD}	$C(1)F_2$	$C(2)F_2$	CF_3
			α-CD-SPFB System, SPFB=5.494×10^{-3} M				
0.000	-120.181	-129.262	-82.666	5.383	-120.027	-128.960	-82.333
0.767	-120.163	-129.219	-82.618	5.731	-120.018	-128.942	-82.316
1.464	-120.142	-129.180	-82.571	6.058	-120.008	-128.929	-82.299
2.102	-120.121	-129.141	-82.528	6.541	-119.997	-128.903	-82.273
2.687	-120.105	-129.107	-82.493	6.980	-119.986	-128.882	-82.251
3.225	-120.090	-129.076	-82.458	8.690	-119.943	-128.808	-82.173
3.723	-120.073	-129.050	-82.428	9.867	-119.917	-128.765	-82.126
4.183	-120.061	-129.024	-82.402	10.728	-119.900	-128.739	-82.100
4.612	-120.047	-129.003	-82.376	11.384	-119.887	-128.713	-82.074
5.010	-120.034	-128.981	-82.355	11.657	-119.882	-128.705	-82.065
			β-CD-SPFB System, SPFB=6.277×10^{-3} M				
0.000	-120.185	-129.267	-82.670	2.968	-119.805	-129.011	-82.666
0.423	-120.124	-129.228	-82.670	3.270	-119.774	-128.990	-82.666
0.808	-120.073	-129.193	-82.670	3.543	-119.748	-128.973	-82.666
1.159	-120.029	-129.163	-82.670	3.849	-119.714	-128.947	-82.662
1.482	-119.986	-129.137	-82.670	4.174	-119.688	-128.925	-82.662
1.779	-119.947	-129.111	-82.670	5.011	-119.614	-128.877	-82.662
2.053	-119.917	-129.085	-82.670	5.599	-119.571	-128.843	-82.662
2.307	-119.882	-129.063	-82.666	6.034	-119.541	-128.821	-82.657
2.543	-119.852	-129.046	-82.666	6.370	-119.515	-128.804	-82.657
2.763	-119.831	-129.029	-82.666				
			RAMEB-SPFB system, SPFB=5.573×10^{-3} M				
0.000	-120.207	-129.284	-82.683	5.149	-119.498	-128.890	-82.554
0.734	-120.086	-129.223	-82.662	5.483	-119.463	-128.869	-82.549
1.401	-119.982	-129.167	-82.644	5.795	-119.429	-128.852	-82.541
2.011	-119.891	-129.115	-82.627	6.257	-119.385	-128.826	-82.534
2.570	-119.809	-129.068	-82.611	6.677	-119.346	-128.804	-82.528
3.085	-119.740	-129.029	-82.598	8.313	-119.208	-128.722	-82.502
3.561	-119.679	-128.994	-82.588	9.439	-119.122	-128.670	-82.489
4.002	-119.627	-128.964	-82.580	10.262	-119.078	-128.640	-82.480
4.412	-119.580	-128.938	-82.571	10.890	-119.044	-128.618	-82.472
4.793	-119.537	-128.912	-82.562	11.384	-119.027	-128.610	-82.471

Table A3: continued

C_{CD}	$C(1)F_2$	$C(2)F_2$	CF_3	C_{CD}	$C(1)F_2$	$C(2)F_2$	CF_3
			DM-β-CD-SPFB system, SPFB=6.103×10^{-3} M				
0.000	-120.189	-129.271	-82.670	3.892	-119.658	-129.003	-82.662
0.554	-120.107	-129.232	-82.675	4.144	-119.632	-128.986	-82.657
1.059	-120.029	-129.193	-82.675	4.380	-119.601	-128.973	-82.653
1.520	-119.965	-129.158	-82.675	4.729	-119.567	-128.951	-82.653
1.943	-119.904	-129.128	-82.675	5.047	-119.532	-128.934	-82.649
2.332	-119.848	-129.102	-82.670	6.283	-119.429	-128.877	-82.636
2.692	-119.800	-129.076	-82.666	7.135	-119.359	-128.839	-82.627
3.025	-119.761	-129.055	-82.666	7.757	-119.325	-128.821	-82.623
3.334	-119.723	-129.033	-82.662	8.231	-119.290	-128.804	-82.618
3.623	-119.692	-129.020	-82.662				
			TM-β-CD-SPFB system, SPFB=5.484×10^{-3} M				
0.000	-120.207	-129.288	-82.683	3.968	-120.029	-129.193	-82.602
0.607	-120.181	-129.275	-82.670	4.263	-120.016	-129.184	-82.597
1.160	-120.155	-129.262	-82.661	4.696	-120.003	-129.176	-82.588
1.665	-120.133	-129.249	-82.650	5.088	-119.986	-129.168	-82.582
2.128	-120.112	-129.236	-82.640	5.528	-119.969	-129.158	-82.575
2.555	-120.090	-129.228	-82.631	5.995	-119.947	-129.147	-82.566
2.948	-120.073	-129.219	-82.623	7.196	-119.908	-129.124	-82.545
3.313	-120.060	-129.210	-82.614	8.041	-119.878	-129.108	-82.532
3.652	-120.042	-129.202	-82.608	8.375	-119.861	-129.102	-82.528
			HP-β-CD-SPFB system, SPFB=5.870×10^{-3} M				
0.000	-120.245	-129.312	-82.715	3.769	-119.808	-128.994	-82.637
0.537	-120.184	-129.271	-82.706	4.013	-119.778	-128.973	-82.633
1.026	-120.115	-129.219	-82.693	4.242	-119.757	-128.955	-82.628
1.882	-120.012	-129.146	-82.676	4.580	-119.726	-128.934	-82.620
2.259	-119.973	-129.115	-82.668	4.888	-119.696	-128.912	-82.615
2.607	-119.925	-129.081	-82.660	6.085	-119.597	-128.834	-82.594
2.930	-119.895	-129.059	-82.654	6.910	-119.540	-128.791	-82.581
3.229	-119.860	-129.033	-82.649	7.512	-119.510	-128.769	-82.572
3.509	-119.830	-129.007	-82.642	7.972	-119.484	-128.748	-82.568

C_{CD}	$C(1)F_2$	$C(2)F_2$	$C(3)F_2$	CF_3	C_{CD}	$C(1)F_2$	$C(2)F_2$	$C(3)F_2$	CF_3
				β-CD-SPFP System, SPFP=5.039×10^{-3} M					
0.000	-119.355	-125.765	-127.723	-82.519	3.378	-118.845	-124.948	-127.547	-82.735
0.908	-119.208	-125.516	-127.675	-82.580	3.472	-118.836	-124.931	-127.546	-82.739
1.132	-119.177	-125.471	-127.663	-82.597	3.807	-118.789	-124.862	-127.529	-82.757
1.356	-119.129	-125.411	-127.649	-82.610	4.538	-118.750	-124.801	-127.516	-82.774
1.748	-119.083	-125.323	-127.630	-82.636	4.085	-118.711	-124.732	-127.499	-82.791
2.080	-119.015	-125.228	-127.611	-82.656	5.605	-118.629	-124.603	-127.473	-82.826
2.381	-118.983	-125.167	-127.594	-82.674	6.853	-118.568	-124.507	-127.451	-82.852
2.768	-118.923	-125.069	-127.576	-82.701	8.065	-118.538	-124.464	-127.438	-82.865
3.142	-118.867	-124.987	-127.560	-82.722					

Table A3: continued

C_{CD}	$C(1)F_2$	$C(2)F_2$	$C(3)F_2$	CF_3	C_{CD}	$C(1)F_2$	$C(2)F_2$	$C(3)F_2$	CF_3
				RAMEB-SPFP System, SPFP=5.137×10^{-3} M					
0.000	-119.372	-125.778	-127.745	-82.528	3.524	-118.374	-124.832	-127.550	-82.631
0.332	-119.264	-125.679	-127.710	-82.532	3.844	-118.296	-124.758	-127.538	-82.640
0.644	-119.174	-125.592	-127.689	-82.541	4.225	-118.195	-124.663	-127.525	-82.657
1.166	-119.022	-125.450	-127.659	-82.554	4.787	-118.097	-124.572	-127.512	-82.670
1.642	-118.893	-125.321	-127.633	-82.566	5.156	-118.045	-124.525	-127.503	-82.679
2.048	-118.741	-125.187	-127.610	-82.584	6.446	-117.864	-124.352	-127.481	-82.705
2.489	-118.638	-125.082	-127.589	-82.597	7.799	-117.726	-124.218	-127.464	-82.726
2.995	-118.491	-124.944	-127.568	-82.614	8.905	-117.643	-124.140	-127.455	-82.739
3.240	-118.443	-124.897	-127.559	-82.618					
				DM-β-CD-SPFP System, SPFP=5.264×10^{-3} M					
0.000	-119.359	-125.770	-127.736	-82.523	3.611	-118.460	-124.832	-127.659	-82.752
0.419	-119.259	-125.662	-127.729	-82.557	3.907	-118.387	-124.758	-127.654	-82.774
1.085	-119.100	-125.497	-127.712	-82.597	4.472	-118.287	-124.654	-127.646	-82.796
1.313	-119.048	-125.445	-127.707	-82.610	5.054	-118.188	-124.551	-127.636	-82.822
1.655	-118.919	-125.307	-127.699	-82.639	6.072	-118.080	-124.434	-127.622	-82.843
1.926	-118.862	-125.251	-127.693	-82.657	8.360	-117.920	-124.270	-127.598	-82.860
2.414	-118.720	-125.104	-127.680	-82.688	10.473	-117.864	-124.209	-127.584	-82.865
2.772	-118.651	-125.039	-127.674	-82.709	17.067	-117.803	-124.136	-127.563	-82.835
3.075	-118.555	-124.935	-127.667	-82.730					
				TM-β-CD-SPFP System, SPFP=5.137×10^{-3} M					
0.000	-119.355	-125.765	-127.732	-82.519	3.817	-118.875	-125.342	-127.663	-82.554
0.995	-119.251	-125.665	-127.699	-82.518	4.221	-118.815	-125.298	-127.663	-82.561
1.188	-119.228	-125.647	-127.697	-82.519	4.602	-118.772	-125.255	-127.663	-82.570
1.451	-119.191	-125.614	-127.689	-82.520	4.816	-118.750	-125.238	-127.663	-82.575
2.164	-119.096	-125.537	-127.676	-82.528	5.444	-118.674	-125.182	-127.663	-82.592
2.679	-119.027	-125.480	-127.672	-82.533	6.008	-118.601	-125.130	-127.667	-82.601
2.936	-118.992	-125.445	-127.672	-82.536	7.579	-118.443	-124.983	-127.672	-82.640
3.163	-118.962	-125.420	-127.672	-82.541	9.964	-118.223	-124.801	-127.684	-82.692
3.546	-118.914	-125.376	-127.667	-82.549					
				HP-β-CD-SPFP System, SPFP=5.039×10^{-3} M					
0.000	-119.382	-125.789	-127.756	-82.534	3.309	-118.705	-124.925	-127.468	-82.546
0.338	-119.311	-125.691	-127.717	-82.538	3.872	-118.618	-124.812	-127.432	-82.546
0.859	-119.199	-125.549	-127.673	-82.538	4.238	-118.558	-124.735	-127.406	-82.546
1.219	-119.094	-125.427	-127.636	-82.538	4.825	-118.484	-124.639	-127.380	-82.546
1.493	-119.046	-125.361	-127.609	-82.542	5.539	-118.406	-124.539	-127.339	-82.546
1.765	-118.990	-125.288	-127.587	-82.538	6.437	-118.311	-124.423	-127.307	-82.546
2.178	-118.908	-125.180	-127.554	-82.542	7.532	-118.238	-124.320	-127.272	-82.551
2.742	-118.795	-125.045	-127.505	-82.542	8.883	-118.164	-124.229	-127.242	-82.555
3.027	-118.764	-124.997	-127.490	-82.542					

Table A3: continued

C_{CD}	$C(1)F_2$	$C(2)F_2$	$C(3)F_2$	$C(4)F_2$	$C(5)F_2$	CF_3
β-CD-SPFH System, SPFH=5.032×10^{-3} M						
0.000	-119.074	-124.840	-123.578	-124.425	-127.672	-82.363
1.104	-119.018	-124.568	-123.479	-124.348	-127.659	-82.373
1.633	-118.983	-124.431	-123.423	-124.300	-127.650	-82.383
2.061	-118.957	-124.320	-123.384	-124.250	-127.646	-82.389
2.884	-118.906	-124.150	-123.293	-124.180	-127.632	-82.403
3.337	-118.884	-124.050	-123.254	-124.140	-127.624	-82.411
3.717	-118.858	-123.969	-123.202	-124.095	-127.620	-82.415
4.058	-118.841	-123.889	-123.185	-124.062	-127.615	-82.420
4.313	-118.823	-123.829	-123.146	-124.036	-127.611	-82.420
4.693	-118.806	-123.738	-123.120	-124.006	-127.607	-82.424
5.127	-118.785	-123.665	-123.081	-123.984	-127.607	-82.428
6.028	-118.776	-123.621	-123.072	-123.980	-127.609	-82.433
6.781	-118.772	-123.621	-123.072	-123.984	-127.611	-82.437
8.106	-118.772	-123.613	-123.072	-123.993	-127.617	-82.441
9.058	-118.767	-123.608	-123.085	-123.993	-127.620	-82.446
10.414	-118.767	-123.617	-123.076	-124.006	-127.624	-82.450
RAMEB-SPFH System, SPFH=5.083×10^{-3} M						
0.000	-119.133	-124.886	-123.637	-124.471	-127.713	-82.395
0.417	-119.020	-124.709	-123.574	-124.426	-127.700	-82.412
0.694	-118.973	-124.631	-123.549	-124.399	-127.691	-82.421
1.166	-118.865	-124.467	-123.498	-124.350	-127.691	-82.443
1.513	-118.774	-124.350	-123.459	-124.323	-127.683	-82.461
1.994	-118.653	-124.177	-123.403	-124.264	-127.674	-82.482
3.037	-118.432	-123.769	-123.291	-124.153	-127.678	-82.537
3.631	-118.290	-123.544	-123.222	-124.091	-127.683	-82.564
3.978	-118.221	-123.428	-123.188	-124.062	-127.683	-82.581
4.349	-118.143	-123.303	-123.148	-124.029	-127.691	-82.598
4.599	-118.069	-123.184	-123.120	-124.008	-127.700	-82.609
5.077	-117.991	-123.066	-123.066	-123.978	-127.709	-82.631
5.578	-117.957	-123.023	-123.023	-123.969	-127.700	-82.642
7.127	-117.927	-122.993	-122.993	-123.957	-127.700	-82.646
8.306	-117.927	-122.988	-122.988	-123.954	-127.704	-82.642
9.524	-117.927	-122.993	-122.993	-123.957	-127.700	-82.642
10.232	-117.927	-122.997	-122.997	-123.957	-127.704	-82.637
12.295	-117.935	-122.997	-122.997	-123.952	-127.704	-82.642

Table A3: continued

C_{CD}	$C(1)F_2$	$C(2)F_2$	$C(3)F_2$	$C(4)F_2$	$C(5)F_2$	CF_3
DM-β-CD-SPFH system, SPFH=4.981×10^{-3} M						
0.000	-119.133	-124.886	-123.637	-124.471	-127.713	-82.395
0.417	-119.020	-124.709	-123.574	-124.426	-127.700	-82.412
0.694	-118.973	-124.631	-123.549	-124.399	-127.691	-82.421
1.166	-118.865	-124.467	-123.498	-124.350	-127.691	-82.443
1.513	-118.774	-124.350	-123.459	-124.323	-127.683	-82.461
1.994	-118.653	-124.177	-123.403	-124.264	-127.674	-82.482
3.037	-118.432	-123.769	-123.291	-124.153	-127.678	-82.537
3.631	-118.290	-123.544	-123.222	-124.091	-127.683	-82.564
3.978	-118.221	-123.428	-123.188	-124.062	-127.683	-82.581
4.349	-118.143	-123.303	-123.148	-124.029	-127.691	-82.598
4.599	-118.069	-123.184	-123.120	-124.008	-127.700	-82.609
5.077	-117.991	-123.066	-123.066	-123.978	-127.709	-82.631
5.578	-117.957	-123.023	-123.023	-123.969	-127.700	-82.642
7.127	-117.927	-122.993	-122.993	-123.957	-127.700	-82.646
8.306	-117.927	-122.988	-122.988	-123.954	-127.704	-82.642
9.524	-117.927	-122.993	-122.993	-123.957	-127.700	-82.642
10.232	-117.927	-122.997	-122.997	-123.957	-127.704	-82.637
12.295	-117.935	-122.997	-122.997	-123.952	-127.704	-82.642
TM-β-CD-SPFH system, SPFH=5.011×10^{-3} M						
0.000	-119.140	-124.900	-123.630	-124.470	-127.720	-82.399
0.626	-118.980	-124.630	-123.560	-124.460	-127.760	-82.400
0.991	-118.880	-124.450	-123.520	-124.450	-127.800	-82.464
1.218	-118.840	-124.350	-123.500	-124.440	-127.820	-82.494
1.978	-118.650	-124.030	-123.420	-124.400	-127.890	-82.590
2.224	-118.600	-123.910	-123.390	-124.390	-127.920	-82.624
2.573	-118.510	-123.750	-123.350	-124.380	-127.950	-82.665
2.883	-118.430	-123.600	-123.320	-124.370	-127.980	-82.698
3.075	-118.380	-123.530	-123.310	-124.360	-128.000	-82.728
3.640	-118.260	-123.260	-123.260	-124.350	-128.050	-82.779
4.192	-118.140	-123.050	-123.200	-124.340	-128.100	-82.834
4.635	-118.060	-122.920	-123.160	-124.330	-128.130	-82.871
5.055	-118.000	-122.820	-123.130	-124.320	-128.150	-82.909
5.409	-117.960	-122.730	-123.110	-124.320	-128.170	-82.948
6.692	-117.910	-122.660	-123.100	-124.310	-128.190	-82.961
8.092	-117.890	-122.600	-123.090	-124.310	-128.190	-82.983
9.112	-117.880	-122.590	-123.090	-124.310	-128.200	-82.992
10.009	-117.890	-122.600	-123.090	-124.310	-128.200	-82.996

Table A3: continued

C_{CD}	$C(1)F_2$	$C(2)F_2$	$C(3)F_2$	$C(4)F_2$	$C(5)F_2$	CF_3
HP-β-CD-SPFH system, SPFH=5.006×10^{-3} M						
0.000	-119.110	-124.900	-123.620	-124.460	-127.700	-82.385
0.644	-119.020	-124.680	-123.530	-124.380	-127.650	-82.368
0.921	-118.980	-124.620	-123.490	-124.350	-127.630	-82.363
1.616	-118.880	-124.400	-123.410	-124.270	-127.590	-82.342
2.104	-118.800	-124.250	-123.340	-124.200	-127.550	-82.324
2.573	-118.730	-124.110	-123.280	-124.140	-127.510	-82.316
3.148	-118.650	-123.950	-123.210	-124.080	-127.470	-82.303
3.625	-118.580	-123.810	-123.160	-124.030	-127.450	-82.286
3.687	-118.580	-123.800	-123.150	-124.030	-127.450	-82.286
4.174	-118.500	-123.640	-123.080	-123.970	-127.400	-82.273
4.578	-118.460	-123.540	-123.040	-123.930	-127.380	-82.264
5.057	-118.400	-123.420	-122.990	-123.900	-127.360	-82.251
5.321	-118.370	-123.370	-122.960	-123.870	-127.350	-82.245
5.573	-118.360	-123.350	-122.940	-123.860	-127.340	-82.242
6.933	-118.310	-123.240	-122.900	-123.830	-127.320	-82.238
8.354	-118.310	-123.230	-122.900	-123.820	-127.320	-82.234
10.202	-118.310	-123.230	-122.890	-123.820	-127.320	-82.238
25.295	-118.310	-123.210	-122.880	-123.820	-127.320	-82.234

C_{CD}	$C(1)F_2$	$C(2)F_2$	$C(3)F_2$	$C(4)F_2$	$C(5)F_2$	$C(6)F_2$	CF_3
β-CD-SPFO system, SPFO=5.098×10^{-3} M							
0.000	-119.121	-124.873	-123.440	-123.663	-124.378	-127.673	-82.381
0.780	-119.101	-124.754	-123.384	-123.599	-124.314	-127.636	-82.373
1.014	-119.091	-124.718	-123.353	-123.576	-124.291	-127.623	-82.370
1.718	-119.068	-124.602	-123.286	-123.505	-124.220	-127.572	-82.367
1.968	-119.058	-124.567	-123.264	-123.497	-124.212	-127.559	-82.363
2.167	-119.048	-124.535	-123.247	-123.457	-124.172	-127.546	-82.361
2.615	-119.035	-124.465	-123.200	-123.423	-124.138	-127.517	-82.358
3.018	-119.022	-124.396	-123.158	-123.379	-124.094	-127.491	-82.356
3.936	-118.987	-124.248	-123.081	-123.294	-124.009	-127.425	-82.357
4.037	-118.981	-124.223	-123.068	-123.291	-124.006	-127.420	-82.354
4.664	-118.955	-124.119	-123.001	-123.228	-123.943	-127.414	-82.355
5.536	-118.929	-124.089	-122.990	-123.232	-123.947	-127.424	-82.366
5.761	-118.916	-124.049	-123.012	-123.258	-123.973	-127.434	-82.384
5.949	-118.907	-124.019	-123.016	-123.267	-123.982	-127.444	-82.389
6.719	-118.878	-123.984	-123.056	-123.337	-124.052	-127.513	-82.424
7.320	-118.846	-123.945	-123.094	-123.371	-124.086	-127.556	-82.449
7.846	-118.828	-123.928	-123.129	-123.414	-124.129	-127.599	-82.471
8.727	-118.798	-123.881	-123.155	-123.479	-124.194	-127.664	-82.503
8.753	-118.791	-123.875	-123.177	-123.470	-124.185	-127.666	-82.502
10.354	-118.733	-123.806	-123.295	-123.595	-124.310	-127.768	-82.566
11.205	-118.697	-123.750	-123.350	-123.650	-124.365	-127.824	-82.591

Table A3: continued

C_{CD}	$C(1)F_2$	$C(2)F_2$	$C(3)F_2$	$C(4)F_2$	$C(5)F_2$	$C(6)F_2$	CF_3
RAMEB-SPFO system, SPFO=5.035×10^{-3} M							
0.000	-119.050	-124.790	-123.360	-123.590	-124.300	-127.620	-82.315
0.867	-118.880	-124.560	-123.270	-123.510	-124.240	-127.600	-82.342
1.265	-118.800	-124.420	-123.200	-123.430	-124.210	-127.610	-82.346
2.076	-118.670	-124.170	-123.130	-123.360	-124.160	-127.610	-82.389
2.644	-118.570	-124.030	-123.050	-123.280	-124.120	-127.630	-82.407
3.170	-118.470	-123.890	-123.000	-123.230	-124.090	-127.620	-82.424
3.810	-118.350	-123.700	-122.930	-123.150	-124.050	-127.620	-82.446
4.322	-118.280	-123.570	-122.870	-123.110	-124.030	-127.620	-82.450
4.777	-118.200	-123.420	-122.820	-123.040	-124.000	-127.630	-82.467
5.231	-118.120	-123.310	-122.750	-123.000	-123.980	-127.630	-82.480
5.629	-118.090	-123.260	-122.740	-122.980	-123.960	-127.610	-82.484
6.312	-118.080	-123.260	-122.730	-122.970	-123.960	-127.600	-82.476
7.136	-118.080	-123.260	-122.730	-122.970	-123.950	-127.600	-82.476
7.690	-118.080	-123.260	-122.730	-122.980	-123.960	-127.610	-82.480
8.103	-118.080	-123.250	-122.730	-122.980	-123.960	-127.610	-82.471
8.941	-118.080	-123.260	-122.730	-122.970	-123.960	-127.600	-82.471
10.590	-118.080	-123.270	-122.730	-122.970	-123.960	-127.600	-82.476
11.045	-118.060	-123.260	-122.730	-122.970	-123.960	-127.600	-82.471
DM-β-CD-SPFO system, SPFO=5.199×10^{-3} M							
0.000	-119.090	-124.840	-123.420	-123.630	-124.370	-127.660	-82.363
0.463	-119.020	-124.730	-123.380	-123.600	-124.350	-127.660	-82.376
1.041	-118.940	-124.580	-123.340	-123.550	-124.320	-127.670	-82.389
1.691	-118.840	-124.410	-123.270	-123.480	-124.280	-127.690	-82.411
2.255	-118.770	-124.290	-123.240	-123.440	-124.260	-127.700	-82.423
3.108	-118.650	-124.100	-123.160	-123.360	-124.220	-127.710	-82.441
3.859	-118.550	-123.940	-123.100	-123.300	-124.190	-127.730	-82.467
4.394	-118.480	-123.820	-123.060	-123.250	-124.170	-127.740	-82.483
4.958	-118.430	-123.720	-123.010	-123.210	-124.140	-127.750	-82.494
5.782	-118.320	-123.550	-122.950	-123.130	-124.120	-127.760	-82.514
6.143	-118.320	-123.570	-122.960	-123.140	-124.100	-127.750	-82.515
7.126	-118.320	-123.560	-122.960	-123.140	-124.100	-127.760	-82.514
7.849	-118.330	-123.540	-122.950	-123.140	-124.100	-127.750	-82.514
8.673	-118.330	-123.560	-122.960	-123.140	-124.100	-127.750	-82.517
10.118	-118.320	-123.560	-122.960	-123.140	-124.100	-127.740	-82.511
10.566	-118.320	-123.560	-122.950	-123.140	-124.100	-127.740	-82.509
11.578	-118.310	-123.540	-122.950	-123.140	-124.100	-127.740	-82.510

Table A3: continued

C_{CD}	$C(1)F_2$	$C(2)F_2$	$C(3)F_2$	$C(4)F_2$	$C(5)F_2$	$C(6)F_2$	CF_3
TM-β-CD-SPFO system, SPFO=5.012×10^{-3} M							
0.000	-119.080	-124.830	-123.430	-123.650	-124.350	-127.660	-82.359
0.703	-118.950	-124.590	-123.320	-123.580	-124.370	-127.710	-82.450
1.137	-118.850	-124.450	-123.250	-123.530	-124.360	-127.740	-82.493
1.553	-118.760	-124.320	-123.190	-123.480	-124.350	-127.760	-82.545
2.480	-118.570	-124.030	-123.030	-123.370	-124.330	-127.820	-82.597
2.559	-118.560	-123.990	-123.020	-123.360	-124.330	-127.820	-82.601
3.502	-118.370	-123.690	-122.840	-123.230	-124.310	-127.870	-82.640
3.904	-118.300	-123.570	-122.770	-123.190	-124.300	-127.890	-82.662
4.570	-118.190	-123.420	-122.680	-123.120	-124.290	-127.930	-82.683
4.882	-118.150	-123.330	-122.640	-123.090	-124.290	-127.940	-82.701
5.466	-118.110	-123.260	-122.580	-123.060	-124.290	-127.950	-82.709
6.155	-118.100	-123.170	-122.580	-123.060	-124.290	-127.960	-82.714
7.321	-118.100	-123.170	-122.580	-123.060	-124.290	-127.960	-82.714
7.851	-118.090	-123.160	-122.590	-123.050	-124.290	-127.960	-82.718
8.263	-118.090	-123.160	-122.590	-123.060	-124.290	-127.960	-82.718
9.102	-118.080	-123.180	-122.590	-123.060	-124.300	-127.960	-82.718
12.232	-118.080	-123.220	-122.590	-123.050	-124.300	-127.950	-82.714
HP-β-CD-SPFO system, SPFO=5.162×10^{-3} M							
0.000	-119.080	-124.830	-123.410	-123.630	-124.360	-127.650	-82.363
0.733	-119.000	-124.650	-123.320	-123.550	-124.280	-127.610	-82.337
0.888	-118.970	-124.600	-123.290	-123.530	-124.270	-127.600	-82.329
1.724	-118.870	-124.370	-123.190	-123.420	-124.170	-127.540	-82.298
2.013	-118.840	-124.300	-123.150	-123.380	-124.140	-127.530	-82.289
2.918	-118.730	-124.080	-123.040	-123.280	-124.060	-127.480	-82.254
3.493	-118.670	-123.940	-122.980	-123.210	-124.000	-127.440	-82.233
4.186	-118.580	-123.780	-122.890	-123.110	-123.920	-127.410	-82.209
4.256	-118.580	-123.770	-122.880	-123.110	-123.920	-127.410	-82.200
5.145	-118.490	-123.570	-122.760	-123.020	-123.840	-127.380	-82.175
5.958	-118.440	-123.460	-122.730	-122.960	-123.830	-127.350	-82.159
6.535	-118.440	-123.440	-122.730	-122.940	-123.820	-127.340	-82.164
7.004	-118.440	-123.440	-122.730	-122.930	-123.820	-127.330	-82.161
8.082	-118.440	-123.440	-122.730	-122.930	-123.820	-127.340	-82.160
8.720	-118.440	-123.430	-122.730	-122.940	-123.820	-127.340	-82.160
9.334	-118.440	-123.440	-122.720	-122.940	-123.820	-127.330	-82.156
9.838	-118.440	-123.450	-122.720	-122.940	-123.810	-127.330	-82.165

Table A3: continued

C_{CD}	$C(1)F_2$	$C(2)F_2$	$C(6)F_2$	$C(7)F_2$	CF_3
β-CD-SPFN System, SPFN=5.061×10^{-3} M					
0.000	-119.056	-124.781	-124.300	-127.625	-82.363
1.065	-119.045	-124.678	-124.266	-127.611	-82.333
1.526	-119.030	-124.626	-124.258	-127.605	-82.323
1.763	-119.022	-124.598	-124.251	-127.600	-82.321
2.176	-119.013	-124.544	-124.243	-127.595	-82.308
2.805	-118.997	-124.473	-124.224	-127.585	-82.295
2.964	-118.993	-124.446	-124.220	-127.582	-82.290
3.298	-118.984	-124.415	-124.216	-127.578	-82.287
4.197	-118.961	-124.300	-124.205	-127.569	-82.265
4.263	-118.959	-124.287	-124.200	-127.567	-82.265
4.829	-118.939	-124.213	-124.220	-127.563	-82.261
5.554	-118.877	-124.150	-124.240	-127.592	-82.291
5.711	-118.857	-124.131	-124.258	-127.604	-82.304
6.706	-118.762	-123.922	-124.373	-127.702	-82.399
6.953	-118.741	-123.889	-124.413	-127.723	-82.425
9.369	-118.515	-123.556	-124.667	-127.900	-82.607
11.996	-118.515	-124.425	-124.827	-128.022	-82.372
RAMEB-SPFN System, SPFN=5.003×10^{-3} M					
0.000	-119.115	-124.861	-124.341	-127.665	-82.382
0.384	-119.068	-124.766	-124.397	-127.772	-82.516
0.791	-118.999	-124.665	-124.462	-127.870	-82.668
1.201	-118.929	-124.570	-124.470	-127.944	-82.752
1.394	-118.896	-124.493	-124.476	-127.948	-82.776
1.790	-118.817	-124.382	-124.472	-127.952	-82.832
2.374	-118.717	-124.227	-124.454	-127.959	-82.840
2.963	-118.623	-124.078	-124.397	-127.907	-82.789
3.316	-118.562	-123.983	-124.329	-127.840	-82.715
3.913	-118.476	-123.840	-124.255	-127.760	-82.624
4.432	-118.411	-123.732	-124.186	-127.708	-82.559
4.862	-118.353	-123.624	-124.142	-127.667	-82.525
5.116	-118.316	-123.574	-124.116	-127.650	-82.516
6.221	-118.281	-123.546	-124.112	-127.645	-82.508
7.691	-118.272	-123.537	-124.116	-127.645	-82.508
9.022	-118.259	-123.530	-124.121	-127.648	-82.512
9.906	-118.250	-123.524	-124.125	-127.648	-82.512
13.099	-118.235	-123.524	-124.129	-127.650	-82.521

Table A3: continued

C_{CD}	$C(1)F_2$	$C(2)F_2$	$C(6)F_2$	$C(7)F_2$	CF_3
DM-β-CD-SPFN System, SPFN=5.020×10^{-3} M					
0.000	-119.104	-124.829	-124.321	-127.650	-82.369
0.590	-119.035	-124.719	-124.352	-127.706	-82.442
1.055	-118.974	-124.620	-124.399	-127.775	-82.533
1.622	-118.904	-124.482	-124.394	-127.784	-82.538
1.957	-118.862	-124.380	-124.370	-127.767	-82.507
2.112	-118.842	-124.320	-124.340	-127.758	-82.503
2.792	-118.749	-124.269	-124.311	-127.729	-82.486
3.292	-118.680	-124.117	-124.281	-127.699	-82.455
3.314	-118.676	-123.994	-124.279	-127.702	-82.447
3.860	-118.602	-123.988	-124.253	-127.690	-82.442
4.272	-118.555	-123.895	-124.231	-127.691	-82.442
4.708	-118.499	-123.811	-124.213	-127.693	-82.447
5.448	-118.468	-123.755	-124.210	-127.695	-82.451
6.333	-118.460	-123.755	-124.211	-127.697	-82.455
8.375	-118.434	-123.742	-124.211	-127.700	-82.464
10.165	-118.425	-123.729	-124.209	-127.699	-82.468
11.144	-118.415	-123.729	-124.209	-127.703	-82.473
TM-β-CD-SPFN System, SPFN=5.426×10^{-3} M					
0.000	-119.101	NR	-124.309	-127.637	-82.350
0.469	-119.091	NR	-124.754	-128.082	-82.886
0.895	-119.030	NR	-124.879	-128.398	-83.340
1.283	-118.897	NR	-124.992	-128.558	-83.643
1.640	-118.694	NR	-125.022	-128.605	-83.755
1.968	-118.577	NR	-125.009	-128.592	-83.751
2.271	-118.495	NR	-124.953	-128.532	-83.682
2.551	-118.443	NR	-124.888	-128.458	-83.582
2.811	-118.378	NR	-124.823	-128.367	-83.474
3.054	-118.331	NR	-124.719	-128.246	-83.319
3.280	-118.287	NR	-124.632	-128.138	-83.167
3.612	-118.257	NR	-124.558	-128.035	-83.029
3.912	-118.233	NR	-124.475	-127.948	-82.904
4.249	-118.214	NR	-124.399	-127.849	-82.770
4.606	-118.192	NR	-124.339	-127.771	-82.662
5.524	-118.175	NR	-124.304	-127.728	-82.605
6.168	-118.153	NR	-124.291	-127.706	-82.580
6.423	-118.145	NR	-124.296	-127.702	-82.575

Table A3: continued

C_{CD}	$C(1)F_2$	$C(2)F_2$	$C(6)F_2$	$C(7)F_2$	CF_3
HP-β-CD-SPFN System, SPFN=5.012×10^{-3} M					
0.000	-119.117	-124.858	NR	-127.666	-82.381
0.694	-119.050	-124.716	NR	-127.633	-82.355
0.956	-119.027	-124.660	NR	-127.620	-82.347
1.374	-118.979	-124.566	NR	-127.599	-82.334
1.993	-118.916	-124.419	NR	-127.565	-82.312
2.181	-118.895	-124.370	NR	-127.554	-82.304
2.697	-118.840	-124.248	NR	-127.525	-82.283
2.906	-118.817	-124.218	NR	-127.515	-82.277
3.552	-118.754	-124.075	NR	-127.482	-82.251
3.973	-118.713	-123.997	NR	-127.460	-82.237
4.102	-118.705	-123.967	NR	-127.452	-82.234
4.427	-118.667	-123.894	NR	-127.438	-82.216
4.812	-118.634	-123.823	NR	-127.420	-82.203
5.349	-118.590	-123.721	NR	-127.395	-82.182
5.780	-118.570	-123.673	NR	-127.382	-82.173
7.090	-118.569	-123.665	NR	-127.383	-82.173
8.793	-118.577	-123.664	NR	-127.382	-82.173
9.655	-118.568	-123.660	NR	-127.382	-82.173
10.305	-118.567	-123.663	NR	-127.382	-82.173

[a]Chemical shifts for the CF2 and CF3 groups are in ppm relative to TFA and C_{CD} is in m($\times10^3$)

NR indicates that the values are not reported due to spectral overlap

APPENDIX A4

Table A4: ^{1}H NMR Chemical Shifts of the H(3) and H(5) Nuclei of β-CD of Cyclodextrin-Sodium Perfluoroalkyl Carboxylate Systems at 295 K.

C_S	H(3)	H(5)	C_S	H(3)	H(5)	C_S	H(3)	H(5)
			β-CD-SPFB system, β-CD=5.264×10^{-3} M					
0.000	3.930	3.814	3.933	3.902	3.795	6.562	3.892	3.780
0.721	3.924	3.807	4.335	3.899	3.789	7.115	3.890	3.777
1.377	3.919	3.804	4.710	3.897	3.787	7.897	3.889	3.775
1.976	3.915	3.801	5.060	3.895	3.785	9.083	3.887	3.771
2.526	3.911	3.798	5.574	3.894	3.784	9.941	3.885	3.767
3.032	3.908	3.795	6.039	3.893	3.782	10.590	3.883	3.764
3.500	3.905	3.793						
			β-CD-SPFP System, β-CD=10.338×10^{-3} M					
0.000	3.929	3.820	8.123e-3	3.843	3.750	0.015	3.808	3.722
2.079e-3	3.904	3.799	8.624e-3	3.839	3.747	0.016	3.805	3.720
2.960e-3	3.893	3.791	9.192e-3	3.835	3.744	0.017	3.803	3.718
3.756e-3	3.884	3.784	0.010	3.831	3.741	0.018	3.801	3.717
4.478e-3	3.877	3.778	0.010	3.827	3.738	0.019	3.799	3.715
5.136e-3	3.870	3.772	0.011	3.824	3.735	0.020	3.798	3.714
5.739e-3	3.864	3.767	0.012	3.821	3.732	0.021	3.797	3.713
6.293e-3	3.858	3.763	0.012	3.818	3.730	0.022	3.795	3.712
6.966e-3	3.852	3.758	0.013	3.816	3.729	0.023	3.794	3.711
7.572e-3	3.847	3.754	0.014	3.811	3.725			
			β-CD-SPFH System, β-CD=7.210×10^{-3} M					
0.000	3.942	3.835	3.173	3.875	3.750	5.523	3.824	3.692
1.170	3.918	3.802	3.726	3.861	3.734	6.201	3.811	3.675
1.824	3.905	3.783	4.403	3.847	3.717	6.773	3.803	3.666
2.359	3.893	3.770	4.811	3.839	3.707	9.386	3.800	3.661
3.024	3.877	3.752	5.195	3.832	3.700	13.357	3.798	3.657
			β-CD-SPFO System, β-CD=6.333×10^{-3} M					
0.000	3.947	3.837	3.003	3.852	3.731	5.251	3.804	3.658
0.847	3.914	3.802	3.462	3.840	3.716	5.376	3.803	3.655
1.873	3.886	3.770	4.280	3.822	3.688	6.293	3.793	3.635
2.259	3.874	3.757	4.644	3.815	3.676	10.735	3.793	3.626
2.943	3.853	3.732	4.754	3.812	3.672	16.358	3.792	3.621

Table A4: continued

C_S	H(3)	H(5)	C_S	H(3)	H(5)	C_S	H(3)	H(5)
			β-CD-SPFN System, β-CD=6.333×10^{-3} M					
0.000	3.939	3.835	2.983	3.790	3.698	5.379	3.786	3.627
1.206	3.863	3.771	3.567	3.782	3.678	5.892	3.787	3.617
1.875	3.834	3.743	4.242	3.777	3.655	6.375	3.786	3.616
2.175	3.822	3.730	4.619	3.780	3.647	10.296	3.787	3.616
2.959	3.790	3.699	5.051	3.784	3.634	11.727	3.788	3.616
			β-CD-SPFD system, β-CD=7.331×10^{-3} M					
0.000	3.944	3.829	3.923	3.743	3.644	5.928	3.753	3.599
0.912	3.879	3.774	4.376	3.742	3.631	6.376	3.754	3.595
2.239	3.799	3.709	5.030	3.744	3.618	6.843	3.755	3.593
2.649	3.778	3.690	5.392	3.749	3.610	7.628	3.758	3.589
3.324	3.753	3.661						
			α-CD-SPFB system, α-CD=11.18×10^{-3} M					
0.000	3.946	3.794	3.897	3.945	3.795	6.502	3.945	3.795
0.714	3.946	3.795	4.296	3.944	3.794	8.095	3.944	3.792
1.364	3.947	3.796	4.668	3.943	3.794	9.192	3.942	3.790
1.958	3.949	3.799	5.014	3.944	3.794	9.994	3.942	3.789
2.503	3.949	3.799	5.339	3.941	3.790	10.605	3.941	3.788
3.005	3.945	3.795	5.644	3.944	3.794	10.859	3.941	3.788
3.468	3.946	3.796	6.093	3.946	3.797			

APPENDIX A5

Table A5: Concentration(C_S), Density Difference($\Delta d = d - d_o$), and Apparent Molar Volume($V_{\phi,S}$) Data of Sodium Akyl Carboxylate Salts in Water and Ternary (w+S+CD) Aqueous Solutions at pH 10.5 and 298 K.

C_s	Δd	$V_{\phi,S}$	C_s	Δd	$V_{\phi,S}$	C_s	Δd	$V_{\phi,S}$
				SP in water				
4.270	0.182	53.4	11.610	0.492	53.7	21.563	0.907	54.0
5.843	0.248	53.7	13.035	0.550	53.9	25.368	1.067	54.0
7.598	0.319	54.1	15.954	0.672	54.0	27.980	1.175	54.0
9.840	0.414	54.0	19.093	0.803	54.0	31.981	1.342	54.1
				β-CD-SP System where $C_{\beta\text{-CD}}=1.343\times10^{-2}$ m				
3.017	5.820	53.8	10.429	6.134	53.7	19.956	6.536	53.8
4.319	5.876	53.7	12.231	6.208	53.9	22.539	6.643	53.8
5.538	5.927	53.7	13.699	6.271	53.8	24.619	6.731	53.8
7.626	6.014	53.9	16.060	6.370	53.8	24.703	6.734	53.8
9.394	6.089	53.9	17.050	6.413	53.8	29.841	6.953	53.8
				SHex in water				
2.924	0.109	101.1	9.458	0.355	100.8	17.787	0.661	101.0
4.662	0.173	101.1	10.894	0.401	101.4	20.705	0.768	101.1
5.996	0.222	101.3	12.143	0.452	101.0	24.426	0.906	101.1
6.930	0.261	100.6	13.179	0.491	101.0	26.460	0.980	101.1
8.420	0.315	100.9	14.164	0.533	100.6	29.937	1.108	101.2
				β-CD-SHex System where $C_{\beta\text{-CD}}=1.326\times10^{-2}$ m				
3.547	0.406	107.8	8.981	1.034	107.0	19.981	2.319	106.0
4.515	0.516	107.9	10.874	1.256	106.7	23.183	2.704	105.3
5.281	0.605	107.7	13.113	1.521	106.1	24.531	2.856	105.5
6.856	0.790	106.9	15.668	1.813	106.4	27.014	3.162	104.9
8.194	0.947	106.6	17.037	1.978	106.0	30.960	3.613	105.2
				DM-β-CD-SHex where [DM-β-CD]=4.002 × 10^{-3} m				
1.798	1.449	103.3	5.950	1.595	103.1	10.81	1.776	102.2
2.368	1.469	103.3	6.134	1.602	103.0	11.59	1.804	102.1
2.960	1.490	103.0	7.243	1.645	102.5	12.32	1.828	102.3
3.600	1.513	102.8	7.720	1.664	102.2	13.13	1.856	102.4
4.191	1.532	103.4	8.897	1.707	102.1	13.87	1.883	102.4
4.806	1.560	102.9	9.733	1.736	102.2	14.88	1.921	102.2
5.332	1.575	102.8						

Table A5: continued

C_s	Δd	$V_{\phi,S}$	C_s	Δd	$V_{\phi,S}$	C_s	Δd	$V_{\phi,S}$
			HP-β-CD-SHex where [HP-β-CD]=5.003 × 10^{-3} m					
1.704	2.180	100.2	5.458	2.314	101.8	10.27	2.484	102.3
2.685	2.215	101.2	6.751	2.361	101.8	11.24	2.519	102.2
3.413	2.241	101.5	6.658	2.355	102.2	12.20	2.552	102.4
4.040	2.264	101.4	8.150	2.408	102.2	12.69	2.569	102.4
4.816	2.291	101.7	9.197	2.446	102.2	13.99	2.615	102.4
5.472	2.315	101.7						
			SHept in Water					
4.599	0.163	117.0	10.617	0.380	116.5	16.586	0.592	116.6
5.456	0.194	116.8	11.507	0.412	116.5	20.462	0.729	116.7
6.213	0.221	116.8	11.791	0.422	116.6	22.715	0.807	116.8
7.183	0.257	116.6	13.291	0.475	116.6	25.072	0.889	116.8
8.177	0.289	117.0	13.684	0.489	116.7	27.613	0.980	116.8
8.378	0.299	116.7	14.048	0.502	116.7	29.933	1.064	116.7
9.488	0.340	116.6	16.137	0.575	116.7	31.374	1.115	116.7
9.655	0.343	116.9						
			β-CD-SHept System where $C_{\beta\text{-}CD}$=1.352×10^{-2} m					
4.383	5.773	129.0	14.197	6.032	126.6	24.853	6.328	125.4
5.876	5.809	128.6	15.977	6.087	125.9	27.837	6.471	123.1
7.737	5.856	128.2	18.638	6.164	125.5	30.483	6.549	123.1
9.443	5.901	127.7	21.499	6.255	124.7	32.214	6.603	123.0
11.445	5.955	127.2	22.205	6.319	122.7	35.645	6.715	122.6
			SO in Water					
3.519	0.121	132.0	10.352	0.341	133.5	25.568	0.840	133.5
5.515	0.195	131.2	11.511	0.382	133.3	29.235	0.958	133.6
5.993	0.199	133.3	12.934	0.425	133.6	33.134	1.085	133.6
7.508	0.248	133.5	15.585	0.518	133.2	30.679	0.984	134.3
8.685	0.287	133.4	19.460	0.639	133.6			
			β-CD-SO System where $C_{\beta\text{-}CD}$=1.304×10^{-2} m					
3.851	5.606	149.0	10.763	5.737	147.6	20.054	5.982	143.9
5.067	5.626	149.0	12.170	5.765	147.4	23.156	6.076	142.7
6.482	5.650	149.1	13.105	5.789	146.9	26.845	6.186	141.8
7.270	5.667	148.5	15.571	5.855	145.7	29.591	6.274	141.0
7.830	5.672	149.1	18.009	5.925	144.5	33.275	6.383	140.5
9.705	5.713	148.1						

Table A5: continued

C_s	Δd	$V_{\phi,S}$	C_s	Δd	$V_{\phi,S}$	C_s	Δd	$V_{\phi,S}$
			DM-β-CD-SO where [DM-β-CD]=3.969 × 10^{-3} m					
1.834	1.490	140.6	6.275	1.613	139.2	11.12	1.757	138.0
2.427	1.506	140.1	6.777	1.627	139.1	11.92	1.782	137.8
2.924	1.514	141.7	7.341	1.642	139.1	12.69	1.809	137.4
3.707	1.537	140.9	8.249	1.670	138.7	13.56	1.836	137.3
4.378	1.554	140.9	9.224	1.697	138.7	14.20	1.856	137.1
4.938	1.571	140.3	10.14	1.727	138.2	15.33	1.896	136.7
5.536	1.588	140.0						
			HP-β-CD-SO where [HP-β-CD]=5.003× 10^{-3} m					
1.537	2.160	140.0	5.420	2.260	140.4	10.30	2.406	138.4
2.500	2.180	142.2	6.340	2.290	139.7	11.11	2.432	138.2
3.150	2.198	141.6	6.683	2.297	139.8	12.10	2.460	138.2
3.826	2.216	141.2	7.100	2.310	139.5	12.81	2.483	137.9
4.326	2.230	140.8	8.097	2.340	139.2	13.70	2.513	137.5
4.958	2.247	140.7	9.355	2.378	138.7	15.49	2.567	137.3
				SN in Water				
3.701	0.121	147.8	10.439	0.342	147.7	17.140	0.550	148.4
4.885	0.160	147.9	10.862	0.348	148.5	20.206	0.659	147.9
4.980	0.164	147.7	11.829	0.387	147.7	22.525	0.732	148.0
5.823	0.191	147.7	12.200	0.395	148.1	25.322	0.822	148.0
6.076	0.197	148.2	13.272	0.430	148.1	27.380	0.888	148.0
7.247	0.233	148.4	14.436	0.464	148.4	29.405	0.952	148.1
8.416	0.271	148.3	14.446	0.471	147.9	33.738	1.093	148.0
9.810	0.317	148.2	16.601	0.542	147.8			
			β-CD-SN System where $C_{\beta\text{-CD}}$=1.354×10^{-2} m					
4.380	5.751	168.1	13.375	5.909	164.1	23.547	6.197	158.6
5.685	5.769	167.6	15.457	5.962	162.8	26.890	6.299	157.5
6.415	5.779	167.4	17.341	6.011	161.8	28.542	6.351	156.9
8.705	5.816	166.4	20.036	6.089	160.3	30.400	6.407	156.5
11.005	5.859	165.3	22.289	6.155	159.3	33.701	6.504	155.9
				SDec in Water				
4.216	0.121	165.8	13.075	0.378	165.6	23.182	0.660	166.0
5.461	0.158	165.6	15.978	0.460	165.8	25.012	0.708	166.2
7.515	0.220	165.2	18.329	0.525	165.9	27.519	0.780	166.1
9.379	0.271	165.7	20.987	0.598	166.0	30.909	0.874	166.2
11.001	0.318	165.7						

Table A5: continued

C_s	Δd	$V_{\phi,S}$	C_s	Δd	$V_{\phi,S}$	C_s	Δd	$V_{\phi,S}$
			β-CD-SDec System where $C_{\beta\text{-}CD}=1.344\times10^{-2}$ m					
3.553	5.692	202.4	12.222	5.866	182.0	21.792	6.114	175.8
5.260	5.708	196.6	13.856	5.902	180.8	24.878	6.187	175.0
6.960	5.778	185.8	16.755	5.973	178.8	29.090	6.292	174.1
7.933	5.792	184.9	17.936	6.000	178.3	32.529	6.399	172.9
9.263	5.821	183.2	19.347	6.035	177.6	36.501	6.504	172.3
10.747	5.840	182.9						
			DM-β-CD-SDec where [DM-β-CD]=3.969 × 10^{-3} m					
1.530	1.456	184.8	4.763	1.510	180.0	7.887	1.594	175.0
2.030	1.463	183.5	5.124	1.519	179.1	8.640	1.616	174.2
2.621	1.471	183.0	5.754	1.535	178.1	8.636	1.618	173.9
3.140	1.483	181.1	6.219	1.547	177.3	9.482	1.642	173.2
3.682	1.488	181.7	7.013	1.570	176.1	10.52	1.673	172.4
4.173	1.498	180.7						
			HP-β-CD-SDec where [HP-β-CD]=5.003× 10^{-3} m					
1.761	2.210	180.7	5.110	2.265	178.9	9.175	2.371	174.2
2.204	2.215	181.1	5.531	2.274	178.4	9.898	2.392	173.5
2.768	2.224	180.6	6.071	2.287	177.7	10.77	2.417	172.8
3.318	2.234	179.9	6.758	2.304	176.9	11.50	2.438	172.3
3.968	2.242	180.2	7.575	2.329	175.4	12.70	2.473	171.7
4.412	2.249	180.0	8.364	2.349	174.9	13.89	2.508	171.1
				SDodec in Water				
3.373	0.087	197.0	7.974	0.203	197.3	18.081	0.458	197.4
5.096	0.128	197.8	11.392	0.274	198.7	20.345	0.515	197.4
4.995	0.130	196.8	12.562	0.321	197.2	22.405	0.568	197.3
6.023	0.155	197.1	13.759	0.341	197.9	24.370	0.607	197.8
7.636	0.197	197.0	16.442	0.419	197.3	28.216	0.689	198.3
			β-CD-SDodec System where $C_{\beta\text{-}CD}=1.364\times10^{-2}$ m					
3.607	5.820	219.7	8.625	5.854	216.9	14.109	5.923	213.9
4.824	5.820	220.0	10.416	5.868	216.3	15.242	5.952	212.5
5.756	5.829	218.7	11.826	5.885	215.6	16.846	5.983	211.5
7.664	5.844	217.5	12.783	5.899	214.9			

Table A5: continued

C_s	Δd	$V_{\phi,S}$	C_s	Δd	$V_{\phi,S}$	C_s	Δd	$V_{\phi,S}$
		DM-β-CD-SDodec where [DM-β-CD]=4.036 × 10^{-3} m						
1.632	1.387	220.9	4.056	1.401	218.5	6.228	1.451	211.9
1.986	1.390	220.0	4.577	1.411	216.9	6.700	1.462	211.1
2.361	1.391	219.9	5.099	1.424	214.7	7.367	1.478	209.8
2.930	1.393	219.6	5.704	1.440	212.9	8.352	1.501	208.6
3.524	1.395	219.5						
		HP-β-CD-SDodec where [HP-β-CD]=5.170 × 10^{-3} m						
2.002	2.202	218.6	6.356	2.255	212.8	11.61	2.378	206.6
2.929	2.205	218.6	7.044	2.269	211.7	12.64	2.397	206.3
3.626	2.205	219.3	8.008	2.289	210.5	13.59	2.428	205.2
4.263	2.213	217.9	8.406	2.301	209.7	14.98	2.458	204.7
5.001	2.242	212.8	9.484	2.327	208.4	16.41	2.485	204.6
5.708	2.256	211.5	10.50	2.351	207.5	17.77	2.561	201.7
				ST in Water				
3.094	0.074	227.1	3.443	0.083	226.7	4.017	0.097	226.8
4.446	0.106	227.1	5.100	0.120	227.4			
		β-CD-ST System where $C_{\beta\text{-CD}}$=1.309×10^{-2} m						
2.072	5.852	264.9	4.922	5.837	259.2	8.086	5.852	253.6
2.550	5.846	264.3	5.537	5.840	257.5	8.192	5.853	253.4
3.205	5.841	262.9	5.970	5.860	253.7	8.451	5.858	252.8
3.797	5.837	261.9	6.601	5.850	254.8	9.593	5.861	252.0
4.342	5.838	260.3	7.067	5.858	253.4	9.719	5.862	251.9
		DM-β-CD-ST where [DM-β-CD]=4.036 × 10^{-3} m						
0.5411	1.380	253.0	1.624	1.384	249.4	2.969	1.383	250.4
0.7288	1.378	256.0	1.875	1.381	251.2	3.000	1.382	250.8
0.8674	1.379	253.5	1.996	1.382	250.8	3.556	1.385	250.0
1.075	1.381	251.7	2.194	1.382	250.8	3.791	1.387	249.5
1.313	1.377	254.1	2.430	1.384	250.0	4.130	1.392	248.3
1.457	1.379	252.4	2.711	1.381	250.9	4.542	1.402	246.3

Table A5: continued

C_s	Δd	$V_{\phi,S}$	C_s	Δd	$V_{\phi,S}$	C_s	Δd	$V_{\phi,S}$
HP-β-CD-ST where [HP-β-CD]=5.013 × 10^{-3} m								
0.5762	2.127	252.1	2.095	2.124	252.5	3.819	2.129	250.3
0.9265	2.122	257.1	2.377	2.122	253.0	4.285	2.134	249.3
1.181	2.121	256.4	2.539	2.125	251.7	4.416	2.134	249.2
1.422	2.123	254.2	2.846	2.124	252.0	4.844	2.140	248.1
1.597	2.125	252.3	3.419	2.124	251.7	5.294	2.147	247.1
1.821	2.125	252.2	3.239	2.125	251.5	5.815	2.161	244.9

[a] C_S in m($\times 10^3$), Δd in g cm^{-3}($\times 10^3$), and $V_{\phi,S}$ in cm^3 mol^{-1}.

APPENDIX A6

Table A6: Concentration(C_S), Density Difference($\Delta d = d - d_o$), and Apparent Molar Volume($V_{\phi,S}$) Data of Perfluorocarbon Sodium Akyl Carboxylate Salts in Water and Ternary (w+S+CD) Aqueous Solutions at pH 10.5 and 298 K.[a]

C_s	Δd	$V_{\phi,S}$	C_s	Δd	$V_{\phi,S}$	C_s	Δd	$V_{\phi,S}$
				SPFA in water				
4.501	0.356	56.8	12.583	0.992	57.1	25.371	1.999	57.0
5.813	0.459	56.9	14.734	1.165	56.8	24.678	1.941	57.2
7.615	0.598	57.4	15.656	1.233	57.1	33.760	2.617	58.3
9.432	0.741	57.4	18.801	1.481	57.1	42.340	3.328	57.2
10.775	0.849	57.1	21.880	1.723	57.1			
				β-CD-SPFA System where $C_{\beta\text{-CD}}=1.390\times10^{-2}$ m				
3.500	6.134	61.1	12.291	6.825	58.4	21.743	7.568	58.0
4.775	6.236	59.8	14.360	6.988	58.3	24.411	7.776	57.9
6.720	6.386	59.6	15.652	7.088	58.3	27.023	7.985	57.8
8.093	6.496	59.0	17.205	7.209	58.2	29.678	8.195	57.7
9.883	6.631	59.2	19.488	7.390	58.1	33.358	8.484	57.6
11.226	6.742	58.5						
				SPFB in Water				
3.502	0.452	106.7	11.823	1.526	106.8	21.817	2.848	105.1
5.998	0.782	105.5	13.519	1.766	105.2	24.650	3.216	105.1
6.193	0.811	104.9	15.557	2.034	105.0	25.922	3.385	105.0
8.105	1.062	104.8	17.486	2.284	105.1	29.791	3.802	107.9
9.929	1.299	105.0	19.747	2.580	105.0	31.076	4.055	105.0
				β-CD-SPFB System where $C_{\beta\text{-CD}}=1.352\times10^{-2}$ m				
4.347	6.250	114.7	13.235	7.358	112.3	24.234	8.747	110.9
5.945	6.444	114.6	16.189	7.732	111.7	26.974	9.102	110.4
5.810	6.428	114.5	17.982	7.958	111.5	28.582	9.313	110.1
7.316	6.615	113.9	18.985	8.081	111.6	30.600	9.572	109.9
9.373	6.875	113.0	21.570	8.409	111.2	33.360	9.926	109.6
11.568	7.146	112.8						
				DM-β-CD-SPFB where [DM-β-CD]=4.000 $\times 10^{-3}$ m				
1.419	1.539	112.6	5.317	2.034	109.8	9.428	2.557	109.2
1.979	1.616	108.6	5.719	2.087	109.4	10.26	2.666	109.0
2.681	1.702	109.8	6.262	2.153	109.8	11.12	2.776	108.8
3.464	1.794	111.7	6.888	2.236	109.2	11.92	2.878	108.8
4.049	1.874	110.0	7.665	2.325	110.5	13.18	3.036	108.9
4.555	1.938	109.8	8.565	2.446	109.5	14.36	3.192	108.5

Table A6: continued

C_s	Δd	$V_{\phi,S}$	C_s	Δd	$V_{\phi,S}$	C_s	Δd	$V_{\phi,S}$
			HP-β-CD-SPFB where [HP-β-CD]=5.013 × 10^{-3} m					
1.678	2.336	109.0	5.644	2.846	107.8	10.11	3.421	107.5
2.323	2.420	108.3	6.135	2.907	108.1	11.08	3.548	107.2
2.936	2.500	107.8	6.758	2.987	108.1	11.97	3.665	107.0
3.707	2.598	107.8	7.236	3.047	108.2	12.77	3.768	107.1
4.277	2.675	107.0	7.984	3.144	108.0	14.06	3.934	107.0
4.945	2.750	109.1	9.132	3.293	107.8	15.47	4.125	106.3
				SPFP in Water				
3.575	0.563	128.3	10.649	1.676	128.4	19.599	3.076	128.6
4.714	0.741	128.6	11.867	1.866	128.5	21.135	3.316	128.6
5.886	0.925	128.7	12.907	2.028	128.6	23.060	3.619	128.5
6.931	1.089	128.6	13.799	2.165	128.8	24.319	3.816	128.5
8.342	1.310	128.8	16.001	2.511	128.7	27.138	4.261	128.4
9.455	1.487	128.5	17.730	2.786	128.5	29.827	4.685	128.3
			β-CD-SPFP System where $C_{\beta\text{-CD}}$=1.357×10^{-2} m					
4.471	6.410	140.5	11.616	7.463	139.2	20.898	8.886	136.1
6.068	6.643	140.3	13.479	7.743	138.7	22.238	9.098	135.5
7.041	6.785	140.3	14.214	7.854	138.5	24.516	9.452	135.0
7.742	6.890	139.9	15.457	8.045	137.9	26.438	9.752	134.5
9.462	7.144	139.6	17.340	8.334	137.2	29.514	10.233	133.9
11.062	7.380	139.4	19.194	8.620	136.7			
				SPFH in Water				
2.893	0.134	176.4	8.139	1.704	176.3	14.323	2.995	176.3
3.926	0.823	176.2	8.645	1.813	175.9	14.609	0.673	176.5
4.459	0.206	176.4	9.230	1.931	176.3	16.596	3.467	176.5
5.032	1.055	176.2	9.330	0.431	176.4	17.257	0.794	176.5
5.287	0.246	176.0	10.244	2.143	176.4	23.650	1.087	176.5
7.003	0.326	176.1	11.337	0.525	176.3	30.018	1.368	176.9
7.197	1.507	176.3	12.257	2.562	176.5			
			β-CD-SPFH System where $C_{\beta\text{-CD}}$=1.381×10^{-2} m					
3.373	6.375	220.8	11.457	8.199	213.0	21.498	10.556	206.9
4.910	6.709	219.9	13.388	8.656	210.9	24.275	11.201	206.3
6.104	6.973	218.9	15.244	9.087	209.8	26.238	11.659	205.8
7.828	7.362	216.8	17.149	9.526	209.2	28.383	12.161	205.3
9.699	7.790	214.9	18.698	9.891	208.3	30.519	12.659	205.0

Table A6: continued

C_s	Δd	$V_{\phi.s}$	C_s	Δd	$V_{\phi.s}$	C_s	Δd	$V_{\phi.s}$
			DM-β-CD-SPFH where [DM-β-CD]=4.112 × 10^{-3} m					
1.253	1.672	190.8	5.221	2.462	187.7	9.245	3.302	182.9
1.811	1.780	191.3	5.883	2.601	186.3	9.854	3.433	182.1
2.524	1.920	190.7	6.314	2.691	185.7	10.49	3.567	181.8
3.182	2.048	190.9	7.056	2.846	184.8	11.25	3.721	181.8
3.654	2.139	191.1	7.347	2.906	184.6	11.87	3.851	181.4
4.207	2.248	191.0	8.373	3.120	183.5	13.17	4.125	180.7
4.760	2.366	188.6						
			HP-β-CD-SPFH where [HP-β-CD]=5.074 × 10^{-3} m					
1.283	2.401	187.7	4.548	3.047	187.9	8.384	3.845	183.1
1.994	2.540	188.9	5.149	3.169	187.2	9.099	3.995	182.6
2.537	2.648	188.2	5.557	3.253	186.7	9.764	4.132	182.3
3.026	2.743	188.8	6.090	3.366	185.6	10.61	4.309	181.9
3.547	2.845	188.9	6.856	3.524	184.8	11.73	4.543	181.4
4.021	2.944	187.6	7.634	3.687	183.9	12.77	4.761	180.8
				SPFO in Water				
3.283	0.778	199.0	11.687	2.750	200.1	21.314	5.002	200.3
4.472	1.062	198.3	13.541	3.192	199.6	23.290	5.459	200.5
5.682	1.339	200.1	15.084	3.540	200.6	24.727	5.799	200.3
7.309	1.722	200.1	17.692	4.154	200.4	29.336	6.870	200.4
9.374	2.211	199.7	18.922	4.444	200.2			
			β-CD-SPFO System where $C_{\beta\text{-CD}}$=1.304×10^{-2} m					
3.373	6.375	220.8	11.457	8.199	213.0	21.498	10.556	206.9
4.910	6.709	219.9	13.388	8.656	210.9	24.275	11.201	206.3
6.104	6.973	218.9	15.244	9.087	209.8	26.238	11.659	205.8
7.828	7.362	216.8	17.149	9.526	209.2	28.383	12.161	205.3
9.699	7.790	214.9	18.698	9.891	208.3	30.519	12.659	205.0
			DM-β-CD-SPFO where [DM-β-CD]=3.975 × 10^{-3} m					
1.314	1.675	215.0	3.430	2.142	215.1	7.056	2.984	208.9
1.534	1.721	216.3	3.743	2.210	215.3	7.446	3.076	208.5
1.767	1.772	216.7	4.346	2.348	214.2	8.203	3.252	207.9
2.249	1.878	215.7	4.861	2.471	212.3	9.215	3.490	207.1
2.429	1.920	215.3	5.464	2.612	211.0	10.15	3.710	206.4
2.935	2.030	215.8	6.518	2.858	209.6			

Table A6: continued

C_s	Δd	$V_{\phi.S}$	C_s	Δd	$V_{\phi.S}$	C_s	Δd	$V_{\phi.S}$
			HP-β-CD-SPFO where [HP-β-CD]=5.074 × 10^{-3} m					
1.749	2.547	208.9	6.086	3.529	209.1	11.20	4.736	204.7
2.789	2.776	211.5	6.832	3.704	208.3	12.23	4.976	204.4
3.335	2.901	210.7	7.495	3.861	207.4	13.29	5.224	204.1
4.235	3.104	210.6	8.110	4.002	207.3	14.20	5.434	204.1
4.731	3.217	210.4	9.005	4.216	206.2	15.36	5.706	203.9
5.447	3.381	209.8	10.08	4.473	205.0			
			DM-β-CD-SPFO where [DM-β-CD]=1.299 × 10^{-3} m					
4.265	5.397	214.0	10.52	6.781	214.1	18.89	8.73	208.6
5.104	5.581	214.3	11.62	7.025	213.8	20.55	9.117	208.0
6.341	5.858	213.6	12.73	7.284	212.8	21.53	9.346	207.7
7.379	6.087	213.9	14.01	7.586	211.5	23.71	9.854	207.1
8.314	6.294	213.9	16.28	8.117	210.1	24.79	10.11	206.7
9.483	6.551	214.0	17.57	8.421	209.3	26.63	10.53	206.5
				SPFN in Water				
3.214	0.840	224.4	6.133	1.607	223.6	9.519	2.495	223.3
4.114	1.080	223.2	5.469	1.433	223.6	10.527	2.757	223.4
4.675	1.224	223.9	8.116	2.127	223.4	11.799	3.080	224.3
5.641	1.478	223.6						
			β-CD-SPFN System where $C_{\beta\text{-}CD}$=1.309×10^{-2} m					
3.423	6.693	258.0	8.612	7.968	247.0	13.312	9.246	235.0
3.818	6.790	256.4	10.007	8.341	242.9	15.228	9.756	232.9
4.808	7.017	256.3	11.087	8.636	239.9	16.566	10.113	231.7
5.782	7.250	254.5	11.614	8.782	238.5	18.694	10.677	230.3
6.418	7.405	253.4	12.418	9.004	236.6	20.652	11.193	229.3
7.227	7.608	251.1						
			DM-β-CD-SPFN where [DM-β-CD]=4.024 × 10^{-3} m					
1.757	1.828	241.6	4.758	2.573	239.1	8.414	3.482	238.0
2.329	1.968	241.6	5.197	2.687	237.9	9.204	3.674	238.3
2.836	2.091	241.8	5.697	2.814	237.3	10.46	3.978	238.9
3.282	2.201	241.5	6.413	2.994	236.9	10.49	3.987	238.7
3.735	2.313	241.12	7.072	3.156	237.2	11.99	4.354	239.0
4.248	2.441	240.4	7.804	3.333	237.8			

Table A6: continued

C_s	Δd	$V_{\phi,S}$	C_s	Δd	$V_{\phi,S}$	C_s	Δd	$V_{\phi,S}$
			DM-β-CD-SPFN where [DM-β-CD]=1.486 × 10^{-3} m					
2.538	5.702	243.8	6.468	6.667	241.5	11.41	7.876	241.0
3.197	5.862	243.6	6.994	6.797	241.3	12.45	8.128	241.0
3.857	6.024	243.0	7.685	6.965	241.3	12.00	8.023	240.8
4.506	6.183	242.7	8.280	7.111	241.2	13.84	8.471	240.9
5.053	6.320	241.9	9.575	7.425	241.3	16.16	9.044	240.4
5.641	6.463	241.9	10.50	7.652	241.2			
			HP-β-CD/$C_9F_{17}O_2Na$ where [HP-β-CD]=5.105 × 10^{-3} m					
0.9805	2.407	237.9	3.586	3.050	238.7	6.566	3.814	234.3
1.502	2.537	237.5	4.006	3.155	238.4	7.178	3.975	233.3
1.982	2.654	238.4	4.377	3.248	238.1	7.732	4.119	232.7
2.438	2.767	238.5	4.765	3.347	237.5	8.394	4.293	231.9
2.781	2.852	238.4	5.366	3.502	236.4	9.228	4.507	231.5
3.182	2.951	238.6	6.000	3.668	235.1	10.06	4.722	231.1
				SPFD in Water				
0.241	0.071	243.7	0.864	0.251	245.1	1.188	0.346	244.6
0.399	0.117	242.2	1.026	0.300	244.1	1.188	0.345	245.3
			β-CD-SPFD System where $C_{\beta\text{-}CD}$=1.323×10^{-2} m					
0.879	5.810	282.9	2.766	6.296	279.7	4.703	6.803	277.3
1.391	5.942	281.3	3.228	6.417	278.9	5.054	6.897	276.6
1.832	6.053	281.7	3.610	6.515	279.0	5.670	7.069	274.3
2.346	6.191	278.7	4.175	6.665	277.7			
			DM-β-CD-SPFD where [DM-β-CD]=4.281 × 10^{-3} m					
1.161	1.800	262.8	2.393	2.137	262.6	3.873	2.545	261.5
1.392	1.863	262.6	2.954	2.290	262.7	3.926	2.560	261.5
1.585	1.915	263.8	2.693	2.220	262.3	4.374	2.685	260.8
1.804	1.976	262.8	3.288	2.383	262.1	4.638	2.760	260.6
2.031	2.038	262.5	3.374	2.407	262.0	5.011	2.867	259.6
2.199	2.083	263.2						

Table A6: continued

C_s	Δd	$V_{\phi,S}$	C_s	Δd	$V_{\phi,S}$	C_s	Δd	$V_{\phi,S}$
HP-β-CD-SPFD where [HP-β-CD]=5.105 × 10^{-3} m								
0.6021	2.328	258.2	2.169	2.755	261.7	4.007	3.260	261.4
0.8717	2.400	261.2	2.432	2.827	261.6	4.354	3.355	261.3
1.252	2.504	261.9	2.696	2.901	261.3	4.648	3.436	261.4
1.549	2.587	260.7	2.901	2.956	261.6	4.723	3.462	260.1
1.745	2.637	262.8	3.307	3.070	260.8	5.597	3.705	259.6
1.960	2.695	263.4	3.633	3.163	259.8	6.121	3.851	259.4

[a] C_S in m($\times 10^3$), Δd in g cm^{-3}($\times 10^3$), and $V_{\phi,S}$ in cm^3 mol^{-1}.

APPENDIX A7

Table A7: Concentration(C_{CD}), Density Difference($\Delta d = d - d_o$), and Apparent Molar Volume($V_{\phi,CD}$) Data of Cyclodextrins in Water at pH 10.5 and 298 K.

C_{CD}	Δd	$V_{\phi,CD}$	C_{CD}	Δd	$V_{\phi,CD}$	C_{CD}	Δd	$V_{\phi,CD}$
				β-CD in water				
2.253	0.965	707.0	5.313	2.268	707.3	8.519	3.635	706.5
2.619	1.123	706.3	5.807	2.482	706.7	9.380	3.999	706.7
2.693	1.155	706.2	5.860	2.504	706.7	9.550	4.072	706.6
3.205	1.372	706.6	6.420	2.741	706.9	10.368	4.417	706.7
3.248	1.392	706.3	6.421	2.743	706.7	10.416	4.437	706.7
3.693	1.581	706.7	6.909	2.950	706.8	10.652	4.538	706.6
3.703	1.586	706.4	7.102	3.034	706.6	11.455	4.876	706.7
4.242	1.816	706.4	7.456	3.182	706.8	11.660	4.963	706.7
4.248	1.816	707.1	7.952	3.394	706.6	12.603	5.365	706.4
4.626	1.977	707.2	7.967	3.398	706.9	13.437	5.711	706.8
4.746	2.031	706.4	8.506	3.629	706.7	13.450	5.722	706.4
5.237	2.240	706.5						
				DM-β-CD in water				
2.403	0.8362	984.1	5.889	2.032	985.8	8.934	3.073	986.0
3.029	1.051	984.9	6.694	2.311	985.4	11.02	3.778	986.2
3.611	1.251	985.3	7.244	2.500	985.4	11.67	3.999	986.4
4.261	1.477	984.3	8.216	2.829	985.8	13.62	4.655	986.6
4.875	1.686	985.4	9.168	3.153	985.9	15.43	5.260	986.8
5.379	1.862	985.0	9.979	3.428	985.9			
				HP-β-CD in water				
1.945	0.8294	958.3	5.002	2.122	959.3	8.966	3.787	959.6
2.462	1.048	958.7	5.411	2.295	959.2	9.802	4.137	959.5
2.973	1.266	958.4	5.943	2.519	959.4	10.44	4.404	959.5
3.396	1.445	958.6	6.751	2.860	959.2	11.41	4.811	959.4
3.990	1.696	958.8	7.387	3.125	959.5	11.73	4.944	959.4
4.495	1.911	958.6	7.976	3.373	959.4			

[a] C_{CD} in m($\times 10^3$), Δd in g cm^{-3}($\times 10^3$), and $V_{\phi,S}$ in cm^3 mol^{-1}.

APPENDIX A8

Table A8: Concentration(C_{CD}), Density Difference($\Delta d=d-d_o$), and Apparent Molar Volume($V_{\phi,CD}$) Data of Cyclodextrins in Water and Ternary (w+S+CD) Aqueous Sodium Alkyl Carboxylate Solutions at pH 10.5 and 298 K.

C_{CD}	Δd	$V_{\phi,CD}$	C_{CD}	Δd	$V_{\phi,CD}$	C_{CD}	Δd	$V_{\phi,CD}$
			β-CD-SHex where [SHex]=5.093×10^{-3} m					
2.197	1.111	714.9	5.386	2.450	714.2	8.565	3.781	713.7
2.656	1.304	714.7	5.951	2.689	713.7	10.510	4.594	713.5
3.229	1.544	715.0	6.457	2.901	713.8	11.335	4.944	712.9
3.797	1.783	714.7	7.218	3.218	713.8	12.192	5.307	712.3
4.349	2.015	714.4	8.166	3.614	713.8	13.568	5.882	712.1
4.870	2.234	714.3	8.828	3.891	713.7			
			β-CD-SHex where [SHex]=2.960×10^{-2} m					
2.908	2.275	723.2	6.280	3.665	721.7	9.868	5.136	721.4
3.472	2.507	723.0	6.868	3.907	721.6	11.265	5.711	721.0
4.002	2.729	721.9	7.783	4.281	721.8	12.103	6.053	720.9
4.592	2.970	722.3	8.630	4.628	721.7	13.211	6.507	720.7
5.147	3.198	722.3	9.506	4.987	721.6	14.486	7.029	720.5
5.725	3.434	722.5						
			β-CD-SHex where [SHex]=6.003×10^{-2} m					
2.554	3.204	725.7	5.555	4.434	724.3	9.170	5.909	723.7
3.084	3.422	725.3	6.150	4.677	724.2	9.993	6.245	723.5
3.650	3.653	725.3	6.895	4.980	724.2	10.713	6.540	723.2
4.072	3.825	725.3	7.629	5.278	724.3	11.786	6.981	722.8
4.619	4.050	724.7	8.460	5.616	724.3	12.882	7.425	722.8
5.141	4.262	724.8						
			β-CD-SHex where [SHex]=1.200×10^{-2} m					
2.825	5.484	730.0	5.965	6.757	728.0	9.775	8.299	727.0
3.232	5.648	729.8	6.472	6.962	727.9	10.559	8.615	726.9
3.698	5.838	729.1	7.172	7.249	727.3	11.505	8.993	727.0
4.283	6.076	728.6	8.143	7.640	727.3	12.017	9.199	727.0
4.912	6.331	728.4	8.948	7.965	727.1	13.675	9.869	726.4
5.632	6.621	728.4						

APPENDIX A8
Table A8: continued

C_{CD}	Δd	$V_{\phi,CD}$	C_{CD}	Δd	$V_{\phi,CD}$	C_{CD}	Δd	$V_{\phi,CD}$
		DM-β-CD-SHex where $[C_6H_{11}O_2Na]=4.006 \times 10^{-3}$ m						
1.576	0.6913	986.1	5.081	1.897	986.4	9.216	3.310	986.4
2.024	0.8452	986.4	5.552	2.060	986.2	10.00	3.571	986.9
2.542	1.025	985.9	5.957	2.198	986.3	10.65	3.797	986.5
3.080	1.208	986.8	6.480	2.375	986.5	11.59	4.113	986.7
3.569	1.377	986.7	7.546	2.738	986.7	12.04	4.264	986.7
4.045	1.542	986.3	8.387	3.022	987.0	12.82	4.528	986.7
4.551	1.715	986.4						
		DM-β-CD-SHex where $[C_6H_{11}O_2Na]=2.000 \times 10^{-3}$ m						
1.995	1.395	988.5	5.358	2.546	987.9	9.563	3.973	987.9
2.576	1.594	988.3	5.850	2.712	988.2	10.43	4.268	987.9
3.198	1.808	987.8	6.379	2.894	987.9	11.18	4.518	988.1
3.673	1.969	988.3	7.069	3.128	987.9	12.09	4.825	987.9
4.124	2.125	987.8	7.891	3.407	987.9	12.67	5.018	988.1
4.908	2.393	987.9	8.867	3.737	988.1	13.42	5.275	987.9
		HP-β-CD-SHex where $[C_6H_{11}O_2Na]=4.999 \times 10^{-3}$ m						
1.347	0.756	960.1	4.632	2.141	960.9	8.527	3.769	961.5
2.031	1.044	961.0	5.139	2.354	961.1	9.305	4.097	961.1
2.576	1.273	961.3	5.716	2.597	960.9	10.01	4.392	961.1
3.050	1.472	961.8	6.201	2.799	961.2	10.81	4.723	961.2
3.543	1.682	961.3	6.948	3.113	961.1	11.74	5.109	961.2
4.079	1.907	961.3	7.526	3.354	961.2	13.01	5.635	961.1
		β-CD-SO where $[SO]=1.515\times10^{-2}$ m						
2.153	1.371	730.4	5.162	2.597	728.1	9.407	4.313	727.7
2.672	1.587	728.4	5.670	2.800	728.5	9.952	4.531	727.8
3.119	1.762	730.2	6.269	3.044	728.2	10.524	4.762	727.7
3.730	2.018	727.9	6.941	3.316	728.1	11.688	5.233	727.4
4.100	2.166	728.2	7.733	3.635	728.2	13.100	5.805	727.0
4.810	2.456	727.8	8.520	3.950	728.3			
		β-CD-SO where $[SO]=5.997\times10^{-2}$ m						
2.637	3.007	730.5	5.739	4.269	728.0	9.451	5.765	728.0
3.129	3.207	729.7	6.213	4.461	728.0	10.119	6.033	728.0
3.619	3.410	728.5	7.004	4.780	728.0	10.921	6.355	728.0
4.186	3.638	728.7	7.746	5.076	728.3	11.901	6.750	727.7
4.669	3.842	726.9	8.602	5.423	728.1	13.153	7.254	727.5
5.201	4.053	727.7						

Table A8: continued

C_{CD}	Δd	$V_{\phi,CD}$	C_{CD}	Δd	$V_{\phi,CD}$	C_{CD}	Δd	$V_{\phi,CD}$
			β-CD-SO where [SO]=1.203×10^{-2} m					
2.471	4.854	732.3	5.450	6.053	730.8	8.762	7.382	730.3
2.940	5.042	732.0	5.932	6.247	730.7	9.524	7.687	730.2
3.441	5.245	731.5	6.630	6.526	730.8	10.389	8.034	730.0
3.930	5.440	731.7	7.368	6.824	730.4	11.384	8.434	729.7
4.430	5.645	730.7	8.162	7.140	730.6	12.411	8.842	729.7
4.891	5.828	731.2						
			DM-β-CD-SO where [$C_8H_{15}O_2Na$]=4.054 × 10^{-3} m					
1.697	0.7116	995.4	4.373	1.620	992.9	6.640	2.391	991.6
2.231	0.8944	993.8	4.886	1.793	992.8	7.596	2.716	991.1
2.818	1.094	993.3	5.531	2.014	992.2	8.243	2.930	991.6
3.297	1.253	994.0	6.103	2.208	991.9	9.086	3.216	991.2
3.802	1.425	993.4						
			HP-β-CD-SO where [$C_8H_{15}O_2Na$]=5.001 × 10^{-3} m					
1.540	0.8098	970.0	4.692	2.122	967.7	8.625	3.758	966.2
2.122	1.052	969.6	5.238	2.348	967.7	9.528	4.131	966.0
2.587	1.246	969.0	5.758	2.566	967.3	10.23	4.423	965.6
3.145	1.479	968.3	6.305	2.794	967.0	10.64	4.592	965.5
3.665	1.695	968.2	7.097	3.123	967.0	11.91	5.116	965.6
4.194	1.915	967.9	7.681	3.363	966.9	13.22	5.664	964.6
			β-CD-SDec where [SDec]=4.995×10^{-3} m					
2.741	1.271	723.3	6.063	2.660	718.7	9.942	4.304	714.3
3.347	1.523	722.1	6.103	2.676	718.8	10.753	4.651	713.2
3.937	1.766	722.1	7.468	3.256	716.7	11.638	5.028	712.5
4.435	1.979	720.4	8.263	3.597	715.3	12.130	5.240	711.9
5.039	2.229	720.2	9.139	3.964	714.9	13.951	6.009	711.1
5.496	2.419	720.0						
			β-CD-SDec where [SDec]=6.137×10^{-2} m					
2.634	2.784	730.5	5.916	4.108	729.8	9.700	5.632	729.2
3.194	3.009	730.6	6.407	4.306	729.7	10.528	5.964	729.1
3.698	3.212	730.6	7.212	4.630	729.7	11.292	6.273	728.8
4.470	3.527	729.7	8.024	4.957	729.5	11.789	6.470	728.9
4.820	3.663	730.6	8.835	5.282	729.6	13.551	7.177	728.6
5.403	3.901	729.9						

Table A8: continued

C_{CD}	Δd	$V_{\phi,CD}$	C_{CD}	Δd	$V_{\phi,CD}$	C_{CD}	Δd	$V_{\phi,CD}$
		DM-β-CD-SDec where $[C_{10}H_{19}O_2Na]=4.027 \times 10^{-3}$ m						
1.469	0.6030	1005.0	4.061	1.466	1000.7	7.622	2.678	994.9
2.055	0.7973	1003.5	4.661	1.666	1000.1	8.360	2.931	994.1
2.312	0.8810	1003.8	5.180	1.844	998.6	8.948	3.129	993.8
2.560	0.9637	1003.2	5.626	1.996	997.9	9.922	3.461	993.1
3.128	1.153	1002.3	6.164	2.178	997.4	10.49	3.655	992.7
3.591	1.308	1001.4	6.960	2.451	996.0			
		HP-β-CD-SDec where $[C_{10}H_{19}O_2Na]=5.121 \times 10^{-3}$ m						
1.196	0.6403	978.8	4.408	1.948	977.0	8.182	3.500	973.4
1.986	0.9631	977.7	4.956	2.173	976.3	8.957	3.818	973.0
2.461	1.154	978.6	5.457	2.378	975.9	9.682	4.120	972.1
2.996	1.376	976.5	5.961	2.582	975.9	10.48	4.450	971.5
3.510	1.581	977.6	6.586	2.840	975.2	11.39	4.828	970.7
3.950	1.760	977.5	7.492	3.214	974.2	12.52	5.300	969.9
		β-CD-SDodec where $[SDodec]=5.170\times10^{-3}$ m						
2.567	1.173	731.3	5.505	2.372	728.0	8.695	3.707	722.7
3.123	1.398	731.0	6.024	2.588	727.2	9.634	4.103	721.3
3.398	1.509	730.7	6.777	2.905	725.3	10.463	4.445	720.9
3.478	1.543	730.5	7.488	3.201	724.3	11.359	4.821	720.0
3.913	1.720	730.0	8.318	3.549	723.1	12.581	5.329	719.4
4.950	2.143	729.0						
		β-CD-SDodec where $[SDodec]=1.997\times10^{-2}$ m						
2.681	1.587	731.0	5.607	2.767	730.6	9.009	4.143	729.2
3.150	1.777	730.7	6.183	3.000	730.2	10.112	4.589	728.8
3.599	1.955	731.6	6.777	3.241	730.0	10.515	4.753	728.6
3.908	2.081	731.2	7.772	3.642	729.7	11.462	5.138	728.1
4.649	2.380	730.8	8.406	3.900	729.4	12.968	5.748	727.6
5.114	2.567	730.9						
		DM-β-CD-SDodec System where $[C_{12}H_{23}O_2Na]=4.010 \times 10^{-3}$ m						
1.602	0.6491	1006.3	5.247	1.851	1002.5	9.386	3.264	995.5
2.107	0.8114	1007.3	5.822	2.048	1001.0	10.25	3.558	994.6
2.677	0.9958	1007.5	6.371	2.237	999.5	10.90	3.777	994.2
3.126	1.142	1007.2	6.618	2.325	998.5	11.54	3.994	993.8
3.665	1.319	1006.5	7.103	2.488	998.1	12.66	4.372	993.2
4.270	1.519	1005.4	7.757	2.711	997.2	13.29	4.585	993.0
4.709	1.668	1004.0						

Table A8: continued

C_{CD}	Δd	$V_{\phi,CD}$	C_{CD}	Δd	$V_{\phi,CD}$	C_{CD}	Δd	$V_{\phi,CD}$
			HP-β-CD-SDodec where $[C_{12}H_{23}O_2Na]=5.017\times10^{-3}$ m					
1.335	0.6724	988.2	4.842	2.095	983.0	8.854	3.761	974.7
2.170	1.010	990.7	5.375	2.312	982.0	9.622	4.090	973.9
3.269	1.455	986.6	5.950	2.551	980.5	10.44	4.419	972.7
3.765	1.655	985.7	6.466	2.751	981.4	11.41	4.824	971.7
2.722	1.234	987.9	7.244	3.089	977.6	11.94	5.044	971.2
4.225	1.843	984.4	7.963	3.388	976.3	13.54	5.710	969.8
			β-CD-ST where $[ST]=2.034\times10^{-3}$ m					
2.512	1.089	723.4	5.604	2.395	716.5	9.348	3.983	712.7
2.930	1.263	722.2	6.251	2.670	715.5	10.117	4.304	712.7
3.774	1.619	720.0	7.227	3.085	714.3	10.880	4.633	711.7
4.157	1.782	718.9	7.893	3.366	713.9	11.787	5.014	711.5
5.871	2.026	798.9	8.649	3.688	713.1	13.383	5.696	710.3
5.146	2.202	717.0						
			β-CD-ST where $[ST]=5.158\times10^{-3}$ m					
3.627	1.604	728.3	6.054	2.584	728.8	9.814	4.126	725.8
4.175	1.829	727.6	6.720	2.856	728.3	10.393	4.362	725.6
4.410	1.918	729.1	7.544	3.194	727.5	10.923	4.579	725.3
4.988	2.156	728.3	8.309	3.508	726.9	12.832	5.363	724.3
5.568	2.391	728.2	8.979	3.785	726.6			
			DM-β-CD-ST where $[C_{14}H_{27}O_2Na]=1.004\times10^{-3}$ m					
0.7941	0.2828	1010.1	2.009	0.6975	998.4	3.553	1.234	992.0
0.9880	0.3465	1008.9	2.179	0.7585	996.3	3.885	1.345	992.2
1.168	0.4064	1007.3	2.394	0.8315	995.9	4.036	1.399	991.6
1.438	0.4991	1003.8	2.668	0.9264	994.7	3.699	1.283	992.0
1.613	0.5600	1001.7	2.973	1.029	994.9	4.522	1.562	991.8
1.763	0.6134	999.4	3.315	1.149	993.3	5.012	1.739	989.5
			HP-β-CD-ST where $[C_{14}H_{27}O_2Na]=1.002\times10^{-3}$ m					
1.347	0.5777	976.2	4.751	2.012	965.9	8.701	3.667	963.6
2.012	0.8557	973.0	5.239	2.216	965.7	9.101	3.835	963.5
2.675	1.136	970.1	5.697	2.408	965.3	10.25	4.315	963.1
3.165	1.343	968.6	6.322	2.671	964.8	11.10	4.668	962.9
3.659	1.552	967.3	7.229	3.052	964.2	11.86	4.989	962.5
4.247	1.798	966.9	8.051	3.397	963.8			

[a] C_{CD} in m($\times10^3$), Δd in g cm^{-3}($\times10^3$), and $V_{\phi,CD}$ in cm^3 mol^{-1}.

APPENDIX A9

Table A9: Concentration(C_{CD}), Density Difference($\Delta d=d-d_o$), and Apparent Molar Volume($V_{\phi,CD}$) Data of Cyclodextrins in Water and Ternary (w+S+CD) Aqueous Sodium Perfluoroalkyl Carboxylate Solutions at pH 10.5 and 298 K.

C_{CD}	Δd	$V_{\phi,CD}$	C_{CD}	Δd	$V_{\phi,CD}$	C_{CD}	Δd	$V_{\phi,CD}$
			β-CD-SPFA where [SPFA]=4.691×10^{-3} m					
1.980	1.208	711.8	4.870	2.432	710.7	8.782	4.080	710.6
2.448	1.407	711.2	5.352	2.636	710.6	9.216	4.270	709.7
2.946	1.617	711.5	5.863	2.851	710.7	10.218	4.686	710.3
3.467	1.839	711.0	6.632	3.175	710.7	11.306	5.140	710.4
3.958	2.046	711.1	7.337	3.471	710.9	12.357	5.583	710.2
4.458	2.257	711.1	7.874	3.699	710.6			
			β-CD-SPFA where [SPFA]=5.950×10^{-2} m					
2.735	5.793	715.5	5.886	7.121	712.9	9.656	8.704	711.7
3.245	6.010	714.3	6.391	7.337	712.0	10.450	9.040	711.2
3.677	6.192	714.0	6.655	7.443	712.7	11.179	9.340	711.6
4.321	6.463	713.5	7.970	7.995	712.4	12.294	9.810	711.1
4.813	6.670	713.3	8.836	8.361	711.8	13.432	10.285	710.9
5.295	6.874	712.8						
			β-CD-SPFA where [SPFA]=1.200×10^{-1} m					
2.476	10.005	719.6	5.535	11.288	715.0	8.977	12.722	714.0
2.983	10.215	719.1	6.001	11.485	714.6	9.805	13.070	713.5
3.405	10.392	718.2	6.697	11.772	714.8	10.755	13.462	713.6
3.907	10.602	717.6	7.368	12.058	713.7	11.406	13.728	713.9
4.499	10.851	716.7	8.205	12.415	712.5	12.551	14.203	713.5
5.024	11.071	716.1						
			β-CD-SPFA where [SPFA]=2.330×10^{-1} m					
2.649	19.024	725.6	5.760	20.308	719.9	9.641	21.904	717.8
3.236	19.264	724.2	6.092	20.444	719.7	10.412	22.218	717.7
3.777	19.491	722.1	7.204	20.907	718.2	11.195	22.540	717.3
4.248	19.684	721.8	7.970	21.218	718.4	11.872	22.817	717.2
4.818	19.922	720.4	8.971	21.631	717.7	13.441	23.463	716.5
5.311	20.125	720.0						
			β-CD-SPFB where [SPFB]=4.900×10^{-3} m					
2.552	1.734	715.8	5.638	3.025	715.3	9.045	4.450	714.5
3.084	1.956	716.1	6.115	3.222	715.7	9.924	4.820	714.0
3.609	2.174	716.4	6.985	3.591	714.7	10.680	5.138	713.6
4.118	2.388	716.0	7.659	3.870	714.6	12.890	6.065	712.9
5.116	2.805	715.9						

Table A9: continued

C_{CD}	Δd	$V_{\phi,CD}$	C_{CD}	Δd	$V_{\phi,CD}$	C_{CD}	Δd	$V_{\phi,CD}$
			β-CD-SPFB where [SPFB]=6.000×10^{-2} m					
2.551	8.908	723.2	5.772	10.237	720.5	9.372	11.720	719.2
3.143	9.152	722.5	6.319	10.464	720.1	10.294	12.098	719.0
3.641	9.359	721.6	7.145	10.801	720.3	10.431	12.155	718.9
4.231	9.598	722.0	7.898	11.104	720.7	12.077	12.833	718.4
4.691	9.791	721.1	8.443	11.335	719.7	13.329	13.357	717.4
5.240	10.019	720.5						
			β-CD-SPFB where [SPFB]=1.200×10^{-1} m					
2.692	16.479	731.0	5.821	17.755	725.5	9.201	19.141	722.3
3.215	16.696	728.4	6.371	17.986	723.9	10.405	19.622	722.6
3.630	16.861	728.8	7.082	18.278	723.3	11.062	19.897	721.7
4.189	17.092	727.0	7.963	18.635	723.0	12.248	20.380	721.3
4.845	17.357	726.5	8.759	18.954	723.2	13.556	20.915	720.6
5.356	17.571	724.9						
			DM-β-CD-SPFB System where [$C_4F_7O_2Na$]=5.016 × 10^{-3} m					
1.412	1.128	991.0	4.561	2.200	990.3	8.427	3.511	989.7
2.062	1.349	990.8	5.015	2.352	990.6	9.279	3.796	989.9
2.579	1.524	991.1	5.667	2.576	990.0	10.074	4.067	989.5
3.020	1.674	991.0	6.073	2.713	990.0	10.835	4.320	989.7
3.544	1.852	990.9	7.093	3.056	990.3	11.968	4.701	989.7
4.099	2.041	990.7	7.142	3.073	990.2	13.028	5.060	989.3
			HP-β-CD-SPFB where [$C_4F_7O_2Na$]=5.016 × 10^{-3} m					
1.362	1.219	965.3	4.886	2.700	963.3	9.181	4.492	962.8
2.230	1.584	964.4	5.442	2.931	963.4	9.967	4.819	962.7
2.644	1.757	964.4	6.175	3.238	963.3	10.860	5.190	962.6
3.271	2.020	964.3	6.586	3.411	963.0	11.01	5.252	962.4
3.861	2.269	963.8	7.455	3.772	963.1	12.57	5.903	962.3
4.436	2.509	963.8	8.253	4.105	963.0	13.92	6.470	961.4
			β-CD-SPFH where [SPFH]= 4.983×10^{-3} m					
2.108	1.930	717.4	5.293	3.258	716.8	9.303	4.957	712.9
2.544	2.109	718.7	5.777	3.463	716.2	10.189	5.330	712.5
3.158	2.366	717.9	6.354	3.709	715.2	11.041	5.689	712.1
3.689	2.586	718.0	6.988	3.977	714.6	10.833	5.601	712.2
4.251	2.822	717.6	7.850	4.342	713.9	13.354	6.664	711.2
4.736	3.023	717.7	8.619	4.666	713.4			

Table A9: continued

C_{CD}	Δd	$V_{\phi,CD}$	C_{CD}	Δd	$V_{\phi,CD}$	C_{CD}	Δd	$V_{\phi,CD}$
			β-CD-SPFH where [SPFH]= 3.031×10^{-2} m					
2.160	7.213	720.5	5.354	8.530	719.7	9.513	10.242	718.9
2.658	7.422	718.9	5.902	8.754	720.1	9.687	10.311	719.2
3.256	7.665	720.2	6.434	8.974	719.8	11.363	10.999	718.9
3.780	7.881	720.1	7.279	9.322	719.6	12.369	11.411	718.8
4.353	8.119	719.7	8.018	9.625	719.4	13.616	11.918	718.9
4.833	8.316	719.8	8.972	10.018	719.3			
			DM-β-CD-SPFH where $[C_7F_{13}O_2Na]=3.998\times10^{-3}$ m					
1.740	1.421	999.1	5.173	2.570	996.6	9.183	3.941	991.9
2.020	1.513	999.4	5.642	2.731	995.7	10.22	4.293	991.3
2.631	1.716	999.2	5.913	2.824	995.2	10.78	4.482	991.0
2.964	1.828	998.6	6.480	3.016	994.7	11.39	4.690	990.7
3.532	2.017	998.5	7.674	3.426	993.1	13.09	5.265	990.1
4.662	2.395	997.7	8.542	3.723	992.2			
			DM-β-CD-SPFH where $[C_7F_{13}O_2Na]=2.515\times10^{-2}$ m					
2.048	5.916	1000.9	5.098	6.911	1001.0	9.171	8.246	999.2
2.584	6.091	1001.0	5.647	7.089	1000.9	10.06	8.522	1000.3
3.036	6.239	1001.0	6.082	7.231	1000.9	10.79	8.762	1000.1
3.605	6.423	1001.5	6.880	7.492	1000.6	11.45	8.977	999.7
4.127	6.594	1001.2	7.762	7.779	1000.4	12.00	9.155	999.6
4.635	6.761	1000.9	8.500	8.019	1000.3	12.98	9.486	998.5
			HP-β-CD-SPFH where $[C_7F_{13}O_2Na]=5.016\times10^{-3}$ m					
1.360	1.617	970.5	4.751	3.010	971.4	8.993	4.775	967.6
2.140	1.935	972.1	5.368	3.265	971.0	9.847	5.132	967.0
2.691	2.166	970.5	5.971	3.515	970.5	10.53	5.415	966.6
3.285	2.408	971.6	6.603	3.779	969.6	11.40	5.778	966.1
3.771	2.607	971.6	7.293	4.066	969.1	12.32	6.162	965.6
4.314	2.830	971.6	7.819	4.286	968.6	13.74	6.751	964.7
			β-CD-SPFO where [SPFO]= 5.190×10^{-3} m					
2.110	2.095	724.2	5.224	3.380	722.1	9.384	5.112	718.8
2.645	2.318	722.8	5.691	3.582	720.1	10.108	5.414	718.5
3.141	2.520	723.3	6.256	3.810	720.9	10.891	5.739	718.1
3.649	2.730	723.0	7.092	4.159	720.2	11.827	6.131	717.5
4.184	2.952	722.2	7.794	4.449	720.0	13.091	6.660	716.7
4.759	3.188	722.3	8.637	4.804	719.0			

Table A9: continued

C_{CD}	Δd	$V_{\phi,CD}$	C_{CD}	Δd	$V_{\phi,CD}$	C_{CD}	Δd	$V_{\phi,CD}$
			β-CD-SPFO where [SPFO]= 3.009×10^{-2} m					
2.507	8.068	725.3	5.557	9.317	723.3	9.011	10.726	722.7
3.008	8.277	723.6	6.074	9.528	723.3	9.934	11.102	722.6
3.548	8.496	724.1	6.869	9.851	723.3	10.694	11.412	722.3
4.072	8.708	724.4	7.564	10.136	722.9	11.683	11.811	722.4
4.519	8.891	724.0	8.248	10.415	722.8	12.798	12.271	721.7
5.131	9.142	723.7						
			DM-β-CD-SPFO where [$C_8F_{15}O_2Na$]=4.147×10^{-3} m					
1.530	1.487	999.7	4.622	2.513	998.8	8.153	3.724	992.8
2.014	1.645	1000.5	5.142	2.692	997.4	9.102	4.049	991.9
2.292	1.738	1000.2	5.577	2.843	996.1	10.34	4.470	991.2
2.536	1.818	1000.0	6.200	3.055	995.4	10.54	4.537	991.1
3.030	1.982	1000.3	6.599	3.190	994.9	11.43	4.840	990.5
3.574	2.160	1000.7	7.288	3.427	994.0	13.00	5.374	989.9
4.074	2.327	1000.1						
			DM-β-CD-SPFO where [$C_8F_{15}O_2Na$]=2.5192×10^{-2} m					
2.061	6.492	1040.1	5.099	7.440	1025.0	9.179	8.765	1013.7
2.529	6.636	1036.5	5.591	7.598	1023.2	9.934	9.014	1012.2
3.005	6.782	1034.1	6.122	7.769	1021.5	10.24	9.113	1011.7
3.539	6.948	1031.2	6.893	8.016	1019.5	11.32	9.473	1009.5
4.197	7.156	1028.1	7.463	8.203	1017.8	11.76	9.617	1009.1
4.525	7.257	1027.3	8.378	8.502	1015.5	12.87	9.988	1007.0
			HP-β-CD-SPFO where [$C_8F_{15}O_2Na$]=5.009×10^{-3} m					
1.294	1.718	973.3	4.785	3.149	972.9	8.798	4.815	968.9
2.150	2.073	971.5	5.476	3.430	972.9	9.760	5.218	967.9
2.675	2.285	973.1	5.967	3.634	972.2	10.46	5.511	967.4
3.214	2.505	973.2	6.661	3.923	971.4	11.39	5.898	966.8
3.831	2.758	972.9	6.937	4.039	971.0	12.33	6.287	966.4
4.306	2.952	973.0	8.160	4.551	969.3	13.75	6.882	965.4
			β-CD-SPFN where [SPFN]= 2.005×10^{-3} m					
2.171	1.437	717.9	5.258	2.720	717.8	9.442	4.482	714.5
2.629	1.625	718.9	5.763	2.932	717.4	10.337	4.861	713.8
3.128	1.832	719.0	6.307	3.160	717.0	11.049	5.163	713.2
3.648	2.047	719.0	6.950	3.429	716.7	11.284	5.258	713.4
4.122	2.245	718.8	7.960	3.856	715.6	13.351	6.127	712.6
4.826	2.538	718.4	8.796	4.208	715.0			

Table A9: continued

C_{CD}	Δd	$V_{\phi,CD}$	C_{CD}	Δd	$V_{\phi,CD}$	C_{CD}	Δd	$V_{\phi,CD}$
			β-CD-SPFN where [SPFN]= 3.005×10^{-3} m					
1.519	1.420	718.6	4.667	2.719	720.5	8.577	4.347	718.1
2.052	1.641	719.2	5.236	2.954	720.3	9.359	4.673	717.7
2.585	1.861	719.5	5.680	3.138	720.1	10.172	5.014	717.1
3.134	2.088	719.9	6.201	3.357	719.5	10.936	5.334	716.7
3.531	2.251	720.1	7.047	3.709	718.9	12.113	5.834	715.4
4.176	2.516	720.5	7.805	4.027	718.3	13.149	6.271	714.7
			β-CD-SPFN where [SPFN]= 5.009×10^{-3} m					
2.197	2.251	718.1	6.004	3.817	720.3	10.742	5.753	721.1
2.798	2.500	718.4	6.639	4.075	720.9	11.320	5.966	721.0
3.280	2.700	718.5	7.437	4.401	721.1	11.608	6.110	720.7
3.862	2.940	718.7	8.286	4.747	721.3	11.888	6.202	720.6
4.401	3.162	718.9	9.192	5.117	721.3	11.934	6.246	720.5
5.050	3.430	719.3	9.876	5.397	721.3	13.587	6.906	719.7
5.633	3.667	719.9	10.546	5.648	721.2	13.942	7.080	719.3
			DM-β-CD-SPFN where $[C_9F_{17}O_2Na]=5.0267\times10^{-3}$ m					
1.191	1.707	1005.6	3.586	2.502	1000.9	6.669	3.542	996.5
1.567	1.830	1005.4	4.012	2.642	1001.0	6.989	3.652	996.0
1.971	1.965	1003.7	4.395	2.769	1000.7	7.862	3.949	995.0
2.318	2.082	1002.4	4.800	2.903	1000.5	8.477	4.158	994.3
2.527	2.151	1001.4	5.446	3.122	999.2	9.312	4.442	993.6
3.227	2.385	1000.8	6.051	3.330	997.7	10.20	4.743	992.9
			DM-β-CD-SPFN where $[C_9F_{17}O_2Na]=7.023\times10^{-3}$ m					
1.072	2.147	1024.3	2.888	2.745	1010.0	6.636	4.002	1000.4
1.467	2.275	1020.2	3.160	2.836	1008.7	9.686	5.035	996.4
1.864	2.404	1017.0	3.451	2.934	1007.2	11.20	5.547	995.1
1.958	2.435	1016.0	4.072	3.145	1004.6	12.46	5.974	994.2
2.324	2.555	1014.0	5.816	3.732	1000.8	14.05	6.511	993.1
2.592	2.647	1011.1	6.893	4.086	1000.5			
			DM-β-CD-SPFN where $[C_9F_{17}O_2Na]=9.045\times10^{-3}$ m					
1.775	2.903	1034.4	3.890	3.602	1015.2	8.054	5.013	1001.5
2.396	3.105	1026.9	4.151	3.691	1013.5	8.959	5.310	1001.1
2.683	3.200	1023.8	4.512	3.812	1011.8	10.44	5.812	999.1
2.971	3.294	1021.9	5.343	4.097	1007.8	12.01	6.339	997.5
3.220	3.377	1020.0	6.447	4.471	1004.5	13.06	6.695	996.6
3.576	3.496	1017.3	7.068	4.683	1002.8	15.09	7.375	995.1

Table A9: continued

C_{CD}	Δd	$V_{\phi,CD}$	C_{CD}	Δd	$V_{\phi,CD}$	C_{CD}	Δd	$V_{\phi,CD}$
HP-β-CD-SPFN System where $[C_9F_{17}O_2Na]=5.009\times10^{-3}$ m								
1.357	1.873	976.1	4.964	3.349	974.1	9.133	5.087	968.0
2.164	2.205	974.9	5.560	3.592	973.9	9.894	5.403	968.2
2.718	2.430	975.1	6.157	3.843	972.6	10.72	5.746	967.7
3.384	2.703	974.6	6.757	4.094	971.6	11.78	6.188	967.0
4.047	2.976	974.1	7.553	4.426	970.5	12.44	6.471	965.9
4.476	3.150	974.0	8.417	4.788	969.4	14.06	7.140	965.3
β-CD-SPFD where $[SPFD]=1.013\times10^{-3}$ m								
1.397	0.886	717.1	3.400	1.723	716.6	6.262	2.940	712.5
1.720	1.018	718.8	3.860	1.920	715.4	7.257	3.362	711.9
1.951	1.113	719.2	4.371	2.136	714.9	8.008	3.681	711.4
2.186	1.211	718.9	5.054	2.425	714.0	8.949	4.080	710.8
2.470	1.329	719.1	5.423	2.582	713.6	10.179	4.598	710.7
2.880	1.502	718.1	5.858	2.766	713.2	12.304	5.498	709.8
β-CD-SPFD where $[SPFD]=1.903\times10^{-3}$ m								
1.551	1.230	720.7	3.695	2.111	722.2	7.016	3.510	717.0
1.932	1.389	719.9	4.310	2.367	721.4	8.088	3.964	715.7
2.169	1.485	721.0	4.775	2.564	720.3	9.590	4.599	714.5
2.375	1.570	721.2	5.319	2.791	719.8	10.692	5.062	714.0
2.687	1.698	721.6	5.853	3.018	718.5	11.892	5.577	712.6
3.149	1.886	722.3	6.486	3.286	717.7	13.565	6.273	712.5
DM-β-CD-SPFD where $[C_{10}F_{19}O_2Na]=1.031\times10^{-3}$ m								
0.4621	0.4467	1002.5	1.555	0.8184	995.1	2.985	1.314	990.2
0.6731	0.5151	1004.4	1.847	0.9206	993.0	3.397	1.456	989.5
0.7898	0.5557	1001.4	2.037	0.9857	992.5	3.847	1.611	989.0
0.9152	0.5957	1003.1	2.231	1.053	991.7	4.426	1.810	988.6
1.002	0.6249	1002.6	2.456	1.130	991.6	5.039	2.019	988.7
1.096	0.6598	998.7	2.675	1.204	991.7	5.622	2.221	988.2
1.370	0.7539	996.8						
DM-β-CD-SPFD where $[C_{10}F_{19}O_2Na]=2.001\times10^{-3}$ m								
0.5803	0.7527	1008.2	1.463	1.051	999.7	3.217	1.652	993.4
0.7550	0.8154	1000.2	1.659	1.116	999.8	3.673	1.809	992.5
0.8681	0.8490	1004.6	1.891	1.193	999.4	4.074	1.946	992.1
0.9502	0.8788	1001.6	2.100	1.264	998.9	4.477	2.086	991.1
1.046	0.9107	1001.4	2.375	1.361	996.7	4.914	2.236	990.7
1.242	0.9793	998.3	2.831	1.517	995.1	5.352	2.386	990.4

Table A9: continued

C_{CD}	Δd	$V_{\phi.CD}$	C_{CD}	Δd	$V_{\phi.CD}$	C_{CD}	Δd	$V_{\phi.CD}$
HP-β-CD-SPFD System where $[C_{10}F_{19}O_2Na]=1.004 \times 10^{-3}$ m								
1.438	0.8886	971.3	4.988	2.386	964.0	9.306	4.199	962.0
2.114	1.173	968.8	5.372	2.551	963.2	10.13	4.541	962.0
2.872	1.495	966.2	6.137	2.870	963.1	10.69	4.777	961.7
3.376	1.715	963.0	7.522	3.450	962.8	11.80	5.230	962.5
3.998	1.973	963.8	6.720	3.115	962.9	13.07	5.769	961.3
4.493	2.1788	964.0	8.497	3.860	962.3	14.13	6.223	960.2

[a] C_{CD} in m($\times 10^3$), Δd in g cm^{-3}($\times 10^3$), and $V_{\phi.CD}$ in cm^3 mol^{-1}.

APPENDIX A10

Table A10-1: Absorbance of phenolphthalein and concentration of β-CD in 0.1 M Na_2CO_3 at pH=10.5 and 295 K.[a]

$C_{\beta\text{-CD}}$	A	$C_{\beta\text{-CD}}$	A	$C_{\beta\text{-CD}}$	A
9.320e-7	0.628	2.490e-5	0.430	4.980e-4	0.054
1.090e-6	0.616	2.610e-5	0.432	5.220e-4	0.052
2.330e-6	0.614	5.230e-5	0.310	7.470e-4	0.039
2.720e-6	0.600	5.480e-5	0.299	7.830e-4	0.038
4.660e-6	0.592	7.840e-5	0.245	9.960e-4	0.032
5.440e-6	0.574	8.220e-5	0.222	1.040e-3	0.031
6.990e-6	0.572	1.050e-4	0.182	1.570e-3	0.024
8.160e-6	0.552	1.050e-4	0.194	2.490e-3	0.018
9.320e-6	0.550	2.490e-4	0.098	2.610e-3	0.019
1.090e-5	0.526	2.610e-4	0.087	2.940e-3	0.017

[a] $C_{Phth}=2.411\times10^{-5}$ M, $C_{\beta\text{-CD}}$ is in M, and A is the absorbance at 550 nm.

Table A10-2: Absorbance of Phenolphthalein and Concentration Data for β-CD-Surfactant Systems in 0.1 M Na_2CO_3 at pH=10.5 and 295 K.[a]

C_S	A	C_S	A	C_S	A
Surfactant=SHex, $C_{\beta\text{-CD}}=2.940\times10^{-4}$ M, $C_{Phth}=2.410\times10^{-5}$ M					
0.00816	0.110	0.033	0.183	0.057	0.246
0.013	0.125	0.038	0.198	0.062	0.257
0.018	0.138	0.042	0.210	0.067	0.268
0.023	0.152	0.047	0.224	0.072	0.278
0.028	0.173	0.052	0.234	0.077	0.290
Surfactant=SHept, $C_{\beta\text{-CD}}=2.940\times10^{-4}$ M, $C_{Phth}=2.410\times10^{-5}$ M					
2.240e-3	0.102	0.027	0.304	0.063	0.458
4.480e-3	0.126	0.036	0.358	0.072	0.466
8.950e-3	0.171	0.045	0.394	0.081	0.492
0.018	0.247	0.054	0.430	0.090	0.510
Surfactant=SO, $C_{\beta\text{-CD}}=2.940\times10^{-4}$ M, $C_{Phth}=2.410\times10^{-5}$ M					
9.050e-4	0.104	3.620e-3	0.199	8.140e-3	0.296
1.090e-3	0.108	4.970e-3	0.217	9.050e-3	0.312
1.810e-3	0.134	5.880e-3	0.248	0.010	0.322
2.710e-3	0.162	6.780e-3	0.270	0.011	0.340

Table A10-2: continued

C_S	A	C_S	A	C_S	A
Surfactant=SN, $C_{\beta\text{-}CD}$=2.942×10^{-4} M, C_{Phth}=2.410×10^{-5} M					
6.990e-4	0.154	4.660e-3	0.386	0.00851	0.474
1.400e-3	0.215	5.480e-3	0.410	0.00933	0.488
2.330e-3	0.284	6.180e-3	0.432	0.010	0.486
3.150e-3	0.324	6.990e-3	0.450	0.011	0.498
3.850e-3	0.360	7.810e-3	0.452	0.012	0.504
Surfactant=Sodium 1-Octyl sulfonate, $C_{\beta\text{-}CD}$=2.940×10^{-4} M, C_{Phth}=2.410×10^{-5} M					
6.920e-4	0.087	2.350e-3	0.168	7.610e-3	0.296
9.680e-4	0.107	2.770e-3	0.187	9.680e-3	0.336
1.250e-3	0.112	3.800e-3	0.215	0.011	0.340
1.660e-3	0.139	6.230e-3	0.273	0.014	0.364
Surfactant=SDec, $C_{\beta\text{-}CD}$=2.940×10^{-4} M, C_{Phth}=2.410×10^{-5} M					
8.260e-5	0.095	2.480e-4	0.123	4.130e-4	0.156
1.240e-4	0.101	2.890e-4	0.133	4.540e-4	0.167
1.650e-4	0.109	3.300e-4	0.138	4.950e-4	0.172
2.060e-4	0.117	3.720e-4	0.147	5.160e-4	0.177
Surfactant=SDodec, $C_{\beta\text{-}CD}$=2.940×10^{-4} M, C_{Phth}=2.410×10^{-5} M					
4.530e-5	0.089	4.530e-4	0.249	9.060e-4	0.384
1.130e-4	0.108	6.790e-4	0.335	1.020e-3	0.406
2.260e-4	0.151	7.930e-4	0.362	1.130e-3	0.426
2.720e-4	0.164				
Surfactant=SPFB, $C_{\beta\text{-}CD}$=2.942×10^{-4} M, C_{Phth}=2.418×10^{-5} M					
5.200e-3	0.138	0.016	0.258	0.026	0.336
7.800e-3	0.172	0.018	0.274	0.028	0.344
0.010	0.199	0.020	0.289	0.029	0.352
0.013	0.227	0.023	0.316	0.033	0.378
Surfactant=SPFP, $C_{\beta\text{-}CD}$=2.940×10^{-4} M, C_{Phth}=2.409×10^{-5} M					
1.980e-4	0.103	2.980e-3	0.349	0.00695	0.476
3.970e-4	0.127	3.970e-3	0.394	0.00794	0.486
9.920e-4	0.197	4.960e-3	0.426	0.00893	0.508
1.980e-3	0.285	5.950e-3	0.448	0.010	0.516

Table A10-2: continued

C_S	A	C_S	A	C_S	A
Surfactant=SPFH, $C_{\beta\text{-CD}}=2.942\times10^{-4}$ M, $C_{Phth}=2.412\times10^{-5}$ M					
2.030e-5	0.081	2.440e-4	0.223	5.690e-4	0.488
4.060e-5	0.086	3.250e-4	0.325	6.500e-4	0.506
8.130e-5	0.090	4.060e-4	0.400	7.320e-4	0.526
1.630e-4	0.144	4.880e-4	0.452	8.130e-4	0.538
Surfactant=SPFO, $C_{\beta\text{-CD}}=2.940\times10^{-4}$ M, $C_{Phth}=2.418\times10^{-5}$ M					
1.050e-4	0.113	2.530e-4	0.297	3.790e-4	0.516
1.690e-4	0.157	2.740e-4	0.350	4.220e-4	0.544
1.900e-4	0.186	3.160e-4	0.434	4.740e-4	0.568
2.110e-4	0.217	3.580e-4	0.494	5.270e-4	0.584
Surfactant=SPFN, $C_{\beta\text{-CD}}=2.939\times10^{-4}$ M, $C_{Phth}=2.418\times10^{-5}$ M					
4.410e-5	0.090	1.650e-4	0.168	3.860e-4	0.572
6.620e-5	0.101	2.210e-4	0.255	4.410e-4	0.592
8.820e-5	0.112	2.760e-4	0.402	4.960e-4	0.604
1.100e-4	0.123	3.310e-4	0.522	5.510e-4	0.612

[a] C_{Phth} is in M, $C_{\beta\text{-CD}}$ is in M, and A is the absorbance at 550 nm.

IMAGE EVALUATION
TEST TARGET (QA-3)

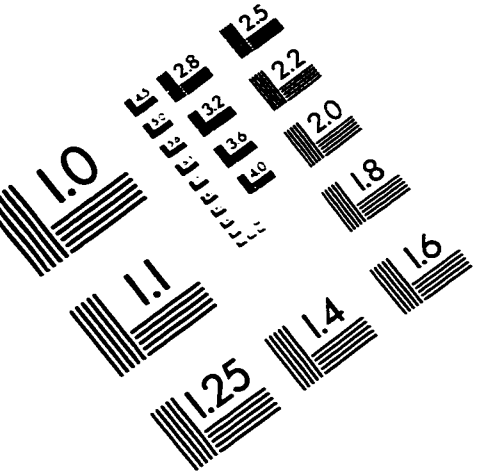

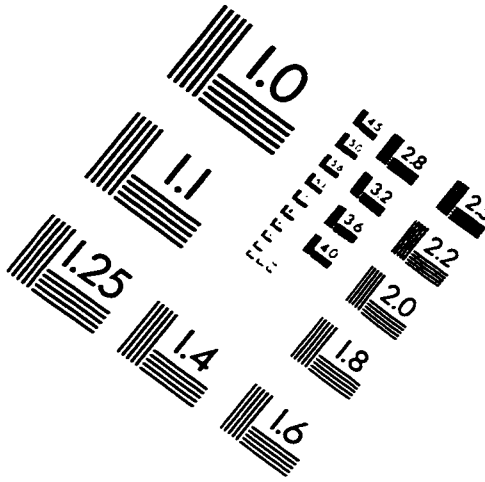

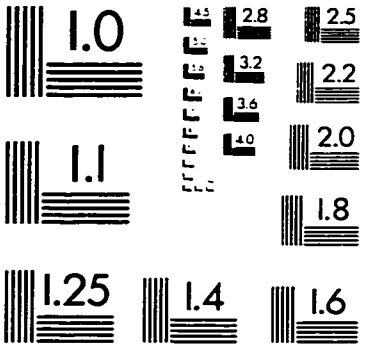

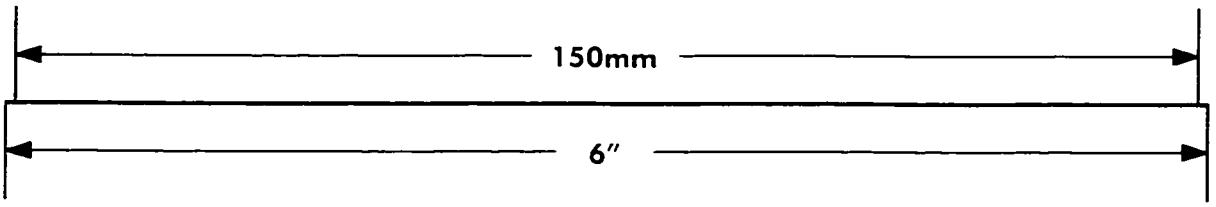

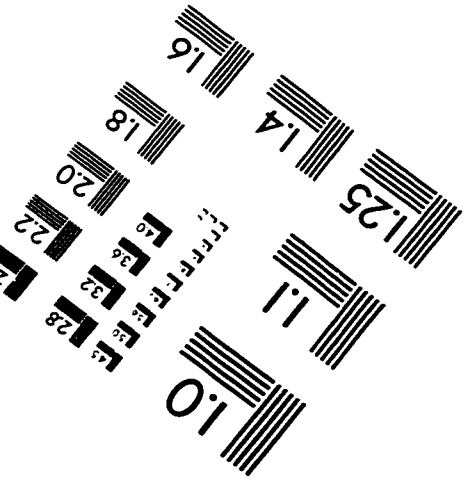

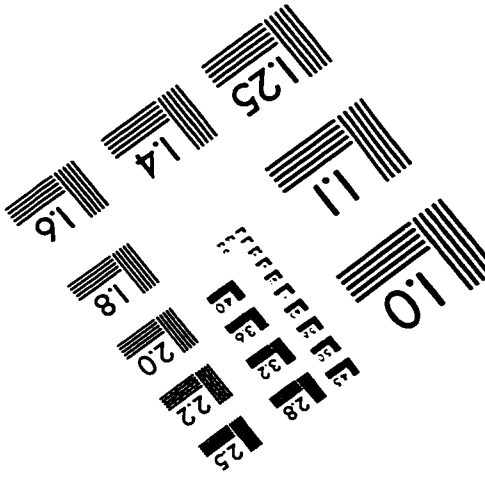

APPLIED IMAGE . Inc
1653 East Main Street
Rochester, NY 14609 USA
Phone: 716/482-0300
Fax: 716/288-5989